Nuclear Medicine Pioneer Citation, 1978: Benedict Cassen, Ph.D.

Benedict Cassen was a distinguished and honoured member of this Society, serving as a Trustee for many years and receiving in 1970 the Society's first Distinguished Scientist award with an honorarium of $5,000. He received world-wide recognition for his invention in 1950 of the automated scintillation scanner, a development which launched the specialty of nuclear medicine upon the sea of organ imaging.

Ben was born in New York City Nov. 13, 1902, and lived during his childhood in the tobacco farming region of Connecticut. He graduated in 1927 in Physics and Mathematics from the Royal College of Science, London, England, and received an M.S. degree in 1928 and a Doctor of Philosophy degree, magna cum laude, in Mathematics-Physics in 1930 from the California Institute of Technology. His dissertation subject was on high-potential x-ray tubes. He was a National Research Council Fellow at Princeton from 1930 to 1932 and became Hospital Physicist at the Harper Hospital in Detroit from 1934 to 1939. This was followed by a period of five years' work on x-rays as a Research Physicist in the Westinghouse Research Laboratory in Pittsburgh, Pennsylvania. He returned to Cal Tech in 1944 to work on a war-related project and then became a research physicist associated with the Naval Ordnance Test Station in Pasadena from 1945 to 1947.

Ben joined the newly formed UCLA-U.S. Atomic Energy Commission Project in 1947 (now the Laboratory of Nuclear Medicine and Radiation Biology), where he continued to work until his death from acute myocardial infarction in 1972. He became Professor of Biophysics at UCLA in 1949 and made valuable contributions to the education of medical and graduate students and research Fellows.

Dr. Cassen, in 1949, established the scientific and practical foundation for successful clinical imaging of body organs by radioisotopic techniques. Although quantitation of the fraction of an administered dose of iodine-131 deposited in the thyroid gland had been a routine procedure for a decade, the efficiency of the Geiger-Müller tube in detecting I-131 gamma rays necessitated administration of several millicuries of radioactive iodine, and imaging of the gland was not a practical procedure. Ben conceived the idea of using calcium tungstate crystals, which have excellent photoelectric absorption of I-131 gamma radiations, cemented to a sensitive photomultiplier tube and thereby obtained a counting efficiency for I-131 of 26% in contrast to the 1 or 2% efficiency achieved by most Geiger-Müller tubes. Shielding of the calcium tungstate crystals made the apparatus highly directional and made possible accurate localization and "mapping" of the thyroid gland following administration of between 10 and 200 μCi of I-131.

Initial clinical studies on human subjects were conducted with Dr. Herbert Allen, Jr., at the Wadsworth Veterans Administration Hospital. These

early studies were accomplished by painstaking manual location of the tube over a grid which overlay the neck and thyroid gland. They were extremely laborious, requiring from 60 to 90 min to determine the outline of the gland. Dr. Cassen resolved this problem by designing the first automated scanning detector. This instrument was first described in *Nucleonics* in 1950, and commercial production of the instrument was undertaken in 1951 by Reed and Curtis, Dr. Cassen's former associates at UCLA. Many of these instruments were used for thyroid gland mapping in United States hospitals during the next 10 years.

The success of the scanning device developed by Dr. Cassen was followed rapidly by the development of photoscanning in 1956 by Dr. David Kuhl and subsequently by the invention of the Anger camera. These and other sophisticated approaches have replaced in large measure the mechanical scanner developed by Dr. Cassen. However, it was Dr. Cassen's original concept and invention which started the whole clinical specialty of imaging, and actually placed the new specialty of nuclear medicine on a strong clinical and financial basis.

Although Ben is best known for his invention and development of the scintillation scanner, he made other significant scientific contributions. He investigated the effects of shock waves on mammalian organisms, developing techniques for producing intense air blast effects under controlled laboratory conditions, and evaluated the effects of such trauma on the respiratory, vascular, and nervous systems. This work contributed materially to our understanding of the effects of explosions on human beings. He invented a method of administering radioisotopes by a jet injection system, which found applications in jet administration of other medications. He conceived the idea of testing closed systems—e.g., pipelines—for leaks, with the use of radioactive gas. Working with Dr. William Blahd, he quantitated total body potassium and body water in primary muscle diseases. During his final years, he worked on methods of characterizing and separating the several populations of white blood cells and successfully separated leucocytes of different types without seriously damaging their physiologic properties.

At the time of his death he was developing a large wide-angle hydraulically driven 2,000-hole collimator scanner for in-depth scanning of the brain which held promise of aiding in the precise localization of deep-seated lesions in the central nervous system.

With Dr. Blahd and Franz Bauer, Dr. Cassen wrote and published in 1958 *The Practice of Nuclear Medicine*, the first definitive American text on Nuclear Medicine. He wrote many articles in the scientific literature and many chapters in books concerned with nuclear medicine. He also prepared many reports to the Atomic Energy Commission, many of which were of a confidential nature.

Ben is survived by his wife, Wylie Balfour Cassen—a delightful Scots lady—who complemented Ben's serious scientific nature with her wonderful Scottish wit. Their son Balfour is Librarian at Woodbury University in Los Angeles.

Ben was an insightful, creative scientist, a perceptive critic, and a sincere friend. His contributions to mankind were great and his position of distinction will survive in history. The Society of Nuclear Medicine is privileged indeed to recognize Dr. Benedict Cassen as one of its Nuclear Pioneers!

JOSEPH F. ROSS, M.D.
UCLA School of Medicine
Center for the Health Sciences
Los Angeles, California

NUCLEAR PIONEER LECTURER—1978 JOSEPH FOSTER ROSS, M.D.

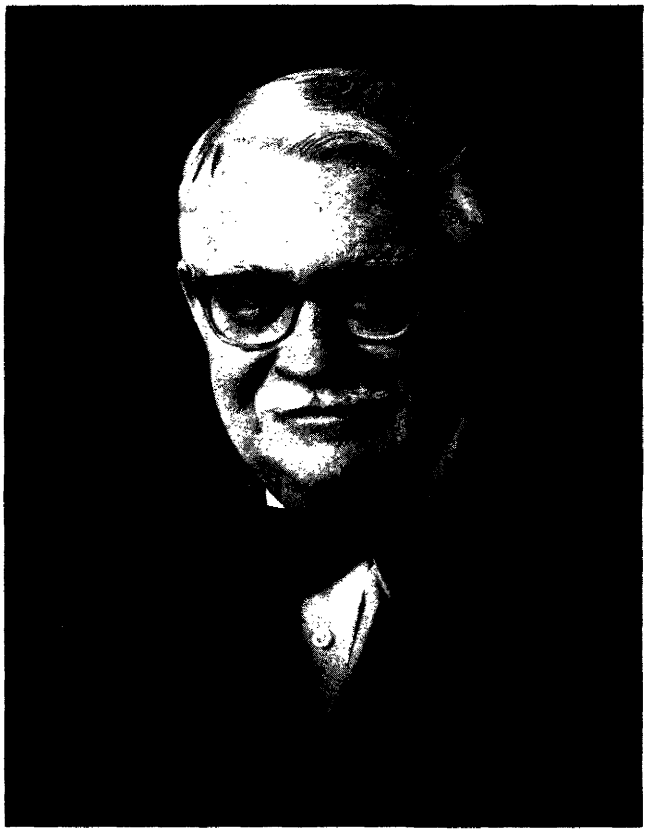

Dr. Joseph Foster Ross, Professor of Medicine and Chief of the Division of Hematology at the University of California at Los Angeles, was educated at Stanford University and Harvard Medical School and completed intern and residency training in Internal Medicine and Pathology at the Boston City Hospital.

In 1939, as an intern in Pathology at the University of Rochester School of Medicine, working with Doctors George H. Whipple and Paul F. Hahn, he used the newly discovered cyclotron-produced isotope Fe-59 in the study of iron metabolism and blood formation in dogs. Moving to Boston University in 1940 as an Assistant Professor of Medicine, he was among the first to apply radioiron tracer methods to the study of iron metabolism and erythropoiesis in human subjects. During the next 14 years he and a series of colleagues studied the patterns of ferrokinetics in normal subjects and in patients with hematologic diseases, contributing significant information concerning the mechanisms of anemia in neoplastic and inflammatory diseases.

With the need for large quantities of whole blood for blood transfusions in World War II, Dr. Ross and his associate, Dr. Clement Finch, studied methods of in vitro preservation of red cells in bank blood. By following the post-transfusion survival of erythrocytes biologically labeled with Fe-59, they developed a method of storage with "ACD solution" which satisfactorily preserved erythrocyte viability for storage periods of 21 days. This method was used for the preservation of hundreds of thousands of pints of blood which were flown to battle areas all over the world, and the method still is in general use in blood banks. This work was recognized by President Harry Truman as "an invaluable contribution to the war effort of the United States" with the Award of the Presidential Certificate of Merit.

Following the war, in collaboration with Doctors Franklin Ebaugh, Jr., and Charles Emerson, Jr., the use of radioactive chromium-labeled erythrocytes to determine the in vivo survival of red cells was developed and applied to the study of erythrocyte survival in pathological conditions—a method still widely used.

Working with Dr. Belton Burrows, Dr. Ross investigated thyroid physiology and pathology with radioactive iodine, studies which were recognized by the American Goiter Society with the Award of the Van Meter Prize in 1953.

In 1948 Dr. Ross established one of the first Veterans Administration Radioisotope Units—at the Framingham and the Boston Veterans Administration Hospitals. During the ensuing 30 years, he has

continued his interest and association with the Veterans Administration Radioisotope Research and Nuclear Medicine Services, and served as National Chairman of the Veterans Administration Committee on Training in Nuclear Medicine.

Returning to his home state of California in 1954, Dr. Ross served as Associate Dean, Professor of Medicine and Professor of Radiation Biology of the new UCLA School of Medicine, and Chief of Staff of the UCLA Hospital. In 1958 he developed and became Director of the United States Atomic Energy Commission supported UCLA Laboratory of Nuclear Medicine and Radiation Biology, working with Doctors Stafford L. Warren, George Taplin, and Benedict Cassen. His interest in environmental radiation and radiation ecology was recognized in 1964 by the American Clinical and Climatological Society with the Gordon Wilson Lectureship and the Award of the Gordon Wilson Medal.

An active member of the Board of Trustees of the Society of Nuclear Medicine from 1962 to 1972, Dr. Ross served as Chairman of the Program Committee in 1966–1967 and Chairman of the Bylaws Committee from 1967 to 1969, during which time a revision of the organization of the Society was proposed and adopted by the membership of the Society. He also has been active in other professional organizations, serving as President of the American Society of Hematology, of the Western Association of Physicians, of the Southern California Chapter of the Society of Nuclear Medicine, and Councillor of the Radiation Research Society.

He has represented the United States Atomic Energy Commission and Department of State, the International Atomic Energy Agency, and the World Health Organization on numerous international missions concerned with research and education in nuclear medicine.

A long-standing interest in medical publications is reflected in membership on the Editorial Boards of the journal *Blood*, the *Annals of Internal Medicine*, *The Journal of Nuclear Medicine*, the Medical Book Division of Little, Brown & Company, and the University of California Press Medical Book Series.

During the 40 years of his association with nuclear medicine, Dr. Ross has worked toward the establishment of nuclear medicine as a recognized medical specialty with high standards of medical excellence. To this end, working with colleagues, he was instrumental in establishing in 1971 the conjoint American Board of Nuclear Medicine, of which he served as Secretary from 1971 to 1973 and as Chairman and President from 1973 until 1977. He represents the American Board of Nuclear Medicine as a member of the American Board of Medical Specialties and represents the Society of Nuclear Medicine on the Council of Medical Specialty Societies. He also is a member of the American Board of Internal Medicine.

The Western Region of the Society of Nuclear Medicine honored Dr. Ross with its first Distinguished Scientist Award in 1977 for his "distinguished contributions to Nuclear Medicine, including founding the American Board of Nuclear Medicine."

ANAHEIM 1978: COLOR IT SILVER

As we take part in the Silver Anniversary Meeting of the Society of Nuclear Medicine, we can reflect with satisfaction both on its growth—total membership is now nearing the 10,000 mark—and on its role in gaining recognition for nuclear medicine as a vital medical specialty.

To extend these accomplishments into the next quarter-century, the Scientific Program Committee for this 25th Annual Meeting at Anaheim has organized the proceedings with the objective of addressing the diverse interests of the Society's heterogeneous membership. The variety of presentations should appeal both to the clinician and the researcher, as well as to those involved in the development of correlative techniques.

The 1978 meeting will be the Society's biggest ever, in terms of numbers of scientific offerings. Of the more than 600 abstracts submitted and reviewed, some 340 were accepted and will be presented in a program extending over four days, from Tuesday, June 27, to Friday, June 30.

This year, for the first time, the program has been planned as a "track" system, with five categories of sessions running concurrently throughout the week. The diagrams on pages 667 and 668 illustrate the basic setup, and in the abstract listings which follow, each session is identified as belonging to one of five tracks: (1) Continuing Education; (2) Clinical Science; (3) Basic Science; (4) In Vitro and Correlative Techniques; and (5) Clinical Practice. Except for the Continuing Education track, proferred papers constitute the basic framework for the scientific sessions, but a variety of formats—rapporteur discussions, panels, poster sessions, and mini-symposia—have been employed.

Cardiovascular Nuclear Medicine is featured throughout the meeting as this year's "scintillating" topic, and schedules have been arranged so that no competing cardiovascular sessions occur at any time. In designing schedules, the Committee has also taken care to leave noon and evening hours for the most part free for visiting an outstanding array of commercial and scientific exhibits. Scientific Exhibit Rounds, supervised by recognized experts in their fields, will also be among the offerings, and will concentrate on cardiovascular nuclear medicine, bone imaging, and instrumentation. In addition, a series of Radioassay Workshops will be in operation Wednesday, Thursday, and Friday mornings.

With the scope of this year's program expanded both in the numbers and types of sessions being presented, it is hoped that meeting-goers can pre-plan their activities to obtain the maximum benefits of the Committee's planning efforts. Attendees are therefore encouraged to peruse the abstracts on the following pages and to carefully survey the meeting program so as to make the best possible use of their time at Anaheim.

With sincere thanks to all who helped in the preparation of this program, I offer my hope that this will prove an enlightening and productive experience for everyone. Happy 25th Anniversary, SNM!

RICHARD A. HOLMES
1978 Scientific Program Chairman
Society of Nuclear Medicine

TABLES OF SCIENTIFIC SESSIONS

MONDAY	TUESDAY, JUNE 27 • SNM 25TH ANNUAL MEETING					
9:00 to **5:00** **Board of Trustees Meeting** (South Ballroom, Disneyland Hotel)	7:30 to **5:30** ***REGISTRATION OPEN***		8:00 to 8:25 ***SPECIAL LECTURE:*** **Nuclear Medicine Milestones** (Santa Ana Room)			
	8:30 to 10:30	**OPENING SESSION:** • **Keynote Address** • **Presentation of Aebersold Award** • **Report of Task Group on Future Directions in Nuclear Medicine** (Anaheim Room, Convention Center)				
	10:30 to 10:45	***GRAND OPENING OF EXHIBITION HALL***—Convention Center				
2:00 to **8:30** ***REGISTRATION OPEN*** (Convention Center)	10:45 to **2:00**	***VISIT THE EXHIBITS/LUNCH***				
		CONTINUING EDUCATION	**CLINICAL SCIENCE**	**BASIC SCIENCE**	**IN VITRO AND CORRELATIVE TECHIQUES**	**CLINICAL PRACTICE**
	2:00 to **3:30**	**Renal Imaging; Pulmonary Diagnosis** (Garden Grove Room) page 2	**Cardiovascular I** (Anaheim Room) page 3	**Radiopharmaceuticals I** (Santa Ana Room) page 5	**Hematology I (Clinical Science)** (California B Room) page 6	**Neurology** (California A Room) page 8
	3:30 to **4:00**	***VISIT THE EXHIBITS***				
6:30 to **8:30** **Ice-Breaker Cocktail Party** (California Room, Convention Center)	**4:00** to **5:30**	**Cardiovascular Nuclear Medicine** (Garden Grove Room) page 9	**Pulmonary I** (Anaheim Room) page 10	**Radiopharmaceuticals II** (Santa Ana Room) page 12	**Endocrinology I (Clinical Science)** (California B Room) page 13	**Exhibit Rounds** (North Exhibition Hall)
	6:30 to **11:30** ***AN EVENING AT KNOTT'S BERRY FARM***				***NOTE:*** In these schematics, times printed in lightface type are a.m.; those in bold are p m	

WEDNESDAY, JUNE 28 • SNM 25TH ANNUAL MEETING					
7.30 to **5:30** ***REGISTRATION OPEN***		9:00 to 11:30 **RIA Workshop A** (Huntington Beach Room); **RIA Workshop B** (Orange County Room 18)			
	CONTINUING EDUCATION	**CLINICAL SCIENCE**	**BASIC SCIENCE**	**IN VITRO AND CORRELATIVE TECHNIQUES**	**CLINICAL PRACTICE**
8:30 to 10:00	**Hematology; Gastrointestinal Imaging** (Garden Grove Room) page 15	**Cardiovascular II** (Anaheim Room) page 16	**Basic Nuclear Science** (Santa Ana Room) page 18	**Computed Tomography** (California B Room) page 20	**Instrumentation** (California A Room) page 22
10:00 to 10:30	***VISIT THE EXHIBITS***				
10:30 to **12:00**	**Central Nervous System; Bones and Joints** (Garden Grove Room) page 29	**Gastroenterology I** (Anaheim Room) page 24	**Radiopharmaceuticals III: Poster Session** (South Exhibition Hall) page 26	**Ultrasound** (California B Room) page 28	**Exhibit Rounds** (North Exhibition Hall)
12:00 to **2:00** ***LUNCH/VISIT THE EXHIBITS***		**12:00** to **1:00** **Exhibit Rounds** (North Exhibition Hall)			
2:00 to **3:30**	**Pediatrics I (Clinical Science)** (Garden Grove Room) page 29	**Oncology I** (Anaheim Room) page 30	**Radiopharmaceuticals IV** (Santa Ana Room) page 32	**Radioassay I; Berson-Yalow Award** (California B Room) page 34	**Bone/Joint** (California A Room) page 35
3:30 to **3:45**	***VISIT THE EXHIBITS***				
3:45 to **5:15**	**Pediatrics II (Clinical Science)** (Garden Grove Room) page 36	**Neurology** (Anaheim Room) page 38	**Radiopharmaceuticals V** (Santa Ana Room) page 40	**Radioassay II** (California B Room) page 42	**Cardiovascular I** (California A Room) page 43
5:30 to **6:30** **Exhibit Rounds** (North Exhibition Hall)					

TABLES OF SCIENTIFIC SESSIONS (continued)

THURSDAY, JUNE 29 • SNM 25TH ANNUAL MEETING

8:00 to 5:30 *REGISTRATION OPEN* — 9:00 to 11:30 **RIA Workshop A** (Huntington Beach Room); **RIA Workshop C** (Orange County Room 18)

	CONTINUING EDUCATION	CLINICAL SCIENCE	BASIC SCIENCE	IN VITRO AND CORRELATIVE TECHNIQUES	CLINICAL PRACTICE
8:30 to 10:00	**Endocrinology and Radioimmunoassay** (Garden Grove Room) page 44	**Bone/Joint** (Anaheim Room) page 45	**Instrumentation I** (Santa Ana Room) page 46	**Hematology II (Clinical Science)** California B Room) page 48	**Quality Control** (California A Room) page 49
10:00 to 10:30	*VISIT THE EXHIBITS*				
10:30 to **12:00**	**Radiopharmaceutical Advances** (Garden Grove Room) page 50	**Cardiovascular III** (Anaheim Room) page 51	**Instrumentation II** (Santa Ana Room) page 53	**Endocrinology II** (California B Room) page 55	
12:00 to **1:30**	*LUNCH/VISIT THE EXHIBITS*	**12:00** to **1:00**	**Exhibit Rounds** (North Exhibition Hall)		
1:30 to **3:00**	**Current Status of Radiation Biology** (Garden Grove Room) page 57	**Oncology II** (Anaheim Room) page 58	**Radiopharmaceuticals VI** (Santa Ana Room) page 60	**Radioassay III** California B Room page 62	**Pediatrics** (California A Room) page 63
3:00 to **3:15**	*VISIT THE EXHIBITS*				
3:15 to **4:45**	**Instrumentation** (Garden Grove Room) page 64	**Renal/Electrolyte/ Hypertension** (Anaheim Room) page 65	**Data Processing I** (Santa Ana Room) page 67	**Radioassay IV** (California B Room) page 68	**Pulmonary** (California A Room) page 69
4:45 to **5:00**	*VISIT THE EXHIBITS*	**5:00** to **5:30**	**Nuclear Pioneer Lecture** (Anaheim Room)		
		5:30 to **6:30**	**SNM Business Meeting** (Anaheim Room)		
8:00 to **9:45**		**Cardiovascular IV: Poster Session** (South Exhibition Hall) page 71			

FRIDAY, JUNE 30 • SNM 25TH ANNUAL MEETING

8:00 to 4:00 *REGISTRATION OPEN* — 9:00 to 11:30 **RIA Workshop B** (Huntington Beach Room); **RIA Workshop C** (Orange County Room 18)

	CONTINUING EDUCATION	CLINICAL SCIENCE	BASIC SCIENCE	IN VITRO AND CORRELATIVE TECHNIQUES	CLINICAL PRACTICE
8:30 to 10:00	**Highlights of the Scientific Sessions** (Garden Grove Room) page 73	**Pulmonary II** (Anaheim Room) page 74	**Instrumentation III** (Santa Ana Room page 76	**Radiopharmaceuticals VII (Basic Science)** (California B Room) page 78	**Gastroenterology and Gallium** (California A Room) page 80
10:00 to 10:30	*VISIT THE EXHIBITS*				
10:30 to **12:00**	**Cardiovascular V (Clinical Science)** (Garden Grove Room) page 81	**Gastroenterology II** (Anaheim Room) page 83	**Data Processing II** (Santa Ana Room) page 85	**Endocrinology III (Clinical Science)** (California B Room) page 86	**Radiopharmacy and Hematology** (California A Room) page 88
12:00 to **2:00**	*LUNCH/VISIT THE EXHIBITS*				
2:00 to **3:30**		**Cardiovascular VI** (Anaheim Room) page 89	**Data Processing III** (Santa Ana Room) page 91	**Radioassay V** (California B Room) page 92	**Governmental Affairs** (Garden Grove Room) page 94
3:30 to **3:45**	*BREAK*				
3:45 to **5:15**			**Data Processing IV** (Santa Ana Room) page 95		**Cardiovascular II** (Garden Grove Room) page 96
5:15	*MEETING ADJOURNS*	*NOTE:* The Exhibition Hall closes at 2:15 p.m. Friday.			

Proceedings of the 25th Annual Meeting

SCIENTIFIC PROGRAM

TUESDAY, JUNE 27, 1978

TUESDAY, JUNE 27
8:30 a.m.-10:30 a.m.

ANAHEIM ROOM

OPENING SESSION

OPENING REMARKS. William H. Blahd, President, Society of Nuclear Medicine.

KEYNOTE ADDRESS: THERE IS A FUTURE FOR NUCLEAR BRAIN SCANNING. William H. Oldendorf, UCLA School of Medicine, Los Angeles, CA.

REPORT OF THE TASK GROUP ON FUTURE DIRECTIONS IN NUCLEAR MEDICINE. INTRODUCTION--Leonard M. Freeman, Task Group Chairman, Montefiore Hospital, Bronx, NY; INSTRUMENTATION--F. David Rollo, Vanderbilt University Hospital, Nashville, TN; RADIOCHEMISTRY AND RADIOPHARMACEUTICALS--Harold L. Atkins, Brookhaven National Laboratory, Upton, NY; RADIOIMMUNOASSAY--Stanley J. Goldsmith, Mt. Sinai Medical Center, New York, NY; CONCLUSIONS--S. James Adelstein, Peter Bent Brigham Hospital, Boston, MA.

CLOSING REMARKS. Richard A. Holmes, Scientific Program Chairman, Society of Nuclear Medicine.

TUESDAY, JUNE 27
2:00 p.m.-3:30 p.m.

GARDEN GROVE ROOM

CONTINUING EDUCATION

RENAL IMAGING AND FUNCTION

PARTICIPANTS: M. Donald Blaufox, Chairman, Albert Einstein College of Medicine; James J. Conway, Co-Chairman, Children's Memorial Hospital, Chicago, IL; Peter T. Kirchner, University of Chicago, Chicago, IL; Leonard Rosenthall, The Montreal General Hospital, Montreal, Quebec, Canada; and Claude Raynaud, Hopital d'Orsay, Orsay, France.

PULMONARY FUNCTION, IMAGING, AND DIAGNOSIS

PARTICIPANTS: Roger Secker-Walker, Chairman, St. Louis University Hospitals, St. Louis, MO; Philip O. Alderson, Co-Chairman, The Johns Hopkins University, Baltimore, MD.

TUESDAY, JUNE 27
2:00 p.m.-3:30 p.m.

ANAHEIM ROOM

CLINICAL SCIENCE

CARDIOVASCULAR I

Chairman: Henry N. Wagner, Jr.
Co-Chairman: Robert E. Henkin

VALIDATION OF A TWO MINUTE TECHNIQUE FOR MULTIPLE GATED SCINTIGRAPHIC ASSESSMENT OF LEFT VENTRICULAR EJECTION FRACTION AND REGIONAL WALL MOTION. J. Maddahi, D. Berman, R. Silverberg, Y. Charuzi, N. Buchbinder, R. Gray, A. Waxman, R. Vas, P.K. Shah, H.J.C. Swan, J. Forrester. Cedars-Sinai Medical Center, Los Angeles, CA

Few radionuclide methods permit the rapid, repeated determination of left ventricular (LV) ejection fraction(EF) and regional wall motion (RWM) necessary for evaluation of exercise LV function. This study assesses the validity of 2-minute (min) and 6-min multiple gated cardiac blood pool scintigraphy (MSc) in 70 pts using Tc-99m-RBC's, gamma camera, computer, and computerized edge detection with multiple frame region of interest. In 35 pts EF and RWM of 6-min MSc were compared with biplane LV cineangiograms (Cine) and in 35 additional pts EF and RWM of 2 and 6-min MSc were compared. RWM was quantitated by a 6 point scoring system for each of 7 LV segments observed on anterior and LAO views. Reproducibility was assessed by repeated 2-min MSc without intervention 1 hour after initial study. Excellent correlation for EF was found between 6-min MSc and Cine (r=.93) and between 2 and 6-min MSc (r=.99). RWM on 6-min MSc and Cine demonstrated high correlation: in 233 of 245 segments RWM scores differed by one point or less. Comparison of RWM on 2 and 6-min MSc showed even better correlation: RWM score was identical in 220 of 245 segments, and in only 3 segments was the difference >1. Reproducibility for 2-min MSc EF demonstrated an absolute deviation of 5.7% ± 4.8% of EF value (mean ± SD). Interobserver variation in EF measurement was minimal (r=.99) reflecting the high degree of automation of the system. Thus, two-minute multiple gated scintigraphy is an accurate and reproducible technique for EF and RWM measurement which is well suited to assessment of LV performance during exercise.

THE R-WAVE SYNCHRONIZED BLOOD POOL EJECTION FRACTION: A COMPARISON OF ACCURACY AND REPRODUCIBILITY OF FIXED AND COMPUTER-AUTOMATED, VARYING LEFT VENTRICULAR REGIONS-OF-INTEREST. S.G. Sorensen, D.L. Williams, J.E. Hannah, and G.W. Hamilton. VA Hospital, Seattle, WA.

The systolic ejection fraction (EF) is the best single measure of left ventricular (LV) performance and may be quantitated noninvasively by gated radionuclide angiography

(RNA). We compared 3 methods of RNA analysis of EF in 40 patients (pts) with RAO contrast EF. Tc-99m-labeled RBC RNA EF was calculated from the LAO view using computer based ECG-gated data collection by 3 methods: I) operator-defined nonvarying end-diastolic LV region-of-interest (ROI); II) computer-defined varying ROI from end-diastole (ED) through end-systole (ES); and III) computer-defined varying ROI from ED through ES following image processing by a nonstationary resolution-recovery algorithm which enhances edge definition. Reproducibility was assessed by repeat analysis on separate days. Mean EF (±SD) by each method was: contrast .51 ± .17; I - .34 ± .15; II - .51 ± .16; and III - .51 ± .16. I differed from contrast ($p < .001$) while II and III did not. Correlation of each method vs. contrast with respective reproducibility data was:

Contrast Correlation (r/SEE)		Reproducibility (r/SEE)	
I. .70/.10	p=NS	I. .97/.03	p=.06
II. .83/.09	p=NS p=NS	II. .93/.06	p=.06 p=NS
III. .80/.10		III. .97/.04	

We conclude that: 1) all 3 methods correlate well with contrast angiography and are highly reproducible, 2) computer defined variable ROI methods (II,III) improved accuracy over nonvariable methods, and 3) image processing may improve reproducibility when varying regions-of-interest are used (p=.06).

EQUILIBRIUM RADIONUCLIDE ANGIOGRAPHY-VALIDATION STUDIES USING A NON-COMPUTERIZED CARDIAC MODULE TO DETERMINE LEFT VENTRICULAR EJECTION FRACTION. M. Pfisterer, S. Swanson, B. Ioannou, R. Sano, J. Verba, W. Ashburn, University of California, San Diego, CA & Picker Corp., Northford, CT.

The Cardiac Module (CM), a new non-computerized Anger camera accessory, has been designed to determine left ventricular (LV) ejection fraction (EF) from equilibrium (EQ) radionuclide angiography. An elliptical region-of-interest is positioned over the LV. The background (Bkg) counts are collected in the left mid lung field (Bkg A) or from a ring-shaped region around the LV (Bkg B) for EQ. A time-activity (T/A) curve is generated integrating the LV minus Bkg counts over a number of heart beats (R-R intervals). To assess the validity of EF by CM we studied 15 pts with CAD at rest in the LAO view. Data were acquired by the CM until 500 counts were reached in the 1st 20 msec. channel of the T/A curve. Average EF values of 3 to 5 measurements were compared to contrast ventriculography (CV) and to a computer-method (MUGA) to determine EF.

EQ-EF derived from the CM compared to CV showed a correlation of r = .71 using Bkg A and r = .90 using Bkg B. The correlation between CM and MUGA was r = .77 (Bkg A) and r = .94 (Bkg B). The results of 2 independent observers correlated much better using Bkg B (r = .97) than Bkg A (r = .69). The intraobserver variability was ± 3.5%. The time necessary to acquire one EF value was 52 ± 20 sec.

We conclude that the CM is a simple and comparatively inexpensive addition to an Anger Camera which provides valid EF results at EQ. Using Bkg B, excellent interobserver agreement can be achieved with an acceptable intraobserver variability. The Cardiac Module permits easy bedside determination of serial EF in 1-2 min of EQ, promising to be most useful during interventions and stress studies.

CHARACTERISTICS OF LEFT VENTRICULAR TIME-ACTIVITY CURVES IN NORMAL VOLUNTEERS. K.H. Douglass, H.N. Wagner, Jr., P.O. Alderson, and P. Rigo. Johns Hopkins Medical Institutions, Baltimore, Md.

After equilibration of Tc-99m human serum albumin in the vascular compartment, left ventricular volume curves were obtained in 21 normal male volunteers ($\bar{x}$ age 28, range 18-50). Supine rest-exercise studies were obtained in 10 of the subjects. ECG-synchronized data were acquired by a scintillation camera-computer system at 64 intervals during the cardiac cycle. The 40° LAO image was used to generate a background subtracted LV time-activity curve. LV function indices derived from the curves included ejection fraction (EF), peak rates of ventricular ejection and filling, and systolic and diastolic time intervals (pre-ejection period-PEP, LV emptying time-LVET, LV fast filling time $LVFT_1$, and LV slow filling time-$LVFT_2$). The mean observed EF was 0.55 (± 0.10 SD) at rest (heart rate 66± 10), and 0.65 (± 0.13) during supine exercise (heart rate 125± 14). During exercise the duration of LVET in msec decreased minimally and all other indices shortened significantly. Thus, the LVET/R-R increased significantly during exercise. The peak rate of ejection (normalized to end-diastolic volume) increased from 2.49 ± .55 at rest to 4.79 ± 1.4 during exercise ($p < 0.01$). There was no significant change in the LV filling rate with exercise. At rest the peak filling rate exceeded the ejection rate in 14 of 18 subjects, but was less than or equal to the ejection rate in 6 of 10 during exercise ($p < .01$). Three of the ten volunteers who exercised did not increase EF with stress, but did show normal increases in the peak LV ejection rate. The peak LV ejection rate is a sensitive indicator of a normal response to exercise.

IMPROVED HIGH FRAMING RATE TIME-ACTIVITY CURVES IN FIRST TRANSIT CARDIAC STUDIES: ADVANTAGES OF A BILATERAL COLLIMATOR. E. Byrom and D.G. Pavel. University of Illinois Medical Center, Chicago, IL.

Computer analysis of radionuclide first transit studies, for ejection fraction and wall motion, is based on left ventricular (LV) time-activity curves generated at high framing rates (50 ms or less per frame). At the count rates of 300-600 counts/50 ms routinely obtained on our system (Searle LFOV camera interfaced to an Informatek computer) the statistical fluctuations are quite evident in the activity curves, especially at framing rates below 50 msec. Fitting and smoothing procedures are limited in their ability to recover accurately the essential features of the curve. In particular, the maxima and minima used in the construction of a composite cardiac cycle must be reviewed by the operator since extraneous peaks may remain in the curve and some cycles are too poorly fitted to be used.

Significant increases in the count rate have been obtained by using a bilateral collimator (Cardiac Medical Systems). Two views (30 RAO and 30 LAO) are obtained simultaneously and thus two ROIs can be used, simultaneously for the generation of LV time-activity curves, essentially doubling the count rate. The main advantages of the improved statistics are: 1) the curves include fewer extraneous maxima and minima, reducing the need for operator intervention; 2) more cardiac cycles can confidently and rapidly be selected for the composite cycle; 3) for a given study, the temporal resolution may be increased (e.g. from 50 ms to 20 ms).

ANALYSIS OF RADIOCARDIOGRAPHIC DATA BY VARIABLE VOLUME (PULSATILE) MODELS OF THE CENTRAL CIRCULATION: A PRELIMINARY REPORT. Jordan L. Spencer, Alba Regina, Marvin I. Friedman, Arun V. Prabhu, and Richard N. Pierson, Jr. Columbia University and St. Luke's Hospital Center, NYC, NY.

First pass time activity curves (TAC) inherently contain data which relate to volumes and ejection fractions of all cardiac chambers and lung, and which can define shunts and valvular insufficiencies. To accomplish these measurements, "background" counts not actually arising in a given chamber must be accurately stripped from measured TAC. Previous efforts in this laboratory have used continuous flow models to analyze these data, with substantial although incomplete success. We have recently applied variable volume models to analysis of radiocardiographic data, to focus on ejection fraction in addition to other volumes and flows.

First pass radiocardiographic data were taken on an Anger camera/mini-computer system, and processed to generate five region-of-interest TAC sampled for 40 msec intervals. The pulsatile model is synchronized with the EKG signal, and incorporates a dead-time correction. Model parameters include volumes of constant volume pools (lung and atria), ventricular volumes with ejection fractions, and crosstalk coefficients. The parameters are determined by using general nonlinear regression programs which iterate for simultaneous weighted least-squares fit for several region-of-interest TAC. In 15 patients studied at cardiac catheterization, the results of model-based analysis are compared with indicator dilution and angiographic measurements.

Initial results show that even relatively simple pulsatile models are able to fit data from both normal and abnormal subjects, and that simultaneous estimation of pool volumes, ejection fractions, and crosstalk coefficients is possible using programs that require minimal operator intervention. In certain cases the parameters are not well determined, and the possibility of non-unique solutions has to be considered from both mathematical and physical perspectives.

RADIONUCLIDE EJECTION FRACTION: PREDICTION OF ADRIAMYCIN CARDIOTOXICITY. J.L. Ritchie, S.G. Sorensen, K.A. Narahara, J.W. Singer, and G.W. Hamilton. Veterans Administration Hospital, Seattle, WA.

Adriamycin, an effective antineoplastic agent, produces severe and often fatal cardiac toxicity in some patients (pts) at high doses. Clinical prediction of toxicity has been unsuccessful.

Fifteen pts receiving Adriamycin had serial measurement of radionuclide ejection fraction (EF) (21 determinations) at monthly intervals, prior to each Adriamycin dose. The reproducibility of the radionuclide EF technique has been established in 10 other pts with repeat studies on day-1 and day-2 (r=.95). Cumulative dose of Adriamycin correlated with reduced EF (r=.70; p<.001). All 4 pts with cumulative Adriamycin dosage of >500 mg/M^2 had EF below .50 (range .19-.42; normal EF is >.5). EF improved in 3 pts 14-24 weeks after termination of Adriamycin therapy (EF on Adriamycin=.32±.08; EF after Adriamycin=.54±.11; p=.01). Eight pts were studied serially before and 5 min, 1 hr, 4 hrs, and 24 hrs following acute Adriamycin administration. Three showed depression of EF at 24 hrs (basal EF .60±.09; 24 hr EF .39±.24; p=.1); one of these was studied at 72 hrs and showed complete recovery (basal EF .50, 24 hr EF .12, 72 hr EF .65). One pt, whose EF had fallen from .57 to .28, with cumulative Adriamycin dosage of 550 mg/M^2, developed fatal CHF. Adriamycin cardiomyopathy was documented at autopsy.

We conclude that: 1) EF correlates inversely with cumulative Adriamycin dose; 2) a chronically reduced EF may partially recover; 3) acute toxicity is maximal at 24 hrs; and 4) serial acute and chronic EF determinations may predict the onset of Adriamycin cardiotoxicity.

TUESDAY, JUNE 27 SANTA ANA ROOM
2:00 p.m.-3:30 p.m.

BASIC SCIENCE

RADIOPHARMACEUTICALS I: MINI-SYMPOSIUM ON TRACERS FOR PHYSIOLOGIC, BIOCHEMICAL, AND DRUG STUDIES

Chairman: Michael L. Welch
Co-Chairman: Harold A. O'Brien, Jr.

PHOTOAFFINITY LABELING OF STEROID RECEPTORS. J. Katzenellenbogen, University of Illinois, Urbana, IL.

USE OF IN VITRO TESTS FOR RECEPTOR BINDING RADIOTRACERS. W.C. Eckelman, R.E. Gibson, W.J. Rzeszotarski, R.C. Reba. George Washington University Med. Ctr., Washington, D.C.

A molecule which binds to a specific cell receptor would seem to be useful as a site directed radiotracer because changes in receptor concentration or the appearance of receptors in tumors suggest a definite pathologic state. However the interaction of a compound with its receptor is the result of complicated pharmacokinetics, and therefore in vitro tests should be used to identify the factors controlling the final distribution. Using such tests, affinity constants were determined for the binding of five iodinated estrogen derivatives to the estrogen receptor and five derivatives of beta blockers for the beta adrenoceptor. The in vitro analyses of beta adrenoceptor drug binding to heart receptors (beta-1) and lung receptors (beta-2) gave cardioselectivities ranging from 5 for 4-hydroxyphenethylamino-3-(4-acetamidophenoxy)-propan-2-ol (TP) to 430 for (4-hydroxy-5-methoxy) phenethylamino-3-(m-tolyloxy)-propan-2-ol (PD3). However the reverse was true in vivo; TP had the most cardioselective distribution and the highest heart to blood ratio (∿20), whereas PD3 had the lowest cardioselectivity and heart to blood ratio. In this instance factors other than receptor binding are controlling the in vivo distribution. The in vivo assay using estrogen receptors showed that iodohexestrol and iodoethynylestradiol bound to the receptor with the highest affinity. In vivo studies confirmed these results. Iodohexestrol gave uterus to blood ratios of 10 in immature rats when plasma protein binding was blocked. Protein binding seemed to be a major factor in low target to blood ratios. In general, in vitro tests are helpful in establishing if a new derivative is a true tracer for the parent compound.

IN VIVO STUDIES OF THE HUMAN BRAIN WITH POSITRON-EMITTING RADIOPHARMACEUTICALS. M. E. Raichle, Washington University, St. Louis, MO.

TUESDAY, JUNE 27 CALIFORNIA B ROOM
2:00 p.m.-3:30 p.m.

IN VITRO AND CORRELATIVE TECHNIQUES

HEMATOLOGY I (CLINICAL SCIENCE)

Chairman: Patricia A. McIntyre
Co-Chairman: David C. Price

FACTORS INFLUENCING THE LABELING OF HUMAN PLATELETS IN PLASMA WITH IN-111. U. Scheffel and P.A. McIntyre. The Johns Hopkins Medical Institutions, Baltimore, MD.

This investigation was designed to study and optimize the factors influencing labeling of human platelets with In-111 oxine. The labeling efficiency was found to be dependent on several factors: 1) Time and temperature. 2) Platelet concentration; beyond ∿1 x 10^{10} platelets/ml there was no further significant increase in labeling. 3) A concentration of 6.25 µg oxine/ml platelet suspension maximized the efficiency of labeling. With other concentrations the percent labeling decreased rapidly. Measurement of the free and complex-bound In-111 showed that the low labeling yield below the optimum oxine concentration might be due to partial dissociation of the In-111-oxine complex. No significant elution occurred once platelets were labeled with In-111 and subsequently incubated in plasma for up to 4 hours. In contrast, ∿80% of the previously platelet-bound In-111 was released within 30 minutes when 50 µg oxine/ml was added to the plasma. This suggests that an equilibrium exists for In-111 between binding sites in platelets and oxine in the medium. 4) The effect of transferrin saturation on the labeling of platelets in the presence of plasma was studied. No consistent relationship was found. Citrate ions alone significantly lowered the percent labeling.

Using a protocol based on these findings we can label human platelets from normal donors in the presence of autologous ACD-plasma with an efficiency of 37%-50%.

SHORTENED PLATELET SURVIVAL, CIGARETTE SMOKING AND POSITIVE FAMILY HISTORY AS PREDICTORS OF CORONARY ARTERY DISEASE UNDER AGE OF 50. V. Fuster, J.H. Chesebro, H.W. Wahner, R.L. Frye, Mayo Clinic, Rochester, MN.

From January till June 1977, 35 patients (pts) under age 50 had the diagnosis of symptomatic coronary artery disease

(SCAD) confirmed at arteriography. We recorded cigarette smoking (at least 10 pack-years) in 77% of the pts, strong family history (FH) (first degree family member under age 50) in 52% of the pts, and one or the other in 93% of the pts.

Platelet deposition to the damaged endothelium appears important in the pathogenesis of atherosclerosis. Accordingly, platelet consumption, as estimated by platelet survival half life with ^{51}Cr. (PS) was measured in 25 of the pts with SCAD and in 36 apparently normal (AN) individuals under age 50. A shortened PS ($\leq$92 hours) occurred in 76% of the SCAD pts and in only 33% of the AN individuals ($p \leq 0.01$). Smoking or FH were present in 96% of the SCAD pts, in 66% of the AN individuals with a shortened PS and in only 8% of the AN with the longer PS (>92 hours) ($p < 0.01$). Lengthening of the shortened PS (79.3 hours to 90.0 hours) was obtained in 9 out of 11 SCAD pts ($p < 0.001$) by using Dipyridamole, 75 mgs combined with Aspirin, 325 mgs t.i.d. Whether such platelet inhibitors will arrest the progression of the coronary disease is under investigation.

This study of coronary disease under age of 50 indicates: 1) a striking association between smoking or FH with the development of the disease; 2) a probable role of platelets as suggested by the shortened PS; and 3) the possibility that in AN individuals the incidence of coronary disease may decrease by avoiding smoking and by using platelet inhibitors in those with FH and shortened PS.

USE OF TECHNETIUM-99m AS A RADIOISOTOPIC LABEL TO STUDY THE MIGRATORY PATTERNS OF LEUKOCYTES AND PLATELETS. T. Uchida and S. Kariyone. Fukushima Medical College, Fukushima, Japan.

The greater usefullness of Tc-99m labeled blood cells is likely to be in the study of cell migration and organ uptake using external scanning techniques. Its use in the study of neutrophil kinetics and thrombokinetics would overcome the difficulty in elucidating the sites of neutrophil margination and platelet distribution or destruction. A method labeling leukocytes and platelets in vitro is that separated cells from 200 ml of whole blood are incubated with Tc-99m, followed by reduction with stannous chloride and washing with acid citrate dextrose. After infusion of labeled cells, organ distribution was observed by scintillation camera. Organ distribution of Tc-99m labeled white cells in 10 subjects with normal and hematological diseases showed that cells were trapped into pulmonary vasculature, then released gradually to localize to spleen and liver, which suggests lungs, liver and spleen as the site of marginal neutrophil pool. In turpentine induced inflamation rats, Tc-99m labeled neutrophils accumulated into infected lesions. Tc-99m labeled lymphocytes were not trapped into lungs. In 16 studies labeled with Tc-99m and Cr-51 simultaneously, labeled platelets were sequestered or destructed into liver and spleen, and no uptake into lungs. In congestive splenomegaly, more than 90% of the labeled platelets were found to have accumulated in the spleen. Sequestration patterns by body surface counting with Cr-51 coincided with sites of sequestration observed using a scintillation camera.

IN VITRO EVALUATION OF INDIUM-111 LABELED NEUTROPHILS: MOBILITY, CHEMOTAXIS AND MICROBICIDAL ACTIVITY. M.L. Thakur, B. Zakhireh, M. Cohen, A. Gottschalk, and R. Root. Yale University School of Medicine, New Haven, CT.

In Indium-111 labeling procedure the neutrophils (PMN) are exposed to oxine, ethanol and to radiation itself. The labeled PMN have been shown to enter inflammatory sites in vivo, however their ability to respond to various stimuli has not been studied.

(PMN) were isolated from the blood of normal healthy donors, suspended in normal saline (10 million/ml) and labeled (L) with In-111-oxine at room temperature with varied concentration of In-111, ethanol or oxine. Equal numbers of PMN treated similarly but unexposed to radioactivity, ethanol or oxine served as reference (R) and untreated PMN as control (C) cells.

In vivo chemotaxis of L and R PMN measured by penetration of the leading front of a PMN population into 1.2 μ micropore filters in Boyden chambers in response to endotoxin activated serum was equivalent to that of C PMN (9 experiments). Spontaneous random migration of L, R and CPMN populations was similar in the chambers or when examined directly on coverslips by phase contrast microscopy. Activated random migration on coverslips in response to the synthetic polypeptide, N-Formyl-Met-Leu-Phe or activated serum was (a) 96.59 $\pm$ 5.25% for R and (b) 87.77 $\pm$ 4.64% for L of C PMN ($P < 0.05$). Phagocytosis and killing of Staphylococcus aureus was equal in all three cell groups.

The data indicates that although there is slight depression in activated random migration of PMN exposed to oxine, ethanol or In-111 radioactivity do not alter the spontaneous random migration and their chemotactic and microbicidial functions remain normal.

SCINTIGRAPHIC EVALUATION OF INDIUM-111 LABELED FILTRATION GRANULOCYTES. J.B. Alavi, A. Alavi, and M. Staum. Hospital of the University of Pennsylvania, Philadelphia, PA.

Transfusion of normal donor granulocytes (PMN) is now accepted as a supportive measure in the treatment of infection in granulocytopenic hosts. However, questions have been raised about the efficacy and function of such PMN. We designed a study to evaluate the in vivo distribution of PMN prepared by filtration leukapheresis (FL). The preliminary results are reported here.

An aliquot (3ml, or approximately 10^8 PMN) of the FL transfusion was labeled with 250 uCi of In-111 oxine according to the method of Thakur. The labeled cells were resuspended in saline and infused into the recipients, who were granulocytopenic patients with leukemia and infection. Scintigrams were performed at 12 to 24 hours after the transfusion.

Two patients have been studied. The first had a left lung infiltrate, found at open biopsy to be due to Aspergillus. The In-111 labeled PMN migrated to the site of infiltrate and left thoractomy. The second patient had left neck pain and erythema, and blood cultures grew Serratia. Scintigrams showed high activity at the base of the tongue and upper left neck. Distribution of labeled cells was otherwise similar in both patients, with intense activity in liver and spleen and minimal activity in the skeleton. These studies suggest that FL cells migrate to sites of inflammation. This method may be useful to detect subtle infections in granulocytopenic patients. Since FL cells are 95% PMN, these preparations should be further evaluated in white cell labeling methods.

CLINICAL USE OF INDIUM-111 OXINE LABELED LEUCOCYTES IN THE DETECTION OF INFLAMMATION OR ABSCESS. L. Forstrom, L. Gomez, B. Weiblen, D. Hoogland, J. McCullough, and M. Loken, University of Minnesota Hospitals, Minneapolis, MN 55455.

Leucocyte suspensions rich in granulocytes (≈65%) were labeled with Indium-111 oxine (In-111 WBC). Studies with this agent have been performed in 17 subjects, including 3 normal volunteers and 14 patients with clinically suspected sites of inflammation or abscess. Images were obtained at 4 and 24 hours after administration of approximately 0.5 mCi In-111 WBC (adult dose). Leucocytes (WBC) for labeling were obtained either from the patient (9 cases) or, in granulocytopenic subjects, from compatible donors (5). Donor WBC were prepared by the standard method, or obtained by leukapheresis. Granulocyte labeling efficiency (50-60%) was not significantly different between these methods of WBC preparation. Neither did method of WBC preparation noticeably affect the in-vivo distribution of In-111 WBC, except for early increase in lung activity seen with the use of donor WBC. This activity normally cleared by 24 hours. Persistent increase in lung activity was observed in a patient with pneumonitis documented by biopsy. Ten male and 4 female patients have been studied, ranging in age from 3 to 69 years. Six patients had had recent abdominal surgery. In these, wound uptake of In-111 WBC was observed only in the presence of infection. There were 6 sites in which acute inflammation was diagnosed, most (5) confirmed by pathologic examination, with abscess present in 2. All 6 showed (+) uptake of In-111 WBC, generally

een best at 24 hours. There were no definite false (+) tudies. Our results confirm the usefulness of In-111 WBC n the detection of inflammation or abscess. Moreover, we ave shown that when necessary donor WBC can be safely and ffectively used in such studies.

NDIUM-111 OXINE GRANULOCYTE LABELING: A MODIFIED METHOD ESULTING IN AN IMPROVED GRANULOCYTE FUNCTION. Syed S.H. ilani, Vincent Salvatori and Donald J. Higby. Roswell ark Memorial Institute, Buffalo, N.Y.

Granulocyte transfusions used adjunctively in the managment of infected, neutropenic cancer patients have improved survival and morbidity. Several methods of procuring granulocytes exist, and there is question as to which esults in the best product for clinical use. To study in itro function, Thakur developed an intracellular label sing Indium-111 oxine. We have developed two modifications of his technique. a) In Thakur's method, chloroform s used to dissolve the oxine complex; this requires evapration of the solvent on steam bath, posing the theoretial risk of phosgene formation. Using methylene chloride s a solvent, the evaporation phase can be done at room emperature using nitrogen. With this modification, we chieved a > 90% efficiency of complex formation, and it is table at room temperature for thirty days. b) In Thakur's ethod, the Indium oxine complex is dissolved in ethyl lcohol. With his method, while nitroblue tetrazolium reuction (unstimulated and stimulated with TPA) and granuloyte adhesion were normal, chemotaxis was not demonstratale. When we used propylene glycol as the solvent, chemoaxis and other functions were normal. These modifications esult in a simpler and mild procedure which results in ore functional granulocytes for study. Care should be aken to assure that labelled granulocytes are fully unctional in vitro before concluding that they will behave imilarly to normal granulocytes in vivo.

UESDAY, JUNE 27 CALIFORNIA A ROOM
:00 p.m.-3:30 p.m.

CLINICAL PRACTICE

NEUROLOGY

Chairman: Norman R. Vincent
Co-Chairman: Sheldon Baum

UCLEAR CEREBRAL ANGIOGRAPHY. J. F. Rockett, Baptist Memrial Hospital, Memphis, TN.

AROTID RADIOANGIOGRAPHY. J. F. Rockett, Baptist Memorial ospital, Memphis, TN.

ADIONUCLIDE ANGIOGRAPHY IN THERAPY: REDUCING ARTERIAL SUPLY TO BRAIN TUMORS BY GELFOAM EMBOLISM. S. Baum, Milton . Hershey Medical Center, Hershey, PA.

HE OPTIMAL PHARMACEUTICAL FOR BRAIN IMAGING. M.R. etalman, A.H. Deutchman, J. Scheu, J. Olsen, and J.Chiles. he Ohio State University Hospital, Columbus, OH.

A study was undertaken to compare the sensitivity of rain imaging agents: NaTc-99mO4, Tc-99m glucoheptonate, nd Tc-99m DTPA. The following image pairing was made: lucoheptonate and DTPA (312 patients); DTPA and pertechneate (361 patients); glucoheptonate and pertechnetate (289 atients). Both images for each patient were obtained with-n 48 hours using the same imaging system and the same maging time post injection (60-90 minutes) in all cases. Only those patients who had images documented as positive either by CT, arteriography, or surgery were intercompared in the final analysis. They were as follows: glucoheptonate and DTPA - 13 patients; DTPA and Tc-99mO4 - 14 patients; glucoheptonate and Tc-99mO4 - 12 patients. With the exception of one primary brain tumor, the lesions were metastases - either single or multiple (30 patients) - or CVA (8 patients). All 78 images were read independently by six nuclear medicine physicians who were asked to determine only whether each image was normal or abnormal. The comparisons were made by tabulating the number of false negatives reported using each of the three agents. The sensitivity for lesion detectability for Tc-99mO4 was 74.4%, glucoheptonate - 80.7%, and DTPA - 94.4%. While others have stated that glucoheptonate may be the agent of choice because of active incorporation into a lesion over a 4 to 6 hour period, in our study DTPA proved to be the most sensitive for lesion detection at 1 to 1½ hours post injection.

EVALUATION OF THE EARLY Tc-99m GLUCOHEPTONATE BRAIN SCAN. D.T. Tanasescu, R.S. Wolfstein, M.B. Brachman, A.D. Waxman. Cedars-Sinai Medical Center, Los Angeles, Ca

The purpose of this study was to evaluate the sensitivity of the early brain scan using Tc-99m glucoheptonate (TcGH), and to determine when the early brain scans are indicated as a complement to, or replacement of the delayed study.

15 mCi TcGH brain scans were obtained immediately following a flow study and repeated at 2-4 hours. Comparisons were then made between the early and delayed static images, using the lesion to calvarial ratio as well as size, as a criteria of abnormality. Documentation was by surgery, angiography, autopsy, or clinical followup.

859 patients with 927 studies were evaluated. 100 patients were not documented, and were excluded from this study. 123 patients were found to have 126 detectable lesions. 634 patients had negative brain scans. Our data showed the early TcGH brain scan to be negative, and the delayed scan positive in 29% of the demonstrated lesions. 41% showed the delayed scan to be superior. In 6% the early study was superior to delayed scan. This group contained only 1 case with a true CNS abnormality (AVM).

In lesions of the posterior fossa or near major vascular areas, the blood pool scan appeared to help in differentiating normal anatomic structures from true lesions. If an AVM or venous malformation is suspected, or if an abnormality detected on the delayed scan is in close proximity to a normal vascular structure, a repeat blood pool study can be done immediately following the delayed scans.

The results suggest that routine early brain scans are inferior to delayed scans in the evaluation of most central nervous system lesions. However, both studies when used serially may be helpful in differentiating skull or scalp abnormalities from true lesions of the brain.

RADIONUCLIDE CEREBRAL PERFUSION SCINTIPHOTOGRAPHY IN THE DIFFERENTIAL DIAGNOSIS OF INTRACRANIAL NEOPLASMS. S.Q. Liao, W.J. Hu, M.K. Chang and S.D.J. Yeh. Tri-service General Hospital and Naval General Hospital, Taiwan.

210 histologically proved cases with various brain tumors were evaluated. The anterior or posterior dynamic study was performed after i.v. injection of a bolus containing 10 mCi of radiopertechnetate with two seconds per frame for 8 frames begining at the visualization of the neck arteries. Static study of the same view was obtained within 5 minutes. Another static study of conventional 4 views was taken within ½-2 hrs. The dynamic scintiphotos were classified into 4 phases and static studies as phase V and VI. The activity in the lesions was graded into 6 grades (-, N and 1-4+).

Most cases of meningioma have grade N in phase I, 2-3+ in phase II and higher grade thereafter. The hemangiomas are similar to the meningiomas. The glioblastomas show mostly grade N in phases I-II, gradually build up to 2-3+ in phases III-IV and to 3-4+ in phases V-VI. The astrocytomas and metastatic tumors have grade N throughout the phases I-IV, N-2+ in phase V and 2-4+

in phase VI. The neurinomas are similar to astrocytomas but build up a higher grade in phases V and VI. A-V malformation have grade N-3+ in phase I, 3-4+ in phase II and washout to N-2+ in phases III-IV, N-4+ in phases V-VI. Other tumors of lower incidence have the tendency similar to astrocytomas.

This method would be very useful in the differential diagnosis of brain tumors especially in those institutions without a minicomputer and the diagnosis is dependent on visual interpretation of the scintiphotos.

TUESDAY, JUNE 27 GARDEN GROVE ROOM
4:00 p.m.-5:30 p.m.

CONTINUING EDUCATION

CARDIOVASCULAR NUCLEAR MEDICINE: MYOCARDIAL PERFORMANCE AND PERFUSION, PERIPHERAL VASCULAR DISEASE

PARTICIPANTS: William L. Ashburn, Chairman, University of California, San Diego, CA, and Glen W. Hamilton, Co-Chairman, V.A. Hospital, Seattle, WA.

TUESDAY, JUNE 27 ANAHEIM ROOM
4:00 p.m.-5:30 p.m.

CLINICAL SCIENCE

PULMONARY I

Chairman: Merle K. Loken
Co-Chairman: Max S. Lin

DIAGNOSTIC ACCURACY OF PULMONARY IMAGING WITH INHALED ^{15}O-CARBON DIOXIDE FOR DETECTION OF PULMONARY EMBOLI. A.B. Nichols, S. Cochavi, C.A. Hales, K.A. McKusick, G.A. Beller, A.C. Waltman, and H.W. Strauss. Massachusetts General Hospital, Boston, MA.

We investigated the clinical utility and diagnostic accuracy of positron imaging of inhaled $C^{15}O_2$ for the detection of pulmonary emboli (PE) in 30 patients with suspected PE. Following pulmonary arteriography, each patient underwent serial imaging with a multicrystal positron camera after single breath inhalation of 2 mCi $C^{15}O_2$ (T 1/2=2min). Inhaled $C^{15}O_2$ rapidly labels pulmonary capillary blood and is cleared from the lungs at a rate proportional to regional pulmonary blood flow. For patients with arteriographically documented PE, clearance of ^{15}O activity was markedly delayed over embolized pulmonary segments (mean halftime 47.0 sec $\pm$ 11.3 SEM), *in comparison to normal segments* (mean 3.6 sec $\pm$ 0.1 SEM; $p < 0.001$). "Hot spots" of ^{15}O activity were present on positron imaging, correctly identifying the site and magnitude of emboli for 12 of 14 patients with documented PE (sensitivity=85.7%). Among 16 patients with pulmonary disorders or heart failure without PE, only one patient displayed a hot spot (specificity =93.7%). These data validate the sensitivity and specificity of $C^{15}O_2$ imaging for the detection of PE in patients with underlying pulmonary disease or congestive heart failure. Since $C^{15}O_2$ imaging is rapidly performed with minimal radiation exposure to the patient, it can be repeated at short intervals for following the resolution of PE and for analyzing persisting perfusion in embolized segments.

* * *

The following four papers constitute a Rapporteur Session. Rapporteur for this group is Merle K. Loken, University of Minnesota, Minneapolis, MN.

POSTURAL CHANGES IN REGIONAL FUNCTIONAL RESIDUAL CAPACITY (FRC) DEMONSTRATED BY Xe-133. K.F. Witztum, H.G. Greditzer, J.W. Fletcher, M.F. Feldman, R.M. Donati, G.F. Dolan and V.-D. Minh. St. Louis VA Hospital and St. Louis University School of Medicine, St. Louis, MO.

Change from upright to supine position results in a decrease in FRC. Understanding the relative contribution of regional lung units, from apex to base, to this change would be helpful in determining why basal regional lung units develop atelectasis in the supine position, and in predicting the distribution of ventilation that might be achieved by rocking bed therapy in paralyzed patients. Postural changes in regional FRC were evaluated in 9 normal human volunteers. Upright and supine posterior images of the lungs were obtained by a gamma camera at total lung capacity after the inhalation of Xe-133 gas (10 mCi/L), at equilibrium and after dilution with room air (Sutherland, P.W., J. Appl. Physiol. 25:566, 1968). Images stored in a minicomputer were divided into 7 consecutive equal-length zones from apex to base, and the radioactivity in each zone determined as a measure of regional FRC. All values were expressed as % of regional total lung capacity. Differences in upright and supine regional FRC were reported as change in regional FRC. Results indicate that all regional lung units from apex to base contribute to the postural change in FRC, but the greatest relative change occurs at the apex. Since the basal regional lung units have the smallest volume in the supine position, these findings provide an explanation for the tendency for basal atelectasis to develop in this position. The data further suggests that rocking bed ventilation therapy, based on cyclic postural changes in FRC, would preferentially ventilate the apical regional lung units.

DETECTION OF CHRONIC OBSTRUCTIVE PULMONARY DISEASE (COPD) WITH FUNCTIONAL VENTILATION IMAGES. L.E. Williams, M.K. Loken, R.A. Ponto, and R.S. Kronenberg. Nuclear Medicine Clinic, University of Minnesota Hospitals, Minneapolis, MN.

A fundamental tenent of Nuclear Medicine is that quantitative imaging permits specific disease diagnosis. Here, the Nuclear Medical practitioner has to demonstrate at least the dichotomy between normal and abnormal states of a patient population. We report here the use of regional ventilation indices to separate old normals from chronic obstructive pulmonary disease (COPD) patients of the same approximate age group. The populations studied included 23 young normals (22-28 years) 25 older normals (63-77 years) and 10 clinically diagnosed COPD patients (46-65 years). All subjects were imaged in the posterior projection using a gamma camera and inhalation of approximately 20 mCi of Xenon-133. Scintillation events were stored on magnetic tape with CDC 3300 computer processing. Regional ventilation (V) and clearance (K) indices were determined for 18 regions per lung with nine slices from apex to base. Following MacIntyre and Wagner, we consider the spatial distribution of either parameter a ventilation functional image. We have found that the frequency distributions of V or K are gaussian curves for the two normal classes. The COPD patients, however, were distinctive in that each patient had at least two regions where indices were more than four standard deviations away from the regional mean. All old normals had every regional index within three σ of the local mean. This last result was predictable from the old normal gaussian distributions. Thus, the functional ventilation images were able to distinguish all of the COPD patients with no false positives being selected from the old normal class.

CORRELATION OF PULMONARY FUNCTION ABNORMALITIES SUGGESTING SMALL AIRWAY DYSFUNCTION WITH XENON WASHOUT CURVES. R. Rosenberg, S. Dhand, B. Shon and L.S. Malmud. Temple University Hospital, Philadelphia, PA.

Pulmonary function tests for the detection of small airway dysfunction were performed in 18 smoking and 16 non-smoking young adults, with forced expiratory volume in one second expressed as a percent of forced vital capacity greater than 75 per cent. Half of the smokers were asymptomatic. A computer modulated quantitative xenon ventilation study was performed within one day of the pulmonary function tests. Xenon washout curves were generated for each lung as well as for three vertical zones in each lung. The xenon washout constant, K, ($\ln 2/T_{\frac{1}{2}}$) was calculated for each curve. Volume of isoflow and slope of Phase III of the curves were the most frequently abnormal (67 per cent and 47 percent respectively) pulmonary function tests in smoking subjects. Washout constant, K, from the lower lung zones and the ratio of K of the upper and lower lung zones were the commonest (60 per cent and 50 per cent respectively) xenon washout abnormalities in smokers. When xenon washout was abnormal, one or more of the pulmonary functions was abnormal 93 per cent of the time, and, conversely, an abnormal pulmonary function was associated with an abnormal xenon washout 88 per cent of the times.

Xenon ventilation scanning with calculation of the washout constant is a sensitive method of detecting small airway dysfunction, correlates well with pulmonary function studies, is a more sensitive indicator of early small airway disease than is any other single pulmonary function test, and has the additional advantage of being able to localize airway abnormalities.

COMPARISON OF Xe-127 AND Xe-133 IN VENTILATION-PERFUSION IMAGING IN DIAGNOSIS OF PULMONARY EMBOLUS. W.H. McCartney, J. R. Perry, E. V. Staab, and L. A. Parker. University of North Carolina at Chapel Hill.

Ventilation-perfusion lung scans were correlated with pulmonary angiograms to compare the efficacies of Xe-133 and Xe-127 in the diagnosis of pulmonary embolus (PE). Xe-133 ventilation studies were performed prior to perfusion, whereas Xe-127 studies were performed after selection of the optimum viewing angle(s) from the perfusion scan. All ventilation studies had washin, equilibrium and washout phases. The studies were interpreted as high probability (at least 50% chance), low probability or indeterminate for PE according to a system similar to that of McNeil. Correlation with the angiograms showed accuracies for Xe-133 of 77% for high probability and 91% for low probability. Correlations for Xe-127 were 100% for high probability and 100% for low probability. These initial results suggest an improved specificity with Xe-127 in perfusion-ventilation imaging for PE.

* * *

GAMMA CAMERA IMAGING OF CLOSING PHENOMENON IN THE LUNG. Y. Ishii, T. Suzuki, H. Itoh, Y. Yonekura, D. Hamanaka, K. Torizuka, and T.Fujita. Kyoto University Medical school, Kyoto, Japan.

We attempted to visualize closing phenomenon, a sensitive expression of early changes of the small airway, using radioactive gas and gamma camera, and compared it with the conventional resident gas method. 20 normals comprising smokers and non-smokers were studied. A bolus of Kr-81m or Xe-133 gas was inhaled at the reserve volume with the subsequent slow maximum inspiration, and the inhaled image was recorded by the gamma camera. This image was compared with the image of equilibrated distribution of Xe-133 gas within a closed circuit or with the rebreathing distribution of Kr-81m gas. In the smokers, closing phenomenon was observed as inspiratory defect at the dependent lower lung region with a horizontal demarcation clearly seen in lateral view using Kr-81m gas. The level of this boundary from the apex was well correlated with the closing capacity measured by the resident gas method ($r=-0.897$, $p<0.005$). In 6 cases using Xe-133 gas, the radioactivity value was converted into volume value to calculate closing capacity, and this estimated value was better correlated with the closing capacity by the resident gas method ($r=0.947$, $p<0.005$). Concerning the quantitative evaluation in the term of volume, Xe-133 gas is superior to Kr-81m with ultra-short half life. However, the latter can provide repeatable test for this phenomenon.

EVALUATION OF AERODYNAMIC CHANGE IN THE AIRWAY OF PATIENTS WITH CHRONIC OBSTRUCTIVE PULMONARY DISEASE USING RADIOAEROSOL SCINTIGRAPHY. T. Suzuki, Y. Ishii, H. Itoh, Y. Yonekura, D. Hamanaka, and K. Torizuka. Kyoto University Medical School, Kyoto, Japan.

In the chronic obstructive pulmonary disease (COPD), radioaerosol inhalation scintigraphy reveals "hot spot" formation in the central airway. We established 4 grades for this findings according to the extent of peripheral irregularity and hot spot formation, which were well correlated with FEV1.0 and respiratory resistance by the oscillation method (Rp). Hence, these abnormal findings were sensitive regional expressions of airway narrowing or obstruction in the central airway. To elucidate these findings on the basis of the aerodynamic change in the airway, flow and volume patterns at the mouth during the aerosol inhalation were monitored to be analyzed. In the case of COPD, increased flow rate followed by diminished flow rate in prolonged expiratory phase was evident, which suggests expiratory failure due to the obstruction with compensational increase of inspiratory flow. Indices for this phenomenon in 25 patients with various stages of COPD were well correlated with the grading as well as FEV1.0 and Rp. It is concluded that these abnormal scintigraphic findings were probably due to the fact of enhanced inspiratory turbulancy at the central airway, which was compensational phenomenon of the expiratory failure of the COPD.

GENERATION OF MONODISPERSED RADIOAEROSOL FOR SCINTILLATION IMAGING. H. Ito, G.C.Smaldone, R.S. Florek, W.H. Wells, D. L. Swift, H.N. Wagner, Jr. The Johns Hopkins Medical Institutions, Baltimore, MD.

Although an ultrasonic generator is the most popular radioaerosol generator in nuclear medicine, the non-uniformity in size of the particles generated makes it difficult to analyze deposition patterns in the lung; since particle behavior is often dependent on size. The purpose of this study was to produce uniform radioaerosol for scintillation imaging. A well established condensation technique was used for this.

Di-2-ethylhexyl sebacate which is non-volatile at body temperature was heated and its vapor mixed with technetium-99m labelled human serum albumin (99m-Tc-HSA) produced in an ultrasonic nebulizer. While passing through a condensation chimney sebacate vapor condensed on 99m-Tc-HSA aerosol, forming radioactive sebacate aerosol. The particle size was determined by several techniques; cascade impactor, Schaefer sedimentation cell and light scattering. There was good agreement between these methods. The size distributions were sensitive to gas flow and temperature, and 1 to 2 micron aerosols with geometric standard deviations of 1.1-1.2 were obtained by adjusting these variables. The aerosol contained less than 2% particles larger than 4

micron. Thus the size distributions were far superior to those produced with usual ultrasonic generator.

Lung images obtained in atropinized intact dogs remained stable for several hours. This modified condensation generator produced monodispersed radioaerosol and worked in a stable condition until the HSA sourse was exhausted(~1 h). In addition, the aerosol can easily be generated in different carrier gas such as helium.

EFFECT OF CARRIER GAS ON THE DISTRIBUTION OF INHALED AEROSOLS. H. Ito, G.C. Smaldone, D.L. Swift, D.F. Proctor, K.H. Douglass, P.O. Alderson, H.N. Wagner, Jr. The Johns Hopkins Medical Institutions, Baltimore, MD.

The purpose of this study was to prove that increased aerosol deposition in post-stenotic areas was directly related to local turbulent flow.

Evans blue aerosols, (mass median diameter = 1 micron), were produced from an atomizer using either air, helium or 80% sulfur hexafluoride (SF_6). The aerosol carried by each individual gas was delivered at a constant flow. The dye deposited on the walls of the tube was dissolved in distilled water at one centimeter intervals and its concentration was determined by photometric methods. The greatest deposition was observed with SF_6-carried aerosol, decreasing with air and helium-carried aerosols, respectively. Pressure differences measured across the constriction at a fixed flow rate also decreased in the same manner (SF_6 > air > helium). This clear-cut gas density dependence of the aerosol deposition and pressure-flow relation suggested strongly that the aerosol deposition was created by turbulent flow.

After clamping a dog's trachea, technetium-99m labeled human serum albumin aerosols carried by air or 80% helium + 20% oxygen were delivered to the trachea using an ultrasonic generator. The radioaerosol deposition in the trachea was much less with helium-carried aerosol. Thus, aerosol deposition in post-stenotic areas was dependent on the density of the carrier gas, suggesting strongly that it was created by turbulent flow. This also suggests that penetration of aerosols used in clinical imaging studies will be improved by using helium gas as the carrier.

INTERCOMPARISON OF INHALATION LUNG IMAGES WITH RADIOACTIVE XENON,KRYPTON AND AEROSOLS. S.K.Chopra,G.V.Taplin and D.Elam.UCLA,School of Medicine,Los Angeles,California.

The main purpose of this study was to determine the practical diagnostic merits and limitations of Xenon-133 (Xe),Krypton-81m(Kr) gases and aerosol(Tc-99m)inhalation lung imaging procedures in revealing regional airways and ventilatory abnormalities.200 pulmonary embolism(PE)suspects underwent ventilation(V) and perfusion(P)imaging procedures. Approximately the same number had perfusion examinations only,plus chest roentgenography.The diagnosis of PE was excluded by either a normal perfusion image or the imaging findings correlated with radiographic abnormalities.Imaging with Kr and aerosols of Tc-S colloid, TcO_4 or Tc-DTPA was performed in multiple projections immediately following the perfusion examination whereas Xe rebreathing and washout procedures were done before or 24 hours later. Thirty-one patients had Xe,118 Tc aerosols and 56 had Kr procedures. A scintigraphic diagnosis of PE(V/P mismatching)was made in 10,19 and 22% of the cases examined with Xe,Kr and radioaerosol inhalation procedures,respectively.Small ventilation defects were better visualized in 190 KeV Kr and 140 KeV-Tc aerosol than in 80 KeV Xe images. It was concluded that the Kr continuous inhalation procedure is ideal in PE suspects for obtaining directly comparable pairs of V/P images with minimal patient cooperation.However,Rubidium-Krypton generators are not commercially available.Therefore from a practical standpoint, aerosol imaging with the same energy radioindicator(140 KeV Tc-99m S.colloid or DTPA)immediately following a perfusion examination with Tc-MAA is considered the ventilation procedure of choice.The aerosol and perfusion lung images provide strong evidence of PE,obstructive airway disease or the coexistence of both.

A WIDELY APPLICABLE PERFUSION-RADIOAEROSOL INHALATION PROCEDURE IN DIAGNOSING PULMONARY EMBOLISM.G.V.Taplin, L.Feigenbaum,S.K.Chopra and D.Elam.UCLA School of Medicine, Los Angeles, California

This study of 311 pulmonary embolism(PE)suspects was made to determine the specific advantages of performing a Tc-99m DTPA radioaerosol lung imaging procedure(V)immediately after a Tc-99m MAA perfusion(P)examination.Multiple view perfusion images were obtained after injecting a 1.0 mCi dose of MAA.When perfusion abnormalities were found, DTPA radioaerosol administration was begun.Aerosol inhalation was continued until a count rate equivalent to that obtained with 3.0mCi of Tc-MAA was registered.Aerosol images were obtained only in the projections showing perfusion abnormalities.In most patients the combined procedure could be completed in approximately one hour.Perfusion examinations alone were done in 138;P/V studies with MAA and DTPA aerosol were made in 168.Forty-seven of these 168 showed distinctly mismatching lesions indicative of PE, whereas 126 patients had matching P/V defects and/or strong aerosol image evidence of obstructive airway disease(OAD). Sixty percent of patients studied had roentgenographic abnormalities and matching P/V images.Chest x-ray,P/V images and angiographic correlation was possible in 21. Three had moderate probability of PE by nuclear imaging. Of the remaining 18,nine had high probability of PE by imaging and 8 of these had positive angiograms.Of the 9 patients with low probability of PE, the angiogram was positive in only one.In conclusion,the new P/V procedure has many advantages over Xenon methods and can provide a highly accurate diagnosis of PE,OAD or the coexistence of both disorders following a single one hour examination.The aerosol administration system is inexpensive,disposable and can be assembled easily in nuclear medicine clinics.

TUESDAY, JUNE 27 — SANTA ANA ROOM
4:00 p.m.-5:30 p.m.

BASIC SCIENCE

RADIOPHARMACEUTICALS II: MINI-SYMPOSIUM ON TRACERS FOR PHYSIOLOGIC, BIOCHEMICAL, AND DRUG STUDIES (continued)

Chairman: William C. Eckelman
Co-Chairman: Kenneth A. Krohn

THE SYNTHESIS OF 1-C-11-2-DEOXY-D-GLUCOSE (C-11-2-DG) FOR MEASURING REGIONAL BRAIN GLUCOSE METABOLISM IN VIVO. C. Y. Shiue, R. R. MacGregor, R. E. Lade, C. N. Wan and A. P. Wolf. Brookhaven National Laboratory, Upton, N.Y.

The use of C-14-deoxyglucose and autoradiography to determine regional glucose metabolism in animals has become a widely employed technique. Recently this method has been extended to study in humans by utilizing a positron-emitting deoxyglucose analog, F-18-2-deoxy-2-fluoro-D-glucose, and positron emission tomography. In order to lower the radiation dose to the patient and to allow rapid serial studies of regional brain glucose metabolism, C-11-2-DG was synthesized from the labeled precursor C-11-NaCN.

C-11-2-DG was synthesized from D-(-)-arabinose (1) in 7 steps. Thioacetalation of (1) with ethanethiol gave D-arabinose diethyl dithioacetal (2) in 72% yield. Treatment of (2) with acetone in dil. HCl gave 2,3:4,5-di-O-isopropylidene-D-arabinose diethyl dithioacetal (3) in 85% yield. Hydrolysis of (3) with mercuric oxide and mercuric chloride gave 2,3:4,5-di-O-isopropylidenealdehydro-D-arabinose (4) in 65% yield. Reduction of (4) with lithium aluminum hydride gave 2,3:4,5-di-O-isopropylidene-D-arabinitol (5) in 99% yield. Reaction of (5) with trifluoromethanesulfonyl anhydride gave 1-O-trifluoromethanesulfonyl-2-3:4,5-di-O-isopropylidene-D-arabinitol (6). Reaction of (6) with NaI

gave 1-deoxy-1-iodo-2,3:4,5-di-O-isopropylidene-D-arabinitol (7) in 85% yield. Treatment of either (6) or (7) with C-11-NaCN in DMF gave 1-deoxy-1-cyano[C-11]-2,3:4,5-di-O-isopropylidene-D-arabinitol (8) in 50% yield. Reduction of (8) with Raney alloy or di-isobutylaluminum hydride followed by hydrolysis gave C-11-2-DG in 50% yield. (Research carried out at BNL under contract with the U.S. DOE and supported by NIH Grants No. 3 P41-BE00657-0351 and 5-RO1-GM16248).

F-18 DEOXYGLUCOSE AND C-11 PALMITIC ACID FOR THE TOMOGRAPHIC MEASURE OF MYOCARDIAL GLUCOSE AND FREE FATTY ACID METABOLIC RATE. M.E. Phelps, E.J. Hoffman, H.R. Schelbert, C. Selin, S.C. Huang, G. Robinson, N.S. MacDonald, D.E. Kuhl. UCLA School of Medicine, Los Angeles, California.

Emission computed tomography (ECT) was used to investigate use of F-18 deoxyglucose (FDG) and C-11 palmitic acid (PA) for regional measure of myocardial metabolic rate for glucose (MMRGlu) and free fatty acids (MMRFFA). The ECAT positron tomograph was used to measure uptake, tissue clearance rates, species dependence (dog, monkey, man) and effect of diet. In vitro studies were performed to measure blood clearance rates. Normal myocardial FDG uptake was 3 to 4% in dog and monkey and 1 to 4% of injected dose in man. MMRGlu in non fasting (glycolytic) state was 2.8 times that of fasting (ketogenic) state. Human subjects showed higher myocardial FDG uptake after normal meal than meal of mostly PA. FDG blood clearance rate was rapid with initial $t_{1/2}$ (82%) of 0.2 to 0.3 min followed by a $t_{1/2}$ (10%) of 8.4 ± 1.2 min in dog and 11.6 ± 1.1 min in man. A third component (8%) had a $t_{1/2}$ of 59 ± 10 min and 88 ± 4 min in dog and man, respectively. PA showed a clearance $t_{1/2}$ of 2.5 min in dog. High image contrast ratios between heart and blood (dog 1.5/1; man 14/1), heart and lung (dog 9/1; man 20/1), heart and liver (dog 15/1; man 10/1) were found with ECAT tomograph. FDG taken up by myocardium showed no significant clearance in 4 hrs and model used to calculate MMRGlu was accurate to ± 6% for time period of 0.5 to 4 hrs. PA has a myocardial clearance $t_{1/2}$ of 290 min. Determination of MMRGlu and MMRFFA in vivo and non invasively with ECT provides a method for investigation and assessment of changing aerobic and anaerobic metabolic rates in ischemic heart disease in man. Supported in part by DOE contract #EY-76-C-03-0012 and NIH grant GM-24839-01.

APPROACHES IN THE DESIGN OF TISSUE BINDING STRUCTURES. J. H. Soloway, Ohio State University, Columbus, OH.

RADIOLABELED ENZYME INHIBITORS - ENHANCED LOCALIZATION FOLLOWING ENANTIOMERIC PURIFICATION. J.L. Wu, D.M. Weland, W.H. Beierwaltes, D.P. Swanson, L.E. Brown. University of Michigan Medical Center, Ann Arbor, MI.

Dog adrenals have recently been imaged with I-123-(±)-(3-iodo-4-aminophenyl)-2-phenethylamine(I), a reversible inhibitor of steroid 11β hydroxylase. In view of the stereoselectivity of adrenocortical enzymes, studies were performed to determine if the enantiomers of I show different affinities for the adrenal cortex.

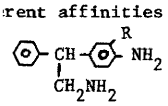

I:R = *I

II:R = H

Racemic-II was resolved by fractional crystallization of the diastereomeric tartarate salts. Conversion to the respective di-HCl salts gave [α]=-9.4 degrees for (-)-II and [α]=+9.6 degrees for (+)-II. The enantiomers were radiolabeled with I-125 in 90% yield by the chloramine-T method. The mild iodination conditions gave no racemization as determined by [α] measurements and N.M.R. analysis of the europium-comphorato complexes of the I-127 labeled compounds.

The tissue distributions of I-125 labeled-(+)-and(-)-I were determined in 5 dogs each at 2 hours post-injection. The (-)-I form gave a 100% greater uptake in the adrenal cortex (3.47±0.12% Kg·dose/gm) and nearly a 3-fold increase in both the [adrenal cortex/liver] and [adrenal cortex/medulla] compared to the (+)-I enantiomer. The uptake values for racemic-I were intermediate between those obtained for the two pure enantiomers.

These results demonstrate the importance of enantiomer evaluation in maximizing the possible clinical utility of a chiral radiopharmaceutical.

TUESDAY, JUNE 27
4:00 p.m.-5:30 p.m.

CALIFORNIA B ROOM

IN VITRO AND CORRELATIVE TECHNIQUES

ENDOCRINOLOGY I (CLINICAL SCIENCE)

Chairman: Henry N. Wellman
Co-Chairman: Harry R. Maxon

PREOPERATIVE ALDOSTERONOMA LOCALIZATION: COMPARISON OF ADRENAL IMAGING AGENTS. J.E. Freitas, R.J. Grekin, J.H. Thrall, M.D. Gross, D.P. Swanson, and W.H. Beierwaltes. University of Michigan Medical Center, Ann Arbor, MI.

I-131-19-iodocholesterol (NM-145) suppression scanning has been efficacious in preoperative aldosteronoma localization. Using a new adrenal imaging agent, I-131-6-iodomethyl-19-norcholesterol (NP-59), 19 patients with Primary Aldosteronism (PA) were imaged to evaluate the sensitivity, rapidity of localization, specificity and predictive accuracy of NP-59 suppression scanning compared to that reported with NM-145. PA was confirmed by low plasma renin activity, elevated urinary and plasma aldosterone values, and the responses of these parameters to salt and postural changes. Dexamethasone 1 mg p.o. q.i.d., and Lugol's iodine 3 gtts b.i.d., were begun 48 hours prior to intravenous injection of 1-2 mCi of NP-59 and continued through the imaging sequence. Posterior adrenal views were obtained on at least 2 occasions within 6 days.

Nine of 19 patients imaged with NP-59 and 19 of 26 patients imaged with NM-145 had an aldosteronoma. Correct localization was achieved with NP-59 in 8/9 (89%) patients as compared to 15/19 (79%) patients with NM-145. Localization was achieved in a mean time of 2.9 days with NP-59 and 4.8 days with NM-145. The specificity of a localizing adrenal scan with NP-59 was 8/9 (89%) as compared to 15/16 (94%) with NM-145. The histologically confirmed predictive accuracy in PA for NP-59 was 12/14 (86%) as compared to 20/26 (77%) with NM-145.

Compared to NM-145, NP-59 shows: 1) better sensitivity, 2) quicker localization, 3) similar specificity of the localizing adrenal scan, and 4) better predictive accuracy. Because of these advantages, NP-59 should replace NM-145 in the preoperative localization of aldosteronomas.

DEXAMETHASONE SUPPRESSION (DS) ADRENAL SCANS IN NORMAL CONTROLS. M. Gross, J. Freitas, D. Swanson, W. Beierwaltes. University of Michigan Medical Center, Ann Arbor, MI.

The degree of DS achieved biochemically and that demonstrated on the I-131-6β-iodomethyl-19-norcholesterol (NP-59) adrenal scan have heretofore not been defined.

To assess the completeness of DS upon NP-59 uptake, 11 normotensive male controls (MC) were studied to determine the doses and duration of DS that would reliably suppress 17-hydroxysteroids (17-OH), 17-ketosteroids (17-KS), and cortisol, and give the least uptake as seen on the adrenal scan. Controls were divided into four groups. Two groups received either DS 4 mg a day for 7 days (6 MC) or 8 mg a day for 2 days (5 MC) prior to injection of NP-59. DS was continued at the assigned dosage level throughout the scanning period (3-7 days). NP-59 was given intravenously in dosages of either 1 mCi (6 MC) or 2 mCi (5 MC). Scans were

interpreted as visualizing when demonstrating uptake on two successive days by two observers.

No significant differences were noted in plasma cortisol, 17-KS or 17-OH between groups that received either the 8 mg or 4 mg DS regimen. Early visualization of the adrenals (day 3-4 post-injection) was noted in the groups receiving the 8 mg DS regimen either with 1 or 2 mCi of NP-59. Late visualization (day 5-7 post-injection) was noted in the group that received the 4 mg DS and 2 mCi of NP-59. No visualization was evident up to 7 days after injection in the group that received 4 mg DS and 1 mCi NP-59.

The administration of 4 mg of DS for 7 days prior to injection of 1 mCi of NP-59 gives adrenal biochemical suppression that is no different from other DS schemes but does provide almost complete suppression of NP-59 uptake in the normal. This provides a basis for the diagnosis of adrenal hyperfunction on the NP-59 adrenal scan.

ISOTOPIC AND SEROLOGIC DETECTION OF THYROID CANCER: I-131 SCANNING AND SERUM THYROGLOBULIN RADIOIMMUNOASSAY IN 100 PATIENTS. M.D.Okerlund, J. Sommers, B. Chuck, E. Lam, M.Galante, and T. Hunt. University of California Medical Center, San Francisco, California.

100 patients with known or suspected thyroid cancer were studied by pre-op scanning of I-123 , and post-op scanning with I-131 and a sensitive thyroglobulin(TG) RIA.

		Serum TG (ng/ml.)		
	N	Range	Mean	Post-operative imaging
Normals	155	ND-11	6±2	Not applicable
Cancer, untreated				
Thyroidal	26	7-21	12±3	26/26 tumor negative
Metastatic	16	11-600	88±80	16/16 tumor positive
Carcinoma after total thyroidectomy				
Active	24	3-560	70±61	22/24 tumor positive
Inactive	34	ND-1.2	ND	0/34 tumor positive

*By examinations, radiographs, and scans.

100% of metastatic tumors had elevated TG, disappearing after I-131 documented total thyroidectomy. 93% of cases with detectable TG after thyroidectomy had positive scans. Serum TG is of limited usefulness in pre-op evaluations but the presence of any serum TG after documented thyroidectomy is unique, and correlates well with positive scans with I-131. There has been no previously specific method of evaluating cancer patients on thyroid medication, but discontinuation of thyroxine in patients with detectable TG is a valuable method for selection of patients for scan. Serum TG RIA and positive tumor scans after I-131 both depend on thyroid tumor cell differentiation and provide good means of evaluating thyroid cancer patients after thyroidectomy, and deserve routine post-operative use in the life long management of these patients.

SERUM THYROGLOBULIN AS AN INDICATOR OF METASTATIC WELL DIFFERENTIATED THYROID CARCINOMA: J.D. Denney, R. Marty, R.A. Schor and A.J. Van Herle. The Swedish Hospital Medical Center, Seattle, WA. and School of Medicine, University of Califonia at Los Angeles, Los Angeles, CA.

Over a two year period sixty-three patients with well differentiated thyroid carcinoma post thyroidectomy had serum thyroglobulin determinations to evaluate the usefulness of this assay as a marker of recurrent or residual thyroid carcinoma.

Fifty-five female and eight male patients were studied ranging in age from 12 - 80 years (mean 41). Forty-seven had papillary and sixteen had follicular carcinoma. All patients had physical examinations and chest radiographs, and some had whole body radioiodine scans and bone scans. A double antibody radioimmunoassay was used to measure thyroglobulin (normal value 0 - 20.7 ng/ml).

All sixteen patients with elevated serum thyroglobulin (mean 163 ng/ml, range 34 - 553 ng/ml) had metastatic thyroid carcinoma found on subsequent evaluation. Only one of the forty-seven patients with normal serum thyroglobulin (mean 8, range 1 - 19.0 ng/ml) has been found to have metastatic thyroid carcinoma. Five of six patients treated with therapeutic radioiodine have had marked lowering of serum thyroglobulin (four to values less than 20.7 ng/ml) and have had excellent clinical responses.

Our data supports the usefulness of serum thyroglobulin as a marker for residual or recurrent well differentiated thyroid carcinoma. An elevated serum thyroglobulin post thyroidectomy in a patient with well differentiated thyroid carcinoma is strong evidence of residual or recurrent carcinoma. A normal value in this same patient population is supportive, but not conclusive evidence of the absence of disease.

M-B ISOENZYME ACTIVITY IN HYPOTHYROIDISM. D.H.Woodbury, G.Washington, J.Batsakis, S.Sarkar. University of Michigan and Wayne County General Hospital, Ann Arbor, MI.

Nine patients admitted to the hospital with nonendocrine diagnosis, and without known pre-existing endocrinopathy, were found to be hypothyroid. Six of the nine patients had elevation of total creatine phosphokinase; two patients had positive M-B isoenzyme activity. All serial LDH isoenzymes and EKG determinations were normal; there were no other stigmata of acute ischemic cardiac disease in the latter patients. One patient with positive activity expired in pulmonary edema and renal failure in spite of hormone therapy. Hormone replacement in the second patient resulted in normalization of values and resumption of activity.

M-B isoenzyme elevation is generally associated with acute myocardial damage, although there have been reports of elevation of this isoenzyme in dermatomyositis, atrial fibrillation, musculodystrophy, and pulmonary embolus. One study in hypothyroid rats revealed faint M-B as an incidental finding. This is believed to be the first description of M-B isoenzyme elevation in hypothyroid patients, with no evidence of the other previously described clinical entities in which M-B isoenzyme elevation might be expected.

Currently patients presenting with cardiopulmonary aberration and elevated total CPK and M-B activity are managed as if acute myocardial infarction has occurred; some proceed to intractable failure and expire. This study suggests the prudency of screening this group of patients for possible unsuspected hypothyroidism.

EFFECT OF GROWTH HORMONE ON PANCREAS UPTAKE OF Se-75 SELENOMETHIONINE. H.L. Atkins and P. Som. Brookhaven National Laboratory, Upton, NY.

Previous studies have shown an enhancement of uptake of zinc thioglucose by the pancreas following administration of growth hormone (GH). This study was undertaken to investigate the effect of GH on the accumulation of Se-75 selenomethionine by the pancreas for comparison. GH and somatostatin (somatotrophin release inhibiting factor, SRIF) were administered intraperitoneally and by infusion to mice. One hour after the intravenous administration of selenomethionine they were sacrificed and radioactivity in pancreas, liver, kidneys, and intestines was assayed. Dogs received infusions of GH and SRIF and sacrificed at one hour after selenomethionine administration. Radioactivity in pancreas, liver, intestines and kidneys was determined.

In the mice given SRIF intraperitoneally, there was a significant increase in the pancreas uptake of Se-75 but the pancreas/liver ratio was not significantly changed. GH caused a decrease in pancreas uptake which was not statistically significant but the decrease in pancreas/liver ratio was highly significant. In dogs administering GH and SRIF by infusion caused no significant changes following SRIF but there was a highly significant decrease of pancreas uptake and pancreas/liver ratio following GH. The most dramatic effect was seen in dogs where GH decreased pancreas uptake to 1.24% and the P/L ratio to 0.97 from control values of 5.60% and 4.78 respectively. SRIF had no effect.

The results suggest that hypothalmic and pituitary factors may play a role in the function of the exocrine pancreas.

EFFECT OF ETHANOL ON OXIDATION OF GALACTOSE-CARBON-13 TO CARBON DIOXIDE IN ALCOHOLIC LIVER DISEASE. C.T. Gregg, J. Rudnick, B.B.McInteer, T. W. Whaley and W.W. Shreeve. Los Alamos Scientific Laboratory, Los Alamos, NM and VA Hospital, Northport, NY.

Measurement of carbon-13 (C-13) or carbon-14 (C-14) in respiratory carbon dioxide (CO-2) of cirrhotic patients after oral administration of galactose labeled uniformly (U) with C-13 or C-14 appears to be a good test for liver function (Shreeve et al., Gastroenterology, 71, 98-101, 1976). Since ethanol load decreases galactose tolerance in normal subjects but much less in patients with cirrhosis, conversion of galactose-U-C-13 to CO-2 has been measured in the absence and presence of ethanol (3.5 g./square meter body area p.o.) in 19 persons. On the basis of the C-13 results, the subjects were classified into four groups: normal, probable normal, probable liver damage and liver damage. There was good correlation with elevation of serum gamma-glutamyl transpeptidase (GGTP), especially a combination of elevated GGTP and serum glutamic pyruvic transaminase, and with drinking history. Serum glutamic oxaloacetic transaminase, alkaline phosphatase, albumin or bilirubin levels did not correlate with each other or C-13 findings. Ethanol-priming particularly helped to identify the intermediate groups. Because of its apparent sensitivity, the ethanol-primed galactose-C-13 (or C-14) oxidation test merits further study as a measure of liver function. (This work was supported by the U.S. Dept. of Energy.)

WEDNESDAY, JUNE 28, 1978

WEDNESDAY, JUNE 28 GARDEN GROVE ROOM
8:30 a.m.-10:00 a.m.

CONTINUING EDUCATION

HEMATOLOGY: FERROKINETICS, ERYTTHROKINETICS, BONE MARROW SPACE IMAGING, B_{12} AND FOLIC ACID METABOLISM

PARTICIPANTS: Gerald S. Johnston, Chairman, National Institutes of Health, Bethesda, MD; A. Eric Jones, National Institutes of Health, Bethesda, MD; James Ryan, University of Maryland Hospital, Baltimore, MD; Pablo Dibos, Franklin Square Hospital, Baltimore, MD; and Patricia A. McIntyre, The Johns Hopkins Hospital, Baltimore, MD.

GASTROINTESTINAL IMAGING AND FUNCTION

PARTICIPANTS: Richard C. Reba, Chairman, George Washington University Medical Center, Washington, DC; and Leon Malmud, Co-Chairman, Temple University Hospital, Philadelphia, PA.

WEDNESDAY, JUNE 28 ANAHEIM ROOM
8:30 a.m.-10:00 a.m.

CLINICAL SCIENCE

CARDIOVASCULAR II

Chairman: John A. Burdine
Co-Chairman: Richard N. Pierson, Jr.

THE EFFECT OF ISCHEMIA ON THALLIUM-201 CLEARANCE FROM THE MYOCARDIUM. H. Gewirtz, D.D. O'Keefe, G.M. Pohost, H.W. Strauss, J.B. MacIlduff, K.A. McKusick, and W.M. Daggett. Massachusetts General Hospital, Boston, MA.

To determine the effect of ischemia on myocardial clearance of thallium-201 (Tl), we studied twelve dogs with ischemia produced after the injection of Tl. Ten minutes before tying a suture around the left anterior descending (LAD) coronary artery, Tl was given IV. Five minutes later, Sr-85 microspheres (MS) were given via the left atrium to determine regional myocardial blood flow (RMBF). Then, one minute prior to LAD ligation, a biopsy (Bx) was obtained from myocardium supplied by the LAD (designated ischemic zone-IZ) and by the circumflex coronary artery (normal zone-NZ). The LAD was tied, and repeat Bx's obtained from IZ and NZ 15 minutes and 2 hours after occlusion (Occ). Sc-46-MS were given immediately prior to the 2 hour Bx. The animals were then sacrificed and MS activity determined in the IZ and NZ. Tl activity in the IZ was not significantly different from that in the NZ both prior to Occ and at 15 minutes and 2 hours after Occ. During the study, RMBF decreased to 24±6% ($p<.01$) control in the IZ and increased to 147±14% ($p<.01$) control in the NZ. Nevertheless, Tl clearance at 2 hours post Occ was 27±5% and 28±5% from the IZ and NZ respectively. Based on these data, the half-time of Tl clearance from the myocardium was calculated at 4.5 hours for both IZ and NZ; a value consistent with previously reported normal clearance half-times.

We conclude that myocardial ischemia does not alter the normal rate of Tl clearance from the myocardium. These results also suggest that myocardial binding of Tl differs from that of potassium (K+), since K+ is known to leak rapidly from ischemic cells, whereas Tl does not.

FACTORS AFFECTING PERCEPTION OF MYOCARDIAL PERFUSION DEFECTS USING Tl-201. J. C. Goble, H.N. Wagner, Jr., P.O. Alderson, T.G. Mitchell, E.L. Nickoloff. Johns Hopkins Medical Institutions, Baltimore, Md.

Several techniques have been proposed for improving detection of myocardial perfusion defects with Tl-201 (e.g., gated or cinematic display of ^{201}Tl images, color display). To provide an objective measure of these techniques a mechanical model was developed which accurately simulates the motion of the heart. A cyclic pump drove air into a water-filled diaphragm, forcing water into a concentric balloon model of the beating ventricle. The space between an inner and outer balloon was filled with 1 mCi of Tl-201. The ventricle model was immersed in water to simulate scatter and attenuation within the thorax. Myocardial lesions were simulated by one or more 3 cm diameter resin disks that produced filling defects. Images were presented to 5 independent observers in routine "static" mode, gated end-diastole (ED), cinematically, or in arc mode (an ED image smoothly rotating through 90° of obliquity). Displays were presented in black-white (BW) and color. The results were evaluated using the ROC curve approach. Cinematic display resulted in significant ($p< 0.01$) improvements in observer performance over both ED and routine images. There was no significant difference between ED and routine images, cine and arc-mode, or B-W and color display. However, the ROC

curves for BW and color had markedly different shapes,with color images yielding higher true-positive rates in the low false-positive range of the ROC curve. The results demonstrate that cinematic display of Tl-201 images yields the highest lesion detection rates, and support clinical experiences that suggest cinematic display is a useful addition to ^{201}Tl imaging.

SCINTIGRAPHIC IDENTIFICATION OF A HIGH RISK SUBSET OF ACUTE INFERIOR MYOCARDIAL INFARCTION. P.K. Shah, D. Berman, J. Maddahi, M. Pichler, T. Peter, A. Waxman, B. Singh, J. Forrester, H.J.C. Swan. Cedars-Sinai Medical Center, Los Angeles, CA.

Precordial ST degment depression in acute inferior myocardial infarction (MI) is often considered a benign finding. For the first time we are able to evaluate this electrical phenomenon noninvasively with scintigraphic methods.

Left ventricular (LV) ejection fraction (EF) and regional wall motion (WM) were determined by multiple gated cardiac blood pool scintigraphy (MSc) in 19 pts within 48 hours of acute MI. Pts with previous MI or concomitant anterior MI were excluded. MSc used in-vitro labeled Tc-99m-RBC's, gamma camera, computer, and curves derived from 14 regions of interest. Regional WM was evaluated by a 6 point scoring system for each of 7 LV segments. A normalized WM score (nWMS) was derived from the sum of individual segments. Twelve pts had >1 mm ST depression in leads V1-V3 (group A) (Gr A) and 7 had no precordial ST changes (group B) (Gr B). EF in Gr A was significantly lower ($p<.001$) than Gr B (.39±.04 vs .61±.03)(mean ±SEM). Regional WM abnormalities were more extensive in Gr A than Gr B with nWMS values of .43±.06 in Gr A vs .81±.04 in Gr B ($p<.001$). Septal and anterolateral segmental WM abnormalities were more prevalent and severe in Gr A. No in-hospital deaths occurred in Gr B, but 4/12 in Gr A died within 7 days of the acute MI ($p<.05$). Severe heart failure and/or shock occurred in 6/12 in Gr A and 0/7 in Gr B ($p<.05$).

Thus, multiple gated cardiac blood pool scintigraphy demonstrates that precordial ST depression in acute inferior myocardial infarction is accompanied by severe global and regional LV dysfunction, thereby explaining the attendant high morbidity and mortality.

Tl-201 ASSESSMENT OF INFARCT SIZE IN EARLY INFARCTION. J.W. Fletcher, P.S. Rao, F.K. Herbig, K.F. Witztum, J.L. Daly, H. Mueller, R.M. Donati. VA Hospital and St. Louis University School of Medicine, St. Louis, MO.

To evaluate the sensitivity and accuracy of Tl-201 in sizing acute transmural myocardial infarctions (ATMI) myocardial imaging was performed in 28 patients with documented ATMI within the first 12 hours after the onset of symptoms. Anterior, 45° LAO and 60° LAO images were obtained using a gamma camera/mini-computer system. The size of infarction as determined from computer-assisted analysis of the Tl-201 images was compared to infarct size obtained from completed creatine kinase (CK) curves using serial serum CK values. In each view, the scintigraphically abnormal area was expressed as the percent of the total surface area of the left ventricle, and the size estimate from the view with the largest calculated surface area was compared to the CK infarct size estimate in gram equivalents (GMEQ), and the CK infarct size index (ISI = GMEQ/m^2 body surface area). Eleven patients had anterior ATMI with a mean CK infarct size of 52 GMEQ (range 8-100), ISI of 26 and Tl-201 % surface area of 28; 17 patients had inferior ATMI with a mean CK infarct size of 44 GMEQ (range 9-119), ISI of 23 and Tl-201 % surface area of 21. Infarct size as determined from Tl-201 images correlated well with CK infarct size in GMEQ (anterior infarction, $r = 0.93$, inferior infarction, $r = 0.86$) and CK ISI (anterior $r = 0.96$, inferior $r = 0.88$). These results indicate that Tl-201 infarct size estimates are sensitive over a wide range of CK GMEQ infarct sizes, are slightly better in anterior than inferior ATMI and provide accurate assessment of the extent of ATMI in the first 12 hours of infarction.

THALLIUM REDISTRIBUTION IN THE PRESENCE OF SEVERE FIXED CORONARY STENOSIS. G.M. Pohost, D.D. O'Keefe, H. Gewirtz, H.W. Strauss, G.A. Beller, J.B. Newell, J.B. Chaffin, and W.M. Daggett. Massachusetts General Hospital, Boston, MA.

To define whether redistribution (RD) of Thallium-201 can occur without restoration of normal blood flow to an ischemic zone of myocardium, the following study was carried out on 14 open-chest dogs anesthetized with chlorolose and urethane. The proximal left anterior descending coronary artery (LAD) was isolated and an inflatable cuff occluder placed around it. The mean aortic pressure was maintained at 100mmHg while the distal LAD pressure was maintained at 30-40mmHg throughout the study. Tl-201 was given intravenously and 9±1μ Sr-85 labelled microspheres given into the left atrium. One group of dogs (n=7) was sacrificed 10min and the other group (n=7) 2hrs after Tl-201 administration. Sc-46 microspheres were given immediately prior to sacrifice in the 2hr group and demonstrated no significant change in flow compared with initial Sr-85 microspheres. Relative blood flow in the myocardium supplied by the LAD was 69±3% of normal flow (N) at 2hrs, whereas Tl-201 activity was 79±3% of N in this zone ($p<.001$) In the 10 min group flow was 61±3% of N while Tl-201 activity was 65±3% of N ($p=NS$). Relative Tl-201 activity was significantly greater compared to flow at 2hrs than at 10 mins consistent with significant redistribution of Tl-201 during this interval of constant low flow. By 2hrs low flow regions (50% of normal or less) demonstrated a 23±3% excess in thallium activity over flow compared to a 10±2% excess in the 10 min values ($p<.001$), consistent with RD even in the most severely ischemic zones. These data document that RD of Tl-201 occurs into myocardium distal to a persistant severe coronary stenosis and does not require restoration of normal blood flow.

REDISTRIBUTION OF THALLIUM AT REST IN PATIENTS WITH CORONARY ARTERY DISEASE. B.C. Berger, D.D. Watson, J.N. Sipes, G.M. Pohost, C.D. Teates, and G.A. Beller. University of Virginia Medical Center, Charlottesville, VA.

This study was designed to determine if redistribution (RD) of Thallium-201 (Tl) occurs at rest in patients (pts) with coronary artery disease (CAD). Fifteen consecutive pts referred for angiography for severe angina pectoris underwent serial imaging over 3 hrs beginning 10 min after injection at rest of 1.5 mCi of Tl. No pts were injected or imaged during pain. Myocardial images in the anterior and LAO views were divided into a total of 6 segments (segs) for analysis. Serial changes in segmental Tl uptake were evaluated visually and confirmed by computer quantitation. Of 90 possible segs, 47 showed decreased Tl uptake on initial images. In 32/47 there was RD at 1-3 hrs, whereas 15 segs did not show RD. Angiograms revealed that 27/32 segs with RD had anatomically appropriate severe CAD (>50% stenosis). One pt with clinical and ECG evidence of infarction but angiographically normal coronary arteries had 3 segs demonstrating RD. Ventriculographic analysis of wall motion in 29 segs with RD revealed 27 were normal or hypokinetic and 2 were akinetic. Four pts had repeat imaging at rest after coronary bypass surgery. Twelve of 14 segs with decreased Tl uptake on initial images pre-op, and which demonstrated RD, showed normal uptake of Tl on initial images post-op.

Thus, 1) myocardial segments with redistribution of Thallium at rest generally correspond to severe CAD but normal or hypokinetic LV wall motion, 2) most segments with redistribution preoperatively, show normal early uptake following coronary artery bypass surgery, and 3) both early and delayed images are necessary to evaluate myocardial perfusion and viability at rest.

A KINETIC MODEL FOR THALLIUM MYOCARDIAL REDISTRIBUTION. D.D. Watson, G.A. Beller, J. F. Irving, C.D. Teates. University of Va. Medical Center, Charlottesville, VA.

It has been widely assumed that after Thallium (Tl) is initially extracted from blood following intravenous injection it will be fixed within myocardial cells for

several hours with very little kinetic exchange. However, recent observations have shown early myocardial Tl redistribution not only with transient perfusion defects, but also in instances of stable perfusion defects at rest. These findings are inconsistent with the conventional view of Tl kinetics and require a more comprehensive evaluation. A multicompartmental model for the in-vivo distribution of Tl has been derived and model parameters compared with human and animal studies. The model indicates three separate phases of Tl uptake. 1) The "perfusion" phase where the concentration of Tl is proportional to the perfusion/extraction-fraction product(EFP). 2) A "delayed uptake" phase with myocardial uptake due to continued exposure to low levels of Tl being reintroduced into the blood from other body organs. 3) An "equilibrium" phase where the rate of Tl input by recirculation equals the rate of output from myocardial cells.

The Tl concentration in phase 2 and 3 is not simply related to EFP as in phase 1. Phase 2 is observed in resting and decreased perfusion states. The equilibrium distribution is not necessarily equivalent to the initial resting distribution. These aspects of Tl kinetics should be considered for both the performance and clinical interpretation, particularly of delayed Tl scans. Myocardial redistribution kinetics could be employed to evaluate areas of decreased perfusion and to differentiate perfusion defects from scar even in patients who cannot undergo exercise stress testing.

WEDNESDAY, JUNE 28 SANTA ANA ROOM
8:30 a.m.-10:00 a.m.

BASIC SCIENCE

BASIC NUCLEAR SCIENCE

Chairman: Bernard A. Sachs
Co-Chairman: Hiram E. Hart

MECHANISM OF HEPATIC EXTRACTION OF GELATIN STABILIZED Tc-99m SULFUR COLLOID (TSC). Erica A. George, Robert E. Henry, James W. Fletcher, and Robert M. Donati. VA Hospitals, St. Louis, MO and Tucson, AZ.

The specific mechanism of hepatic extraction of TSC was studied in rats by time sequenced microscopic autoradiography and electron microscopy following the administration of Tc-99m or osmium labeled TSC. Rats were killed 15 min, 2 hr, 4 hr, 6 hr and 24 hr after the i.v. administration of either 8 mCi Tc-99m TSC or osmium labeled TSC. Livers were removed for autoradiography or electron microscopy. Previous studies had demonstrated similar organ partitions of osmium labeled TSC and Tc-99m TSC. In microautoradiographic sections, a preponderance of grain clusters were associated with Kupffer cells in the peripheral sinusoids in juxtaposition to the portal triads, whereas single file grain patterns were seen distributed equally in peripheral and central sinusoids. This zonal distribution of radioactivity persisted unchanged for 24 hr. The topographic relationship of grains and Kupffer cells did not suggest intracellular radioactivity at any time. Electron microscopic preparations demonstrated clusters of TSC particles attached to and partially surrounded by the pseudopods of hepatic sinusoidal macrophages, however, no intracellular TSC particles could be identified in liver sections obtained within the first 24 hr after osmium labeled TSC administration. These results suggest that the mechanism by which TSC is rapidly removed from the circulation and localized in the liver is Kupffer cell membrane attachment without subsequent pinocytosis; and provide an explanation for the fact that quantitative extraction of TSC is not altered by increasing amounts or repeated administration of TSC nor by particulate reticuloendothelial blockade.

SCINTILLATION PROXIMITY ASSAY (SPA) OF ANTIGEN-ANTIBODY BINDING KINETICS. H. E. Hart and E. B. Greenwald - Dept. of Physics, CCNY. N.Y. and Montefiore Hospital & Medical Center, Bronx, N.Y.

A new very sensitive method has been developed for the direct assay of antigens and antibodies. Human albumin was covalently bound to the carboxylate modified surfaces of tritiated 0.926 μ diameter Dow polystyrene particles (LH) and to $\sim$1 μ polystyrene scintillant particles (L*). Aqueous suspensions of a mixture of these 2 types of particles were incubated under various conditions with Rabbit Anti-Human Albumin sera. Since the mean range of a H-3 β ray in water is only $\sim$1μ, it was statistically unlikely at the dilute particulate concentrations employed ($\sim$1 μgm/ml) and in the absence of (LH) (L*) binding, that the β rays arising from LH particles would strike the scintillant particles L*. The count rate in the tritium energy range was then measured in a standard liquid scintillation system. Characteristically, a grossly enhanced count rate was noted within several hours for titers of 1,000, 10,000, and 100,000, while 24 to 48 hours were required for statistically significant differences from control values at titers of $\sim$1,000,000. Longer term changes in the count rates occurred at lower antibody concentrations depending upon the media and the conditions of incubation, but the results were variable and the evidence is not yet conclusive. In view of the repetitive structure of viral coats, a bridge formed between antibody coated particles by even a single virus or polymeric antigen might well involve multiple stable bonds. This suggests that SPA might prove to be very sensitive for virus detection. A general theory of SPA will be presented, indicating its potential, and describing related multiple-fluorescence techniques and instrumentation under development.

EFFECTS OF DIAGNOSTIC ULTRASOUND ON T-1 HUMAN KIDNEY CELLS. Edward Siegel, Elsie P. Siegel, John Goddard, and A. Everette James. Dept. of Radiology and Radiological Sciences, Vanderbilt University School of Medicine, Nashville, TN.

The application of ultrasonography for diagnostic procedures to ever-increasing numbers of patients is the impetus for investigating the effects of ultrasound irradiation on cultured human cells. To perform these experiments, T-1 human kidney cells, growing exponentially as monolayers, were released and dispersed with trypsin and gentle agitation, seeded into plastic Petri dishes, and irradiated from 5 to 60 minutes with an Ekoline 20 Ultrasonoscope (circa 0.025 watts/cm^2/minute). Alterations the radiation produces could be discerned by evaluating indices that reflect proliferation, colony formation, and attachment; as examples, irradiation of the cells for 15 minutes results in modifications of the following parameters (changes relative to controls indicated in parenthesis): mitotic index (-13.8%), plating efficiency (-6.48%), and attachment to plastic (-18.2%). It is concluded that in vitro exposure to ultrasound in the diagnostic range affects replication, aggregation, and adhesion of T-1 cells.

These studies were supported, in part, by a research grant from the John A. Hartford Foundation of New York City.

GA-67 UPTAKES BY CULTURED TUMOR CELLS. R.G. Sephton and A.W. Harris. Cancer Institute; Walter and Eliza Hall Institute, Melbourne.

To interpret tissue culture findings on Ga-67, one needs an appreciation of system properties influencing the availability of Ga-67 to the cells. This paper concerns cultured mouse tumor cells growing exponentially in medium containing 10% fetal calf serum. The basic experiment involves dispersing Ga-67 citrate into cell cultures and, following the incubation (24 hr, 37°), separating and washing the labeled cells. Uptake promotion due to an extrinsic component (e.g. added serum, transferrin) is studied by comparing uptakes for 'promoted' and 'control' cultures. Our dual tracer studies have documented Ga-67 and Fe-59 uptakes for different cell lines, their

dependence on transferrin dose and species of origin, effects of iron additions. Here we combine such findings with additional data on the fetal calf serum influence, to explain some aspects of tracer uptake responses shown by these cultured cells. Technical questions include: 'uptake' contributions arising from precipitable as opposed to cell-bound Ga-67, the need for distinguishing substantial from trivial uptakes. More fundamentally we then consider transferrin-promoted uptake in terms of - transferrin interactions with cell-receptors, the tracer's distribution between extracellular binding entities (e.g. the added transferrin, the fetal calf serum component) and the influence of the system's iron distribution.

RADIATION DOSIMETRY OF I-131-6β-IODOMETHYL-19-NORCHOLESTEROL (NP-59). J.E. Carey, J.H. Thrall, J.E. Freitas, and W.H. Beierwaltes. University of Michigan, Ann Arbor, MI.

The absorbed dose to the human adrenal from NP-59 has been reported to be 150 rads/mCi. This estimate was calculated using tissue distribution data obtained from rats and dogs. The animal data was the only extensive concentration data available at the time.

Percent adrenal uptake values measured in humans over the past two years using an external counting technique have suggested that the absorbed dose to the adrenals is significantly less than estimated using the animal adrenal concentration values.

Percent adrenal uptake values, measured in over 40 patients, were used to calculate absorbed doses to the human adrenals following the MIRD formalism. The measured percent uptake values for both adrenals ranged from 0.15 to 0.52% in 21 patients without evidence of adrenal disease with a mean uptake of .33±.1% and from 0.22 to 1.5% in 22 patients with Cushing's Disease with a mean uptake of .78± .35%. The absorbed dose to the adrenals for patients without evidence of adrenal disease was estimated to be 26 rads/mCi and for patients with Cushing's Disease was estimated to be 60 rads/mCi (both values calculated for the respective mean percent uptakes).

The significantly lower adrenal radiation dose is an important consideration for general implementation of adrenal imaging which would not have been recognized without systematic percent uptake determinations in actual clinical studies. Although calculated using an external counting technique rather than direct tissue distribution data, the uptake procedure has been previously verified, and the current estimates based on human data are felt to represent the best available information at this time.

TOTAL BODY DISTRIBUTION STUDIES OF 99m-Tc-GLUCOHEPTONATE USING A NEW TOTAL BODY SCANNING SYSTEM. G.H. Simmons, F.H. DeLand and C. Young. Veterans Administration Hospital and University of Kentucky Medical Center, Lexington, KY.

A new scanning system designed for quantitative measurement of the total body distribution of millicurie amounts of radiopharmaceuticals was used to obtain human data for estimating the radiation dose to the kidneys and total body from Tc-99m-glucoheptonate. The system uses a linear array of 16 NaI(Tl) crystals each with its own phototube and focussing collimator. Each detector output feeds into a separate amplifier and PHA channel. The detector assembly oscillates in the lateral dimension as the patient is moved across the detector bank in the orthogonal direction producing a total body scan in a single pass. The system is interfaced to a PDP-11/40 digital computer. A unique feature is the utilization of the DEC NCIIA camera interface for data acquisition. X and Y addresses are generated from the PHA outputs along with digitized transducer signals that mark bed and detector bank positions. The addresses are stored as gamma-11 files on a magnetic disk. A major advantage of such an approach is apparent in that the gamma-11 software is used for data acquisition and analyses thereby allowing the user to interface a custom detector system without the necessity of developing extensive software. The data are displayed as 128 x 384 images. Data from two patients studied to date show the average radiation doses from Tc-99m-glucoheptonate to be 0.01 rads/mCi to the total body and 0.16 rads/mCi to the kidneys. The maximum activity in the kidneys at any time is 5%-8% of the injected activity. The remainder appears to accumulate in soft tissue. There appears to be no biological turnover once the material is fixed in the kidneys. (Supported in part by NCI Grant #PO1-CA-17786).

QUANTITATIVE ORGAN VISUALIZATION USING EMISSION COMPUTED TOMOGRAPHY. L.T. Kircos, J.E. Carey and J.W. Keyes, Jr. University of Michigan Medical Center, Ann Arbor, MI.

Quantitative organ visualization (QOV) has been defined as "the knowledge of the absolute radioactivity of each volume element of the organ of interest". The use of single photon emission computed tomography (ECT) to perform QOV was evaluated using the Humongotron, a scintillation camera transaxial tomograph.

The boundaries of the organs of interest were determined by finding the maximum gradient and the extent of radioactivity in the organs was defined by the extent of the first derivative. An expression for the absolute activity in the organ was derived in terms of the ECT counts and size, imaging system efficiency, imaging time and attenuation factors. Following analytical and phantom studies, 7 dogs and 1 human were studied and the QOV results compared with direct tissue measurements. The liver, bladder, kidneys and spleen were the organs studied.

Absolute organ activity and organ size could be determined to an accuracy of about ± 10% providing: 1) the minimum dimensions of the organ of interest are greater than the FWHM of the imaging system and 2) the total radioactivity within the organ of interest exceeds 5 μCi for dog sized torsos and imaging times less than 45 minutes.

Limits on the accuracy of this technique are imposed by imaging resolution and sensitivity and by subject size. However, the accuracy of the technique appears to be sufficient to allow quantification of human radiopharmaceutical distribution data for internal dosimetry calculation rather than data extrapolated from animals. In addition, the technique of QOV introduces the possibility of quantitating in-vivo physiologic processes and increasing the diagnostic benefit of some procedures in nuclear medicine.

WEDNESDAY, JUNE 28 — CALIFORNIA B ROOM
8:30 a.m.-10:00 a.m.

IN VITRO AND CORRELATIVE TECHNIQUES

COMPUTED TOMOGRAPHY

Chairman: R. Edward Coleman
Co-Chairman: John W. Keyes

A METHOD FOR NON INVASIVE REGIONAL MEASURE OF CEREBRAL GLUCOSE METABOLIC RATE WITH EMISSION COMPUTED TOMOGRAPHY (ECT) M.E. Phelps, S.C. Huang, E.J. Hoffman, C. Selin, D.E. Kuhl. UCLA School of Medicine, Los Angeles, California.

Quantitative imaging capabilities of ECT are combined with a compartmental model for cerebral metabolic rate for glucose (CMRGlu) to provide regional assessment of cellular metabolic rates non invasively. The CMRGlu is based upon models developed by Sokoloff, Reivich et al for autoradiography with (C-14)-deoxyglucose and by Reivich et al for (F-18)-deoxyglucose (FDG). We have reduced these complex models to CMRGlu=[Glu]C(T)-C(b)K)/(LC[A]), where [Glu] and [A] are plasma glucose concentration and area under FDG venous blood curve. LC is a constant accounting for difference in CMRGlu of glucose and FDG. C(T) and C(b)are regional tissue and blood concentration of F-18 at time, T. C(T) is measured with ECT. In the past, blood data have been obtained from arterial samples. We have shown that CMRGlu can be determined by venous sampling without loss in accuracy. Measurement requires venous injection of FDG, withdrawals of

about 10 venous blood samples and ECT images. Ten in vitro dog studies and 20 human studies using the ECAT positron ECT were carried out to test the model. Human images allow clear delineation and calculation of CMRGlu (mg glucose utilized/min/gm tissue) in regional areas of cortex, left and right caudate nucleus and thalamus, internal and external capsule, cerebellum, brain stem etc. Measurements as a function of time showed method to be stable (+ 5%) over a period of 0.6-3 hrs post injection. Tissue to blood activity was found to be > 100 at > 20 min post injection. Method exemplifies combined use of ECT, labeled substrates and physiologic models to form the basis of a new modality of physiologic tomography. Supported in part by DOE #EY-76-C-03-0012, NIH #GM-24839-01.

EFFECT OF OBJECT SIZE IN QUANTITATIVE POSITRON COMPUTED TOMOGRAPHY. E.J. Hoffman, S.C. Huang and M.E. Phelps. UCLA School of Medicine, Los Angeles, California.

Quantitative measurement of isotope concentrations from images obtained in positron computed tomography (PCT) is ambiguous for small structures, unless, the response of the instrument is known as a function of object size.

The response of a positron tomograph (ECAT, Ortec, Inc.) was measured as a function of object size and instrument resolution. Test objects were 18-20 cm cylinders containing various sized cylindrical or variable thickness annular cavities for radioisotope. Each phantom was imaged with three different instrument resolutions and all images were corrected for attenuation.

Integration of counts in images of multiple cylinder phantoms with equal isotope concentration in each cavity showed direct correlation (r>.99) of integral counts with cross-sectional area of cylinder for a 16 to 1 range of sizes (11.4 to .7 sq. cm.). The concentration of activity in the images for each source was obtained at three image resolutions (1.14, 1.45 and 1.8 cm FWHM). As a point of reference, the response of an ideal system with gaussian line spread functions was calculated, giving 50% and 94% recovery for cylinders with diameters of one FWHM and two FWHM, respectively. The measured values were 44±1.5% and 87±2% for one FWHM and two FWHM diameters, respectively.The annular isotope distribution showed about a 50% increase in recovery over a cylinder at thicknesses of one FWHM and were generally in good agreement with calculated values.

PCT is found in good agreement with theoretical limits on recovery of information in images as a function of object size. Care must be exercised in quantitative interpretation in PCT, since many structures in the body are small enough to have significantly attenuated responses.

QUANTITATIVE UPTAKE MEASUREMENTS USING THE SEARLE POSITRON CAMERA SYSTEM. P.V. Harper, F. Atkins, R. Scott, J. Dudek, and M. Buchin. University of Chicago, Chicago, IL. and Searle Radiographics, DesPlaines, IL.

Quantitative uptake measurements are not in general possible with conventional imaging equipment. Such measurements have been possible using the Searle two-camera positron system. In order to accomplish this, a number of corrections are necessary. Correction for geometrical distortion, i.e., radial variation of sensitivity, is accomplished by normalization to a uniform sheet source. Correction for variation of attenuation across the object is accomplished by normalization to a transmission image using a sheet source. This correction gives a close approximation and includes the correction for geometric distortion. Correction for random events is accomplished on line by the use of a parallel coincidence system with offset timing windows which collects a random image for subsequent subtraction from the composite image. Small angle scatter (∿30°) does not degrade the photon energy sufficiently to remove it from the pulse height analyzer windows (20%). This gives rise to a 30-40% background. The use of a second window just below the primary photopeak window permits point by point compensation for scatter using spectral analysis techniques similar to that of simultaneous determination of two radionuclides with overlapping spectra. Information from these various simultaneous measurements is digitized, labeled in the least significant bit and subjected to longitudinal reconstruction. Quantitative results have been thus obtained at count rates of up to 8000/sec, permitting for instance inert gas washout studies of the brain using N-13-nitrous oxide, quantitation of relative myocardial perfusion using N-13-ammonia, and equilibrium imaging with O-15 for brain studies.

SINGLE PHOTON EMISSION COMPUTED TOMOGRAPHY (ECT) OF THE BODY. P. Murphy, J. Burdine, M. Moore, R. Jaszczak, W. Thompson, and G. Depuey. Baylor College of Medicine, St. Luke's Episcopal/Texas Children's Hospitals, Houston, TX, and Searle Radiographics Inc, Des Plaines, IL.

A single photon body ECT system was constructed using two opposed large-field scintillation cameras because of encouraging results from a prototype ECT head unit (J Nucl Med 18:373, 1977). Eleven adjacent slices were reconstructed from data collected with either parallel-hole or specially designed fan-beam converging collimators. A variety of major organ ECT scans were obtained in 130 patients using Tc-99m radiopharmaceuticals and compared with standard scintiphotos. Preliminary conclusions are; (1) ECT images of the brain are superior in resolution and contrast to the standard scintiphotos; (2) Lung ECT perfusion images provide better anatomic separation of lesions with equivalent resolution to the standard scintiphotos, but an overall perspective of the lung is more difficult to obtain in viewing 11 separate sections. This display problem applies to organs of complex shape or internal structure such as the lung and liver, and a simulated three-dimensional display is currently being pursued as a potential solution; (3) In the abdomen, images show little change in qualitative characteristics with or without correction for gamma ray attenuation; (4) Sectional views are particularly helpful in separating internal from external organ structure, such as the porta hepatis and lesions at the surface of the brain; (5) Pyrophosphate and ECG gated blood pool images of the heart appear promising for evaluating infarct size and wall motion abnormalities. These results indicate that a significant potential exists in the further development of single-photon ECT.

A NONMOVING SYSTEM FOR MYOCARDIAL PERFUSION TOMOGRAPHY USING AN ANGER CAMERA AND COMPUTER. D.L. Kirch, R. A. Vogel, M.T. LeFree, and P.P. Steele. VA Hospital, Denver, CO.

A system is described which utilizes a standard large-field Anger camera and dedicated minicomputer for tomographic imaging which has proven superior to conventional planar imaging for myocardial perfusion studies. This approach utilizes a multiple pinhole plate to project 7 simultaneous views of the heart as separate 13 cm diameter images onto the camera detector. The heart is positioned in the LAO projection about 13 cm from the pinhole plate to take advantage of the pinhole resolution characteristics as a function of distance. Following injection of 1.5 mCi of Tl-201 during treadmill stress a total of 750,000 counts are accumulated in less than 10 minutes and the digitized data is stored as 7 individual matrices (64 x 64 pixels each). Uniformity correction is then performed using a flood imaged with the pinhole plate and the digitized data is processed into 12 tomographic planes spaced 6 cm to 24 cm from the pinhole plate. Reconstruction is accomplished by the Simultaneous Multiple Angle Reconstruction Technique (SMART) which shifts and computes the 12 tomographic images in less than 5 minutes. Iterative techniques are then used to perform attentuation correction and refocussing of the data. The point source resolution 13 cm from the pinhole plate was measured to be 11 mm FWHM parallel to the detector and 15 mm perpendicular. The probability of detection in a group of patients with known coronary artery disease was improved from .72 for visual interpretation of planar images to .92 by the tomographic method. Statistical analysis of the maximum count-rate profiles around the annular ring of the tomographic heart image was found to be even more reliable than visual interpretation.

PRELIMINARY OBSERVATION ON THE CLINICAL VALUE OF EMISSION COMPUTED TOMOGRAPHY. T.C. Hill, P. Costello, H.F. Gramm, B.J. Mc Neil. New England Deaconess Hospital, Peter Bent Brigham Hospital and Harvard Medical School, Boston, MA.

Preliminary data comparing emission tomography (ECT), transmission tomography, and conventional radionuclide imaging suggest that in many patients unique diagnostic information is available from emission tomography. ECT was performed during a four month period on 200 of 235 patients referred to Nuclear Medicine for brain scans. The emission tomography was performed on a single photon system, the Cleon Transverse Section Brain Imager. Among the areas in which ECT provided unique information were differentiation of superficial from deep intracranial pathology, localization in depth of lesions, early abnormality in stroke, early detection of metastatic tumor, and a more precise diagnosis of subdural hematoma.

EMISSION COMPUTED TOMOGRAPHY: APPLICATION TO ACUTE MYOCARDIAL INFARCT IMAGING IN INTACT DOGS USING Tc-99m PYROPHOSPHATE. D. E. Gustafson, M. Singh, M. J. Berggren, M. K. Dewanjee, R. C. Bahn, and E. L. Ritman. Mayo Foundation, Rochester, MN.

Emission computed tomography techniques have been used to obtain in vivo quantitative estimates of the distribution of gamma emitting radionuclides in dog hearts. Conjugate views obtained for 60 equiangular projections around 360 degrees by rotating the dogs in front of a gamma camera were used to reconstruct multiple level parallel emission transaxial images of dogs with surgically induced acute myocardial infarcts. Corrections of gamma ray attenuation were performed in a convolution type reconstruction algorithm by weighting the backprojected data with values derived from a corresponding multiple level transmission reconstruction using a prototype cylindrical scanner. By combining the emission and transmission techniques, the size, shape, and location of regions of Tc-99m pyrophosphate uptake were estimated in three dimensions and the concentration of activity was quantitated to 10-15% rms error. Correlations were obtained of the radionuclide and histopathological estimates of the extent of injury (linear correlation coefficient, r=0.99) demonstrating that emission CT techniques provide a method of estimating the extent of myocardial damage. (Research supported in part by grants NIH HL-04664, HL-07111, and RR-00007 and AHA CI-10.)

WEDNESDAY, JUNE 28 CALIFORNIA A ROOM
8:30 a.m.-10:00 a.m.

CLINICAL PRACTICE

INSTRUMENTATION

Chairman: F. David Rollo
Co-Chairman: Perry P. Mandel

USE OF AUTOMATIC WINDOW TRACKING AND FIELD UNIFORMITY CORRECTIONS IN CLINICAL PRACTICE. L.S. Graham, F.E. Holly, J.M. Uszler, and L.R. Bennett. UCLA School of Medicine, University of California, Los Angeles, CA 90024

Recent advancements in Anger camera electronics include automatic tracking of analyzer windows and live correction of field non-uniformities. The purpose of this study was to evaluate the effect the use of these devices would have on clinical studies.

When the analyzer windows were set automatically in the presence of scatter, they were positioned lower on the energy spectrum than when they were set in the absence of scatter. Also, the use of auto peak at high count rates caused the window to be set at a lower position on the energy spectrum. In addition, the use of Co-57 markers caused a downward shift of the window.

Storage of a flood for the correction circuitry required six minutes at a data input of 10K cps. When reference floods were stored at a data input rate of 58K cps, the corrected floods obtained at low rates (8K cps) showed a 10% loss in the number of cells falling within ±5% of the mean. When a flood phantom was used as the source, our camera required 13% more time to collect a given number of counts when the correction circuit was operating. A 4 x 8 cm source required from 3 to 17% more time depending on where it was located within the field.

To evaluate the influence of scatter, a reference flood was stored using a flood phantom. The presence of as much as 4" of scatter had only a minimal effect (2%) on the number of cells falling within a uniformity limit of ±5%.

As long as collimators were of the same type (parallel hole), there was virtually no change in the number of cells falling within ±5%. Use of a different collimator type caused marked changes.

PERFORMANCE CAPABILITIES AND LIMITATIONS OF CURRENT IMAGING DEVICES. L. S. Graham, UCLA School of Medicine, Los Angeles, CA.

PRACTICAL CONSIDERATIONS IN THE CLINICAL STUDY. J. W. Keyes, Jr., University of Michigan Medical Center, Ann Arbor, MI.

SCINTILLATION CAMERA METHODS FOR IODINE-123 THYROID UPTAKE MEASUREMENT. M.L. Born, F.D. Rollo. Vanderbilt University Medical Center, Nashville, TN.

Iodine-123 is used with scintillation cameras for measuring thyroid uptake. Both the collimator type and physical factors have a significant effect upon the reproducibility as well as accuracy of the uptake determinations. In this study, the count rate response for the LEAP, converging and pinhole collimator was determined. The count rate variation at a collimator-to-source distance of 5 cm. was found to be less than 5% per cm. for vertical and horizontal displacements for the LEAP and converging collimators. For the pinhole collimator, count rate variations greater than 25% per cm. and 8% per cm. were obtained for vertical and horizontal displacements respectively. A change from a point source geometry to an extended source causes a 50% change in the count rate with the pinhole collimator. These results demonstrate the need for meticulous patient placement when using the pinhole collimator.

Thyroid uptake measurements were made on 15 patients at 6 and 24 hours following administration of 100 uCi of I-123 p.o. Flat field collimator uptake measurements were compared with scintillation camera measurements made with the LEAP and pinhole collimators. LEAP collimator measurements showed excellent correlation: $r = .98$, $b = .18 \pm .96$, $m = 1.13 \pm .04$ ($y = mx + b$). While pinhole measurements also correlate well ($r + .92$, $b + 1.8 \pm 1.25$, $m = .62 \pm .06$), the pinhole values are less precise and are significantly different from the flat field collimator measurements ($P < .01$). LEAP collimator measurements have the same normal range as those obtained with the flat field collimator. A different normal range was shown for the pinhole collimator measurements.

CLINICAL APPLICATION OF MAGNIFICATION IMAGING TECHNIQUES. **R.B. Grove, R.D. Bowen, R.E. Melton, and F.D. Rollo. V.A. Hospital and Vanderbilt University, Nashville, TN.**

The ability to detect small lesions is fundamental to the early diagnosis of many diseases. The purpose of this study was to evaluate the ability of magnification techniques to increase the detectability of small lesions in clinical practice using equipment readily available in the average nuclear medicine clinic. The principles and characteristics of converging and pinhole collimators for the gamma camera were evaluated. The advantage of magnification and the practical disadvantages of both were studied. Quantitation of the degree of magnification which can be

obtained with the pinhole and converging collimator compared to a parallel hole collimator was performed. Magnification techniques were applied to the study of small lesions of the posterior fossa, orbits, thyroid, kidneys, and skeleton. Illustrative studies include the detection of a 4 x 5 mm intraoccular melanoma, an occult sphenoid ridge meningioma and posterior fossa cystic astrocytoma, as well as improved lesion detection in the thyroid and kidneys. These results clearly demonstrate the utility and practicality of the application of magnification imaging techniques in the clinical practice of nuclear medicine.

UNCOMMON PROCEDURES WITH COMMON EQUIPMENT. F. D. Rollo, Vanderbilt University, Nashville, TN.

A CONCISE ASSESSMENT OF THE VALUE OF COMPUTERS IN CLINICAL PRACTICE. F. D. Rollo, Vanderbilt University, Nashville, TN.

WEDNESDAY, JUNE 28 GARDEN GROVE ROOM
10:30 a.m.-12:00 p.m.

CONTINUING EDUCATION

CENTRAL NERVOUS SYSTEM: RADIOPHARMACEUTICAL DEVELOPMENTS, DYNAMIC AND STATIC IMAGING

PARTICIPANTS: Kenneth A. McKusick, Chairman, Massachusetts General Hospital, Boston, MA; and Warren R. Janowitz, Co-Chairman, National Naval Medical Center, Bethesda, MD.

BONES AND JOINTS: DIAGNOSIS OF PRIMARY AND SECONDARY BONE DISORDERS

PARTICIPANTS: Robert E. O'Mara, Chairman, Strong Memorial Hospital, Rochester, NY; George Wilson, Co-Chairman, Strong Memorial Hospital, Rochester, NY; Edward G. Bell, Crouse-Irving Memorial Hospital, Syracuse, NY; and Jon D. Shoop, Geisinger Medical Center, Danville, PA.

WEDNESDAY, JUNE 28 ANAHEIM ROOM
10:30 a.m.-12:00 p.m.

CLINICAL SCIENCE

GASTROENTEROLOGY

Chairman: Robert C. Stadalnik
Co-Chairman: Edward A. Eikman

LIVER IMAGING VIA LABELED HEPATIC BINDING PROTEIN LIGANDS. D.R. Vera, K.A. Krohn, and R.C. Stadalnik. Department of Nuclear Medicine, University of California at Davis, CA.

Can the molecular biology of hepatic binding protein HBP be utilized to upgrade nuclear diagnosis of the liver?

We have characterized the hepatic uptake of three asialoproteins, asialoceruloplasmin, asialoorosomucoid and asialofetuin using 2 radiolabels, I-123 and Tc-99m. In a normal anesthetized rabbit I-123-asialoceruloplasmin reached 63% of its peak liver activity 90 s after injection. Within 10 min the peak is reached and it returns to 63% at 30-35 min. During this time the plasma activity declined to less than 10% of the injected dose, resulting in superb liver images. Different asialoproteins and variation in percent sialic acid removed from each glycoprotein will alter the above kinetic parameters. The above combinations produce rise times which range from 75-125 s.

For any labeled HBP ligand, the kinetic parameters are constant over the entire liver field. HBP is not involved in bilirubin transport, thus its localization may not be inhibited by bilirubin. Asialoproteins are excellent candidates for functional imaging. The moderate rise time permits sufficient points with adequate statastics for curve fitting, the kinetic model uses only 2 compartments, and HBP molecular properties are well characterized, allowing for use of allosteric kinetics.

Recent work by Marshall (J.C.I. 54:555) indicated decreased HBP avidity with various liver diseases; cirrhosis, cholestasis, hepatitis and hepatic metastases. We are now investigating the ability of labeled asialoprotein functional imaging to differentiate normal from diseased animals. Asialoproteins have the selectivity, specificity and kinetic characteristics needed to yield effective diagnostic imaging of the hepatocyte. (Amer. Cancer Soc. Grant PDT-94A)

HEPATIC XENON-133 RETENTION: CORRELATION WITH LIVER BIOPSY. M.L. Ahmad, R.P. Perrillo, Y.C. Sunwoo and R.M. Donati. St. Louis VA Hospital, St. Louis and Washington University Schools of Medicine, St. Louis, MO.

We have previously demonstrated increased xenon accumulation in acute alcohol-induced fatty liver in rats and a parallel between the degree of suspected alcoholic fatty infiltration determined clinically and the degree of hepatic xenon accumulation in patients. The present study presents the results of comparison of hepatic fat content from liver biopsy with hepatic xenon accumulation in 44 patients. After 4 min of inhalation of 5-7 mCi of Xenon-133 from a closed-circuit rebreathing system and 10 min of pulmonary washout while breathing room air the degree of hepatic xenon retention was measured. Xenon retention was graded (0 to 4+) and correlated with the amount of steatosis (0 to 4+) graded on H&E stained histologic liver sections obtained by needle biopsy. Of the eight patients with 0 fat, 6 had no xenon uptake and 2 were graded as 1+. In 23 patients with 1+ fat, 4 had no xenon uptake, 12 demonstrated 1+ and 6 demonstrated 2+ xenon retention. Six patients had 2+ fat and of this group, all 6 had 2+ retention. Five patients had 3+ fat and were graded as 3+ xenon retention. Three patients had 4+ fat, 2 of these were graded as 3+ xenon retention and third patient as 4+ hepatic xenon activity. In the 9 patients who had significant hepatomegaly xenon retention proved useful in the differential diagnosis. In addition, xenon retention was useful in establishing hepatic fatty infiltration in all patients even in the absence of hepatomegaly. These data suggest that Xenon-133 retention in the liver is a simple, sensitive, and specific index of fatty infiltration of the liver, and that this technique has value as a non-invasive means of investigating hepatic fatty infiltration.

DOES HUMAN SERUM CAUSE AGGREGATION OF INJECTED RADIOCOLLOID? E.E. Kim, J.J. Coupal, F.H. DeLand and D.R. Lovelace. Veterans Administration Hospital, Lexington, KY.

It has been suggested that in vivo aggregation of liver colloid agents has been responsible for visualization of lung activity. The purpose of this study was to evaluate Tc-99m sulfur colloid (Tc-SC) particle size (a) after incubation with patient serum in vitro and (b) after a short residence in blood following IV administration to the same patient. Particle size was determined by selective filtration through polycarbonate membranes. Ten adult males with and without cirrhosis referred for liver-spleen imaging were entered into the study. Eight of the ten demon-

strated abnormal LFT's. Mean particle size of Tc-SC radiopharmaceutical was 0.38±0.09μm. Incubation of Tc-SC with serum for one hour at 37C led to reduced particle size of 0.27±0.06μm ($p<.01$). Filtration of serum obtained from the patients one minute after the Tc-SC radiopharmaceutical had been administered yielded Tc-SC particle size of 0.18±0.10μm. This value was smaller than both the injected Tc-SC ($p<.01$) and the product from in vitro incubation ($p<.05$). No relationship existed between particle size and serum albumin (observed range 2.4-4.4 gm%), total protein (6.6-8.1 gm%) or other standard clinical chemistry findings under either in vitro or in vivo conditions. In all patients with abnormal LFT's radioactivity was detectable in the lungs. This study did not substantiate the hypothesis of in-vivo aggregation of colloid, but instead demonstrated an actual decrease in colloid size.

TECHNETIUM-99m SULFUR COLLOID SCANS IN THE EVALUATION OF ABDOMINAL TRAUMA. A. Alavi, B. Berg, and R. Dann. Hospital of the University of Pennsylvania, Phila., PA. and St. Francis Hospital, Peoria, IL.

Blunt abdominal trauma can result in injuries to the liver, spleen, kidneys, vasculature, and remaining abdominal structures. The value of liver-spleen scanning is well established in the detection of injuries to these two organs. In this study, by using Tc-99m sulfur colloid as an imaging agent, we have attempted to detect and localize the site of hemorrhage in the rest of the abdomen. In seven dogs injuries were made to the liver, spleen, inferior vena cava, mesenteric arteries and veins, kidneys, and small bowel after laparotomy. 15 mCi of Tc sulfur colloid were injected intravenously and immediately the abdomen was imaged at frequent intervals. All the bleeding sites were clearly visualized. The early images were crucial in the accurate localization of the bleeding sites. Delayed images showed spread of activity to a larger area. This is especially true of high bleeding rate areas. Retroperitoneal bleeding from the kidneys appeared more confined compared to intraperitoneal hemorrhage.

Using the above technique in six patients with injuries to the vessels of the mesentery(4), kidney(1), and pelvis (1), we were able to successfully detect and localize the bleeding sites. These findings played an important role in the management of these patients.

In conclusion, Tc-99m sulfur colloid imaging in abdominal trauma appears to be of significant value not only in the detection of injuries to the liver and spleen, but to the contents of the abdomen as well.

SCANNING OF THE HUMAN PANCREAS WITH DL-VALINE-1-C-11 AND DL-TRYPTOPHAN-1-C-11. K. F. Hübner, R. L. Hayes, L. C. Washburn, W. Gibbs, B. L. Byrd, and T. A. Butler. Oak Ridge Associated Universities (ORAU) and Oak Ridge National Laboratory (ORNL), Oak Ridge, TN

Our previous animal studies with the C-14-labeled compounds demonstrated that DL-valine and DL-tryptophan have much greater pancreatic specificities than 75-Se-L-selenomethionine. This made the use of C-11-carboxyl-labeled DL-valine and DL-tryptophan for clinical pancreatic imaging obvious. Nine patient studies were done with 11-C-DL-valine and highly shielded conventional rectilinear scanning equipment using doses of between 13.5 to 45 mCi. C-11-DL-Tryptophan was used for rectilinear pancreas scanning in two patients and with a positron tomograph (ECAT) in 16 patients using doses of between 5 and 35 mCi. Both radiopharmaceuticals were well tolerated, producing no toxic or other side effects and did not alter hematological or biochemical parameters of the patients. Prompt (5 min.) visualization of the human pancreas was demonstrated for both amino acids. Initial clinical results were promising with regard to demonstration of normal pancreatic tissue and the clarity of the images obtained. Application of positron computerized axial tomography offers unique possibilities for dynamic functional studies of the pancreas.

(This work was supported by USPHS Research Grant CA-14669 from NCI. Both ORAU and ORNL are under contract with the U.S. DOE.)

GASTRIC FUNCTION IN DIABETIC PATIENTS -- GASTRIC SCANNING AND MEASUREMENT OF ACID SECRETION. S.E. Lewis, D. B. Corbett, C.T. Richardson, J.S. Fordtran. University of Texas Health Science Center, Dallas, TX.

Management of the longstanding insulin-dependent diabetic may be complicated by unpredictable diabetic control and prominent GI symptoms such as vomiting and diarrhea. Longstanding (>8 yrs) diabetics with neuropathy (DN) and diabetics without neuropathy (D) were studied and compared to normal controls (N) and truncal vagotomy (V) patients. Acid secretion (meq/hr) was measured in response to sham feeding (SF) and pentagastrin. Gastric emptying was evaluated by serial gamma camera imaging following the ingestion of 1 mci Tc-DTPA mixed with a test meal.

	N(n=10)	DN(n=11)	D(n=6)	V(n=24)
Sham feeding	12±2	2±.8	4±2	3±1
Pentagastrin (12 μg/kg)	33±5	30±3	29±7	30±3
Gastric retention @ 90 min	<20%	>50%	>30%	>50%

Diabetics had a normal response to pentagastrin but only minimal response to sham feeding, similar to vagotomized patients. Sham feeding was repeated in 3 diabetic patients during i.v. insulin infusion to normalize blood sugar. No change in response indicates that poor sham feeding response in diabetics is not due to hyperglycemia. Conclusions: 1)Longstanding diabetics, with & without clinical evidence of neuropathy, have decreased acid secretory response to sham feeding suggestive of autovagotomy; 2)Most of these patients have clearly abnormal gastric emptying, presumably because of abnormal vagal innervation; 3)Autovagotomy may precede other clinical evidence of neuropathy; 4) Gastric scanning is a sensitive indicator of neuropathy in such patients.

THE MODE OF ACTION OF ALGINIC ACID COMPOUND IN THE REDUCTION OF GASTROESOPHAGEAL (G-E) REFLUX USING THE G-E SCINTISCAN. L.S. Malmud, R.S. Fisher, J.L. Littlefield, R. Rosenberg, S. Dessel, P.T. Makler, Jr., N.D. Charkes, Temple University Hospital, Philadelphia, PA.

The G-E scintiscan (GES) has been employed previously to quantitate the effect of anti-reflux therapy on G-E reflux (GER). The results were compared to lower esophageal sphincter (LES) pressure measurements. With some therapies, a direct relationship between LES pressure and GER was confirmed; but alginic acid compound (AA) reduced GER without altering LES pressure. This study was designed to evaluate and quantitate the mode of action of AA, Sodium alginate labeled with Sr87m was reconstituted into a tablet with the antacid mixture. Following a standard GES, a dual isotope study was performed using 300 uCi Tc99m sulfur colloid (SC) in water plus 500 uCi Sr87m AA. Ten patients with symptomatic GER and 10 normals were studied in the upright position. Serial 30 second images were obtained while the G-E pressure gradient was increased from 10 to 35 mmHg at 5 mm Hg increments using an inflatable abdominal binder. Data were processed on a digital computer with corrections made for Sr87m scatter. Areas of interest in the esophagus and stomach were selected. Most of the AA (75±20%) appeared to float in the upper half of the stomach in both patients and controls regardless of the order of administration. In symptomatic patients, following AA, the GER index decreased by 34.3±2.0% ($p<.01$). When reflux did occur, the Sr87m AA refluxed preferentially as a greater percent of the administered dose than did the Tc99m SC. Conclusions: (1) AA reduces GER, (2) in the upright position AA floats on the top of the gastric meniscus,(3) AA refluxes preferentially to other gastric contents. This study suggests that AA reduces reflux by its foaming and viscous properties.

WEDNESDAY, JUNE 28 SOUTH EXHIBITION HALL
10:30 a.m.-12:00 p.m.

BASIC SCIENCE

RADIOPHARMACEUTICALS III: POSTER SESSION

Chairman: David A. Goodwin
Co-Chairman: Frank P. Castronovo, Jr.

SELECTION OF TARGET AND TARGET CLADDING MATERIALS FOR ISOTOPE PRODUCTION AT THE LOS ALAMOS MESON PHYSICS FACILITY (LAMPF). J. W. Barnes, G. E. Bentley, T. P. DeBusk, P. M. Grant, H. A. O'Brien, Jr., A. E. Ogard, and M. A. Ott. Los Alamos Scientific Laboratory (LASL), Los Alamos, NM.

Irradiation of targets with 600-800 MeV protons to provide biomedical isotopes at LAMPF requires that the choice of target and/or target cladding materials be given special consideration. The presently available beam intensity is 300μA with a projected design intensity of 1mA. Energy deposition rates in targets are sufficiently high that without adequate cooling target melt-down would result. Radiation induced reactions in the cooling water result in the formation of significant concentrations of H_2, O_2, H_2O_2, and other potentially corrosive species.

The criteria used to establish the need for, and the type of cladding for a target are the reactivity of the target material, the melting point of the target, the possibility of contamination of a product isotope with carrier impurities, and the establishment of localized oxidation reduction couples.

Steady state temperature profiles of the target plus cladding are calculated using a computer code developed at LASL. The code utilizes target dimensional, thermal, and energy deposition parameters, and the thermal and flow parameters of the cooling medium to calculate isotherms, and the maximum temperature to be expected during an irradiation.

TECHNETIUM-99m(Sn)PYRIDOXYLIDENEAMINATES AS HEPATOBILIARY TRACT IMAGING RADIOPHARMACEUTICALS: PREPARATION AND BIOLOGICAL EVALUATION. M. KATO and M. HAZUE. Nihon Medi-Physics Co., Ltd. Takarazuka, Hyogo, JAPAN.

A new method of labeling pyridoxylideneaminates with Tc-99m has been established using divalent tin as the reductant. Several Tc-99m(Sn)pyridoxylideneaminates have been prepared by the simple mixing of a kit reagent with pertechnetate at room temperature, and their chromatographic and in vivo properties were compared with those of corresponding Tc-99m pyridoxylideneaminates prepared by Baker's autoclaving method.

Both Tc-99m(Sn)pyridoxylidenevaline[Tc-99m(Sn)PVal] and the isoleucine analog[Tc-99m(Sn)PIle], the most hydrophobic complexes among the tested ones, showed marked and rapid biliary excretion in rats; over 90% of the activity retained by the body has been excreted into the gut through the liver during the first hour, with 10-15% of the total dose appearing in the urine. Scintigraphic studies using rabbits gave similar results; the gallbladder was visualized within 5 min of injection.

Toxicity studies in four animal species indicated a wide margin of safety for the proposed dose of Tc-99m(Sn)-PVal and Tc-99m(Sn)PIle for the diagnosis of human hepatobiliary disorders.

Following the i.v. injection of Tc-99m(Sn)PIle in a normal human subject, clear visualization of the hepatic duct, cystic duct, gallbladder, and common bile duct was obtained within 15 min of injection.

The results described above, and considerations on the chemistry of the preparation and the structure of the complexes led us to the conclusion that Tc-99m(Sn)PIle is a promising agent for the diagnosis of hepatobiliary disorders.

THE EFFECT OF IONOPHORES ON THE BIODISTRIBUTION OF THALLIUM IN THE RAT. R.C. Gatson, L.R. Hendershott, F.S. Ordway, and J.W. Fletcher. St. Louis VA Hospital and St. Louis University School of Medicine, St. Louis, MO.

The ability of ionophores to transport cations across lipid membranes indicates that these compounds might have an effect on the biodistribution of Tl-201, a monovalent cation currently used as a heart imaging agent. In the present study the distribution of Tl-201 in the rat was assessed alone or in combination with 3 ionophores: RO2-2985, valinomycin or 18-Crown-6 ether. Parallel in vitro TLC, partition ratios and back extraction studies were done to evaluate ionophore-cation complex stability. Groups of rats received either Tl-201 followed by ionophore 5 min later, or Tl-201 and ionophore simultaneously. Control groups received Tl-201. All rats were killed 30 min after Tl-201 and the radioactivity in the blood, plasma, muscle, heart, lungs, spleen, liver and kidney measured. In parallel in vitro experiments a simulated lipid biolayer and TLC was used to measure complexation and to evaluate stability of the complex. Valinomycin and 18-Crown-6 had little or no effect on the biodistribution or TLC pattern of Tl-201. Both failed to partition more than 28% of the Tl-201 to the organic phase of the lipid biolayer. RO2-2985 increased blood Tl-201 concentration 2-fold, and decreased heart and lung concentrations. Seventy-seven % of Tl-201 was partitioned to the organic phase at concentrations affecting biodistribution but only 35% at concentrations that did not affect biodistribution. These data suggest that the simulated lipid biolayer may provide an in vitro measure of biologic activity, that no or only transient complexation occurs between the ionophores tested and thallium, and that RO2-2985 affects the biodistribution of Tl-201.

USE OF LABELED ANTIBODIES TO DETECT OCCULT INFECTION. M.K. Elson, L.R. Peterson, A.J. Kozak, and R.B. Shafer. V.A. Hospital, Nuclear Medicine Svc., Minneapolis, MN.

The ability to prepare labeled antibodies with unique specificity to pyrogenic bacteria would permit imaging deep-seated infection. Gallium-67 citrate is commonly used as a radiopharmaceutical for localizating occult infection. Specificity of this pharmaceutical is limited by its concentration in the liver, spleen, axial skeleton and gastrointestinal tract. This study was undertaken to determine the feasibility of using labeled autologous antibody to image sites of occult infection.

An experimental rabbit model of intraabdominal abscess was used to produce antibody to E. coli. Four perforated table tennis balls were implanted intraperitoneally. Six weeks after implantation, two of the balls were injected with 10^8 colony-forming units of E. coli. Ten weeks after innoculation, 15 cc of serum was obtained for antibody labeling. The serum was fractionated by starch block electrophoresis, and the γ-globulin fraction containing specific E. coli agglutinating activity was eluted and labeled with Iodine-131. Chromatography showed 97.5% activity bound to protein. Four hundred μCi's of labeled antibody were injected and the animal sequentially monitored. Uptake in the table tennis balls of the infected rabbit was demonstrated 8 hours after administration. Similar monitoring of a non-infected rabbit showed no appreciable localization in the area of the table tennis balls.

At sacrifice, the infected table tennis balls showed increased uptake of radioactivity relative to other tissues. This study demonstrates the possibility of imaging with labeled antibodies to localize occult infection.

TC-99m LABELED STEROIDS AS HEPATOBILIARY RADIOPHARMACEUTICALS. D.W. Porter, M.D. Loberg, A.T. Fields. University of Maryland, Baltimore, Maryland 21201

Various steroids particularly the endogenous steroid, cholic acid, are known to be actively secreted by the liver. Two steroidal iminodiacetic acid analogs, compounds I and II, were synthesized from the steroids pregnenolone and cholic acid, respectively. Structure determination of these analogs was accom-

plished by the use of melting point data, thin-layer chromatography, NMR, and CHN analysis. Both compounds were labeled with Tc-99m using the stannous reduction method in aqueous-alcohol (50:50) at a pH of 5.5. Radiochromatographic data indicated that both compounds chelated with reduced Tc-99m in yields approaching 100%. HPLC data demonstrated that compound I formed a single stable radiochemical, whereas compound II formed a number of radiochemicals. The carbamoylmethyl IDA chelating group in compound I favored the formation of a pure Tc-99m labeled radiopharmaceutical. Tissue distribution in mice demonstrated that C-14 II and C-14 cholic acid had rapid hepatic clearance with 60 min intestinal activity of 67.3% and 75.5% respectively. The Tc-99m labeled steroids displayed slower hepatic clearance. Tc-99m-II and Tc-99m-I exhibited 60 min intestinal activity of 30.3% and 40.0% respectively. Imaging studies of these agents in normal dogs demonstrated rapid and prominent uptake in the gallbladder. 24 hour scans clearly showed liver, gallbladder, and intestinal activity. These studies demonstrated that in general, Tc-99m can be chelated by steroidal analogs to form stable and radiochemically pure radiopharmaceuticals and specifically that certain steroidal analogs may be useful in determining both hepatobiliary function and liver morphology.

MODIFICATION IN THE METHOD OF LABELING PLATELETS WITH INDIUM-111. M.J. Welch, C.J. Mathias, H.H. Davis, W.A. Heaton, H.J. Joist, L.A. Sherman and B.A. Siegel. Mallinckrodt Institute of Radiology, Washington University School of Medicine, St. Louis, MO.

Recently a procedure was developed for the labeling of dog and human platelets with indium-111.[1] The procedure for the labeling of human platelets utilized Tyrode's solution which contains apyrase, a material not approved for human use. While adapting the preparation for human studies the following modifications have been made to our original preparation. (1) The labeling of platelets is carried out in a modified Tyrode's solution which contains no protein and no phosphate, the buffer system being citrate and the anticoagulant heparin (50 U/ml). (2) The indium 8-hydroxyquinoline is no longer prepared using an organic extraction. Oxine (50 µg in 50 µl ethanol) is simply added to the indium-111 chloride and this solution added to the modified Tyrode's solution which is used to resuspend washed platelets. The addition should proceed immediately or else lower yields are obtained. (3) After the labeling procedure the labeled platelets are mixed with the patient's plasma to remove any indium that is not intracellular. The platelets are washed before the plasma incubation as in the presence of oxine labeled platelets release indium-111 in plasma.

Utilizing this technique we have shown that the platelets function in vitro (aggregation studies with ADP and collagen), show no aggregation and preliminary data show good in vivo function. Following in vitro incubation of the platelets with plasma or whole blood, little release of indium-111 is observed.

1. Thakur ML, Welch MJ, Joist JH and Coleman RE. Thrombosis Res. 9:345, 1976.

EVALUATION OF A NEW 5-COMPARTMENTAL MODEL OF F-18-FLUORIDE KINETICS IN RATS. N.D. Charkes, M. Brookes, and P.T. Makler, Jr., Temple University Medical School, Philadelphia, PA., and Guy's Hospital Medical School, London, U.K.

We have recently described a new 5-compartment model of F-18-fluoride (F-18) kinetics in humans, which accords well with available data. The model assumes rapid dispersion of F-18 from blood into extracellular fluid (ECF), including bone-ECF, with subsequent uptake by bone substance and urinary excretion. The model is fitted by the SAAM-25 program on an IBM-370 computer, which generates bidirectional rate constants between compartments, given only blood and urine values. The purpose of this study was to test, in rats, the basic assumptions underlying the model. Sixty-eight male Wistar rats, 10-12 weeks old, were injected with Br-77-bromide (an ECF tracer) and F-18 simultaneously, and with Cr-51-labeled rbc's, and killed by hemisection at frequent intervals up to 2 hr post-dose. The ratio of the virtual volumes of distribution of fluoride and bromide was not significantly different from unity (0.96±.05 CL95), corroborating the assumption of initial F-18 distribution into ECF. There was excellent agreement between computer-generated values for bone F-18 uptake and measured concentrations, as well as with bone-ECF concentrations. Cardiac output in these rats was measured by a new isotopic technique and found to be about 138 ml/100 gm bone-min; skeletal blood flow was 16.1% of cardiac output, or 22 ml/100 gm bone-min. Transfer of F-18 from bone-ECF to bone was observed in dead rats, as predicted by the computer. Conclusions: Fluoride is a freely diffusible ion which rapidly penetrates body ECF spaces. Measured concentrations in rats accord well with projections made by computer analysis of a new 5-compartment model.

NORMALITY OF RADIOPHARMACEUTICAL DISTRIBUTION DATA. K.A. Krohn and Horace H. Hines, Department of Nuclear Medicine University of California, Davis, CA.

To test whether radiopharmaceutical tissue distributions conform to the normal probability curve, we analyzed % injected dose/g measurements for Ga-Cit, I-Bleo, and I-Fibrinogen in tumor, liver, and lung of tumored mice. Mean and standard deviation (SD) of the z-transformed data were calculated at all times for which three or more mice had been studied (275 measurements). In addition, the third (skewness) and fourth (kurtosis) moments of the distribution were calculated.

All radiopharmaceuticals/organs/times tested were normally distributed except for I-Bleo in tumor up to 6 hrs after injection. The later finding is probably because of the rapid change in tumor concentration of I-Bleo from 1 to 6 hrs. The higher moments suggested a slight positive skew and were borderline platykurtic but were within P=0.10.

To test the criticality of normal distribution in applying the Student's t-test, we defined an arbitrary right skewed distribution and used a random number program to select values. These numbers were grouped consecutively into 3, 4, 5, or 10/group for which mean and SD were calculated. The means of 1000 sets of numbers were normally distributed about a mean which was equal to the mean of the sampled population. From each of the 1000 means/SD (n=3,4,5,10), 500 pairs were selected at random and the t-statistic calculated. In 0/2000 of these pairs did the t value imply a statistically significant difference at P=0.05.

In summary, concentrations of the radiopharmaceuticals tested were normally distributed. The Student's t-test is valid, indeed conservative, for testing the significance of differences in tissue concentrations of these radiopharmaceuticals. (American Cancer Society Grant #PDT-94A.)

PREPARATION AND EVALUATION OF (F-18) FLUOROANTIPYRINE. P.J. Robbins, D.L. Fortman, and V.J. Sodd. FDA, Nuclear Medicine Laboratory, Cincinnati, OH.

The purpose of this work was to prepare and evaluate (F-18) labeled fluoroantipyrine as a possible regional perfusion imaging agent for central nervous system. Regional perfusion scanning of the central nervous system requires lipophilic radiopharmaceuticals that rapidly penetrate the intact blood-brain barrier and which are labeled with short T-1/2 radionuclides. Because of its lipid solubility and the physical characteristics of fluorine-18, (F-18) fluoroantipyrine was considered a promising agent to evaluate. (F-18) fluoroantipyrine was prepared by the Schiemann reaction scheme as follows: 4'-aminoantipyrine was converted to antipyrine 4'-diazonium fluoroborate. Reactor produced F-18 in an aqueous solution was exchanged with the fluorine of the diazonium salt. The water was evaporated and the salt was pyrolyzed at 165°C. (F-18) 4'-fluoroantipyrine (specific activity 0.83-2.7 µCi/mg) was separated from the decomposition residue by column chromatography on alumina. The maximum radiochemical yield was 1.9%. This is reasonable in light of the 25% maximum possible radiochemical yield of the Schiemann decomposition and the 20% maximum chemical yield obtained in this pyrolysis. Studies of the distribution of this radiopharmaceutical at 12, 30, 60, 120 seconds and 10 minutes in Swiss-Cox mice

weighing approximately 30 g indicate that the radioactivity persists in the brain tissue for up to 120 sec at a level that is greater than that of skin and bone (representative of scalp and skull). It is concluded that F-18 fluoroantipyrine could be used for positron camera imaging of human brain regional perfusion when larger quantities of F-18 fluoroantipyrine are available.

FACILE METHOD FOR THE INTRODUCTION OF Te-123m INTO ORGANIC MOLECULES:SYNTHESIS OF 3-METHYL-TELLURO-Te-123m-CHOLESTEROL. G.P. Basmadjian, G.R. Parker, A.S. Kirschner, R.D. Ice, R.A. Magarian, and S.L. Mills, College of Pharmacy, The University of Oklahoma Health Sciences Center, Oklahoma City, OK.

An easy method of introducing tellurium-123m into organic molecules has been developed. Te-123m has good physical properties (single γ of 159 keV, $t_{\frac{1}{2}}$=117d) and since it forms covalent bonds it is a potential radionuclide for a new generation of radiopharmaceuticals.

The method involves the production of a reactive species (disodium ditelluride,Na_2Te_2) from metallic Te-123m and $NaBH_4$ in ethanol. The introduction of Tellurium-123m was accomplished by two methods:

Route 1: $Te + NaBH_4 \xrightarrow{EtOH\text{-}NaOEt} Na_2Te_2 \xrightarrow{CH_3I} CH_3TeTeCH_3$

$CH_3TeTeCH_3 + NaBH_4 \rightarrow CH_3TeNa \xrightarrow{RY^*} CH_3Te\text{-}R$

Route 2: $Te + NaBH_4 \xrightarrow{EtOH\text{-}NaOEt} Na_2Te_2 \xrightarrow{RY} R\text{-}TeTe\text{-}R$

$R\text{-}TeTe\text{-}R + NaBH_4 \longrightarrow R\text{-}TeNa \xrightarrow{CH_3I} R\text{-}Te\text{-}CH_3$

(*R=cholesterol, Y=p-tosylate)

The solubilization of the Te metal was found to require reflux conditions in a N_2 atmosphere. Route 2 was found to be more suitable to the synthesis of 3-methyl-telluro-cholesterol since yields were higher. 3-Methyl-telluro-cholesterol was characterized by NMR, IR and mass spectroscopy as well as elemental and chromatographic analysis. The molecule containing the Te-123m radionuclide was found to have identical chromatographic properties in two solvent systems as the non-radioactive molecule. Specific activity of the Te-123m compound was 0.2 mCi/mg.

L OR D/L TRYPTOPHAN FOR PANCREAS SCINTIGRAPHY? K.A. Krohn, R.C. Stadalnik*, N.M. Matolo, and L.J. Hein, Departments of Nuclear Medicine and Surgery, University of California, Davis, CA.

Almost every common amino acid has been tested in animals as a potential labeled metabolite for pancreas scintigraphy. From results reported from several independent laboratories, we concluded that labeled tryptophan was the most promising and therefore asked the question posed by this title. The in vivo organ concentrations of commercially available racemic and pure L-C14-tryptophan labeled at the side chain methylene were compared with DL-Se75-selenomethionine in healthy adult Long-Evans rats. Three animals were injected with each agent and sacrificed at 15, 30, 45 60, 90 min. A weighed standard and samples of blood, pancreas, liver, spleen, kidney and muscle were counted by standard liquid scintillation techniques, including quench correction by the channel ratio method. Results were measured as percent injected dose/g and per whole organ.

The spleen and muscle concentrations were indistinguishable for the three compounds at all times studied. Kidney concentration was only slightly higher for racemic trp at later times, reflecting renal excretion of nonmetabolic D-trp. The concentration of L-trp was 1.4 to 1.8 times that of DL-trp in the pancreas and 1.0 to 1.3 times that of DL-trp in the liver at 15 to 45 min, but this differential decreased somewhat at later times. The pancreas/liver ratio is much higher for trp than for Se-met. For L-trp it is at least 5-fold higher. Because the rat is able to partially metabolize D-trp via an inversion step, stereoisomeric differences may be even larger for humans. Enzymatically labeled ^{13}N-L-trp may be a very useful agent for pancreas scintigraphy.

*Picker Scholar, James Picker Foundation.

Mn-52m - A NEW SHORT-LIVED, GENERATOR-PRODUCED RADIONUCLIDE. R.W. Atcher, A.M. Friedman, Argonne National Laboratory, Argonne, IL, J. R. Huizenga, University of Rochester, Rochester, NY, and G.V.S. Rayudu, E.A. Silverstein, D.A. Turner, Rush University Medical Center, Chicago, IL

Dynamic studies would be benefited by the use of short-lived radionuclides. One good radionuclide is Mn-52m, (half-life, 21.1 minutes) a positron emitter. Mn-52m decays in two branches; 98% goes to the ground state of Cr-52 and 2% goes by isomeric transition to Mn-52g. The parent, Fe-52 (half life, 8.3 hours), is produced by He-3 bombardment on natural chromium. Fe-52 is separated from the target and loaded onto an anion exchange column. Mn-52m is eluted in 8 N HCl; the yield is 55% of Mn-52m on the column. Fe-52 breakthrough is 0.01% of the Fe-52 on the column. Typical elution volumes are 0.40 ml. The eluted activity is evaporated to dryness and dissolved in acetate buffer (pH 5). Studies with longer lived Mn-54 have shown that manganese (II) concentrates in the myocardium less than five minutes post-injection and uptake exceeds that of Tl-201. This, coupled with the many oxidation states of manganese enabling one to make a large variety of radiopharmaceuticals, shows the generator to be one of great promise as a diagnostic tool.

RATE OF [C-14]-OCTANOATE OXIDATION TO [C-14]-CARBON DIOXIDE AS A TEST FOR CIRRHOSIS. J.L. Rabinowitz, J. Hansell, and Jean Staeffen. VA Hospital-University of Pennsylvania, Philadelphia, PA and University of Bordeaux, Bordeaux, France

The correlation of the serum octanoate level with the degree of cirrhotic involvement(Rabinowitz, et al., Clin. Chem. 23:2202-6(1977) and J Lab. Clin. Med., 91:223-7 (1978)), suggested to us that the rate of octanoate oxidation to carbon dioxide could be used to evaluate liver cirrhosis in the alcoholic.

The addition of a trace quantity (<1 ng of [C-14]-octanoate) to the octanoate blood-pool of fasted patients, permits the approximate determination of the biological half-time of the octanoate pool in the patient. Experimentally, it was determined that the rate of its oxidation in various subjects was the same whether given orally or by intravenous route. Ingestion of 1-5 microcuries of [1-C-14] or [8-C-14]-octanoate was followed by the collection of the [C-14]-carbon dioxide released in breath at fixed time intervals (Similar to the test for upper GI, bacterial infection, Am. J Med. Sci. 267:35-9(1974)). Micromole equivalents of [C-14]-carbon dioxide were taken and assayed at 5 to 10 minute intervals (for 60 min), then at 15 to 30 minute intervals (for 120 min). Results were plotted (total radioactivity per micromole vs time) for different patients.

The time required for the maxima of [C-14]-carbon dioxide respiratory clearance to be reduced by one-half was judged to be approximately equal to the biological half-life of the octanoate pool. We have observed that patients with a serum octanoate of 0 to 5 microequivalents per liter have a biological half-life between 20 and 75 minutes while patients with a serum octanoate of 8.5 to 15uE/l showed a biological half-life between 85 and 245 minutes.

A METHOD FOR LABELING RED BLOOD CELLS WITH Tc-99m UTILIZING THE AMICON ON-LINE COLUMN ELUATE CONCENTRATOR. Lynn Hendershott, Rita Gatson, Frederick Ordway, Munir Ahmad, St. Louis VA Hospital and St. Louis University School of Medicine, St. Louis, MO.

This method automates the preparation of autologous Tc-99m labeled RBCs utilizing the Amicon on-line column eluate concentrator to separate the plasma from the RBCs. The column eluate concentrator required a 0.6 micron filter over which rat blood was continuously recirculated until all of the plasma was removed and the RBCs remained in a solution of 0.9% sodium chloride. The RBCs were pretreated with stannous diphosphonate to provide 0.017 mg stannous ion as a tin source for the tagging reaction. A 5% solution of EDTA and 0.9% sodium chloride followed by 0.9% sodium chloride were used in the column eluate concentrator until all plasma was removed from the RBCs. Then, Tc-99m sodium pertechnetate solution was added and

incubated for 15 min. These Tc-99m RBCs were compared to Tc-99m RBCs produced in a similar manner except that centrifugation was used to separate the RBCs from the plasma with 5% EDTA and 0.9% sodium chloride rinsings. Both Tc-99m RBC preparations had a 98% or more tagging efficiency and were equally stable in vivo. Rat distribution studies 5 and 30 min post I.V. injection show that both preparations have more than 90% of the injected dose in the intravascular space, and less than 5% in the rat liver which indicated that the RBCs are sufficiently intact to provide adequate intravascular imaging. The column eluate concentrator can be set up in series in order to prepare several samples of autologous Tc-99m RBCs simultaneously thus minimizing technician time and handling of the blood.

RADIOCHEMISTRY AND BIOLOGIC PROPERTIES OF TECHNETIUM-99m EDTA ANALOGS. R.J. Baker, C.I. Diamanti, D.A. Goodwin and C.F. Meares.

We have previously demonstrated that when bifunctional chelating agents are covalently coupled to biologic molecules they provide highly stable, kinetically inert binding sites for In-111 without destroying the biologic properties. Theoretically, Tc-99m should also be an excellent label for these chelate conjugates, thus its binding to various EDTA analogs was examined in vitro and in vivo.

Labeling was carried out under nitrogen using stannous ions as the reducing agent, with analysis by cellulose acetate electrophoresis and thin-layer chromatography. Quantitative distribution was determined in BALB/c mice and computerized renograms were performed on New Zealand rabbits.

In this manner, stable chelates of EDTA and DTPA were produced containing 90-95% of the radioactivity in the chelate form. Binding to phenyl substituted EDTA was less satisfactory under the chosen conditions, but yields of labeled chelate in excess of 70% were obtained. These compounds migrated towards the anode on electrophoresis enabling separation from free pertechnetate and Sn(II)-reduced Tc-99m. In animals, renal clearance was the main excretory route and clear images of the kidneys were obtained during the rabbit study with all three compounds. The renograms showed that maximum activity in the kidneys was achieved in 4-5 min with Tc-99m EDTA, in 2.5-3.5 min with Tc-99m DTPA and in 1.5-2 min with Tc-99m phenyl-EDTA. The very rapid excretion of the phenyl compound suggests a potential use for renal function studies. Further implications of this work are that substituted EDTA derivatives conjugated to other molecules should be capable of producing new Tc-99m radiopharmaceuticals with the stability of binding demonstrated by EDTA.

WEDNESDAY, JUNE 28 CALIFORNIA B ROOM
10:30 a.m.-12:00 p.m.

IN VITRO AND CORRELATIVE TECHNIQUES

ULTRASOUND

Chairman: James H. Pritchard
Co-Chairman: Orlando L. Manfredi

PANORAMIC VIEW OF ULTRASOUND PROCEDURES. E. N. Carlsen, Loma Linda University Medical Center, Loma Linda, CA.

ULTRASOUND AS A DIAGNOSTIC AID FOR UTERINE MYOMAS. B.D. MERER, A.A. Bezjian. University of Miami School of Medicine, Miami, FL.

A retrospective study investigating the clinical utility and accuracy of the ultrasonographic diagnosis of myomas was carried out.

All patients with a diagnosis of uterine myomas by ultrasound were selected for the study. For each case the clinician's initial diagnosis and the final pathologic diagnosis was recorded.

Cases and conditions which resulted in an incorrect sonographic diagnosis of myoma were reviewed. It was found that large extrauterine pelvic masses that were continuous with the uterus and created poor interfaces between uterus and extrauterine mass made identification of the uterus difficult and sometimes resulted in sonographic diagnostic errors. Such conditions include endometrial or ovarian carcinoma, large inflammatory masses and pelvic endometriosis.

Ultrasound alone furnished a correct diagnosis of myomas more often than the clinical diagnosis alone. We feel that when ultrasound examination is added to the clinical exam in patients suspected of having myomas the pre-surgical diagnosis becomes more accurate.

Pelvic ultrasonography in the diagnosis of uterine myomas has a 90% accuracy and therefore is of notable clinical utility.

THE INHOMOGENEOUS LIVER SCAN: ULTRASOUND CORRELATION. N. Chafetz, A. Taylor, N. P. Alazraki, and B. Gosink. Veterans Administration Hospital, San Diego, CA.

Previous studies have evaluated the sensitivity and specificity of liver scanning in the detection of metastatic disease. This study was designed to answer the question: Is an ultrasound liver scan useful in detecting metastatic disease when the nuclear scan shows a "mottled" or inhomogeneous distribution of 99m-technetium sulfur colloid?

We evaluated the hepatic echographic findings in 55 scans of 48 patients with suspected metastatic disease whose nuclear scans showed an inhomogeneous radiocolloid distribution. The inhomogeneity was graded as minimal (42%), moderate (10), or severe (3); the results were correlated with multiple transverse and longitudinal echograms of the liver performed within 10 days of the nuclear study, using a Picker EDC gray scale ultrasonic scanner and a 2.25 Mega Hertz transducer.

Fifty-two of the 55 scans were classified as mild to moderately inhomogeneous. Of the 52 corresponding echograms, 35 (67%) were normal, 11 (21%) were consistent with the hepatocellular disease, 3 were incomplete studies because of abdominal gas, and 2 were falsely suspicious for space occupying lesion. The sonogram in one of three patients with a severely inhomogeneous scan correctly detected the presence of a metastases.

As diagnostic radiographic exams become more sophisticated and expensive, it is important that physicians avoid duplication of information with unnecessary additional procedures. A normal liver scan is strong evidence against a tumor being detected by ultrasonic imaging and a slightly inhomogeneous liver scan probably has similar prognostic value.

GUIDED ULTRASOUND EXAMINATION BASED ON DIRECT MEASUREMENTS OF RADIONUCLIDE LIVER AND GALLIUM SCANS. R.B. Grove, M.L. Born and R.L. Martin, V.A. Hospital, Nashville, TN.

B-mode ultrasound scanning is of proven utility in the investigation of hepatic and abdominal disease. Ultrasound images are tomographic, allowing a lesion to be missed if the proper tomographic cuts are not obtained. The purpose of this study was to evaluate the usefulness of direct measurement of the location of apparent lesions in radionuclide liver and gallium images as a means of directing ultrasound imaging to specific areas of interest. Markers were carefully placed on the xyphoid in anterior and right lateral Tc-99m sulfur colloid liver images and the xyphoid identified in total body Ga-67 citrate scans. Measurements were based on size markers placed in the camera field on liver images and the verified 5:1 minification of the total body gallium scans. The center and extent of potential lesions were measured in cm relative to the xyphoid. These measurements were used to optimize the ultrasound examination. Preliminary results indicate that in each of 8 apparent hepatic focal defects in Tc-99m sulfur colloid images, the radionuclide scan measurements allowed immediate optimum ultrasound localization of lesions as small

as 2-3 cm. In every case, radionuclide measurements corresponded within 1-2 cm of the subsequently identified lesion location and extent in ultrasound images. Similar findings were noted in 3 patients with gallium scan abnormalities. Initial results suggest that direct radionuclide scan measurements can provide increased efficiency of lesion detection in ultrasound examination of the liver and abdomen and increase confidence in negative ultrasound result. Assistance in differentiating bowel uptake of Ga-67 from abdominal lesions is also provided.

WEDNESDAY, JUNE 28 GARDEN GROVE ROOM
2:00 p.m.-3:30 p.m.

CONTINUING EDUCATION

PEDIATRICS I (CLINICAL SCIENCE)

Chairman: Salvador Treves
Co-Chairman: Theodore Harcke

Tc-99m-DIPHOSPHONATE ABDOMINAL IMAGING IN NECROTIZING ENTEROCOLITIS: A PROSPECTIVE STUDY.
G.N. Sfakianakis, V.N. Ortiz, G.M. Haase, and E.T. Boles,Jr. Columbus Children's Hospital, Columbus,OH.

Necrotizing enterocolitis (NEC) a serious disease of the newborn, may respond to medical therapy, or require surgical intervention. A prospective study was performed to evaluate the possibility of diagnosing intestinal necrosis by abdominal imaging using Tc-99m-diphosphonate.

After animal experimentation and experience in newborns and infants who underwent bone imaging for detection of osteomyelitis, the "negative" abdominal image was defined. Imaging was performed 3 to 4 hours after injection using a high resolution parallel hole collimator. With the patient placed on the inverted detector 350,000 counts were accumulated from the xyphoid process to the symphysis pubis. Anterior, lateral and oblique views were taken.

Twenty two studies were performed in patients admitted to the NEC protocol. Three studies showed increased abdominal activity, 2 generalized and 1 focal. The patients had to be operated upon and resected bowel showed transmural necrosis. In a fourth case the injected patient had to be taken to the operating room before imaging. He had a negative study 1 hour post operatively and his resected dead bowel gave positive in vitro images with comparative settings.

Fifteen patients had negative abdominal images. All improved clinically and did not require surgery.

Finally 3 patients had studies which were considered suspicious; they also improved on medical therapy.

The results of this study indicate that abdominal imaging with Tc-99m labeled phosphates may be useful in predicting irreversible intestinal necrosis in NEC.

ABDOMINAL IMAGING FOR ECTOPIC GASTRIC MUCOSA: A REEVALUATION.
G.N. Sfakianakis, G.M. Haase, and V.N. Ortiz, Thomas S. Moore, Columbus Children's Hospital, Columbus, Ohio.

A retrospective analysis of 120 studies of abdominal imaging with Tc-99m-pertechnetate was done. Fifty seven studies were performed with the rectilinear scanner (2 scans, starting immediately and 30 min after injection) and 63 with the gamma camera (serial imaging in 10 min intervals for 60 min). Patient preparation included overnight fasting, withholding of medication and deferring of abdominal barium studies. Additional camera imaging in upright position was necessary to differentiate an abnormal accumulation, which is mobile due to gravity, from the fixed duodenal activity. Imaging after emptying of the urinary bladder helped to clarify lower abdominal accumulations. Renal and ureteral activity was excluded using lateral and upright imaging.

Patient's records were reviewed over the followup period of up to 7 years. All positive(15) and the false negative (5) cases have been explored. True negatives had surgical confirmation (11), another diagnosis (57), or no recurrence of symptoms after a thorough negative workup (32).

All 17 patients with proven bleeding Meckel's diverticuli had hematochesia. Of 57 rectilinear scans, 5 were true positive (TP), 46 true negative (TN), 2 false positive (FP) and 4 false negative (FN). Of the 63 camera studies with strict preparation 7 were TP, 54 TN, 1 FP, 1 FN. Considering only rectal bleeders (96 patients) a diagnostic error of 14% in the former and 4% in the latter group was found. Feeding and barium enema was found associated with FP and FN cases of the camera group.

This analysis showed the value of the properly performed abdominal imaging in the diagnosis of bleeding ectopic gastric mucosa.

THE EXPANDING SPECTRUM OF DISEASE DEMONSTRABLE BY Tc-99m PERTECHNETATE ABDOMINAL IMAGING.
J.E. Ho, W.A. Gleason and J.S. Thompson. St. Louis University, St. Louis, MO, University of Texas Health Sciences Center, San Antonio, TX and Parkway Medical Center, Beachwood, OH.

The results of Tc-99m pertechnetate abdominal images obtained in 83 patients, 3 days to 15 years of age, were reviewed and correlated with endoscopic findings, upper gastrointestinal radiographic examinations or findings at surgery. Nineteen patients had abnormal scans. Five of six patients with Meckels diverticulum were correctly identified by pertechnetate imaging. In addition, one instance of ileal duplication and one instance of appendicitis resulted in a positive abdominal scan. The remaining 12 abnormal abdominal scans were interpreted as consistent with gastric or duodenal ulcer on the basis of a focal accumulation of radioactivity or an irregularity in the gastric configuration. Five of these patients had the diagnosis confirmed either on upper GI or by endoscopy. The upper GI was suggestive of antral ulcer in one of the remaining seven patients, however, none of these patients had endoscopy. Prior studies (Gastroenterology 70:492, 1976) have demonstrated that gastric and duodenal ulcers were diagnosed endoscopically in 88% and radiographically in 47% of pediatric patients. These data suggest that in addition to being the diagnostic procedure of choice in Meckels' diverticulum, pertechnetate abdominal imaging is of potential benefit in identifying ulcer disease in the pediatric patient.

ROLE OF GA-67 CITRATE IMAGING IN MANAGEMENT OF CHILDREN WITH NEOPLASTIC DISEASE.
S.L. Yang, P.O. Alderson, H. Kaisier, and H.N. Wagner, Jr., Johns Hopkins Medical Institutions, Baltimore, Md.

Ga-67 citrate imaging has been advocated for evaluating children with neoplastic disease, but its role in patient management is not clear. We have reviewed the results of 90 Ga-67 scans in 53 children ($\bar{x}$ age 10 yrs) with confirmed neoplastic disease. Twenty of these children had 2 to 5 serial scans while undergoing therapy over periods ranging from 1 mo to 6 yrs (mean follow-up 24 mos). Rectilinear and spot images were performed 48 and 72 hrs after injection of 500 uCi-3mCi of Ga-67 citrate. True-positive rates (TPR) were analyzed in terms of the patient's proven disease status, as site-by-site correlation was often not available. Best results were obtained in Hodgkins and non-Hodgkins lymphoma (n=26, TPR=0.89), hepatoblastoma (3/3 positive), teratoma (4/4 positive), and rhabdomyosarcoma (4/4 positive). The overall TPR was 0.88; the false-positive rate was 0.06. Four children showed persistent Ga-67 uptake on serial scans, and 13 showed decreased tumor uptake after radiation or chemotherapy. These results correlated with their clinical status. Ga-67 avid lesions recurred in 3 patients who had intervening normal Ga-67 studies. These patients were on chemotherapy or radiotherapy at the time of recurrence. Recurrent disease was confirmed by surgery or other

diagnostic techniques. Ga-67 imaging appears to be most useful as an adjunctive technique in children with neoplastic disease. It is helpful in following the progress of children whose primary lesion is Ga-67 avid, and provides whole-body information to direct subsequent diagnostic or therapeutic procedures.

EVALUATION OF BONE MARROW SCINTIMAGING IN PEDIATRIC ONCOLOGY. A.R. Siddiqui, R.S. Oseas, H.N. Wellman, R.L. Baehner. James Whitcomb Riley Hospital for Children and Indiana University School of Medicine, Indianapolis, IN.

The usefulness of technetium-99m-sulfur colloid bone marrow scintimaging (BMS) was evaluated in pediatric oncology patients. All patients had known malignancies or were being worked up for one.

Fifty-six patients had 86 bone marrow scintimages during various phases of management. The normal distribution of marrow was related to age. Under the age of 2 years entire femur and most or all of tibia were visualized. Between the ages of 2 and 5 entire femur and proximal tibia were seen. Between the ages of 5 and 10 years most of the femur had marrow activity. Above the age of 10 years the appearance was similar to that in adults. Chemotherapy and radiation had a definite effect on this distribution.

Thirty-four scintimages showed diffuse or focal defects. Fourteen of those had abnormalities corresponding to the radiation ports. On follow-up BMS 2 of these defects showed recovery in about 6 months. Pathological nature of defects in remaining 20 studies was confirmed by skeletal or gallium scintimaging or biopsy. Some clinical responders (3) had persistent defects on follow-up; biopsy in one showed fibrosis. The remainder showed clearing or worsening of the abnormalities paralleling their clinical courses. In 2 patients BMS was the first study to localize site of the disease.

BMS appears to be a useful adjunct to hepatic scintimaging in initial metastatic work-up and in follow-up. Follow-up studies should be interpretated with care since persistent defects can be seen in patients in clinical remission.

GALLIUM SCANNING AS PROGNOSTIC INDICATOR IN NEUROBLASTOMA. N. Bidani, J.W. Moohr, P. Kirchner, E. Peng, C. Bekerman, M. Cooper. Departments of Radiology and Pediatric Oncology University of Chicago, Chicago, IL.

Gallium-67 citrate imaging has been successfully used in the detection and staging of various cancers. Since many neuroblastomas do not accumulate gallium-67, it appeared initially to have limited clinical value in this disease. At present the principle prognostic indicators in neuroblastoma are: 1) age of onset, 2) initial staging, and 3) size of tumor. This study reports a significant difference in survival between the group of patients in which the tumor accumulated gallium-67 citrate compared with the group in which it did not. (p=.001)

Twenty neuroblastomas were seen in 5 years. Twelve were studied with gallium; 10 prior to treatment. Six of the 10 showed Ga-67 uptake (Group A). Four of the 10 did not (Group B). Age of onset, staging, tumor size, histology, and chemotherapy were comparable in the two groups.

Group	Age of Onset			Stage		Total No.	Disease Free	Mean Survival
	<1	1-2	>2	IV	III			
A. + ve	3	1	2	4	2	6	0	15 mo.
B. - ve	0	1	3	2	2	4	3	49 mo.

Five of the 6 Ga-67 positive patients died (mean survival 15 months); one is alive 8 months post-diagnosis with disease. All 4 of the Ga-67 negative patients are alive (mean survival, 49 months): 3 are disease free.

Our results suggest that gallium scanning may become an important prognostic indicator in neuroblastoma. Its predictive value appears to be independent of age of onset or staging.

WEDNESDAY, JUNE 28 ANAHEIM ROOM
2:00 p.m.-3:30 p.m.

CLINICAL SCIENCE

ONCOLOGY I

Chairman: Raymond Marty
Co-Chairman: Leslie R. Bennett

VISIBILITY OF HOT LESIONS ON GA-67 OR TC-99M SCINTILLATION CAMERA IMAGES. N. Alazraki, J. Verba, H. Nelson, A. Taylor S. Halpern, and B. Palmer. Veterans Administration Hospital and University of California, San Diego, CA.

In response to the frequently asked question, "how small a tumor can be seen on a gallium scan?", we performed this study to examine the effects of varying lesion size, lesion/background count ratios, lesion depth in tissue, and imaging energy of the radioisotope. A chest phantom in which spherical sources (lesions) ranging in size from 0.5 to 2.0 centimeter diameters, were suspended at various distances from the scintillation camera face was devised. The source phantoms were filled with Ga-67 or Tc-99m; activity ratios of source/background were varied from 1.1/1.0 to 650/1 by adding measured increments of the respective isotope to the water bath in the phantom. Imaging was performed for Ga-67 using the 90 Kev peak, the 184 Kev peak, and the 90 plus 184 peaks together. Images were recorded on polaroid, x-ray film, and computer tape for 5 minutes each. Five experienced readers interpreted the images for positive and questionable identification of lesions.

The results showed that Tc-99m smaller sources were more easily detected than Ga-67 at greater depths and lower source/background ratios. Ga-67 imaging with both peaks was more effective than either peak alone (readers averaged 86% correct positive and questionable identifications). Imaging on the 184 peak (80% correct readings) was slightly more effective than 90 Kev peak (75% correct readings). Positive identification of lesions at 1, 4, 6, 10 and 12 centimeter depths corresponded to 100%, 100%, 96%, 64% and 46% respective correct identifications for a 20/1 source/background count ratio. Thresholds for detection of a range of lesion sizes, count ratios, and depths were determined.

GALLIUM-67 CITRATE IN THE STAGING OF DIFFUSE PLEURAL MESOTHELIOMA. M.Sorek, W.N.Rom, and S.J.Goldsmith. Mount Sinai Medical Center, New York.

The incidence of diffuse pleural mesothelioma (DPM) is increasing due to changes in occupational and environmental exposure to asbestos during the last several decades. Accurate staging of the disease is necessary in evaluation and treatment planning.

Ga-67 Citrate scans (GCS) were compared to chest radiographs, thoracoscopy, mediastinoscopy and thoracotomy findings to evaluate their contribution to staging of DPM.

Disease was catagorized anatomically as pleural, mediastinal, pulmonary, peridiaphragmatic and other (peritoneal and bone). In 16 scans performed on 15 patients with DPM, GCS were positive for pleural involvement in 15 whereas chest x-rays identified 12 out of 15. Mediastinal involvement was demonstrated in 8 patients by GCS, and in 6 by chest x-ray. Pulmonary parenchymal lesions were noted in 4 patients by GCS and in 2 by chest x-rays. Peridiaphragmatic disease was documented by GCS in 4 patients, none by chest x-rays. In total GCS identified 32 disease sites compared to 22 on x-rays. In 3 sites (1 mediastinal, 1 pulmonary & 1 lytic rib lesion) x-rays revealed disease not identified by GCS. 8 disease sites were detected by thoracotomy and endoscopic procedures. Of these, 5 were Gallium positive and 3 Gallium negative. It is concluded that GCS is useful in staging of DPM, and that it exceeds the diagnostic yield of chest radiography, especially with regard to the mediastinum, lung parenchyma and the diaphragmatic

region. GCS offers the advantage of non-invasive diagnosis of disease both above and below the diaphragm. A potential role for this procedure is in assessment of response to therapy.

THE GALLIUM-67 CITRATE LIVER SCAN -CRITERIA OF ABNORMALITY. R.B. Grove, S.M. Pinsky, and R.D. Bowen. V.A. Hospital, Nashville, TN., and Michael Reese Hospital, Chicago, ILL.

Gallium-67 citrate has been successfully applied to the detection of malignancy and inflammatory processes in many clinical settings, including the evaluation of liver pathology. Confusion still exists concerning the criteria for a positive Ga-67 liver scan. The purpose of this study was to evaluate the relative uptake of gallium-67 in hepatic lesions with respect to the presence or absence of malignancy or inflammation. Twenty-one patients having focal defects on Tc-99m sulfur colloid liver scans proven to represent malignancy or pyogenic inflammation and 20 patients with proven cirrhosis underwent Ga-67 citrate liver imaging. The concentration of Ga-67 in the hepatic lesions was evaluated as increased, equal, or decreased compared to Ga-67 uptake in areas of normal liver. There was decreased uptake of gallium in the fibrotic liver lesions of all 20 patients with cirrhosis. Four patients with pyogenic liver abscesses had markedly increased gallium concentration in these lesions. In 17 patients with proven tumor, concentration of gallium was increased in 11 (64.8%), equal in 3 (17.6%), and decreased in 3 (17.6%). Inclusion of those patients with equal uptake of gallium in the liver lesion in the positive group increased the correct diagnosis of malignancy from 64.8% to 82.4%. These results indicate that equal uptake of gallium in a hepatic lesion compared to surrounding normal liver should be included along with increased uptake as a criterion of positivity of the Ga-67 citrate liver scan. Uptake of Ga-67 citrate does not differentiate between malignancy and inflammation. However, these data also suggest that in those cases with equal gallium uptake in a lesion, malignancy is more likely than untreated pyogenic inflammation.

IMAGING OF CARCINOMA BY I-131 ANTIBODY TO CEA. F.H. DeLand, E.E. Kim, S. Bennett, F.J. Primus, and D.M. Goldenberg. University of Kentucky Medical Center and Veterans Administration Hospital, Lexington, KY.

Antibody to carcinoembryonic antigen (from colonic carcinoma) was produced in hyperimmunized goats. Purified goat IgG had a 70% immunoreactivity against CEA. The IgG was labeled with I-131 by the chloramine-T method. Two to three μg/kg of IgG were administered intravenously (0.6-1.6 mCi total dose). Patients were imaged by scintillation camera at 4,8,24, and 48 hrs after injection of the labeled antibody. In surgical specimens tumor/non-tumor radioactivity has ranged from 2.0 - 2.5:1, and the average decrease in blood levels has been from about 66% of total dose at one hour to 20% at 48 hrs. Because of persistent high background activity, routine imaging was not satisfactory. By means of IV Tc-99m labeled albumin, background activity was selectively attenuated. The level of plasma CEA (0.7 to 350 ng/ml) had little apparent effect on the localization of antibody or image quality. Of 30 patients studied neoplasms have included gastric, pulmonary, pancreatic, colonic, choledochal, mammary, ovarian, endometrial, cervical, and lymphoma. The computer-processed images in color have readily demonstrated the tumors with the exception of the lymphoma. Metastases have also been identified except in the brain and bone where antibody did not localize consistently in known metastases. The rather broad tumor spectrum of CEA and successful image processing has suggested new possibilities for tumor detection.

CLINICAL TRIAL OF I-123-BLEOMYCIN FOR TUMOR DETECTION. S.J. DeNardo, K.A. Krohn, G.L. DeNardo, J. Mangum, and J. Meyers. University of California at Davis, Sacramento Medical Center, Sacramento, CA.

Oncophilic radiopharmaceuticals which are in current clinical use have disadvantages including marrow and bowel uptake, slow clearance delaying definitive information and non-specific localization in other diseases, including infections. Our earlier work in a murine tumor model indicated that I-123-Bleomycin (I-bleo) rapidly concentrated in the tumor in an amount equal to the maximum concentration of In-111-Bleomycin (In-bleo), but in addition, was much more rapidly cleared from the blood and the animal. Similarly in man, during the initial 2 hours 80% of both I-bleo and In-bleo were cleared from the blood. I-bleo continued to be rapidly cleared with only 1% remaining at 24 hours, whereas most of the remaining 20% of In-bleo persisted at 24 hours. Because of these promising results, we have used I-bleo in 30 patients with biopsy proven cancer. 21 of these patients were also imaged with In-bleo. In 11 patients with primary lung cancer, the lesion was better visualized with I-bleo than In-bleo. Visualization of lymphomatous lesions was equal with the 2 agents except when located near marrow tissue, where I-bleo produced better results. This same result occurred in the other cancers, where the 2 agents most commonly produced comparable results. In all instances I-bleo had the advantage of early imaging (3-6 hrs) compared to In-bleo (18-24 hrs). In 2 patients with pneumonia I-bleo did not localize in the infections whereas In-bleo did, as would Ga-citrate. These results suggest that I-bleo is superior to In-bleo and point out the need for additional clinical trials.
(American Cancer Society Grant #PDT-94A)

AUGMENTED RADIONUCLIDE UPTAKE BY THE SPLEEN IN PATIENTS WITH MALIGNANT MELANOMA. A.J. Sober, M.M. Mintzis, R.A. Lew, H. Lo, C. Whalen, K.A. McKusick, M.S. Potsaid, C. Vialotti, T.B. Fitzpatrick. Massachusetts General Hospital, Boston, MA and New York University, New York, NY.

Augmented splenic uptake with reversal of the usual liver/spleen ratio has been noted on rectilinear scans in patients with malignant melanoma in the absence of apparent liver disease (Goldman, A., Radiology 112:631, 1974). One-hundred and forty-seven patients in the Melanoma Clinical Cooperative Group were injected with Tc-99m sulfur colloid and similar changes were found in 32% of patients early in the course of their disease both by rectilinear and gamma camera imaging. Patients with visceral metastases were excluded from this series. In contrast, augmented splenic uptake was noted in only 1 of 165 patients (0.6%) with various carcinomas ($P<.01$). Recurrence rate by life table analysis was higher for the patients with augmented splenic uptake than for those patients with normal scans ($P<.02$). Age was not a factor. Further life table analysis demonstrated that the difference in survival resulted from a lower recurrence rate in females with normal scans ($P<.05$). The recurrence rates for males with either scan type or females with augmented uptake were similar. While patients with stage II disease (lymph nodal metastases) had a much higher recurrence rate overall - 73% vs. 17% for stage I, patients with stage I (local disease) had a much higher recurrence rate if they had increased splenic uptake 29% vs. 12% ($P<.05$). Scan status may become another prognostic parameter in the selection of high risk groups for potential adjuvant therapies.

INTRACAVITARY COLLOIDAL CHROMIC RADIOACTIVE PHOSPHATE THERAPY. G. L. Jackson, Fred W. Flickinger, Nancy M. Blosser, Harrisburg Hospital, Harrisburg, PA.

Two-hundred forty-five patients have been treated over the past 15 years. Of this number, 95 patients received 122 intrapleural treatments. One-hundred forty-seven patients received 168 intraperitoneal treatments. Two patients received two intrapericardial treatments. The results of therapy according to the site of the primary tumor will be discussed. Evaluation of the results of therapy is best made three months after administration. The overall results indicate that in those patients who have survived three months after intrapleural treatment, improvement (evaluated by referring physician) was observed in 72% of those treatments (47); after intraperitoneal treatment, improvement was observed in 87% of those treatments (79).

In general, we prefer to use 10 mCi in a pleural space;

5 mCi in the pericardial space. For peritoneal disease we recommend the use of two tubes, one placed in the upper abdomen and the second in the pelvis. With two tubes, 20 mCi is used, divided equally per tube. If only one tube is in place, 15 mCi is used. If recurrent effusion requires early removal, assays indicate that less than 1% of administered dose will be found in fluid after 48 hours.

The authors believe this is a significant palliative procedure in the treatment of cavitary malignant disease. In Stage I, ovarian carcinoma, its role is more curative.

WEDNESDAY, JUNE 28 SANTA ANA ROOM
2:00 p.m.-3:30 p.m.

BASIC SCIENCE

RADIOPHARMACEUTICALS IV: TECHNETIUM COMPOUNDS

Chairman: Powell Richards
Co-Chairman: Alun G. Jones

PRODUCTS OF PERTECHNETATE REDUCTION IN COMPLEXING MEDIA. C.D. Russell and A. Cash, Veterans Administration Hospital and University Hospital, Birmingham, Al.

It has proved difficult to identify the chemical structure of many Tc pharmaceuticals. The oxidation state has been identified in only a few, and in others there is no certainty even that the agent is a single species. Polarography is useful for identifying species and determining oxidation state. It has a synthetic counterpart, controlled-potential electrolysis, so that reactions identified by polarography can be used for preparative purposes. We have identified oxidation states and half-wave potentials for products of TcO_4^- reduction in a variety of media, and for the products of electrolytic reoxidation. The first cathodic wave in acidic phosphate was identified as Tc(VII) → Tc(III) by its ratio to the Tc(III) → Tc(IV) reoxidation wave seen on anodic-sweep pulse polarography. This wave was used as a standard to determine the number of electrons transferred in other media of same ionic strength. The first wave in acid occurred at pH-dependent potential and usually corresponded to formation of Tc(III). The Tc(III) could in some media be reoxidized to Tc(IV) or Tc(V). In alkaline or unbuffered media the first wave occurred at -0.8V vs. S.C.E. and a second was sometimes seen at -1.0V. These often corresponded to formation of Tc(IV) or Tc(V), but in some alkaline media mixtures of products were obtained. Insoluble films were formed on the electrode surface in some alkaline media. As we have shown elsewhere, such data are useful in designing methods for radiopharmaceutical preparation.

AN IMPROVED PROCEDURE FOR LABELING PROTEINS WITH Tc-99m. W.A. Pettit and F.H. DeLand. Veterans Administration Hospital, Lexington, KY.

Numerous procedures currently used in Tc-99m labeling of proteins have been found unsatisfactory for two reasons: 1) formation of colloid and 2) loss or transfer of the radionuclide from the protein. Gel filtration on a 2.5 x 87.8 cm Sephacryl S-200 column has proved to be an accurate and reliable assay method for identification of these problems. When small quantities of protein (100 micrograms) are labeled by the currently available procedures, these problems become more pronounced. Since many biologically significant proteins (specific immunoglobulins, enzymes, etc.) are often not available in milligram quantities, attempts were made to adapt current labeling techniques to low concentrations of protein. A procedure has been developed using stannous tartrate which circumvents these problems satisfactorily. The procedure is carried out in a 1 ml reaction vial which contains pertechnetate (Tc-99m), stannous tartrate, and the protein to be labeled, i.e., either albumin, normal goat IgG, or goat anti-CEA IgG. Following incubation at 40°C, the pH of the reaction mixture is adjusted to 8.5 with aqueous sodium bicarbonate, then reincubated at 40°C, and finally placed over a 1.5 x 6.5 cm Sephacryl S-200 column and the appropriate protein fraction collected. The procedure requires about one hour. Goat anti-CEA IgG was prepared by this procedure with no loss of its immunological activity by radioimmunoassay within experimental error. Labeled goat IgG (Tc-99m) could be obtained in 30-35% radiochemical yield. The product was approximately 90% monomeric IgG when assayed by Sephacryl S-200 chromatography.

EFFECT OF LIGAND STRUCTURE AND RADIOLABELING METHODOLOGY ON RADIOCHEMICAL PURITY OF TC-IMINODIACETATES. A.T. Fields, D.W. Porter, P.S. Callery, M.D. Loberg. University of Maryland, Baltimore, Maryland 21201

The preparation of radiochemically pure Tc-labeled N-substituted iminodiacetates (IDA) was investigated. A series of eight N-substituted IDA ligands with structures similar to HIDA were synthesized having pKa values for the imino nitrogen varying from 5.0 to 8.7. The ligands (L) were labeled with Tc-99m at aqueous pH values of 4, 5.5, and 8.0 and in absolute methanol. The radiochemical purity of each chelate was examined by HPLC, paper chromatography, and tissue distribution studies. No radiolabeling was seen for ligands in which the pKa of the imino nitrogen was 5. Radiolabeling in methanol resulted in pure Tc-chelates for the remaining six compounds irrespective of pKa, but aqueous labeling conditions resulted in radiochemically pure chelates only for the two compounds in which the pKa of the imino nitrogen was approximately 6. In these instances, all Tc-chelates chromatographed and possessed in vivo distributions very similar to that of the anionic, bis structured Tc-HIDA (pKa 6.2). When the pKa of the imino nitrogen was 8, aqueous labeling conditions resulted in three major radiochemicals, only one of which had a HPLC retention time (25 min) and an in vivo distribution identical to that of the pure methanolic preparation. The observed multiple products may be attributed to a competitive protonation-induced decrease in $[L^{-2}]$. IDA should be synthetically incorporated into drug analogs in such a fashion as to reduce the electron density on the imino nitrogen from a pKa value of 8 to one of approximately 6. For this purpose, the carbamoylmethyliminodiacetate is a better ligand than iminodiacetate itself.

COMPARISON OF ^{99m}Tc-HEPATOBILIARY AGENTS BASED ON NAPTHALENE AND SIMILAR RING SYSTEMS. A.R. Fritzberg, D. Eshima, W. C. Klingensmith, and W. Whitney. U. of Colorado Medical Center, Denver, CO.

A series of chelating agents which are derivatives of fused bicyclic aromatic ring systems have been complexed with Tc-99m using either stannous chloride or formamidine sulfinic acid. The compounds included 8-hydroxyquinoline-7-carboxylic acid (bioquin-7CA), 1-hydrazinophthalazine (hydralazine), 2-(dicarboxymethylimino)methylnapthalene (NMIDA) and iminodicarboxymethyl 2-napthyl ketone (NAIDA).

These complexes were compared in rabbits and dogs with respect to rates of blood clearance, rates of biliary excretion and amount of renal excretion. Results were compared to N,α-(2,6-diethylacetanilide)-iminodiacetic acid (diethyl-IDA) and Rose Bengal as reference radiopharmaceuticals.

Complexes with bioquin-7CA and hydralazine were much less polar than the iminodiacetates as determined by solvent distributions and had the slowest blood clearance. Thus in dogs at 30 min 39% of bioquin-7CA remained in the blood, 17% of hydralazine, 10.6% of Rose Bengal, 5.6% of NMIDA, 4.4% of NAIDA and 2.8% of diethyl-IDA. Clearance of activity into the gall bladder in order of decreasing rates was diethyl-IDA, NAIDA, hydralazine, NMIDA and Rose Bengal. Two hour urine dose values were 2.2% for bioquin-7CA, 3.0% for hydralazine, 18.0% for NMIDA, 1.8% for NAIDA and 5.7% for diethyl-IDA. The results of these napthalene-like derivatives indicate widely varied biological behavior due largely to different chelating groups. The relatively rap-

id blook clearance, rapid biliary excretion and low renal excretion of NAIDA suggest its clinical evaluation in order to determine the importance of high hepatobiliary specificity in patients with poor liver function.

A STUDY OF THE RELATIONSHIP BETWEEN CHEMICAL STRUCTURE AND BONE LOCALIZATION OF Tc-99m-Sn-DIPHOSPHONIC ACIDS. T.S.T. Wang, G.E. Mojdehi, R.A. Fawwaz, and P.M. Johnson. College of Physicians and Surgeons, Columbia University, New York NY

Technetium-99m-Sn-methylene diphosphonate (MDP) is one of the most commonly used bone imaging radiopharmaceuticals. This study was aimed at determining the bone localizing property of the following analogues of MDP: ethylidenediphosphonic acid, $CH_3CH(PO_3H_2)_2$ (A); benzylmethylenediphosphonic acid, $C_6H_5CH_2CH(PO_3H_2)_2$ (B); isopropylidenediphosphonic acid, $(CH_3)_2C(PO_3H_2)_2$, (C), and dichloromethylenediphosphonic acid, $Cl_2C(PO_3H_2)_2$ (D).

The synthesis of compounds A and B consisted of methylation (with CH_3Br) and benzylation (with $C_6H_5CH_2Cl$) of the sodium salt of tetraethylmethylene diphosphonate respectively. This was followed by acid hydrolysis to yield the corresponding acids. Compound C was prepared by methylation (with CH_3Br) of sodium tetraethylethylidene diphosphonate, followed by acid hydrolysis. Product purity was identified by TLC, elemental analyses, and NMR spectra. Labeling of diphosphonic acids with Tc-99m pertechnetate was carried out with Sn(II) as the reducing agent. Labeling efficiencies were determined by ITLC with acetone and 85% methanol systems.

Tissue distribution studies were done in rats. At two hours after iv injection the data revealed that increasing bone localization occurs in the order B<D<C<MDP=A. These results suggest that in addition to steric hindrance the "keto-enol"type of tautomerism and resonance structure of these ligands may play an important role in bone localization.

STRUCTURAL REQUIREMENTS FOR Tc-99m BONE SCANNING AGENTS: A STUDY BY MEANS OF ANALOGUES, R.P.Spencer, P. Hosain, F. Hosain, T.S.T. Wang. Dept. Nuclear Medicine, Univ. Connecticut Health Center, Farmington, CT.

The angular and structural similarities between P-O-P, P-C-P and P-N-P suggest that these configurations are necessary for Tc-99m binding and bone localization. The validity of this assumption was examined by synthesizing a series of analogues which possessed one or more structural changes. Each new compound was then tested for Tc-99m (Sn) binding and for bone accumulation after intravenous administration to mice, rabbits and dogs. Results were as follows. 1. A single heteroatom separating the phosphates can be replaced by two carbon atoms. That is, P-C-C-P (ethylene diphosphonate) was as usable a bone imaging agent as P-C-P. 2. The second phosphate was not essential, but could be replaced by other groupings such as $H_2N.CO.O-$ (carbamylphosphate and analogues). 3. The phosphate group itself was not a strict requirement for Tc-99m(Sn) binding and bone localization. That is, one or both phosphate groups could be replaced by arsenate (which is a phosphate analogue). Both arsonomethyl phosphoric acid and methylenediarsonic acid bind Tc-99m(Sn) and show bone uptake. 4. The second phosphate group can bear a bulky substituent. For example, thiamine pyrophosphate had slower entry into bone than pyrophosphate (but entry did occur). Whether this represents cleavage of the bulky grouping or its placement "above" the binding site is not known. Hence, while the P-C-P type structure is sufficient for Tc-99m(Sn) binding and bone uptake, it is not necessary. The newer analogues allow a number of substitutions to be made, in an effort to explore the possibility of distinguishing between various types of lesions.

SYNTHESIS, STRUCTURE ELUCIDATION, AND BIODISTRIBUTION OF TECHNETIUM-99 AND TECHNETIUM-99m DITHIOLATES. E.F. Byrne and J.E. Smith. Union Carbide Corporation, Tuxedo, NY.

Since several Tc-99m labeled radiopharmaceuticals, such as dihydrothioctic acid and dimercaptosuccinic acid, appear to involve Tc-S coordination, the reaction of reduced Tc with dithiols was investigated. By working with long-lived Tc-99 rather than short-lived Tc-99m, macroscopic amounts of Tc compounds were isolated and characterized by conventional chemical and spectroscopic methods.

It was observed that the $NaBH_4$ reduction of Tc-99-pertechnetate in the presence of dithiols results in the formation of orange complexes. The complexes formed with 1,2-dimercaptoethane, 1,2-dimercaptopropane, and 1,3-dimercaptopropane were isolated as the tetraphenylarsonium salts and characterized by chromatography, electrophoresis, and chemical analysis as well as infrared, Raman, and ultraviolet-visible spectroscopy.

The analytical data indicate an As:Tc:O:S ratio of 1:1:1:4 in these complexes. The charge of these complexes is -1, the oxidation state of Tc is +5, and the following structures are proposed: $Ph_4AsTcO(SCH_2CH_2S)_2$, $Ph_4AsTcO[SCH_2CH(CH_3)S]_2$, and $Ph_4AsTcO(SCH_2CH_2CH_2S)_2$. The assignment of these compounds as oxotechnetium(V) bisdithiolates was verified by the x-ray diffraction analysis of $Ph_4AsTcO(SCH_2CH_2S)_2$.

The product of the $NaBH_4$ reduction of Tc-99m-pertechnetate in the presence of 1,2-dimercaptoethane has been shown by chromatography, electrophoresis, and biodistribution in mice to be identical to the Tc-99 dithiolates.

WEDNESDAY, JUNE 28 — CALIFORNIA B ROOM
2:00 p.m.-3:30 p.m.

IN VITRO AND CORRELATIVE TECHNIQUES

RADIOASSAY I

Chairman: Stanley J. Goldsmith
Co-Chairman: Eileen J. Nickoloff

* * *

The following paper is the winner of the Second Berson-Yalow Award, presented annually by the Education and Research Foundation of the Society of Nuclear Medicine.

RADIOIMMUNOASSAY OF FIBRINOPEPTIDE A IN PATIENTS WITH CANCER. S.J. DeNardo, G.L. DeNardo, M.A. Swanson, K.A. Wong. Department of Nuclear Medicine, University of California, Davis, CA

Cancer patients frequently have overt and even more often occult coagulopathes. Fibrinopeptide A (FPA) is the specific polypeptide cleaved from fibrinogen by the action of thrombin. By radioimmunoassay, Nossel has shown that FPA is rapidly cleared from the plasma ($T_{\frac{1}{2}}$=3.5 min), so that plasma levels of FPA reflect active coagulation at the time of sampling. The purpose of this study was to evaluate the usefulness of this assay for screening cancer patients. Plasma from 11 patients with histologically proven cancer, 7 patients with thrombophlebitis, 10 normal subjects and 5 normal women on contraceptive drugs was assayed for FPA. After elimination of fibrinogen by ethanol precipitation, the supernatant containing FPA was incubated with FPA antiserum and labeled desaminotyrosyl-FPA. Excess labeled FPA was separated and the bound FPA compared to a standard curve. All cancer patients had FPA levels above the normal range. Nine of 11 cancer patients had levels greater than those of normal women on contraceptive drugs. The remaining 2 patients were men with lung cancer and were not under treatment with extrogenic drugs. The range of FPA for normal controls was 0-2.7ng/ml (mean=1.5ng/ml), for normal women on contraceptive drugs, 3.4-4.4ng/ml(3.9ng/ml), and for cancer patients, 3.9-10.6ng/ml (7.9ng/ml). FPA in patients with thrombophlebitis was 3.8-22.0ng/ml (9.6ng/ml).

This data provides additional evidence that cancer patients have ongoing abnormal coagulation, and suggests that plasma FPA radioimmunoassay may be useful as a screening test for cancer. Plasma FPA may also prove useful to assess tumor burden and follow the effect of therapy.
(Supported by American Cancer Society Grant #PDT-94A)

* * *

RADIOIMMUNOASSAY FOR DETECTION OF MORPHINE IN HAIR. A.M. Baumgartner and P.F. Jones, The Aerospace Corporation, El Segundo, CA, W.A. Baumgartner, V.A. Hospital Wadsworth Center, and C.T. Black, University of California, Los Angeles, CA.

Morphine was detected in hair using the commercially available morphine radioimmunoassay kit with minor sample preparation. Hair samples obtained from morphine-treated mice and from heroin users at a drug abuse treatment center contained nanogram levels of morphine per milligram of hair (a single human hair).

The hair sample has a number of significant advantages over body fluids: accessibility, sample stability and long-term retention of information. It was found that hair retains measureable drug levels for at least two months after the last use of the drugs, while urine and serum analysis is useful only for one to 72 hours after drug use.

In our studies it has been possible to distinguish sections of hair grown prior to drug intake from those grown during drug use, thus suggesting the feasibility of determining the time and extent of drug abuse.

RADIOMETRIC MEASUREMENT OF FATTY ACID METABOLISM BY MYCOBACTERIA. E.E. Camargo, J. Kertcher, M. Chen, S.M. Larson, B.S. Tepper, P. Charache, P.A. McIntyre and H.N. Wagner, Jr. The Johns Hopkins Medical Institutions, Baltimore, MD.

Recently we have developed a 48-hour drug susceptibility test of clinical isolates of M. tuberculosis using 1 ml of 7H9 medium with 1 µCi of C-14 formate and different concentrations of isoniazid (INH), streptomycin, ethambutol, rifampin and gentamicin. The assay system included automated radiometric quantification of C-14 carbon dioxide released as a result of oxidation of the C-14 labeled substrate. Radiometric MIC (50% inhibition of metabolism) correlated well with the agar dilution method for INH, but was lower than routine MIC for protein synthesis blockers.

For both M. tuberculosis and M. lepraemurium (cause of murine leprosy), we observed characteristic patterns of utilization of different fatty acids as indicated by C-14 carbon dioxide release. Two strains of M. tuberculosis (H37Rv and Erdman) and one of M. bovis (BCG) in one ml of 7H9 medium with 1 µCi of one of the fatty acids (progressing in chain length from acetate to stearic), were used. M. lepraemurium was suspended in 1 ml of K-36 buffer with 5 µCi of the same substrates. Both strains of M. tuberculosis preferred hexanoic; however, oxidation of butyric and avid oxidation of lauric were found with H37Rv but not with Erdman. The best substrates for M. bovis were lauric and decanoic. For M. lepraemurium, the best substrates were lauric, decanoic and myristic. Radiochromatograms confirmed transformation of oxidized substrates into byproducts and preservation of the non-oxidized ones.

These data suggest that differential fatty acid metabolism may provide a basis of speciation and strain identification of genus Mycobacterium as well as a means of drug susceptibility testing.

SERUM MYOGLOBIN DETERMINATION: LABORATORY AND CLINICAL EVALUATION. Robert E. Sonnemaker, Douglas L. Daniels, William E. Craig, John L. Floyd, and Robert F. Bode, William Beaumont Army Medical Center, El Paso, TX.

An investigation was undertaken to evaluate the laboratory and clinical efficacy of a commercially available radioimmunoassay for serum myoglobin (MG). Coefficient of variation analysis of precision, accuracy and reproducibility between reagent lots, control values, and technologists averaged 5% or less. During a six month period, multiple MG levels were determined in all patients admitted to the Coronary Care Unit. Results were correlated with the final clinical impression determined by strict criteria based on clinical presentation, electrocardiogram, and serum enzymes including CK-MB (Selective Activation Method). In 113 patients without evidence of acute myocardial infarction (AMI), MG ranged from 6.2 to 79ng/ml (M = 33ng/ml, SD = 17.0ng/ml). In 26 patients with AMI, all peak MG levels were greater than 120ng/ml providing a 3SD separation of normal and abnormal values. In contrast, there was considerable overlap of CK-MB values. All patients with AMI demonstrated elevated MG values at four hours which preceded CK-MB elevation by 4 to 44 hours in over half of the patients. It is concluded that MG radioimmunoassay is an important new parameter for the management of AMI which provides clearer delineation and earlier detection than CK-MB.

WEDNESDAY, JUNE 28 CALIFORNIA A ROOM
2:00 p.m.-3:30 p.m.

CLINICAL PRACTICE

BONE/JOINT

Chairman: Robert A. Kraft
Co-Chairman: John M. Vogel

BONE SCANNING IN THE DIAGNOSIS OF OSTEOMYELITIS. H. T. Nelson, A. Taylor. Nuclear Medicine Service, Veterans Administration Hospital and University of California, San Diego, Ca.

All patients referred to the Nuclear Medicine Department for bone scanning during a 12 month period were reviewed and those patients referred for suspected osteomyelitis (N=59) were examined in detail. All patients were imaged with either a gamma camera or rectilinear scanner after receiving intravenous injections of technetium-99m labeled stannous pyrophosphate. Nineteen patients were determined to have osteomyelitis by biopsy (N=12) or by clinical criteria which included physical examination, history, blood cultures, radiographs, scans, and response to antiobiotic therapy (N=7). Thirty-seven patients did not have osteomyelitis by these criteria. Three patients were indeterminate and excluded from the data.

Bone scans detected 18 of 19 patients with osteomyelitis (sensitivity of 95%) compared to the radiograph which detected 6 of 19 patients with osteomyelitis (sensitivity of 32%). Furthermore, the bone scan had a low false-negative rate (5%), with the only false-negative occurring in a setting of advanced vascular disease. Bone scans and radiographs had specificities of 92% and 89% respectively. An analysis of the data using only biopsy proven cases of osteomyelitis did not change the sensitivity or specificity of either test.

A normal bone scan is strong evidence against the presence of osteomyelitis. In the appropriate clinical setting an abnormal bone scan is highly suspicious for osteomyelitis; in several patients, the bone scan detected additional sites of involvement which were clinically unsuspected. Routine bone scanning should be part of the evaluation of patients with suspected osteomyelitis.

THE ROLE OF GALLIUM AND BONE SCANNING IN MONITORING RESPONSE TO THERAPY IN CHRONIC OSTEOMYELITIS. N.P. Alazraki, J. Fierer, D. Resnick. Veterans Administration Hospital, San Diego and University of California, San Diego, CA.

Clinically it is often difficult to evaluate progression of disease in chronic osteomyelitis. We studied 14 pa-

tients with chronic osteomyelitis over a two year period by clinical, radiographic, and nuclear medicine techniques to evaluate response to various antibiotic therapies. Ga-67 and Tc-99m pyrophosphate bone imaging was performed approximately every 6 months, and the results were correlated with radiographic and clinical findings.

Nuclear imaging of the affected bones and of the bones of the opposite normal extremity was performed at 3 hours following 15 mCi Tc-99m pyro or polyphosphate and 72 hours after 5 mCi Ga-67. All images were performed on the scintillation camera and recorded on computer tape. Computer analysis of the data to obtain ratios of counts in the abnormal bone region relative to a corresponding region selected in the opposite normal bone, with normalization of the regions, was performed on both the gallium and the bone image data every 6 months.

Clinically, 8 patients improved, 5 did not and 1 response was indeterminate. Bone scans and gallium scans correlated well with the clinical evaluation and reflected the response to therapy. In patients who did not improve, the uptake ratios did not change. Generally, the image interpretations did not differ from the computer generated ratios. Radiographic findings did not change over the two year period in either group of patients and therefore were of no value in assessing the response to treatment.

The findings support the use of bone or gallium scan to follow response to therapy in chronic osteomyelitis and indicate increased sensitivity over radiography.

COMBINED IMAGING IN OSTEOMYELITIS. H. Handmaker, Children's Hospital of San Francisco, San Francisco, CA.

BONE AND GALLIUM SCANNING IN PRIMARY BONE AND SOFT TISSUE TUMORS OF THE EXTREMITIES. P.T. Kirchner, M.A. Simon, M. Cooper. Departments of Radiology and Surgery. University of Chicago, Chicago, IL.

Management of bone and soft tissue extremity lesions is based on clinical, x-ray, and biopsy data. X-rays are unreliable for soft tissue and cartilage lesions. Many surgeons seek maximum staging data prior to incisional biopsy. Hence, we studied the value of bone and Ga-67 scans in 67 patients with extremity lesions. All diagnoses were biopsy proven. Of 21 soft tissue lesions, 14 were malignant, 5 were excised before scanning; in this group all scans done were normal and no tumor was subsequently found. Intense Ga-67 uptake was seen in 6/7 patients with tumor present and in 9/10 lesions. A normal bone scan in all but one patient correctly indicated lack of bony invasion. In 4/4 benign tumors both bone and Ga-67 scans were normal. 3/3 inflammatory lesions were Ga-67 positive. 36 patients presented as primary bone lesions; 20 were malignant. Bone scan was positive in 20/20 malignancies but also in 7/8 benign lesions and 8/8 cases of active and inactive osteomyelitis. Ga-67 scan was positive in 12/12 malignancies and 4/4 active osteomyelitis cases. It was negative in the only benign lesion studied. Whereas the bone scan showed half of bone malignancies to have abnormal proximal and distal bone/joint uptake, Ga-67 showed this only once, yielding better correlation with true local tumor extension. Both bone and Ga-67 scans assist the staging of extremety tumors. Only Ga-67 uptake correlated with the presence of soft tissue malignancy and Ga-67 may also be more accurate in delineating local tumor extension. As yet this series does not clarify the role of Ga-67 in differentiating benign and malignant bone tumors.

BONE SCANNING IN PROSTHETIC IMPLANTS. B.J.L. Sauerbrunn, M.P. Lastra, H.R. Bates, P. Kenmore, D.R. Harris, P.F. Richin. VA Hospital, Washington, D.C.

Evaluation of the patient with a painful joint following implantation of a prosthesis is often a diagnostic dilemma to the orthopedic surgeon because the implant may have become loosened, infected, or both entities may be present. In an attempt to add to the diagnostic evaluation in this situation, radionuclide bone and joint scanning was utilized in a series of 12 patients.

Two groups of patients with painful joints following prosthetic implants were studied. Group I (5 patients) had Tc-99m pyrophosphate bone scans in addition to other diagnostic modalities (x-ray, sedimentation rate, joint culture). All had operative intervention. Group II (7 patients) had identical studies and additionally were scanned with Ga 67 Citrate at 24 and 48 hours. Five of 7 were operated.

The Tc-99m pyrophosphate scan showed significant focal increased uptake around the implant in all 12 patients with no difference in uptake being noted in the loose implant as compared to the loose, infected implant. The erythrocyte sedimentation rate did not correlate with infection being relatively high in 3 cases having simple loosening and relatively low to normal in 2 cases with positive cultures. The Ga 67 Citrate scan was positive only in those patients with operative evidence of infection or positive cultures.

Tc-99m phosphate scanning may be helpful in the evaluation of a painful joint prosthetic implant, but cannot differentiate between loosening of the implant and an infected loosened implant. Our preliminary study indicates that the addition of Ga 67 Citrate scanning to the diagnostic regimen may offer more of a diagnostic aid.

THE ROLE OF BONE SCANNING IN DIAGNOSIS AND MANAGEMENT OF MALIGNANT BONE DISEASE. P. Matin, Roseville Community Hospital, Roseville, GA.

WEDNESDAY, JUNE 28 GARDEN GROVE ROOM
3:45 p.m.-5:15 p.m.

CONTINUING EDUCATION

PEDIATRICS II (CLINICAL SCIENCE)

Chairman: Gary F. Gates
Co-Chairman: Sidney Hagman

QUANTITATION OF LEFT-TO-RIGHT CARDIAC SHUNTS AFTER DECONVOLUTION ANALYSIS OF PULMONARY TIME-ACTIVITY CURVES. P.O. Alderson, K.H. Douglass, K.G. Mendenhall, R.C. Donovan, and H.N. Wagner, Jr., Johns Hopkins Hospital, Baltimore, Md. and Armed Forces Radiobiology Research Institute, Bethesda, Md.

A poor bolus injection results in an unsatisfactory quantitative radionuclide angiocardiogram (QRAC) in as many as 20% of children with possible left-to-right (L-R) cardiac shunts. To determine if dependence on the input bolus could be minimized, the results of 24 bad bolus studies were recalculated after deconvolution analysis (DCVA) of the pulmonary curve. Repeated good bolus, prolonged (>3 sec) and double-peak injections were made in 4 normal dogs and 7 dogs with surgically created atrial septal defects (ASD). QP/QS was determined using the gamma function. The mean QP/QS from 10 good bolus studies in each animal was used as the standard for comparison. In 4 normal animals where a prolonged or double-peak bolus led to a shunt being calculated (QP/QS $>$ 1.2:1), DCVA resulted in QP/QS=1.0. DCVA improved quantitation in 7 of 12 trials in animals with ASDs that received a prolonged bolus. In 4 trials results were similar, and in one case slightly worse. Before DCVA the mean difference between the reference values and calculated shunt was 0.59 ± 0.40 units; after DVCA it was reduced to 0.30 ± 0.15 ($p < .05$). Double-peak boluses were more difficult to correct; results were better in 3 of 8 trials, the same in 2, and worse in 3. Current techniques for DCVA are useful in preventing normals from being classified as shunts and for improving shunt quantitation after a prolonged bolus. Clinical application of DCVA to QRAC should reduce the number of repeat studies required in children with suspected L-R shunts.

SKELETAL IMAGING IN SICKLE CELL DISEASE. M.J. Gelfand, Radioisotope Laboratory, University of Cincinnati and Children's Hospital, Cincinnati, OH and H.T. Harcke, St. Christopher's Hospital for Children, Philadelphia, PA.

37 symptomatic sites in 30 patients (pts) with sickle cell disease (SS,SC,SD,S-Thal) were studied with 99mTc-EHDP or 99mTc-pyrophosphate bone imaging 48+ hours after onset of fever, bone pain and/or localized swelling.

34/37 sites were judged to be free of infection by clinical presentation and after one to 25 months of follow-up. 10/34 sites had uniformly increased (+) uptake in bone. 15/34 sites had an area of decreased (+) uptake in bone, almost always surrounded by + uptake. At each of these 25/34 sites, the abnormality was felt to represent recent bone infarction. 9/34 sites were normal. In addition, three pts had + uptake in bone at asymptomatic locations, two had + uptake in soft tissue and one had splenic uptake. Immediate blood pool images failed at each of 18 sites to yield information in addition to that found on delayed images.

3/37 sites had infectious processes. Single cases of acute osteomyelitis (osteo), chronic osteo, and septic arthritis had +, + and + uptake, respectively.

Four pts, three with bone infarction and one with chronic osteo, had 99mTc-sulfur colloid marrow imaging within three days of a bone imaging study. Absent marrow uptake was seen at symptomatic sites where bone imaging showed +, + or normal uptake.

Bone infarction can be identified and localized by bone or marrow imaging as an area of + uptake. Uniformly + uptake, indistinguishable from osteo in the child with normal red cells, can be seen at symptomatic sites of infarction and at asymptomatic sites in bone. Our experience is too small to determine if bone or marrow imaging can differentiate sterile from infected bone infarction.

GALLIUM-67 CITRATE UPTAKE IN DUCHENNE MUSCULAR DYSTROPHY (DMD). R. G. Brown, J. M. Ash, C. H. Verellen-Domoulin, M. E. Percy, L. S. Chang, The Hospital for Sick Children, Toronto, Canada

Abnormal localization of Ga-67 citrate in the calf muscles of young males with active Duchenne dystrophy and in carrier females has recently been reported. A pilot project was initiated to attempt computer quantitation of Ga-67 citrate uptake forty eight hours post-injection, in the calf muscle as compared with tibial concentration in males with DMD, in known female carriers with normal and elevated serum creatinine phosphokinase (CPK) levels and in normal females in the same age group.

To date we have studied 9 subjects. Two male patients recently diagnosed as DMD had muscle/bone ratios of 1.2 and 1.4. Two normals in this age group had ratios of .5 and 3, carrier females had ratios in the range of 1.3 to 2.1. These ratios are higher than the normals in this age group (1.3-1.4).

Correlative data was obtained by electrophoretically examining the serum proteins of the various individuals as well as assaying for serum CPK and pyruvate kinase (PK). The results indicate that there is significant uptake of Ga-67 citrate in the calf muscle of DMD patients and DMD carriers as compared with normals. This localization appears to be independent of CPK and PK levels. It was found that all Ga-67 positive patients had both abnormal and elevated hemopexin levels. There is probably alteration in the iron transport and heme salvage system which may be instrumental in the Ga-67 citrate localization in the dystrophied muscle.

RADIONUCLIDE RENAL STUDIES IN NEONATAL CLINICAL PROBLEMS. G.N. Sfakianakis, E. Sfakianaki, F. Bowen. Columbus Children's Hospital, Columbus, OH.

A technique was applied to study 35 infants (25 newborn, 10 age 1-2 months) with suspected urinary system abnormalities, in whom radiologic and laboratory tests could not provide sufficient information.

Following 50 μCi/Kg of Tc-99m-Fe-Ascorbate-DTPA injection, gamma camera images were taken for 30 min and also at 2 and 24 hr. Interpretation was based a) on the renal parenchymal and collecting system accumulation and discharge of the radiopharmaceutical and b) on the background activity (BA) and its evolution throughout the study.

In 13 patients (5 renal insufficiency, 4 hypertension, 4 other) no structural abnormality was found and their disorders resolved clinically. Various degrees of bilateral low renal concentrating ability were noticed depending on prematurity, age, hydration and urine output rate.

Of the remaining 22 patients, 4 had acquired and 18 congenital parenchymal and/or collecting system abnormalities. In all but two, this technique suggested the correct diagnosis, proven surgically (8) or clinically(12). Focal defects in BA adjacent to kidneys were noticed in 7 studies (5 dilated collecting systems, 1 cross ectopic multicystic kidney, 2 retroperitoneal hematomas) and in lieu of kidney activity in 5 (2 multicystic, 2 nonfunctioning kidneys, 1 renal artery compression). There were 6 hypoplastic kidneys and 5 cases of agenesis where BA was intact. In hydronephrosis impairment of drainage (12) with or without enlarged kidneys and intrarenal BA defects were shown.

This technique was found to be valuable in the diagnosis of perinatal urinary system abnormalities.

RADIONUCLIDE STUDIES FOR RENAL ANATOMY AND FUNCTION IN CHILDREN. G.N. Sfakianakis, E. Sfakianaki, J.P. Smith, H.A. Wise, and J.F. Sotos. Columbus Children's Hospital, Columbus, OH.

A computer assisted program was used to study structural and functional anatomy of kidneys in 253 urologic and nephrologic pediatric patients. Tc-99mFe-Ascorbate-DTPA, Tc-99m-Tin-DTPA and o-I-131-hippurate were used to perform 316 studies. There were 1 to 5 followup studies in 46 patients. Computer analysis quantitated information mostly evident on sequential imaging.

Of 137 patients (179 studies) referred to study split functional anatomy of the kidneys, 44 had parenchymal (19 dystrophy, 2 ectopia, 10 duplication, 9 medical, 4 other) and 93 collecting system abnormalities (63 obstructive or reflux, 30 neuropathic). Seventy one % of the studies gave results deemed essential to patient management. Twenty eight % of the studies were used to assess medical (10%) or surgical (18%) therapy. Nonsuspected additional information was obtained in 25 patients.

Fifty one patients (61 studies) were referred to study structural anatomy of the kidneys (9 trauma, 22 perinatal problems, 20 suspected focal lesions). The tendative diagnosis was confirmed or ruled out in 48% of the studies, a different diagnosis suggested in another 48% and 4% of the studies were noncontributory.

Finally, 65 patients (76 studies) with a variety of suspected renal disorders were studied to obtain structural and functional information. In 75% the suspected conditions were confirmed or ruled out but in 22% findings that had not been expected were discovered.

Radionuclide renal studies provide structural and/or functional information important in clinical pediatrics.

A COMPUTER ASSISTED METHOD TO STUDY CHANGES IN RENAL FUNCTIONAL ANATOMY. C.N. Sfakianakis, E. Sfakianaki, J.P. Smith, H.A. Wise, and J.F. Sotos. Columbus Children's Hospital, Columbus, OH.

A computer assisted radionuclide method was used to study 39 pediatric patients in whom conventional radiologic and functional studies did not provide sufficient and accurate information to assess effects of therapy.

Hydrated immobilized recumbent patients were injected with 200 μCi/Kg of Tc-99m-Tin-DTPA (blood flow-GFR) and/or 5 μCi/Kg of o-I-131-hippurate (function-drainage). Serial imaging and computer accumulation of data followed each injection. Regions of interest were assigned avoiding ureteral, bowel and stomal areas. Time activity histograms were generated and analyzed. Background clearance indices, renal blood flow indices, split renal function, times of peak kidney activity and of the 50% and 75% of the peak on the upslope and the downslope, and also residual kidney activity were given by the program.

There were 51 pairs of successive studies for comparative analysis, 15 after nonoperative and 36 after operative management, 23 to assess short-term effects and 28 to

assess long term results. It was possible to identify a total of 42 kidneys with parenchymal function improvement, 24 of continued deterioration and 35 of no change. Drainage was improved in 37, progressively worsened in 19 and found unchanged in 24. In 21, peak activity occurred at the end of both studies. In the great majority conventional studies were questionable, inconclusive or contradictory regarding changes in renal function or drainage.

Computer assisted radionuclide studies can provide needed information in assessing results of medical and surgical therapy or changes in renal function in children.

GLUCOHEPTONATE RENAL IMAGING IN A CHILDREN'S HOSPITAL. J.C. Leonard, E.W. Allen, J.E. Wenzl. Oklahoma Children's Memorial Hospital, Oklahoma City, OK.

Our purpose is to share our experience in the utilization of renal imaging in a predominately pediatric population during the past year.

A total of 51 patients, ranging from 5 days to 19 years in age, were studied with Tc-99m glucoheptonate as part of a larger on-going Phase III clinical evaluation.

The distribution of the reasons for renal imaging were: inflammatory disease(4%), renal trauma(6%), abdominal mass lesions(12%), congenital anomalies and anatomic localization(32%), and functional evaluation(46%).

Of particular significance was the ability to image the neonatal kidney at a time when glomerular function was immature, to localize kidneys that were not visualized on intravenous urography, and the ability to obtain images in patients with increased blood urea nitrogen.

Sequential studies to objectively evaluate the renal functional mass, as described by Gilday, have been helpful in permitting assessment of change in differential renal function in chronic renal disease, meningomyelocele, and other urologic disorders, as well as patients with organic iodine allergy. A potential limitation with glucoheptonate is its inability to estimate glomerular filtration rate.

Glucoheptonate renal imaging provides a means of evaluating both renal function and renal structure with less irradiation to both the kidneys and gonads than routine intravenous radiography. The additional information advantage concerning calculi, skeletal abnormalities and other abdominal masses which is obtained with an intravenous urography provided by a supine abdominal film.

SIMULTANEOUS DETERMINATION OF THE SEPARATE GLOMERULAR FILTRATION RATE AND THE INTRARENAL TRANSIT TIMES BY MEANS OF THE Tc-99m-DTPA COMPLEX. VALIDATION AND RESULTS IN PEDIATRIC UROLOGY. A. Piepsz, H.R. Ham, J. Struyven, R. Denis, C.C. Schulman and F. Erbsmann. St-Peter Hospital, Free University of Brussels, Belgium.

Two different and independant parameters quantifying the renal function are obtained from a corrected kidney curve (R) and a curve representing the plasma concentration of the tracer (P) :

a) the separate glomerular filtration rate

$$SGFR\ (ml/min) = \frac{1}{P(t)} \cdot \frac{dR}{dt} \qquad 100 < t < 180\ sec.$$

b) the intrarenal transit times
obtained by deconvolution of R by P.

The test is of short duration. It delivers low radiation dose to the patient, is easy to perform and thus particularly adapted to the pediatric population.

SGFR was validated by comparison with other biological parameters, in 101 well documented cases of children with various kinds of uropathies (hydronephrosis, megaureters, vesicoureteral reflux...). SGFR correlates highly with total and separate creatinine clearance and with the Hg-197 Cl_2 renal uptake.

Direct renal artery injection was performed on six patients, validating the calculated transit times. Normal and obstructed kidneys are clearly discriminated by the calculated intrarenal transit times. In vesicoureteral reflux, normal to very prolonged transit times are observed. They are not related to the grade of the reflux, the SGFR nor the mercury uptake.

WEDNESDAY, JUNE 28
3:45 p.m.-5:15 p.m.

ANAHEIM ROOM

CLINICAL SCIENCE

NEUROLOGY

Chairman: Kenneth McKusick
Co-Chairman: Robert J. Cowan

RELATIONSHIP OF LOCAL CEREBRAL GLUCOSE UTILIZATION AND PERFUSION IN BRAIN ISCHEMIA: DETERMINATION BY EMISSION COMPUTED TOMOGRAPHY OF (F-18) FLUORODEOXYGLUCOSE AND (N-13) AMMONIA. D.Kuhl, M.Phelps, E.Hoffman, G.Robinson, N.MacDonald, A.Kowell, J.Winter. UCLA School of Medicine, Los Angeles, CA

By means of emission computed tomography (ECT), we used (F-18)FDG and (N-13) ammonia as indicators of abnormalities in local cerebral glucose utilization and perfusion respectively. The ECAT positron tomograph was used to scan 10 control subjects and 10 patients with cerebral ischemia. In control subjects, where local perfusion normally is regulated by and matched to local metabolic activity, we found local distributions of (F-18)FDG and (N-13) ammonia matched in all structures, i.e., frontal, temporal, parietal, and occipital grey matter, visual cortex, basal ganglia, and white matter. But patients with acute arterial occlusions had focal inhomogeneities and mismatches of the two indicators which reflected non-coupling of the usual perfusion-metabolism relationship. In regions of complete ischemia, both glucose utilization and perfusion were markedly depressed. Focal reactive zones of increased or "luxury" perfusion had normal, increased, or decreased glucose utilization. The peripheral zone of some early infarcts showed increased glucose utilization, probably due to enhanced anaerobic glycolysis in the hypoxic but still perfused border zone. These findings agree with those of Ginsberg et al who employed the (C-14)DG autoradiographic method to study carotid artery occlusion in cats. Few of these relationships could have been inferred in these patients from results of x-ray CT alone. In one patient with a small internal capsule hemorrhage XCT was the only abnormal study. But in three other patients, XCT was normal yet ECT showed definite metabolic defects which matched clinical dysfunction.

LOCAL CEREBRAL BLOOD VOLUME IN HEAD INJURED PATIENTS: DETERMINATION BY EMISSION COMPUTED TOMOGRAPHY OF (Tc-99m) RED CELLS. D.Kuhl, A.Alavi, E.Hoffman, M.Phelps, R.Zimmerman, W.Obrist, D.Bruce, J.Greenberg, B.Uzzell. UCLA School of Medicine, Los Angeles, CA. University of Pennsylvania School of Medicine, Philadelphia, PA.

This study was undertaken to help clarify the role of cerebral blood volume changes in patients soon after head trauma and during recuperation. Local cerebral blood volume (LCBV) was measured by means of emission computed tomography using the Mk IV tomograph after intravenous injection of technetium-99m red cells. In ten normal subjects, the mean cerebral blood volume (MCBV) for the whole brain was 4.34ml blood per 100gm with a coefficient of variation of 12%; for repeated studies in a single subject the coefficient of variation of MCBV was only 3%. Thirty patients underwent CBV studies after admission to the Hospital of the University of Pennsylvania in a disoriented or comatose state following head trauma. Values of MCBV separated according to clinical status were within one standard deviation of normal, but serial studies in individuals showed consistent trends. While instances of early increased MCBV were recorded, the most common pattern was an average 10% initial global decrease in MCBV compared to the value after recuperation. This was associated with a parallel 31% initial decrease in cerebral blood flow as measured by the Xenon-133 inhalation method. Greater changes were seen in LCBV on individual sections. There were mixed zones of hyper and hypovolemia in regions of infarction and intracerebral hematoma. The acute subdural hematoma had a consistent medial margin of increased LCBV which represented the dilated blood vessels of the underlying cortex. The presence and displacement of this hypervolemic zone was a sensitive indicator of persist-

ent subdural collection and mass effect even when the collection was lucent to x-ray computed tomography.

CLINICAL APPLICATIONS OF SINGLE GAMMA EMISSION COMPUTERIZED TOMOGRAPHY OF THE BRAIN. M.P.Frick, R.A. Ponto and M.K. Loken. University of Minnesota, Minneapolis, MN.

This investigation was undertaken to compare the diagnostic sensitivity and accuracy of emission computerized tomography "Union Carbide 701" (ECT) with conventional scintillation camera imaging (SC) and transmission tomography (TCT) in the detection of cerebral (CNS) pathology. 101 patients were included in our study. 5/5 primary brain tumors were demonstrated by ECT, as well as by SC and TCT. ECT demonstrated 6/6 ischemic brain infarcts, compared to 4/6 by SC and 3/6 by TCT. ECT by virtue of its sectioning capability is more sensitive to differences in radionuclide concentration at various depths in the brain than is true for SC. Ischemic infarcts may be missed by TCT, if the attenuation coefficient for the lesions does not significantly differ from that of normal brain tissue and if there is absence of a significant ventricular shift. TCT was slightly more sensitive in demonstrating multiple metastases (7/7) compared to ECT and SC (6/7). In 9 cases, ECT and SC scans were normal, whereas TCT scans showed various abnormalities, including dilated ventricles, porencephaly and/or brain atrophy. Our preliminary results indicate that the use of ECT appears to be most rewarding in diagnostic cases of acute ischemic infarcts. However, because the overall accuracy of TCT together with SC for determining cerebral mass lesions approaches 90-95%, it remains unclear just what impact ECT will have on the detection and evaluation of CNS lesions. Preliminary studies indicate that ECT can provide reliable information on regional CNS blood flow and metabolism; we are exploring the clinical utility of such data.

QUANTITATIVE IMAGING OF CEREBRAL FUNCTION DURING CONTINUOUS INHALATION OF $C^{15}O_2$ and $^{15}O_2$. J.A. Correia, R.H. Ackerman, N.M. Alpert, J. Chang, A. Gouliamos, J.C. Baron, J.M. Taveras. Massachusetts General Hospital, Boston, Mass.

Fifty-two patients and 8 normal subjects were studied during the continuous inhalation of $C^{15}O_2$ and $^{15}O_2$ using the MGH positron camera. Continuous inhalation of these gases establishes a dynamic equilibrium due to biological transport and radioactive decay. Inhalation of $C^{15}O_2$ results in the in vivo labeling of water of perfusion ($H_2{}^{15}O$). Inhalation of $^{15}O_2$ labels hemoglobin and ultimately produces ^{15}O labeled water of metabolism. The steady state distributions of $H_2{}^{15}O$ which result provide indicies of rCBF and oxygen metabolism(1).

Normal scintigrams were established which showed in the left lateral projection a crescentric area of decreased activity (corresponding anatomically with the centrum semiovale) and a focal area of increased activity in the region of the basal ganglia and overlying opercula and insula.The ratio of the $^{15}O_2$-image to the $C^{15}O_2$ image, which according to theory (1)depends linearly on the O_2-extraction fraction (E), was homogenous. Disturbed patterns of bloodflow and O_2-metabolism were found in patients with stroke, AVM and tumor. Defects in the $C^{15}O_2$ and $^{15}O_2$ images correlated well with the anatomic location of lesions determined by CT scan and cerebral angiography. Dissociation between bloodflow and metabolism was observed in some cases of tumor and acute stroke. Quantitative data was obtained in two subjects, one of which was neurologically normal. In the normal subject rCBF ranged from 40-88 cc/100g/min, E was nearly uniform (±10%) at 0.6 and $rCMRO_2$ ranged from 3-9 ml/100g/min

(1) Subrumanyum R., Alpert N.M., Hoop B. Jr., etal: J. Nucl Med 19, 48-53, 1978.*This work supported in part by USPHS grant #NS10828 and GM16712

TRANSVERSE SECTION IMAGING OF $H_2{}^{15}O$ DURING CONTINUOUS INHALATION OF $C^{15}O_2$ and $^{15}O_2$. N.M. Alpert, J.A. Correia, R.H. Ackerman, A. Gouliamos, G.L. Brownell, and J.M. Taveras. Massachusetts General Hospital, Boston, Mass.

Transverse section images of the distribution of ^{15}O-labeled water ($H_2{}^{15}O$) have been obtained in a group of 14 human subjects during continuous inhalation of $C^{15}O_2$ and $^{15}O_2$. $C^{15}O_2$ labels water in vivo and provides information on rCBF. $^{15}O_2$ provides information on regional oxygen extraction.+ Typically, 8-10 transverse sections are obtained with a resolution of 1.2 cm during a 20 min. imaging time. In normal subjects (4) a cortical increase of activity was found which correlates anatomically with the distribution of grey matter in the brain. The cortical activity in the subjects studied to date is 1.5 - 2 times greater than activity measured in the centrum semiovale. The ratio of the transverse section image obtained using inhalation of $C^{15}O_2$ to the image obtained during inhalation of O_2 provides a map in which the quotient varies linearly with the oxygen extraction fraction, $(C_A-C_V)/C_A$. In subjects with stroke, AVM and tumor focal defects in rCBF and oxygen extraction have been observed which correlate with lesions defined anatomically by CT scan and cerebral angiography.

+Subramanyam R, Alpert, N.M., Hoop, B., Jr. et al: J Nucl Med. 19, 48, 1978.
*This work supported in part under USPHS grants #NS10828 and GM16712

NITROGEN-13 NITROUS OXIDE FOR CEREBRAL IMAGING STUDIES. M. Zalutsky, T. Wickland, J. Nickles, and P.V. Harper. University of Chicago, Chicago, IL. and University of Wisconsin, Madison, WI.

In order to circumvent some of the limitations of the existing inert tracers for cerebral studies, the feasibility of using N-13 nitrous oxide has been explored. This agent which is an inert non-metabolized positron emitter is very soluble in water leading to rapid equilibration and even more soluble in lipid thus providing an excellent means for differentiating gray and white matter in the brain. The agent is easily produced by the pyrolysis of ammonium nitrate in concentrated sulfuric acid at ∿ 210°C. It may be labeled by using either a N-13 ammonium or nitrate ion precursor and by driving the reaction with an excess of the opposite moiety. With N-13 labeled ammonium ion and an excess of nitrate, 15-20 mC of N-13 nitrous oxide are regularly produced from a 10 min, 15-20 μA cyclotron bombardment. Radiochemical purity was 92-97% with the principal impurity being nitrogen. Nitrogen-13 nitrous oxide was administered by inhalation to human subjects and tomographic back projections of the brain were produced with the Searle positron camera. In these studies, the activity was retained sufficiently longer in the white matter to provide clear delineation of this tissue. Tomographic imaging appears to provide the capability of measurement of relative regional time-activity curves with N-13 nitrous oxide. Using tomography this agent should be superior to xenon-133 especially in the deeper regions of the brain because of the intrinsic freedom from attenuation. In addition to the usual applications of an inert tracer, N-13 nitrous oxide may well have potential for the investigation of well-differentiated neoplasms and demyelating disease.

THE USE OF POSITRON EMITTING ANESTHETIC COMPOUNDS FOR REGIONAL CEREBRAL BLOOD FLOW STUDIES. M.T. Madsen, R.J. Nickles, S.J. Gatley, R.D. Hichwa, D.J. Simpkin, and J.L. Martin. University of Wisconsin, Radiology Department, Madison, WI.

Clinical measurements of rCBF are performed almost exclusively with Xe-133. Xe-133 is poorly matched for gamma camera studies for rCBF because the low solubility of xenon in blood results in low brain activity and the low energy gamma limits spatial resolution. We have investigated physiologically inert positron emitting compounds of varying solubility as rCBF agents. The tracers studied in order of increasing solubility were N-13 nitrogen, (Xe-133), N-13 nitrous oxide, C-11 acetylene, and O-15 and O-14 labelled water. The positron emission allows coincidence techniques to be used for high spatial resolution and the high solubilities of nitrous oxide, acetylene, and water enable dynamic gamma camera studies.

The tracers are inhaled (or injected intravenously) followed by breath hold. Brain activity is monitored for a 15 minute period by coincidence probe arrays or is

imaged dynamically with a gamma camera. Arterial concentration of tracers is inferred by monitoring activities of the lung, heart and expired gas. The entire brain activity curve is well fitted to the sum of two exponentials convolved with the lung activity curve utilizing a weighted nonlinear least squares regression program. The verity of the model is further reflected by the stability of the fitted parameters to variations in the respiratory maneuver. Fitted clearance rates are comparable to those obtained with Xe-133. The increased spatial resolution, higher solubility and the ability to utilize all information in the brain activity curve demonstrate the significant advantages of these tracers over Xe-133.

KRYPTON-77 POSITRON EMISSION TOMOGRAPHY FOR EVALUATION OF MEDICAL AND SURGICAL TREATMENT IN STROKE PATIENTS. Y.L. Yamamoto, J. Little, E. Meyer, C. Thompson and W. Feindel. Montreal Neurological Institute, Montreal, Que., Canada.

True topographical and quantitative measurement of regional cerebral blood flow is now possible with a circular positron device using the non-invasive Krypton-77 inhalation technique. We have used this technique to evaluate topographical changes of regional cerebral blood flow before and after medical and surgical treatments in over 80 stroke patients. The results of Krypton-77 positron emission tomography (Kr-77 P.E.T. study) in these patients, in correlation with the results of computed tomography (CT) scans and sequential cerebral dynamic studies, using a gamma scintillation camera with Med II computer, were reviewed. The focal cerebral infarction, shown as a lower density in the CT scans, received none or a minimal amount of Krypton-77 gas with very low rCBF values of 0 to 9 ml/100 g/min. The moderately reduced rCBF values of 15 to 35 ml/100 g/min, shown in the Kr-77 P.E.T. study, are often correlated with moderate to severe reduction of the cerebral perfusion of the gamma emitting, non-diffusible tracer in the cerebral dynamic study but no abnormality is apparent in the CT scans. The results of the Kr-77 P.E.T. study indicate that improvement of rCBF in the cortical and subcortical ischemic lesions, treated by by-pass surgery, is much more extensive and of a higher magnitude than that achieved with medical treatment with 5% carbon dioxide inhalation.

WEDNESDAY, JUNE 28 SANTA ANA ROOM
3:45 p.m.-5:15 p.m.

BASIC SCIENCE

RADIOPHARMACEUTICALS V: CYCLOTRON-PRODUCED RADIONUCLIDES

Chairman: Alfred P. Wolf
Co-Chairman: Roy S. Tilbury

ENZYMATIC SYNTHESIS OF C-11 PYRUVIC ACID, LACTIC ACID AND L-ALANINE. M.B. Cohen, L. Spolter, C.C. Chang and N.S. MacDonald. VAH, Sepulveda and UCLA.

Lactic acid is readily utilized by the myocardium. An enzymatic synthesis for C-11 lactic acid was therefore devised and is performed in two steps: 1) production of C-11 pyruvate from C-11 CO_2 and acetyl CoA in the presence of an enzyme extracted from Clostridium acidi urici 2) Conversion of C-11 pyruvate to lactic acid by lactic dehydrogenase. Alternatively, pyruvate may be transaminated to C-11 L-alanine by glutamic-pyruvic transaminase.

The incubation mixture contained the following substances in a total volume of 2 ml: C-11 carbon dioxide, 30-40 mCi; ferredoxin, 2 x 10^{-6} mmole; ferredoxin reductase, 0.1 unit; NADPH, 8 x 10^{-2} mmole; acetyl CoA, 2 x 10^{-2} mmole; acetyl phosphate, 2.9 x 10^{-2} mmole; phosphotransacetylase, 25 units, cysteine, 2.5 x 10^{-3} mmole; potassium phosphate buffer, 17.6 x 10^{-2} mmole; NADH, 1.25 x 10^{-3} mmole; lactate dehydrogenase, 50 units; pyruvate-ferredoxin oxidoreductase, approx. 1 mg. After anaerobic incubation at 37°C for 10 minutes, the sample was passed through an AG 50W x 8 resin column which had been equilibrated with 0.1N sodium acetate buffer, pH 2.3. The effluent was then passed through an AG 1 x 8 resin column which had been equilibrated with HCL at pH 3 and then washed with double distilled water. A yield of about 3-5% (corrected for decay) was obtained in 20 minutes. The identity of the C-11 lactate was established by paper chromatography and by its behavior in various chromatographic columns, where it acted like standard lactic acid.

Tissue distribution studies in rabbits have demonstrated a 7:1 myocardium to lung ratio for C-11 lactic acid, which is suitable for quantitative tomographic imaging.

SPECIES DIFFERENCES IN THE MYOCARDIAL LOCALIZATION OF N-13-L-ASPARAGINE. C. Majumdar, V. Stark, K. Lathrop, and P.V. Harper. University of Chicago, Chicago, IL.

The spectacular myocardial localization of N-13 labeled L-asparagine in the dog reported by The Sloan Kettering Group led us to study the behavior of this agent in other species including man. The remarkably high localization in the dog heart was confirmed. In the rabbit however the localization was almost trivial, the heart to liver ratio being 1:10 as compared to 1:1 in the dog. In the primate (baboon) the localization in the myocardium was quite good, 6 to 9% of the injected dose, but in the human subject the uptake was only 2.5% of the injected dose giving no advantage over that observed with N-13 labeled ammonia. The agent was prepared by enzymatic synthesis using asparagine synthetase separated from mutant E. coli. The labeled asparagine was identified by electrophoretic comparison with authentic ^{14}C-labeled material and by treatment with asparaginase. Measurements were made with a two-camera coincidence imaging system comparing organ activity to that of a reference injected standard imaged simultaneously. Counts were normalized to a sheet source transmission image to correct for attenuation and adjacent background was subtracted. The mechanisms involved in the exceedingly wide species variation observed are not clear and the dangers of incautious extrapolation of animal data to human studies is well illustrated in this case of an apparently very promising radiopharmaceutical.

F-18 FLUORODEOXYGLUCOSE: REMOTE, SEMI-AUTOMATED PRODUCTION USING A COMPACT CYCLOTRON. G.D. Robinson, Jr., N.S. MacDonald, M.P. Easton, and J.S. Cook. UCLA, School of Medicine, Los Angeles, California.

Synthesis of F-18 labeled 2-deoxy-2-fluoro-D-glucose (FDG) has been reported by the Chemistry Group at BNL. FDG is being evaluated as an in vivo indicator of glucose metabolism. To minimize radiation exposure during synthesis and to maintain vacuum integrity in the target, we modified the BNL procedure and devised a remote, semi-automated method for routine production of FDG on our cyclotron.

Using BNL designed targets and a Ni manifold together with remotely operated valves, all target operations including filling with fluorine (50 torr) and Ne (280 psi) and release of F-18 into the fluorination vessel are controlled from outside of the cyclotron vault. The fluorination vessel is located inside of the vault next to the targets;with fluid access controlled by remotely operated valves. Prior to release of F-18 labeled target gas, 40 mg of triacetyl glucal in 15 ml of Freon 11 are transferred into the vessel This solution is held at -78°C and target gas release rate is 50 ml/min. After delivery of F-18 is complete the crude products are transferred out of the vault for processing. Solvent is evaporated, labeled residue is dissolved in diethyl ether (DEE) and is applied to a 1 cm X 25 cm silica gel column. The F-18 FDG precursor is eluted with 45 ml of 4:1 petroleum ether:DEE. After solvent removal, the residue is hydrolized with 1.0 N HCl at 130° for 30 min. Final purification is by passage through a single column packed sequentially with AG 11A8 resin, neutral alumina, and AG

11A8. The FDG produced exceeds 95% radiochemical purity as measured by TLC. A 25 μAhr bombardment yields 6-8 mCi of FDG at a specific activity of 2-4 mCi/mg at 2½ hr after EOB.

EVALUATION OF THE RADIOPHARMACEUTICAL POTENTIAL OF AN ANALOG OF DIHYDROTESTOSTERONE, LABELED WITH F-18. L.A. Spitznagle, C.A. Marino and P. Rapacz. University of Connecticut Health Center, Farmington, CT.

This laboratory has recently developed a technique for labeling potential radiopharmaceuticals with fluorine-18. The crown ether assisted nucleophilic displacement by fluoride ion of various leaving groups has been adapted to allow preparation of steroid molecules labeled with fluorine-18. We have previously reported the use of this technique to prepare 21-F-18-fluoropregnenolone-3-acetate, and 21-F-18-fluoroprogesterone. We now wish to report the preparation of an F-18-labeled analog of dihydrotestosterone (DHT), 2-F-18-fluoro-5α-androstan-17β-ol-3-one, (I).

I was prepared from 2α-bromo-5α-androstan-17β-ol-3-one 18-crown-6, and KF-18. The maximum radiochemical yield based on total activity present after work-up was 12%. The total time required for the reaction and its work-up was 150 min.

Initial distribution studies in rats indicate that the compound concentrates in steroid target organs such as the adrenal gland, ovaries and the prostate gland. The compound also reaches high concentrations in sites of steroid metabolism and excretion such as the liver and kidney. Significant differences were observed in the handling of the compound by female and male animals. This or similar compounds may prove useful for studying diseases involving steroid hormone metabolism, secretion and/or utilization.

5-[F-18]FLUOROURIDYLATE AS A PROBE FOR MEASURING RNA SYNTHESIS AND TUMOR GROWTH RATES IN VIVO. E. Crawford, M. Friedkin, J. Fowler, B. Gallagher, R. MacGregor, A. Wolf, I. Wodinsky and A. Goldin. Univ. of Calif., San Diego, CA, Brookhaven Nat'l. Lab., Upton, N.Y., A. D. Little, Boston, MA, Nat'l. Cancer Inst., Bethesda, MD.

Since 5-fluorouridine is incorporated into RNA more efficiently than 5-fluorouracil (Harbors, Chaudhuri, and Heidelberger, 1959), we have explored the feasibility of using 5-fluorouridylate labeled with fluorine-18 as a probe for measuring the in vivo synthesis of RNA in tumors. 5-[F-18]fluorouracil was converted enzymically to the nucleotide by incubation with pyrophosphorylribosylphosphate and uridylate pyrophosphorylase (EC 2.4.2.9.). Fluoronucleoside and fluoronucleotide were found to be very effective precursors in mouse spleen and intestine which have a high rate of RNA synthesis. The fluorpyrimidine was poorly utilized. Shortly after intravenous administration of 5-[F-18]fluorouridylate most of the radioactivity in mouse tissues such as liver and intestine was due to F-18 labeled acid-soluble metabolites. With time the acid-soluble radioactivity decreased considerably while the percent of the dose in RNA per gram of tissue remained relatively constant from 2 to 16 hr. The utilization of 5-[F-18]fluorouridylate for RNA synthesis in liver, spleen, kidney, and intestine was markedly inhibited by actinomycin D. Intracranial tumors such as L1210 murine leukemia and ependymoblastoma incorporated significantly higher levels of F-18 than normal mouse brain. The RNA of ependymoblastoma brain tumors contained 40 times as much F-18 than RNA from normal brain. By employing positron emission tomography and 5-[F-18]fluorouridylate or 5-[F-18]fluorouridine it should be possible to determine the in vivo rate of RNA synthesis as an index of tumor growth and response to anticancer drugs.

PREPARATION OF RADIOBROMINATED PROTEINS USING BROMOPEROXIDASE. K.D. McElvany, L.C. Knight, and M.J. Welch. Mallinckrodt Institute of Radiology, Washington University School of Medicine, St. Louis, MO.

Bromoperoxidase, an algal enzyme obtained from Bonnemaisonia hamifera, has been found to catalyze carrier free radiobromination and radioiodination of proteins at pH 7. It is desirable to label proteins with radioisotopes of bromine as bromine forms a stronger bond to carbon than does iodine. Thus the radiohalogen labels should remain more stably attached to proteins. To date, the only method available for direct carrier-free radiobromination of proteins required a pH of 2.8. This pH is too acidic for most proteins, and labeling at this pH results in unstable attachment of bromine atoms to cysteinyl residues (sulfur-bromine bond) rather than stable attachment to tyrosyl residues (carbon-bromine bond). Optimum efficiencies for carrier-free radiobromination at pH 7 can be achieved by mixing protein (25 μg), partially purified bromoperoxidase (25 μl), carrier-free Br-77 as NaBr in aqueous solution, and 20 nanomoles of hydrogen peroxide in a total volume of ∿0.25 ml. The reaction is complete after 35 minutes at 37° C. In vitro hydrolysis studies on proteins labeled with Br-77 in this manner have shown the label to be completely stable toward hydrolysis at pH 7 for at least 10 days. Studies on sites of attachment of the Br-77 label indicate that bromotyrosyl residues are the predominant species formed. This gentle technique for radiobromination is applicable even to the labeling of sensitive proteins such as fibrinogen. In vitro clottability studies on fibrinogen labeled with Br-77 using this method have shown >85% clottability of the labeled fibrinogen. Also, increased stability of the label should make feasible accurate protein turnover studies lasting several days.

AN ON-LINE, AUTOMATED, MULTIGENERATOR SYSTEM FOR RB-81/KR-81M PRODUCTION.* T. J. Ruth, R. M. Lambrecht and A. P. Wolf. Chemistry Department, Brookhaven National Laboratory, Upton, NY 11973, and M. L. Thakur. Yale-New Haven, Hospital, New Haven, CT 06510.

The increase in the demand for short-lived radionuclides at hospital-based cyclotrons for radiopharmaceuticals necessitates the development of on-line, automatic systems. Such a system for the production of from 1-4 Rb-81/Kr-81m generators has been constructed and in routine use at the BNL 60-inch cyclotron. These generators are loaded simultaneously in a shielded container from a remote location at EOB without exposure to the operator. The Rb-81 is produced from the (p,xn) reactions on a natural Kr gas target at 140 psi. The production rate is 7 mCi/μAh when using 33→14 MeV protons. At EOB a valving system vents the Kr from the Ni target, pumps water through the target and collects 90-95% of the Rb activity. The Rb-81 is pumped through the columns in parallel where ∿90% of the activity is removed. Flow rates through the colums varies by <10%. Zirconium phosphate and Dowex-50W resin were used. The extraction of Rb by both materials was studied over a wide range of flow rates (4-35 ml/min) and found to be comparable. A 1-h x ∿20 μA irradiation provides enough activity to load 4 generators with >25 mCi of Rb-81. The loading process including a clean rinse requires <10 minutes. Preliminary experiments with low beam currents (.1-1 μA) indicate that Bromoform can be used as target material in a dynamic target-generator system for production of Rb-81 via the (α,2n) reaction. This would result in the generator being fully loaded at EOB.

*Research carried out at BNL under contract with the U.S. DOE and supported by NIH Grant No. 5 P41 PR00657.

WEDNESDAY, JUNE 28 CALIFORNIA B ROOM
3:45 p.m.-5:15 p.m.

IN VITRO AND CORRELATIVE TECHNIQUES

RADIOASSAY II: THYROID

Chairman: Martin L. Nusynowitz
Co-Chairman: Avir Kagan

PHYSIOLOGY AND CLINICAL RELEVANCE OF TRIIODOTHYRONINE (T_3). L. E. Braverman, University of Massachusetts Medical School, Worcester, MA.

THE EFFECT OF AN ETHANOL-EXTRACTABLE TRIIODTHYRONINE BINDING SUBSTANCE IN PLASMA ON THE MEASUREMENT OF TRIIODOTHYRONINE BY RADIOIMMUNOASSAY. T. H. Hsu, E. L. Nickoloff, R. C. Rock, and A. Herner. The Johns Hopkins Hospital, Baltimore, Md. and Herner Analytic's, Rockville, MD.

A 28-year-old nervous woman was referred for evaluation of T_3-thyrotoxicosis. Her serum T_4 and TBG levels were normal, but serum T_3 was elevated to 450 ng/100 ml using a solid phase radioimmunoassay (RIA) with rabbit antibody coated to glass beads. When the patient was rendered hypothyroid (proven by low T_4 and high TSH), her serum T_3 remained high and unchanged from the pretreatment value. Further studies showed that she had no assayable serum T_3 when it was measured with charcoal and polyethylene glycol separations. Assay of T_3 in ethanol-extracted serum resulted in values 150 to 170 ng/100 ml, regardless of RIA technique. Serum protein electrophoresis was normal as was the distribution of binding radioactive T_3 to her serum proteins.

Studies of T_3 receptor sites showed binding of 864 femtomoles radiolabelled T_3 per mg protein, approximately twice the normal binding capacity. It is postulated that this patient's serum contains a substance which preferentially binds T_3 and thus gives false results in the assay for serum T_3. True serum T_3 value may be altered because of T_3-binding immunoglobulin (JCEM 42:642, 1976) or in the manner as in the present case.

AGE-DEPENDENT CHANGES IN THYROID HORMONE VALUES. A. Lipson, E.L. Nickoloff, T.H. Hsu, R. Shakir, and H.N. Wagner, Jr. The Johns Hopkins Hospital, Baltimore, MD.

Measurement of total serum T4 and T3, T3 Resin Uptake, TSH and reverse T3 were made in 209 healthy adults, age 20-89 (107 males and 102 females). Subjects were studied by decade and age-related changes for each parameter were noted. Thyroxine values were stable for men throughout life, but were significantly higher in females under 60 than in older women (7.90 ± 1.34 vs. 7.39 ± 1.35 ug/dl, $p<0.05$). There were no statistically significant differences in T4 in subjects over 60. Values for T3RU were significantly higher in men than women throughout all decades (31.5 ± 2.3 vs. 29.4 ± 2.4%, $p<0.0005$). Females had significant increases in T3RU after age 60. Free thyroxineindex showed no significant age or sex-related changes. TSH increased significantly in females over 60 (3.379 ± 1.58 vs. 2.347 ± 1.26 uU/ml, $p<0.05$). Men had stable TSH levels throughout life, higher than female results before age 60 and lower thereafter. Mean T3 declined similarly for both sexes with increasing age. Mean values for males and females under 60 were 139.8 ± 19.9 vs. 127.0 ± 20.8 ng/dl for the older group, $p<0.0005$. Men had significantly higher rT3 values over all decades (245.0 ± 46.9 vs. 203.9 ± 41.3 pg/ml, $p<0.0005$). Female rT3 decreased significantly after age 60 (216.0 ± 39 vs. 194.8 ± 41 pg/ml, $p<0.005$), while males maintained stable values.

The physiologic reasons for these findings are unknown, although sex-related changes in binding proteins and alterations in metabolic clearance rates, production, and degradation of these hormones with increasing age may significantly contribute to producing these results.

FREE THYROXINE (FT_4) RADIOASSAY WITH PRESATURATED ANTI-T_4 MICROCAPSULES. F. S. Ashkar, R. Buehler, T. Chan, Jackson Memorial Hospital, Miami, Fla. and Damon Labs., Nedham Heights, Mass.

Free thyroxine is the active hormonal portion in contact with end organs, is unaffected by serum protein alterations, and it's measurement reflects true thyroid function or malfunction, previous FT_4 assay techniques were difficult, long, costly, and inaccurate.

A quick, simple, and accurate radioassay for FT_4 was developed utilizing T_4 antibody (rabbit) complexed with high specific activity T4-125 tracer and encapsulated in nylon microcapsules 30-50μ in size, the microcapsule minidialysis membrane is formed by an emulsification and separation process where Hexanediamine inorganic solution and emulsified antibody solution are treated with acid chloride starting a rapid polymerization process allowing the antibody to be encapsulated, T_4 standards or unknown samples are added where the FT_4 liberates a proportional amount of FT_4-125 from the microcapsules; bound T_4 is excluded from the reactions, centrifugation separates the microcapsules from the freed T_4-125 portion, a standard curve is generated and unknowns are obtained from it.

A panel of known samples as well as a group of normals, pregnant women, hypothyroid and hyperthyroids were tested by this radioassay.

The results showed an excellent co-efficient of variations, and the FT4 values correlated well with the clinical state of the patient and their thyroxine values.

This FT_4 radioassay appears to have the distinct advantages of simplicity, speed, and accurcay unmatched by previous techniques to date.

WEDNESDAY, JUNE 28 CALIFORNIA A ROOM
3:45 p.m.-5:15 p.m.

CLINICAL PRACTICE

CARDIOVASCULAR I

Chairman: Donald A. Podoloff
Co-Chairman: William Turner Harris

PROBE RADIOCARDIOGRAPHY: VALIDATION OF A TECHNIQUE FOR DETERMINING LEFT VENTRICULAR EJECTION FRACTION. John L. Floyd, Robert E. Sonnemaker, Jerome A. Waliszewski, and Robert F. Bode. William Beaumont Army Medical Center, El Paso, TX.

An investigation was undertaken to validate measurements of left ventricular ejection fraction (LVEF) as determined with a commercially available cardiac probe. In fifteen patients undergoing cardiac catheterization, four or five probe radiocardiograms (RCG) were recorded using 1.0-1.5mCi Tc-99m sulfur colloid: 1) right atrial injection of the bolus with the probe positioned by TM echocardiography; 2) if necessary, a second right atrial injection with the probe location adjusted based on inspection of the first RCG; 3) repeat right atrial injection after removing the probe from the subject's side and repositioning at the location for the first (or second) RCG; 4) injection of the bolus into a basilic, cephalic, hand, or wrist vein with a 20cc saline flush; and 5) repeat peripheral injection. Correlation coefficients among the injection groups ranged from .95 to .98 and mean LVEF for all groups was identical. The correlation coefficient with LVEF estimated by single plane ventriculography was .88. Thus, no differences existed between probe positioning, injection site, and rapid sequential injections. It is concluded that the probe yields LVEF with accuracy and precision, that a peripheral injection is suitable, and that rapid serial measurements are feasible.

VALIDITY OF A PROBE TECHNIQUE FOR EJECTION FRACTION DETERMINATION. J.P. Wexler, J. Strom, E.A. Sonnenblick, and M.D. Blaufox, Albert Einstein College of Medicine, Bronx, NY.

The radionuclide determination of ejection fraction is now a proven and accepted noninvasive technique. Cost and size of the equipment needed to perform this evaluation as well as the time and expertise required for processing tends to limit the availability of this procedure to hospitals with extensive nuclear medicine and cardiology facilities. A portable, single-crystal probe (based on a method described by Wagner) coupled to a microprocessor and electrocardiographic gate allows for the bedside determination of ejection fraction, cardiac output, left-to-right shunt and ejection velocity. Acceptance of this technique requires proof of reproducibility and accuracy in spite of blind positioning of the probe. An empirical method has been developed resulting in reproducible placement of the probe for determination of ventricular and background activity. Comparison of scintigraphic ejection fractions determined by conventional gated acquisition with those determined by probe reveal excellent correlation ($r=0.96$, $n=7$, $p < 0.01$) in patients with intrinsic heart disease. Sequential determinations by the same observer and interobserver results agree well. Time for acquisition and processing is less than 5 minutes per determination.

DEMONSTRATION OF SEGMENTAL THALLIUM PERFUSION DEFECTS IN CARDIOMYOPATHIES HAVING NORMAL CORONARY ARTERIES. D. Feiglin, V. Huckell, H. Staniloff, P. McEwen, J. Morch, P. McLaughlin, Divisions of Nuclear Medicine and Cardiology, Toronto General Hospital, Toronto.

57 patients were investigated for various cardiomyopathies. All had selective coronary arteriograms with multiple views; graded exercise test symptom limited (Bruce Protocol) with rest and exercise Thallium studies performed at least one week apart and imaged using two doses of 1.5 mCi. Thallium.

All of these patients had normal coronary arteriograms. Of this group 4 patients had Malignant Hyperthermia (MH); 22 Mitral Valve Prolapse (MVP); 10 Eisenmenger Syndrome (ES); 7 Coronary Artery Spasm (CAS); 9 Muscular Subvalvular Stenosis (MSS) and 5 miscellaneous (MISC) including congestive cardiomyopathy; 2 Loeffler's; one Idiopathic Pulmonary Hypertension and one Mitral Stenosis and Pulmonary Hypertension. Within this total group 26 had negative exercise studies; 17 were non interpretable; 9 were false positive and 5 patients were not studied. Abnormal Thallium studies were seen in MH-2; MVP-11; ES-7; CAS-3; MSS-6; all of the MISC group. 19 of these patients demonstrated exercise induced defects. Only 23 of 57 patients had normal Thallium studies.

In the presence of normal coronary arteries we suggest that perfusion defects indicate one or a combination of cellular loss, dysfunction or regional malperfusion. Abnormal Thallium scans need not indicate presence of coronary artery disease.

Tc-99m METHYLENE DIPHOSPHONATE MYOCARDIAL SCANS IN ADRIAMYCIN THERAPY. A. Alavi, J.Glick, and N. Reichek. Hospital of the University of Pennsylvania, Philadelphia, PA.

Adriamycin (Adr) is a valuable antineoplastic agent, widely used, but associated with significant incidence of myocardial toxicity. Early diagnosis of this complication is of importance to oncologists. This study was designed to evaluate the usefullness of myocardial scanning with Tc-99m MDP in these patients.

Thirteen patients with malignancy were studied during or after completion of Adr therapy. None of the patients had cardiovascular disorder before the study nor developed evidence of congestive heart failure during the study. Myocardial scans were performed at 3 month intervals. In total, 26 scans were obtained. The intensity of activity in the myocardium was graded 0 to +4. Fourteen scans in 8 patients who received 200-300 mg/m^2 of Adr revealed 2 cases of +1 uptake. Five scans in 3 patients with a dose of 300-400 mg/m^2 showed four +1 activity. Six scans in 3 patients who were given 400-500 mg/m^2 of Adr had only one +2 positive scan. Finally 3 scans on one patient who received 550 mg/m^2 showed only one 1+ uptake. In conclusion, no relation was found between the dose of Adr and the uptake of Tc-99m MDP in the myocardium. Until more information becomes available, one must be cautious in the use of this test for detection of myocardial toxicity.

Tc-99m PYROPHOSPHATE MYOCARDIAL IMAGING FOLLOWING CARDIOPULMONARY RESUSCITATION WITH DC COUNTERSHOCK. S.M. Spies, R. Davison and J. Przybylek. Northwestern University, Chicago, IL.

Myocardial infarct imaging was performed in a series of 24 patients who had received cardiopulmonary resuscitation (CPR) including DC countershock to assess the influence of electrical cardioversion in the setting of cardiac arrest on the appearance of Tc-99m pyrophosphate images. All patients had cardiac arrest or life threatening arrhythmias requiring CPR 48 to 72 hours prior to imaging. Images were performed 2 hours after intravenous injection of 15 mCi of Tc-99m stannous pyrophosphate. Anterior, left anterior oblique and left lateral views were interpreted without prior knowledge of clinical history, ECG or serum enzyme determinations. The images were evaluated for the presence of abnormal myocardial uptake and skeletal abnormalities. Patients received from one to seven shocks for a total of from 100 to 2200 watt seconds. Of eleven patients without other evidence of acute myocardial infarction, all but one had normal images. The one patient without clinical evidence of infarction but with positive myocardial images had received intracardiac epinephrine during the course of CPR. Myocardial imaging was abnormal in all four patients with unequivocal transmural infarcts. Three of six patients with subendocardial infarcts had positive studies. Three additional patients had biochemical findings suggestive of infarction but no ECG evidence, and in these patients images were normal. These findings are in general agreement with previously published sensitivity and specificity data for infarct imaging, and suggest that false positive images following cardioversion do not represent a major source of error in interpretation of Tc-99m pyrophosphate myocardial images.

WHY FIRST TRANSIT? D.G. Pavel, E. Byrom, S. Swiryn, and B. Ayres. University of Illinois Medical Center, Chicago, Illinois.

We have recently shown that first transit cardiac studies on Anger type cameras can be used successfully for the evaluation not only of the ejection fraction but also of other aspects of the left ventricular function (several types of functional images, wall motion, slope evaluation of the time activity curves, etc.). Until recently this multifaceted evaluation was considered possible only with multicrystal cameras. The use of Anger type cameras will greatly increase the availability of complete first transit studies. Under these circumstances it is important to establish a clear set of indications. Based on the past 1½ years' experience in our institution, the following set of indications for the study has emerged: 1) when rapid screening is needed; 2) when there is disproportion between the number of requests and the availability of Nuclear Medicine resources; 3) when minimizing cost is essential; 4) when there is a need for frequent follow-up (during and

post therapy); 5) very sick or poorly cooperative patients; 6) when a myocardial scan (Tc-PYP) is needed at the same time (e.g. during routine evaluation for perioperative M.I. post coronary bypass); 7) in combination with Tl-201 scan; 8) in patients with high suspicion of inferior or apical anomalies; 9) during i.v. injection of almost any Tc-labeled compound administered for other studies (e.g. for brain, liver, kidney, etc.); 10) in combination with the EKG synchronized studies.

In conclusion, the well known advantages of first transit techniques (minimal patient, gamma camera and technologist time requirements) coupled with the multiplicity of data which can be obtained result, for both clinical and economic reasons, in a wide spectrum of indications.

MYOCARDIAL VIABILITY: ASSESSMENT WITH FIRST PASS RADIONUCLIDE ANGIOGRAPHY FOLLOWING NITROGLYCERIN. C. Hellman, J. Carpenter, F. Blau, W.D. Johnson, D. Schmidt. University of Wisconsin-Mount Sinai Medical Center, Milwaukee, WI

Myocardial viability is a critical determinant in the selection of patients (pts) for myocardial revascularization surgery (MRS) especially in pts with marked left ventricular (LV) dysfunction. To determine if improved LV function or wall motion (WM) produced by nitroglycerin (NTG) would result in the same effect following successful revascularization, 12 consecutive pts were prospectively studied. They were assessed preoperatively by conventional LV cineangiography (CA) and first pass RAO radionuclide angiography (RNA) to measure ejection fraction (EF) and regional WM both before and 4 minutes after 1/150 grain NTG. Pre-op LVCA and RNA EF's correlated well (r=0.98). Postoperatively (post-op) evaluation was by RAO RNA. Regional LV WM was assessed by dividing the end diastolic volume (EDV) image into 6 segments and analyzing the EDV and end systolic volume perimeters as well as a derived regional distribution of EF image. Average pre-op EF rose from 0.30 to 0.36 after NTG ($p<.01$); average post-op EF was 0.38 ($p<.05$). Nine pts showed a pre-op EF increase after NTG; 6 of these showed an increased EF after MRS. Of a total of 72 segments analyzed for LV WM, 54 showed a baseline study abnormality. Of 40 hypokinetic segments, 17 improved post MRS; 13 segments had been seen to improve in the NTG RNA. Of 7 akinetic segments, 2 improved post MRS; they were the only 2 akinetic segments to improve in the NTG RNA. None of the 7 dyskinetic segments improved either post MRS or in the NTG RNA. These studies indicate that first pass RAO RNA post-NTG is useful for noninvasive prediction of regional WM and overall LV function improvement in pts considered for MRS.

THURSDAY, JUNE 29, 1978

THURSDAY, JUNE 29 — GARDEN GROVE ROOM
8:30 a.m.-10:00 a.m.

CONTINUING EDUCATION

ENDOCRINOLOGY AND RADIOIMMUNOASSAY: METHODOLOGY, INTERPRETATION, AND CURRENT STATUS

PARTICIPANTS: Steven M. Larson, Chairman, V.A. Hospital, Seattle, WA; Stanley J. Goldsmith, Co-Chairman, Mt. Sinai School of Medicine, New York, NY; Robert J. Griep, U.S. Public Health Hospital, Seattle, WA; E. Samols, V.A. Hospital, Louisville, KY; and Thomas G. Rudd, University Hospital, Seattle, WA.

THURSDAY, JUNE 29 — ANAHEIM ROOM
8:30 a.m.-10:00 a.m.

CLINICAL SCIENCE

BONE/JOINT

Chairman: N. David Charkes
Co-Chairman: Tuhin Chaudhuri

QUANTITATIVE EVALUATION OF ARTICULAR DISEASE. K. Rosenspire, M. Blau, L. Russamanno, and F. Green. State University of New York at Buffalo, Buffalo, NY.

The radionuclide evaluation of arthritic involvement is always difficult because of the uptake of scanning agents in normal joints. The purpose of this investigation was to quantitate the uptake of Tc-99m pyrophosphate in normal and arthritic joints. Twenty normal and 20 arthritic patients were studied 2-3 hours after injection of 10-15 mCi of Tc-99m pyrophosphate with images taken of the hands, knees, forearms and thighs. All images were stored for quantitative evaluation in a 64x64 matrix on an MDS computer. Each joint in the hands and knees (a total of 32 joints) was flagged to determine the uptake per unit area (absolute number of counts/channel/minute normalized for body weight and decay).

The normalized uptake in each arthritic joint was then compared to the average normalized uptake in that same joint in the normal group.

There was a distinct difference in uptake between normal and arthritic joints with no overlap between groups. The difference ranged from a 39% increase to an 84% increase with an average of a 60% increase in uptake of arthritic joints over normal joints.

Other calculated parameters, including ratio of joint to mid-femur, total joint uptake and total joint ratio, were ineffective in distinguishing between normal and arthritic joints.

The normalized quantitative uptake per unit area of Tc-99m pyrophosphate in arthritic joints might be useful in detecting minimally involved joints and in following the progression of joint disease and the effectiveness of drug therapy.

SKELETAL TRACER UPTAKE AND BONE BLOOD FLOW IN DOGS. V.Sagar, J.M.Piccone, N.D.Charkes, and P.T.Makler Jr., VA Hospital, Wilmington,DE. & Temple Univ. Med. Sch., Philadelphia, PA.

The relationship between bone blood flow and skeletal tracer uptake is poorly understood. Recent compartmental modelling studies suggest a complex interaction and a saturation effect with increasing flows. We therefore undertook a study to investigate the effect of altering skeletal blood flow on tibial uptake of a bone-seeking tracer, Tc-99m-methylene diphosphonate (MDP), in anesthetized dogs. Aortic blood was diverted through a sigmamotor pump and reinfused into each femoral artery at controlled rates monitored with electromagnetic flowmeters. Normal flow was maintained in the control limb and the flow varied in the experimental limb from 0.3 to 4 times normal. Tibial nutrient perfusion was estimated with labeled microspheres. MDP was injected into the jugular veing and the dogs killed 75 min later; the tibias were dissected out, cleaned, and

crushed, and right/left activity ratios determined by well scintillation counting. In 17 dogs we found that increasing the bone blood flow up to 4x normal increased MDP uptake by only 70%, indicating a saturation effect; an excellent fit to the computer-predicted curve was observed. There was close correlation between tibial nutrient perfusion and femoral artery flow. In nerve-sectioned dogs the resting MDP uptake was twice normal, and early data suggest saturation with increasing flows.
Conclusion: With respect to skeletal blood flow, bone behaves as if it were almost saturated with MDP, in agreement with computer predictions. Nerve section opens normally closed vessels, probably accounting for the "warm" scans seen after stroke and sympathectomy. Markedly increased (>2x nor) MDP uptake is not the result of increased blood flow.

EVOLUTION OF THE BONE IMAGING FINDINGS IN OSTEOMYELITIS. G.N. Sfakianakis, P. Scoles, M. Welch, R. Haynes, M. Hilty, and P. Azimi.
Columbus Children's Hospital, Columbus, OH.

A prospective study of 25 children with osteomyelitis was undertaken to investigate evolution of the bone imaging findings during treatment.

A combination of visual interpretation of gamma camera images and computer-assisted comparison of contralateral or adjacent regions was employed. Tc-99m-diphosphonate was used in 100 μCi/Kg dosage for the first study; 50 μCi/Kg was used at 8 day intervals for subsequent studies.

Three patterns of evolution were found. In virulent disease (acute onset, short history, severe symptoms) the first scan faintly visualized the lesion (ischemia). The second study showed a dramatic increase in activity, at which time radiographs became positive. Of 7 patients in this group, 5 were treated surgically. Resolution began 3-6 weeks after onset.

In compensated disease (slow onset, 1-2 week history, moderate local findings) the original scan showed prominent lesions (hyperemia) and radiographs were occasionally positive. In 10 patients resolution usually began on the second study following successful medical treatment. Two patients not responding to original antibiotics showed increasing activity for more than 4 weeks; resolution began following switch to an effective different antibiotic.

Advanced osteomyelitis (long history, mild symptoms) had strongly positive original scans, and positive radiographs. Resolution was slow after surgical management.

This study indicates that bone imaging reflects well the evolution of osteomyelitic lesions.

STUDY OF HOST-GRAFT ACTIVITY PATTERNS IN DOGS WITH MANDIBULAR BONE GRAFTS USING QUANTITATIVE BONE IMAGING. F.Vieras, R.G. Triplett, K.G. Mendenhall, and J.F. Kelly. Armed Forces Radiobiology Research Institute and Naval Medical Research Institute, Bethesda, MD.

We have investigated the use of quantitative radionuclide bone imaging for assessment of healing in mandibular bone grafts. Full-thickness mandibular defects were surgically created in beagle dogs and replaced by either allogeneic (homo-) or xenogeneic (hetero-) grafts. Allografts (obtained from allogeneic freeze-dried mandibles) provided a model of successful grafts whereas xenografts (obtained from sheep mandibles) provided a model of graft failure. The grafts were evaluated by radionuclide imaging with Tc-99m stannous diphosphonate and a gamma camera-computer system, radiography, and clinical examination at 1, 2, 4, 6, and 8 weeks post-graft. Activity in the graft and proximal host bone was expressed as a ratio of counts per element in the region of interest to counts per element in a control region in the contralateral side of the mandible. In the allografts (n = 5), the serial mean activity ratios (MAR) gradually approached those of the host area. In the xenografts (n = 4), the MAR's never reached the level of the host. Healing occurred in all animals in which the activity ratios in the graft approached or were greater than the host by 6 weeks post-graft, whereas those grafts with ratios remaining considerably below those of the host did not heal. Radiographic evaluation during the 8-week period of study was not a reliable indicator of graft success or failure. Radionuclide bone imaging appears useful for the early identification of graft failure or success.

BONE SCINTIGRAPHY IN OSTEITIS DEFORMANS (M.PAGET) BEFORE, DURING AND AFTER TREATMENT. C.J.L.R. Vellenga, E.K.J. Pauwels, O.L.M. Bijvoet, D.J. Hosking. (Departments of Nuclear Medicine and Endocrinology, University Medical Center, Leiden, The Netherlands).

30 patients with Paget's disease were treated with a combination of E.H.D.P. and calcitonin. Bone scintigraphic results before, during and after treatment were compared with roentgenography, bone biopsy, symptomatology, levels of serum alkaline phosphatase and urine hydroxyproline, and calcium kinetic studies. Dramatic improvement is apparent during the first 6-18 months. However, complete normalization occurs only in 35 out of 106 affected bones. This is in contrast with alkaline phosphatase levels, which normalize in 22 out of 30 patients within 6-12 months.

In 10 patients deterioration of one or more lesions is seen, often during treatment. In 3 instances this decline coincides with a rise of serum alk. phosph., in 2 cases it precedes such a rise. In the remaining 5 patients the follow-up after scintigraphic deterioration possibly was too short to show the biochemical change. Treatment, which usually was concluded 6 months after biochemical normalization, therefore should not be discontinued in these patients. It is suggested that bone scintigraphy is a sensitive parameter for local activity of the disease and is a very useful tool for evaluating the effects of treatment.

This will be particularly true, when in the very near future even more potent therapeutic agents will be available.

PREOPERATIVE EVALUATION OF AMPUTATION LEVEL UTILIZING Tc-99m PYROPHOSPHATE. D.C.Hickey, W.R.Gray,JR, S.E.Lewis, E.R. Thal, R.W.Parkey. U. Texas Hlth. Sci. Ctr., Dallas, TX.

This study evaluated the usefulness of Tc-99m pyrophosphate (Tc-99m) in delineating recent lower extremity muscle necrosis. In 17 patients with various diseases who were candidates for amputation, dual-probe rectilinear scans of the legs and camera scintigrams of the feet were performed 1½ hrs after IV injection of Tc-PYP. Absent soft-tissue activity indicated absent perfusion, and abnormally increased activity was interpreted as recent muscle necrosis. After independent surgical evaluation the patients were operated, the specimens examined pathologically, and surgical results followed clinically. Of 12 patients with atherosclerotic peripheral vascular disease (ASPVD) 9 underwent amputations, and the courses of 8 correlated well with scan interpretation. Of 3 patients who underwent less extensive amputation than suggested by scan, 2 required second operations to the level suggested, and the third healed poorly. Of 3 patients who underwent more extensive amputations than suggested, 2 had only normal muscle in the proximal surgical specimen. In 5 other patients without ASPVD who had undergone trauma scans were less reliable (accurate correlation in 2 cases) but were useful in identifying necrotic areas needing debridement. This suggests than in spite of the presence of muscle necrosis, good perfusion enables viability. Preoperative evaluation of lower extremities with Tc-PYP is of definite value and should enable both identification of areas needing debridement and more accuarte levels of amputation to preserve maximum function and decrease the number of operations required.

THURSDAY, JUNE 29
8:30 a.m.-10:00 a.m.

SANTA ANA ROOM

BASIC SCIENCE

INSTRUMENTATION I: SPECIALIZED IMAGING DEVICES

Chairman: F. David Rollo
Co-Chairman: Raleigh F. Johnson, Jr.

IMAGING AND QUANTITATION CHARACTERISTICS OF FOUR THYROID FLUORESCENT SCANNERS. D.W. Palmer, Medical College of Wisconsin, Milwaukee, WI., and L. Kaufman, University of California, San Francisco, CA.

Thyroidal imaging and iodine quantitation have been compared for thyroid fluorescent scanners manufactured by KEVEX Corp., Oak Ridge Technical Enterprises Corp. (ORTEC), and Princeton Gamma-Tech (PGT). Imaging of lesions of diameter D is compared with the imaging performance parameter $IP=(S/B)^{*}EXP(-2R^2/D^2)$ using measured values for S, the sensitivity in counts/min. per part per million iodine (CPM/ppm) registered from a 2 cm diameter vial placed in the most sensitive region; B, the equivalent iodine background in CPM/ppm from a blank vial; and R, the measured line spread function full-width-at-half-max. averaged over a 2 cm depth. KEVEX appears best for lesions larger than 8 mm, and PGT is best for smaller lesions.

Precision of intrathyroidal iodine measurements are compared with $(B/S)^{1/2}$. The ORTEC Si(Li) and KEVEX systems provide the best quantitation precision.

Detector*	ORTEC Si(Li)	ORTEC HPGe	KEVEX Si(Li)	PGT Si(Li)
Excitation Source	Am-241	Am-241	Am-241	X-ray tube
R (mm)	9.6	7.8	7.6	3.7
S (CPM/ppm)	18.8	6.7	21.1	5.1
B (CPM/ppm)	48	324	54	51
IP (D=10mm)	0.062	0.006	0.12	0.076
IP (D=7mm)	0.009	0.002	0.037	0.057
$(B/S)^{1/2}$	1.6	6.9	1.6	3.2

*HPGe: high purity germanium

ABSORPTION-EDGE TRANSMISSION TECHNIQUE USING Ce-139 FOR MEASUREMENT OF STABLE IODINE. J.A. Sorenson and J.A. Nelson, University of Utah, Salt Lake City, UT.

A technique for determining stable iodine concentrations by measuring differential absorption of photons having energies just above and just below the absorption edge of iodine (33.2 keV) has been developed. The radiation source is Ce-139 (EC, $T_{\frac{1}{2}}$=140 d), which emits characteristic x rays of lanthanum ($K_{\alpha 2}$=33.0 keV, $K_{\alpha 1}$=33.4 keV). Separation of these closely-spaced energies is accomplished with a NaI(Tl) detector system by energy-selective beam filtration. An iodine filter (155 mg/cm^2) transmits only the $K_{\alpha 2}$ photons, whereas a brass or other neutral filter transmits both energies. The ratio of filtered-beam transmissions through a sample can be used to determine its $K_{\alpha 1}/K_{\alpha 2}$ transmission ratio, and thus its iodine concentration. Alternatively, a thin (~0.1 mm) NaI(Tl) detector can be used to measure the ratio of x-ray photopeak (33 keV) to iodine x-ray escape-peak (~6 keV) counts. Only the $K_{\alpha 1}$ x rays have energy sufficient to cause escape-peak events, and therefore the photopeak/escape-peak ratio is an indicator of sample $K_{\alpha 1}/K_{\alpha 2}$ transmission. With a 20-mCi source activity we have achieved ±15 µg/ml precision in measuring times of 20 minutes on in vitro samples, and ±100 µg/ml in measuring times of 15-20 seconds. Visualization of stable iodine in vivo is technically possible by this technique using a conventional Anger camera as the detector system. However, studies on humans are not feasible at the present time, because very long measuring times are needed to achieve statistically reliable data with 10-15 cm thick absorbers, and because of contamination of the transmitted beam by 166-keV gamma rays also emitted by Ce-139. Comparative aspects of the Ce-139 absorption-edge technique and the fluorescence excitation method will also be discussed.

POSITRON EMISSION LONGITUDINAL TOMOGRAPHY WITH STATIONARY PLANAR MWPC POSITRON CAMERA. C.B. Lim, V. Perez-Mendez, A. Cheng, R.S. Hattner, and L. Kaufman. University of California, San Francisco, CA.

A prototype positron camera using two opposed converter-coupled multi-wire proportional chambers was built two years ago and has been undergoing evaluations and upgrading processes. New improved response of the camera will be presented together with design criteria. A markedly improved performance of the camera has been achieved by combinations of installation of newly developed converters and improved electronics for detection and position timing. In each detector box, two old converters were replaced by 3 smaller cell size converters, which have enhanced lead conversion surface area to increase both the basic detection efficiency and spatial resolution. Detection efficiency of small amplitude pulses in the chambers, which reside in bulk originating from escaping process of the conversion electrons in lead, has been increased by using low noise amplifiers in combination with 6% Xenon to the original 70% Argon and 30% methan gas mixture, which amplifies the chamber pulse amplitude by a factor of 3. The net effect of these upgrading processes is the increased system sensitivity and improved spatial resolution. The new system sensitivity of the cameras is 1600 counts/min-µCi for a point source located in the middle of the camera field and 463 counts/min-µCi or 48.5K counts/sec per µCi/ml for a water-filled cylindrical phantom of 20 cm diameter and 20 cm height, which incorporates varying point sensitivity in the camera field and gamma attenuation inside the phantom. In image scheme extends the basic idea of focal plan tomography in an iterative manner. Clinical results from the improved system with new reconstruction algorithm will also be presented.

EMISSION TOMOGRAPHIC IMAGES OF A CANINE HEAD WITH FLUORINE-18. D.J. Hnatowich, D. Elmaleh, S. Cochavi, S. Kulprathipanja and G.L. Brownell. Massachusetts General Hospital, Boston, Mass.

Approximately 2 mCi of F-18 as F^- (produced by the Ne-20 (d,α)F-18 reaction in a compact medical cyclotron) was administered intraveneously to an anesthetized dog after positioning the animal in the MGH positron camera and after collecting a set of transmission images. Both the transmission images (obtained with a flood source containing Ga-68) and a set of emission images were collected at 30 equally-spaced angles in a half circle about the animal. A total of 180 2-dimensional images were collected in 18 min. These data were sufficient to reconstruct 23 transverse section images corrected for random coincidences, photon absorption, and radioactive decay. The sections are spaced 1.4 cm apart and exhibit a spacial resolution of approximately 1 cm (FWHM). The activity distribution in the skull is displayed in the first 10 sections; the images clearly show the frontal, parietal, occipital and temporal bones. Also visible as regions of decreased uptake are the optical orbits, temporal fossa, cranial cavity and foramen magnum.

*This work supported in part by ERDA (E(11-1)-4115)

A COMPUTERIZED ROTATING LAMINAR RADIONUCLIDE CAMERA. W. Mauderli, L.T. Fitzgerald, R. Luthmann, C.M. Williams, University of Florida, Gainesville, FL, C.H. Tosswill, Galileo ElectroOptics, Sturbridge, MA, and G. Entine, Radiation Monitoring Devices, Newton, MA.

A new type of radionuclide camera has been designed and constructed which has dramatically higher spatial resolution and sensitivity. Using a new approach based on a one-dimensional parallel plate collimator and a computerized image reconstruction technique, camera resolution on the order of 2 mm has been obtained without increased counting time. The camera uses an array of

linear cadmium telluride gamma detectors as its sensing element. These sensors are placed between thin vertical plates of tungsten. This geometry prevents interdetector scatter and restricts the field of view to one dimension. A series of image projections are obtained in 7° angular increments until a total angle of 180° has been traversed. Well-known mathematical techniques of image reconstruction from projections are then used to produce a viewable image which is displayed in gray scale (16 levels) on a video display device. An important principle of the device is that sensitivity decreases linearly with increased resolution rather than with the square as in the multihole collimator case. The 40 mm x 40 mm prototype has been used clinically to perform a bone scan of a wrist. The image clearly resolved the detailed shape of a fracture of the triquetrum.

LONGITUDINAL AND TRANSVERSE SINGLE-PHOTON EMISSION COMPUTED BODY TOMOGRAPHY USING AN ANGER TOMOGRAPHIC SCANNER. E.V. Garcia, A.E. Inglis, Jr., J.E. Diaz, A. Miale, Jr., and A.N. Serafini. University of Miami School of Medicine, Miami, FL.

The dual probe multiplane tomographic scanner developed by Anger (Pho-Con-Searle Radiographics) has been interfaced to standard nuclear medicine computer system (32K Modumed Medical Data Systems). This combination provides single-photon emission computed body tomography, with longitudinal and transverse section capabilities.

During acquisition, the computer digitizes and records on magnetic disk the positioned information generated by each scintillation event. Tomograms are reconstructed by back projection of each scintillation event along a line passing through the focal point of the collimators.

Longitudinal tomograms are reconstructed as an image of the desired plane in focus with over and underlying activity out of focus. This produces low contrast images but with good depth and spatial resolution (Tc-99m 13mm FWHM at 3.5 inches in tissue). Transverse section reconstruction of a point source appear as two 60° cones meeting tip-to-tip at the source location creating a "cone beam geometry" similar to the positron camera as described by Muehllehner. These cones give rise to a blurring effect in both the longitudinal and transverse slices. In order to obtain higher image contrast, we are currently developing algorithms to correct for the blur effect and for photon absorption.

At this point using the above described system, we are routinely obtaining, clinically useful longitudinal and transverse body sections.

STEREOSCOPIC IMAGING OF GAMMA RAY SOURCES. J. A. McIntyre. Texas A&M University, College Station, TX.

A three-dimensional stereoscopic image of a gamma ray source provides an image completely in focus in contrast to a tomographic image which is in focus in only one plane. The stereoscopic image is produced by the viewer's brain while the viewer is looking at two different plane images with his two eyes. These plane images can be obtained with gamma ray cameras by using either diverging or converging collimators; in each case the two pictures are obtained by viewing the gamma ray source from two slightly different directions corresponding to the different viewing directions of the viewer's two eyes.

Pairs of plane images can also be obtained if the gamma ray source emits annihilation radiation; in this case, no collimators are required but two gamma ray cameras are used on opposite sides of the gamma ray source. By selecting gamma ray pairs directed toward either of two imaginary eyes, a pair of plane images is also obtained. With the two cameras, however, gamma ray pairs for many eyes can also be selected simultaneously and later displayed, two eyes at a time, so that the viewer can effectively move around the source by viewing the source from different directions.

One of the methods was tested by using a camera and diverging collimator to view a radioactive source having discrete parts placed at different distances from the camera. Two plane images were obtained from two viewing angles. By photographing one image in red and the other in green, the three-dimensional nature of the source becomes apparent when viewing the two images through glasses with one red and one green lens.

THURSDAY, JUNE 29 — CALIFORNIA B ROOM
8:30 a.m.-10:00 a.m.

IN VITRO AND CORRELATIVE TECHNIQUES

HEMATOLOGY II: PERIPHERAL VASCULAR (CLINICAL SCIENCE)

Chairman: Barry A. Siegel
Co-Chairman: James H. Thrall

NON-INVASIVE DIAGNOSIS FOR INTERMITTENT CLAUDICATION USING Tl-201. Y. Ishii, D. Hamanaka, Y. Yonekura, T. Fujita, K. Kumada, and K. Torizuka. Kyoto University Medical School, Kyoto, Japan.

Present attempt was to applicate Tl-201 to visualise peripheral blood flow distribution of lower extremities and to establish quantitative assessment of the intermittent claudication.

After intravenous injection of Tl-201 with or without exercise loading by treadmill, distribution of this tracer throughout the body was obtained using a whole body scanner. According to the indicator fractionation principle, fractional blood flow of cardiac output for each segment of the lower extremities (FBF/CO) was expressed as a fractional deposited radioactivity at these segments of that of whole body. In order to validate this principle, depositional radioactivity of Tl-201 at each segment was compared with that of I-131-MAA on intraarterial injection, and found to be a good correlation ($r=0.947$). FBF/CO in 10 normals (N) and of diseased segment in 15 patients with arteriosclerosis obliterans (ASO) at rest (R) and on exercise loading (E) were as follows;

	Thigh	Calf	Foot
N (R)	3.25±0.82(%)	1.64±0.45(%)	0.50±0.20(%)
N (E)	10.69±2.30(%)	6.05±0.64(%)	0.74±0.25(%)
ASO(R)	2.68±0.41(%)	1.22±0.31(%)	0.52±0.19(%)
ASO(E)	6.54±0.88(%)	4.09±0.58(%)	0.59±0.15(%)

Significant decrease of blood flow supply for increased demand on exercise was evident in ASO ($p<0.001$) compared with normals.

NON-CARDIAC ORGAN PERFUSION IMAGING WITH THALLIUM-201. J. Thrall, J. Freitas, M. Gross, D. Rucknagel, D. Swanson, B. Pitt. University of Michigan Medical Center, Ann Arbor, MI.

To assess the applicability of thallium-201 (Tl) for non-cardiac imaging, total body Tl scan patterns were analyzed in 50 individuals (10 normals, 40 patients). Studies were obtained 5-10 minutes post-injection of 1.5 mCi of Tl intravenously.

Proper interpretation of abnormal studies required recognition of the normal pattern: Tl is excluded from brain and rapid blood clearance precludes dural sinus visualization; scalp activity is faint but salivary glands and thyroid show marked uptake; myocardial uptake is intense witl diffuse and variable lung activity; homogeneous liver activity is present with variable gut uptake; renal uptake is also homogeneous with the most intense uptake of any organ (including heart); skeletal structures are relatively photon deficient with uniform activity in all muscle groups, especially in the lower extremities.

Abnormal imaging patterns were seen in 1) peripheral vascular disease-focal and diffuse areas of diminished activity were seen in 12 patient's muscle groups with reactive hyperemia demonstrated in 4 of 7 ischemic ulcers; 2) sickle cell anemia-areas of expanded bone marrow in 10 patients showed marked Tl uptake with clear demarcation of focal defects due to infarction; 3) other patterns included lack of increased uptake in sclerotic Pagetic bone, faint but definite uptake in scalp and skeletal breast metastases, intense uptake in a thymoma and 2 abscesses and poor renal visualization in renal failure.

Since Tl demonstrates both organ perfusion and cellular uptake, it appears potentially useful in various non-cardiac applications.

EFFECTS OF EXERCISE OR SURGERY ON UPTAKE OF THALLIUM-201 INTO LEGS IN PERIPHERAL VASCULAR DISEASE. W.W. Shreeve, L. Giwa, M.A. Ficek, B.G. Spoering and J. Hui. VA Hospital, Northport, NY.

Blood flow and function of leg skeletal muscles in peripheral vascular disease might be evaluated objectively by uptake of thallium-201 (Tl). After peripheral intravenous injection of Tl (1-2 mCi.) uptake into the legs under resting and exercise conditions has been examined with the gamma camera and computer analysis in 13 patients and one normal subject. In some cases effects of bicycle exercise programs or of vascular surgery have been evaluated. Repeated counting during 1-1/2 hours post-injection has indicated variable changes in Tl content, particularly under exercise conditions, which may have pathological significance. Lesser uptake into upper or lower leg on the side of greater disease is usually observed. Ratios of activity in the thighs between exercise (bicycle ergometer, 4-6 mets) and resting states have ranged from 1.5 to 7.6 (intermediate values for the normal). In 3 of 4 patients the incremental uptake upon exercise (same amount) was greater following the exercise program. A differential effect on the side of greater disease was not seen. In two patients there was increased uptake in the operated leg after by-pass graft relative to the opposite leg. Tl uptake can help evaluate quantitatively the degree of unilateral vascular impairment in the legs and the possible benefits of therapy.

A NEW, NONINVASIVE APPROACH TO PERIPHERAL VASCULAR DISEASE: Tl-201 LEG SCANS. M.E. Siegel and Jan K. Siemsen. LAC/USC Medical Center, Los Angeles, CA

The purpose of this report is to describe a new, noninvasive technique to evaluate the physiologic effect on the distribution of perfusion intra-arterial disease of the lower extremities.

The technique employs the intravenous administration of Tl-201. A 1.5 mCi dose of tracer is given at rest and a second dose is given a week later during maximum physiologic exercise. Rectilinear scans of the legs of 40 patients were obtained after each administration of the tracer. Point counting over the thighs, knees, calves and ankles is performed during rest and after stress to objectively quantify the distribution of the perfusion.

In the normal patient, the distribution of perfusion is proportional to muscle mass with a thigh to calf ratio of 1.3 $\pm$ .4. The mean increase in thigh to knee perfusion with exercise is 85%. Because of the nature of the tracer, mixing is not a concern, and the normal left to right thigh ratio is 1 + .05. In the abnormal patient, the perfusion abnormalities are documented subjectively, via images, and objectively, via point counting, and they vary depending on the physiologic significance and degree of arterial disease. Perfusion distribution patterns closely resemble those reported using intra-arterial injections of microspheres.

The Tl-201 peripheral vascular perfusion scan provides a unique noninvasive means of evaluating and localizing physiologically significant arterial pathology and may be useful in objectively evaluating the various therapeutic interventions.

TRANSVERSE SECTION IMAGING OF VASCULAR STRUCTURES WITH ^{11}CO. Gordon L. Brownell, Massachusetts General Hospital, Boston, Mass.

The inhalation of small quantities of C-11 labeled CO provides a convenient method for imaging vascular structures within the body. The CO is rapidly labeled to carboxyhemaglobin. The biological turnover is sufficiently slow that excellent images of vascular structures in the body and red cell distribution in other organs can be obtained. Transverse section images of the head, upper torso and lower torso have been obtained using the MGH Positron Camera, PC-II, that has a capability of obtaining simultaneous information for 22 planes spaced at 1.4 centimeters. Because of the detail in the vascular structure, large number of planes are required for useful information to be obtained.

Transverse section images of the head indicate principally vascular structures such as the carotid arteries and transverse sinus. However, information on cerebral blood volume can also be obtained. In the face, vascular structures as well as the sinus cavity are clearly shown.

In the body the obvious vascular structures such as the heart, descending aorta etc. are clearly seen.Other vascular organs such as the spleen and kidney may be clearly identified.

In all cases, the anatomical information may be of use. However, high resolution transverse section images may well provide further information on blood volume and vascular kinetics of body organs.

MEASUREMENT OF SKIN PERFUSION WITH XENON-133. M.J. Daly, R.E. Henry, and D.D. Patton. University of Arizona and Veterans' Administration Hospital, Tucson, AZ.

Quantitation of skin perfusion provides objective criteria to determine the optimal amputation level in ischemic limb disease, to assess the maturation of pedicle flaps in reconstructive surgery, and to select appropriate treatment for chronic skin ulcers. Previous investigators used the disappearance of intradermal (I.D.) Xe-133 measured by probe and scaler to calculate skin perfusion rates. We have adapted this technique for the gamma camera interfaced to a minicomputer which allows rapid, reproducible determination of skin perfusion rates in multiple sites simultaneously.

Following I.D. injection of 0.05 ml of Xe-133 in saline into one or more sites, activity is recorded on computer disc for 10 min. Using a least squares fit for a monoexponential function, the rate of regional Xe-133 washout is calculated from time activity curves and entered into the Schmidt-Kety equation. Perfusion rates are expressed as ml/min/100gm (MM%).

Perfusion rates in normals, above knee (9.8$\pm$2.6 MM%), below knee (10.6$\pm$1.3 MM%)and dorsal foot (14.3$\pm$2.6 MM%) were similar to results obtained by probe technique. Reproducibility of duplicate measurements in normals was good with no significant difference on the same day ($P>0.2$) or between different days ($p>0.2$). Perfusion rates in ischemic limbs ranged from 0.5 MM% to normal depending on the level of injection, whereas rates near non-ischemic ulcers were in the normal range.

This procedure is an easy, reproducible means of measuring skin perfusion at multiple sites simultaneously which is not possible with previously described techniques.

THURSDAY, JUNE 29 CALIFORNIA A ROOM
8:30 a.m.-10:00 a.m.

CLINICAL PRACTICE

QUALITY CONTROL

Chairman: Richard Meidinger
Co-Chairman: L. David Wells

QUALITY CONTROL OF SCINTILLATION CAMERAS, DATA STORAGE, AND DISPLAY DEVICES. E. M. Smith, Walland, TN.

SIMPLE, PRACTICAL RADIOPHARMACEUTICAL QUALITY CONTROL FOR THE COMMUNITY NUCLEAR MEDICINE DEPARTMENT. B. A. Rhodes, University of New Mexico, Albuquerque, NM.

PATIENT QUALITY ASSURANCE--IMPORTANT WAYS TO IMPROVE PATIENT CARE IN NUCLEAR MEDICINE. L. D. Wells, University of Kansas Medical Center, Kansas City, KS.

THURSDAY, JUNE 29 GARDEN GROVE ROOM
10:30 a.m.-12:00 p.m.

CONTINUING EDUCATION

RADIOPHARMACEUTICAL ADVANCES: REACTOR PRODUCTS, CYCLOTRON PRODUCTS, AND GENERATOR SYSTEMS

PARTICIPANTS: William C. Eckelman, Chairman, George Washington University School of Medicine, Washington, DC; Michael J. Welch, Co-Chairman, Edward Mallinckrodt Institute of Radiology, St. Louis, MO; Alun G. Jones, Harvard Medical School, Boston, MA; and Kenneth A. Krohn, University of California at Davis, Sacramento, CA.

THURSDAY, JUNE 29 ANAHEIM ROOM
10:30 a.m.-12:00 p.m.

CLINICAL SCIENCE

CARDIOVASCULAR III

Chairman: H. William Strauss
Co-Chairman: Ismael Mena

PROFILES OF LEFT VENTRICULAR EJECTION FRACTION BY EQUILIBRIUM RADIONUCLIDE ANGIOGRAPHY DURING EXERCISE AND IN THE RECOVERY PERIOD IN NORMALS AND PATIENTS WITH CAD. M. Pfisterer, G. Schuler, D. Ricci, S. Swanson, D. Gordon, R. Slutsky, K. Peterson, W. Ashburn, University of California, San Diego, CA.

The profile of left ventricular (LV) ejection fraction during and following exercise (ex) and its relation to symptoms, stress ECG and contrast ventriculography (CV) is unknown. Thus, we studied 8 normal men and 23 pts with proven CAD using gated equilibrium radionuclide angiography (EQ) after injecting 20 mCi of Tc-99mHSA. Data were collected at rest, during the last 2 min of each 3 min stage of supine bicycle ex, and post ex. The ex limiting symptom was angina in 14 pts (group A) and fatigue in 9 pts (group B).

During ex, EF increased in all normals (27.6 ± 11.2%). In contrast, EF decreased in group A by 19.1 ± 12.9% and showed little change in group B (+ 0.6 ± 6.9%) [$p < .001$ between all groups]. Overshoot elevation of EF above basal level was noted 2-5 min post ex in all pts not on propranolol (17.6 ± 11.6%), but was significantly less in 12 pts on this medication. Of 11 pts with a significant fall in ex EF, 9 developed ST depression in V5 and 8 had ant/lat hypokinesis by CV while in the remaining 12 pts there were 5 positive stress ECG's and 5 hypokinetic areas.

We conclude that (1) there are significantly different profiles in LVEF during ex between normals, CAD pts limited by angina and those limited by fatigue, (2) an overshoot increase in EF in the early recovery period may be catecholamine mediated and (3) pts decreasing their EF during exercise more often develop a positive stress ECG and have more severe regional LV dysfunction.

QUANTITATIVE, SEMI-AUTOMATED RADIONUCLIDE TECHNIQUE FOR DETERMINATION OF REGIONAL LEFT VENTRICULAR FUNCTION DURING REST AND EXERCISE. J.H. Caldwell, D.L. Williams, J.W. Kennedy, and G.W. Hamilton. Veterans Administration Hospital, Seattle, WA.

A quantitative method for analysis of regional left ventricular (LV) function at rest and exercise has been developed for the noninvasive evaluation of patients (pts) with coronary artery disease. Using a commercially available second derivative method, edge recognition computer program, the outline of the LV is defined on the ECG-gated left anterior oblique blood pool image. The geometric center of the LV region at end-diastole is determined and radians are projected to divide the LV into 3 regions -- anterior (Ant), inferior (Inf), and posterior (Post). Time-activity curves are generated and regional ejection fractions (REF) determined.

In 12 pts with normal coronary arteries and contrast LV angiograms, the Ant-REF was 0.49±.10, the Inf-REF 0.74±.13, and the Post-REF 0.61±.09 (mean ± SD). Duplicate, blinded studies were done by a single observer for each segment with the following correlation: Ant-REF r=0.96, SEE=0.04; Inf-REF r=0.94, SEE=0.06; and Post-REF r=0.86, SEE=0.06. During maximal supine exercise in 2 pts, the Ant-REF and the Inf-REF increased while the Post-REF was unchanged.

A quantitative, semi-automated, and highly reproducible system for evaluating regional LV function has been developed and the range of normal values at rest reported. This method is also applicable for analysis of regional changes during maximal exercise. It is now possible to quantitatively compare regional LV function in patients with coronary artery disease to that in normal pts using radionuclide techniques.

GLOBAL AND REGIONAL LEFT VENTRICULAR PERFORMANCE DURING GRADED BICYCLE EXERCISE: ASSESSMENT BY FIRST-PASS RADIONUCLIDE ANGIOCARDIOGRAPHY. H.Berger, L.Reduto, D.Johnstone, M.Sands, H.Borkowski, R.Langou, L.Cohen, A.Gottschalk and B.Zaret. Yale University Sch. of Medicine, New Haven, Conn.

Left ventricular ejection fraction (LVEF) and regional wall motion (RWM) were assessed noninvasively at rest and during either supine or upright graded bicycle exercise (EX). First-pass radionuclide angiocardiograms were obtained in <15 secs with a computerized multicrystal scintillation camera in 51 patients (pts) with documented coronary artery disease (CAD) and in 11 normal (nl) controls. Twenty-seven CAD pts were exercised to angina and/or ischemic ECG changes, while 24 CAD pts and all 11 nls were exercised to symptom-limiting fatigue without ischemia.

LVEF increased by ≥ 10% in all nls ({Mean±SEM} rest, 66±2%; EX, 83±1%, $p<0.001$). In CAD with ischemia, LVEF fell or remained the same in 27/27 pts (rest, 66±2%; EX, 57±2%, $p<0.001$). New or exagerated RWM abnormalities were detected in 17/27 pts. In contrast, in CAD with fatigue, LVEF remained the same in 9/24 pts and increased in 15/24 pts (rest, 52±4%; EX, 58±4%, $p<0.01$). New RWM abnormalities developed in 6/24 pts, including two in whom LVEF increased. The peak heart rates achieved in pts limited by ischemia

(115±4 bpm) and fatigue (119±5 bpm) were not significantly different (p>0.05). The magnitude and direction of the LV response to EX was similar whether studies were performed supine or upright.

Thus, first-pass radionuclide angiocardiography consistently demonstrates compromised LV reserve during EX-induced ischemia, but not during fatigue. Whether performed with supine or upright EX, the sensitivity of this technique appears to be greater than that of conventional EX testing, but also is dependent upon the end-point of EX.

COMPARATIVE SENSITIVITY AND SPECIFICITY OF RADIONUCLIDE ANGIOGRAPHIC ASSESSMENT OF WALL MOTION AND REGIONAL EJECTION FRACTION AT REST AND DURING EXERCISE IN THE DIAGNOSIS OF CORONARY HEART DISEASE. M. Bodenheimer, V.Banka, C.Fooshee, G. Hermann, and R. Helfant. Presbyterian-U. of Penn Med. Center, Philadelphia, PA.

The detection of regional left ventricular (LV) wall motion (WM) abnormalities provides strong evidence for the presence of coronary heart disease (CHD). In 129 patients (pt) undergoing cardiac catheterization the relative value of radionuclide angiographic (RA) assessment of WM was compared with computer generated regional ejection fraction (REF) at rest and during handgrip (HG) exercise. WM was determined by superimposition of computer derived end-diastolic and end-systolic perimeters. REF was determined using a computer generated 16 color isocount image which permitted a quantitative assessment of zonal contribution to ejection fraction. Of the 129 pt, 31 had normal coronaries while 98 had CHD. At rest, WM abnormalities were present in 55 of 98 pt (56%) with CHD while REF was abnormal in 65 of 98 pt (66%). During HG, WM abnormalites were present in 67 pt (68%). In contrast, REF was abnormal in 89 of 98 pt (91%) ($p<.005$). Assessment of the severity of CHD was also enhanced by REF with HG. Of 24 pt with one vessel disease, 20 (83%) had an abnormal REF compared to 15 (63%) on WM. Similarly, of 74 pt with multivessel CHD, 69 (93%) had an abnormal REF compared to 52 (70%) by WM ($p<.02$). Of the 31 pt with normal coronaries WM correctly identified 29 (94%) and REF 27 (87%). Overall sensitivity of WM was 68% and REF 91% ($p<.005$). Specificity of WM was 94% and for REF 87%. Thus, RA assessment of REF during HG is both highly sensitive and specific for CHD. Also, it has enhanced sensitivity compared to WM with little loss in specificity.

EVALUATION OF LEFT VENTRICULAR FUNCTION DURING SITTING BICYCLE EXERCISE BY MULTIPLE GATED SCINTIGRAPHY: VALIDATION AND CLINICAL APPLICATION IN CORONARY DISEASE. D. Berman, J. Maddahi, Y. Charuzi, R. Gray, A. Waxman, R. Vas, H.J.C. Swan, and J.Forrester.Cedars-Sinai Med.Ctr., Los Angeles,CA.

This study was undertaken to evaluate the validity of 2-minute (2min) multiple gated scintigraphy (MSc) and to clinically apply MSc in assessing left ventricular (LV) ejection fraction (EF) and regional wall motion (RWM) during sitting bicycle exercise (Ex). Left anterior oblique (LAO) MSc employed in-vitro Tc-99m-RBC's, gamma camera, computer, and curves from 14 LV regions of interest for EF. Accuracy and reproducibility of 2min MSc were assessed in 35 pts by comparing 2min MSc to standard 6min MSc for EF and RWM and to repeated resting 2min MSc 1 hour after control (C). RWM was evaluated using 6 point scoring for 3 LV segments on LAO view. 2min MSc was performed during successive stages of graded bicycle Ex in 8 normals (N) and 10 pts with angiographically documented coronary disease (CAD). High correlation was found between 2 and 6min MSc for EF ($r=.99$) and for RWM with identical score in 96/105 segments and >1 score difference in only 2/105. Reproducibility for 2min MSc EF demonstrated absolute deviation of 5.7%±4.8% of EF value (mean±SD). During peak Ex in N, MSc EF rose markedly (.66±.05 to .83±.05) (mean±SEM) ($p<.001$) with >15% EF↑ in 8/8. No RWM abnormalities were observed during C or Ex in N. In contrast, during peak Ex in CAD pts, mean EF did not rise (.55±.17 to .55±.19) (p=ns) with >15% EF↑ in only 2/10 pts. New RWM abnormalities were seen in 6/10 pts during Ex, and RWM was abnormal at C or Ex in 8/10. Thus, (1)2min MSc is accurate and reproducible for assessment of EF and RWM and is well-suited to evaluation of LV function during Ex and (2)preliminary pt results suggest MSc with sitting bicycle Ex may be applicable in detection of CAD.

RESPONSE OF LEFT VENTRICULAR VOLUME TO EXERCISE IN NORMALS AND PATIENTS WITH ANGINA PECTORIS AS CALCULATED BY EQUILIBRIUM RADIONUCLIDE ANGIOGRAPHY. R. Slutsky, G. Schuler M. Pfisterer, J. Karliner and W. Ashburn. University of California, San Diego, CA

To assess the effects of exercise on left ventricular volumes we studied 9 normal men and 15 patients (pts) with angina pectoris using gated LAO radionuclide blood pool imaging after injection of Tc-99m human serum albumin. All subjects performed supine bicycle exercise until angina or fatigue resulted. Data were collected at rest and during the last 2 minutes of each 3 minute stage of exercise and after exercise. Volumes were calculated by a new radionuclide technique that correlates well with cineangiography and is expressed in nondimensional units. In normals, end-diastolic volume (EDV) at rest was not different than EDV at peak exercise; 15.8 ± 6 vs. 15.4 ± 7.2 units (NS), whereas end-systolic volume (ESV) decreased from 5.6 ± 2.9 at rest to 2.6 ± 1.6 units at peak exercise ($p<.01$). ESV decreased in all but one of 27 exercise periods. Pts with CAD had larger EDV, 23.5 ± 8.8, at rest ($p<.01$) and at angina (A), 23.5 ± 9.8, ($p<.01$) than normals. Pts increased ESV from 10.9 ± 6.7 at rest to 14.2 ± 7.5 at A ($p<.001$) resulting in a decreased ejection fraction (EF) [.57 ± 0.15 to .45 ± 0.16, ($p<.001$)]. All pts had an increased ESV at angina compared with the exercise stage just prior to angina. We conclude: normals exhibit an increase in EF during exercise because of a decrease in ESV; in angina pts. EF declines because the ESV actually increases. Thus radionuclide equilibrium angiography may provide a useful method for assessing alterations in left ventricular volume and EF that occur during angina pectoris.

CHANGES IN CARDIOPULMONARY BLOOD VOLUME DURING UPRIGHT EXERCISE STRESS TESTING IN PATIENTS WITH CORONARY ARTERY DISEASE. A. B. Nichols, S. Cochavi, H. W. Strauss, T. E. Guiney, M. B. Leavitt, G. A. Beller, G. M. Pohost, Massachusetts General Hospital, Boston, Massachusetts.

Alterations in regional cardiopulmonary blood volume during myocardial ischemia were evaluated in 15 patients with chest pain syndromes undergoing exercise stress testing. Each patient was exercised on a bicycle ergometer with a multicrystal positron camera positioned over the chest. Inhaled ^{11}C-carbon monoxide ($T_{1/2}$ = 20.3 min) was used as a blood label (^{11}C-carboxyhemoglobin). Blood volume was calculated by comparison of regional chest activity to activity measured over a venous blood specimen. Chest wall attenuation was corrected by positron transmission imaging with a ^{68}Ga plane source. After equilibrium of ^{11}CO-Hgb in the blood, the regional activity of this blood label was continuously measured over the heart and lungs during rest, exercise, and recovery periods. For the group of patients (n=9) developing an ischemic response to exercise manifested by RS-T segment depression and angina pectoris, regional activity rose 18.9 ± 4 (SEM)% over the upper lobes, 10.4 ± 5% over the lower lobes, and 7.4 ± 5% over the heart. In contrast, among patients (n=6) not demonstrating an ischemic response to exercise, regional activity declined 7.2 ± 4% over the upper lobes, 13.1 ± 1% over the lower lobes, and 13.9 ± 6% over the heart. These changes in regional activity were significantly different for the two groups (all $P<0.05$). The data indicate that an ischemic response to exercise stress testing is associated with an acute rise in pulmonary and cardiac blood volume. This rise in cardiopulmonary blood volume may be due to ischemia-induced left ventricular dysfunction.

THURSDAY, JUNE 29
10:30 a.m.-12:00 p.m.

SANTA ANA ROOM

BASIC SCIENCE

INSTRUMENTATION II: IMAGING DEVICE PERFORMANCE

Chairman: L. Stephen Graham
Co-Chairman: Robert Richardson

THE PITFALLS OF FIELD CORRECTION. R. Wicks and M. Blau. State University of New York at Buffalo, Buffalo, NY.

In Anger camera-computer systems the camera's nonuniform field response is generally corrected for by multiplying the images by an inverse flood matrix. The purpose of this investigation was to study the causes of this field nonuniformity and the effect that field correction (FC) has on quantitative data.

In order to measure field uniformity, a ¼ in. dia. source of Tc-99m was imaged at 25 positions across the collimator face. The percent standard deviation (%SD) of the counts in these 25 images was 3%. Our flood field, however, shows a %SD of 18%. Moreover, when these 25 images were field corrected in the usual manner their %SD went up to 9%. This experiment was repeated with up to 6 inches of scattering medium. No significant changes were noted.

Since the inverse flood matrix FC technique in reality corrects for counts per unit area, we did a second experiment to estimate the error in area determination. A 1.75 in. dia. source of Tc-99m was imaged on the Anger camera at 61 positions of a hexagonal array. The area of the source in the resulting images at each of these positions was determined along with the total counts within these areas. The number of counts within the areas had a %SD of 2.1% while the size of these areas varied with a %SD of 9.7%.

We conclude that the major cause of field nonuniformity for the Anger camera is spatial distortion and not varing sensitivities across the crystal face. Furthermore while FC may improve the quality of the pictures, it may distort the quantitative data contained in these images.

ANGER CAMERA NONUNIFORMITY -- THE SOURCE AND THE CURE. D.L. Kirch, L. Shabason, M.T. LeFree, and P.P. Steele. Veterans Administration Hospital, Denver, Co.

The full-field flood (FFF) nonuniformity of the Anger camera does not primarily reflect variations in the instrument sensitivity. A series of objective tests indicates that FFF nonuniformities are mainly due to spatial distortions which displace the coordinates of gamma events inward or outward to create "hot" or "cold" regions, respectively. First, the point-source sensitivity (PSS) was measured at random positions over the camera detector using a collimated point source and a 5 million count FFF image was obtained under the same conditions so that FFF count density values were determined at the same locations. The probability distribution functions for the PSS and FFF count density were then compared. The percentage standard deviation for the PSS was 1.0% while that of the FFF count density was 4.7%. The PSS values along a diameter of the detector were also compared with the corresponding FFF values and no significant relationship was noted. The final test compared data from an image of an Orthogonal Hole Phantom (OHP) with the FFF count density data. The area between each four hole group of the OHP image compared with the average value of the FFF count density over the same region showed a strong inverse relationship. Thus, we conclude that FFF nonuniformities are primarily due to dot displacements. An algorithm has been developed whereby a series of ray sums are formed at several angles and a one-dimensional correction is determined for each projection. The two-dimensional shift vector is then computed as the vector sum of these one-dimensional corrections. This method lends itself to online digital implimentation and does not result in unnecessary count losses.

UNIFORMITY CORRECTION WITH THE MICRO Z PROCESSOR. J. W. Steidley and D. S. Kearns. Picker Corp., Northford, CT. P. B. Hoffer. Yale University, New Haven, CT.

This study evaluates the performance capabilities of a microprocessor controlled system (Micro Z Processor) which has been developed for uniformity correction using a sliding energy window concept. The Micro Z Processor corrects for gamma camera nonuniformity in two stages. The first stage corrects for misalignment of the energy pulse height window relative to the actual energy signal level in each of 4096 regions in the detector. The second stage corrects for any residual nonuniformity by rejecting pulses based on an automatic flood field calibration which is accumulated with a correctly aligned energy window.

In order to test the system, several phototubes in a gamma camera were detuned to clearly demonstrate the concepts and performance of the device. In the bypass mode, the uncorrected flood of such a detuned camera shows several gross cold spots. Operation of the device using only the sliding energy window correction stage noticeably improves the flood. The gross cold spots are significantly reduced and other areas of the flood field are also improved. This improvement shows that energy window misalignment is a major cause of nonuniformity. Using both stages of correction, the residual nonuniformities are removed and the flood field is restored to within statistical variations in nonuniformity. Intrinsic spatial resolution and count rate capability are unchanged while indepth spatial resolution through scatter media is slightly improved due to an overall improvement in energy resolution from 13% to 11% for Tc-99m. These improvements occur during on-line operation with no sacrifice in sensitivity.

MEASUREMENTS OF INTRINSIC AND OVERALL RESOLUTION AND SENSITIVITY IN THE SCINTILLATION CAMERA. G.H. Simmons, P.W. Grigsby, G.A. White. Veterans Administration Hospital, University of Kentucky Medical Center, Lexington, KY.

Measurements of the intrinsic resolution and sensitivity of scintillation cameras have long been recognized as important ones in the total performance evaluation of those systems. The measurements are especially valuable as part of a battery of acceptance tests to ascertain whether or not a new camera meets the manufacturer's specifications. They are seldom done however, because of the difficulties in making the measurements with conventional equipment. Even with a digital computer that acquires data in a 128 x 128 format too few data points are obtained to ascertain the shape of the line spread function (LSF). To circumvent these problems a device has been constructed that moves a line source at a constant velocity across the face of the camera crystal. The source is collimated for intrinsic measurements and uncollimated for extrinsic measurements in either water or air. Data are acquired in the dynamic mode with a computer or other digital recording device as the source moves across the crystal face. A region of interest (ROI) one pixel wide is defined at a point in the image field. The data are replayed and a count rate vs time curve generated for the ROI. By relating the frame time for data acquisition to the velocity of the source the dynamic curve becomes a LSF. One can easily generate LSF's at multiple locations over the face of the crystal simply by moving the ROI. Results for a Searle LFOV camera show the resolution index (integral of the MTF) to vary from 0.502 to 0.594 and the sensitivity (integral of the LSF) from 1.32 to 1.89 for 5 different locations across the diameter of the crystal.

CONSEQUENCES OF CRYSTAL THICKNESS REDUCTION ON GAMMA CAMERA RESOLUTION AND SENSITIVITY. R. M. Sano, J. B. Tinkel. Picker Corp., Northford, CT. C. A. LaVallee, G. S. Freedman. Yale University School of Medicine.

The crystal thickness for the original anger detectors was optimized for clinical studies of the past decade at 1/2" (12.5mm). The shift of clinical dependence towards Tc-99m and the introduction of Tl-201 permits significant improvements in resolution and overall performance by reduction of the thickness of the

NaI crystal.

Several small field of view mobile camera models now utilize 1/4" (6.25mm) crystal detectors which optimize low energy applications. These have shown significant improvements in intrinsic resolution (3.8mm F.W.H.M. vs. 5.5mm F.W.H.M.). Large field cameras, however, are utilized for all energy applications. Therefore, a detector designed to optimize the improvement of resolution at 70 kev and 140 kev and minimize the sensitivity loss at 360 kev resulted in a detector with a 9.4mm thick crystal. The standard 12.5mm thick crystal has an intrinsic resolution for Tl-201 (70 kev) of 6.5mm vs. 8mm F.W.H. M. at Tc-99m (140 kev) the difference is 4.4mm F.W.H.M. vs. 5.5mm F.W.H.M. for the thin (9.4mm) detector. The loss in sensitivity at Tc-99m is only 6% and, at Tl-201, less than 1%. For the lower two peaks of Ga-67 (94 kev and 184) the resolution improvement is 18% and the sensitivity loss is 6%. At 360 kev the resolution is 3.3mm F.W.H.M., while the sensitivity is only 23% lower. Clinical studies and phantom tests demonstrate significant improvements in resolution which outweighs the minimal loss in sensitivity at higher energies when evaluated for typical applications of today.

IMAGING I-125 WITH A SCINTILLATION CAMERA. R. Adams, G.A. Kirk, E. Schulz, and B. Snell. Loma Linda University, Loma Linda, CA.

We report our experience imaging I-125 with certain unmodified scintillation camera models.

The 27-35 KeV radiations from I-125 are generally considered to be well below the energy range of Anger type cameras. At lower energies the spatial resolution is adversely affected by statistical variation in the number of electrons released in the photomultiplier tubes. None of the camera manufacturers claim I-125 imaging capability nor to our knowledge have other investigators previously reported it. However, new camera models, providing at least 37 photomultiplier tubes of high efficiency, might be expected to show improved performance at low energy.

We have successfully imaged I-125 with an Ohio-Nuclear model 120. When the controls for the high voltage supply and window width are both set to maximum the I-125 photopeak appears within the lower energy portion of the window. Models 410 and 420 we have tested afford even greater high voltage flexibility, permitting centering of the photopeak within a 40% window. Several other instruments tested were not capable of imaging I-125. As expected, the spatial resolution is somewhat inferior to that measured with Tc-99m. Line spread data from capillary tubes imaged with a high sensitivity collimator through 2 cm scattering material provided FWHM's of 1.16 and 0.77 cm respectively. We present corresponding MTF curves.

I-125 imaging appears to be useful in the display of labeled fibrinogen in deep-vein thrombosis of the leg. Camera images show considerably more detail of clot formation than is available from conventional probe measurements. However, adequate evaluation of this application of I-125 imaging awaits further study.

DUAL WINDOW TECHNIQUE FOR IMPROVING I-123 THYROID SCANS. F.D. Rollo and D. Williams. Vanderbilt University Hospital, Nashville, TN. and V.A. Hospital, San Francisco, CA.

I-123 is becoming widely used for thyroid scanning. Improved images result from recording not only the 159 keV primary photopeak but also the 27.5 keV x-ray peak. The ratio of counting rates of a 20-50 keV window to a 130-190 keV window is 0.8 or greater in scattering media. Line spread function imply comparable resolution for these two energy windows. A Picker thyroid phantom was imaged with a Picker Magna-scanner 1000 at three energy window conditions (1) 20-50 keV, (2) 130-190 keV, and (3) both windows simultaneously (dual window). Three collimators, four dot sizes and four contrast levels were evaluated. The L217 Ackerman-Schmehl collimator with 1mm dot and 85% contrast provided the best images. For the same information density the dual window allowed an 80% increase in scan speed. Twenty-five patients were evaluated. The best images resulted with the dual window. Conclusion: Superior I-123 images result with the dual window. This technique allows either improved statistics, a decrease in scan time or a decrease in administered dose.

THURSDAY, JUNE 29 CALIFORNIA B ROOM
10:30 a.m.-12:00 p.m.

IN VITRO AND CORRELATIVE TECHNIQUES

ENDOCRINOLOGY II: THYROID (CLINICAL SCIENCE)

Chairman: Lewis E. Braverman
Co-Chairman: William H. Beierwaltes

MINI-SYMPOSIUM: RADIOIODINE THERAPY FOR HYPERTHYROIDISM

* * *

The following three papers constitute a Rapporteur Session. Rapporteur for this session is Lewis E. Braverman, University of Massachusetts Medical Center, Worcester, MA.

CALCULATED LOW DOSE RADIO-IODINE THERAPY FOR THYROTOXICOSIS. George L. Jackson, Fred W. Flickinger, Nancy M. Blosser, Harrisburg Hospital, Harrisburg, PA 17101.

Four-hundred eighty-seven patients have been treated since 1963 with radio-iodine, ^{131}I, for thyrotoxicosis. The present schedule of therapy is for the initial administration of 3500 RADS. In the 45% of patients who have required more than one treatment, a second treatment dose with 5000 RADS is generally employed. If a third treatment is required, 10,000 RADS are administered. The patients have been followed at frequent intervals during the early stages of therapy and then generally at not less than one year intervals. Most patients receive Propranolol. Some patients also receive goitrogen therapy in order to help relieve the symptoms of their disease earlier than if radio-iodine therapy alone were used. The overall incidence of permanent hypothyroidism is 12%. A life table analysis will be presented showing the incidence of hypothyroidism every six months after therapy. Forty percent of all patients who become hypothyroid after therapy do so transiently. This series of patient has been further subdivided into groups according to gland size, diffuse nature of enlargement, nodularity, or if postoperative. Subgroups according to the presence of eye manifestations or pretibial myxedema are also noted. These divisions are analyzed according to the number of treatments required, the number of millicuries and RADS administered, and the incidence of hypothyroidism. The authors conclude that it is possible and desirable to treat hyperthyroidism with ^{131}I without producing another disease (hypothyroidism). This can be accomplished with minimal inconvenience to the patient if concomitant Propranolol and goitrogen therapy is employed.

TREATMENT OF THYROTOXICOSIS WITH IODINE-131. A 25-YEAR EXPERIENCE. H. Katz, S.B. Majid, E.M.

Lopez, J. Eisenberg, and M.L. Maayan. Veterans Administration Hospital, Brooklyn, New York.

130 male patients representing approximately 1% of hospital admissions over a 25-year period were treated with I-131 for thyrotoxicosis (91.6% diffuse goiter; 8.4% toxic nodules) with the intent of cure by a single dose. The amount of the dose was established in relation to the gland size, 24-hr. RAI uptake, clinical symptomatology, and other pertinent laboratory results. In 67% of cases this dose varied between 1-10 mCi of I-131, of which 50% were 5 mCi or less. 20% of the patients received more than 10 mCi and the rest more than 20 mCi. In 57.6% of the treated patients, cure was achieved with a single dose during the first 12 months after therapy. In all of these, the doses were below 10 mCi, and in 33%, 5 mCi or less. 45% of all treated patients became hypothyroid; of these, 68% within the first 12 months succeeding a single dose of 1-10 mCi of I-131. Patients receiving 2 (25%), 3 (12%), and exceptionally up to 7 doses, became euthyroid or hypothyroid in 2-3 or more years after treatment. The data suggests that both - cure of thyrotoxicosis and induction of myxedema - are related to individual sensitivity to radioactive iodine rather than to the size or number of doses given.

I-131 THERAPY OF HYPERTHYROIDISM IN CHILDREN. J.E. Freitas, D.P. Swanson, M.D. Gross, and J.C. Sisson. University of Michigan Medical Center, Ann Arbor, MI.

All children treated with I-131 for hyperthyroidism over a 25 year period (1951-1976) were evaluated to assess the long term effects of such therapy. Sixty-three patients (11 males and 52 females) had hyperthyroidism established by standard clinical and laboratory criteria. Sixty-one of these 63 patients were examined by either one of our clinic physicians or by their private physician within the past year.

The mean age at the time of initial treatment was 15.4 years (range 3-18) with a mean total dose of 8.8 mCi (range 3-81.6). Hyperthyroidism subsided in 5.6±4.1 months. In 45 patients (74%), hyperthyroidism was ended by the first dose, 13 (21%) by the second dose, and one required a third and another a fourth dose. In one patient, I-131 then total thyroidectomy were required to terminate her thyrotoxicosis. One patient developed recurrent hyperthyroidism 11 years after initial therapy, but responded to a second treatment. Ophthalmopathy (grade II-III) was present in 43%, but did not progress after treatment.

The follow-up period was 11.5±8.7 years. The prevalence of hypothyroidism 6 months after treatment was 54% and at the time of latest follow-up was 84%. No patient developed head or neck neoplasms or leukemia. Two patients are infertile. Of 60 progeny, 1 child had cryptorchidism and 2 have learning disabilities.

From this and other series, it is apparent that the theoretical risks (thyroid cancer, leukemia and genetic change) of I-131 therapy for hyperthyroidism in children are not realized. Hypothyroidism occurs in most patients, but is easily treated. I-131 should be considered a safe and simple primary therapy of hyperthyroidism in children.

* * *

RADIOIODINE THERAPY OF HYPERTHYROIDISM. David V. Becker, New York Hospital, New York, NY.

MINI-SYMPOSIUM: RADIATION AND THE THYROID

ABNORMALITIES OF THE THYROID GLAND AFTER IRRADIATION OF NECK FOR HODGKINS DISEASE. D.F. Nelson, R.E. O'Mara, K.V. Reddy and P. Rubin. University of Rochester Medical Center, Rochester NY

An investigation has been carried out to determine the risk of patients developing thyroid abnormalities (nodules, functional abnormalities, etc.) after neck irradiation for Hodgkins disease. Although much has been written concerning the development of abnormalities after low-dose childhood irradiation to the neck, little is known about the development of such abnormalities in patients who fall into this treatment dosage range (median 4400 rads). A total of 50 patients are currently being followed in this institution. All patients are free of evidence of Hodgkins disease with a median duration of followup of six years (range 2-16 years). Sixteen patients from the group scanned presented the following abnormalities: a nonfunctioning, palpable nodule; adenoma at surgery-1; multinodularity-3; mottled activity pattern without palpable nodularity-5; decreased uptake with decreased perfusion-4; increased perfusion, uptake and size of one lobe with respect to the other-3. One other patient showed a pattern consistent with thyroiditis at initial study which reverted to normal with one year. Ten of the 50 patients are clinically and chemically hypothyroid; some with minimal symptoms. One patient with normal chemistries but abnormal perfusion and size of the gland has developed bilateral exophthalmos.

These data, obtained within the relatively short follow-up period, indicate that morphological and functional abnormalities of the thyroid gland are not uncommon in such patients and underscore the need for continuous reevaluation of thyroid status.

HASHIMOTO'S THYROIDITIS: THE COMMONEST RADIATION INDUCED THYROID DISEASE. M.D.Okerlund, A. Beckmann, M. Caro, J. Sommers, L. Kaufman, F. Greenspan, M.Galante, and T. Hunt. University of California Medical Center, San Francisco, CA.

Thyroid cancer is usually emphasized as resulting from neck radiation, but when 319 patients with a history of childhood radiation were studied 64(20%) had stigmata of thyroiditis (positive antibody tests, goiter, iodide depletion,or hypothyroidism) they were then compared with 200 patients with these criteria but without radiation.

Radiation	Yes	No
Age	37±5	41±9
%Female	63	88
%Hypothyroid	8	22
%Palpable nodule	26	18
Family history +	12	41

100% had 1(and 86% had 2) positive antibody tests, using antithyroglobulin by RIA and agglutination test for thyroid microsomal antibody.

All 15 nodule-bearing patients meeting thyroiditis criteria had this confirmed at surgey when operated for the nodule: 6 glands contained cancer, and 8 adenomas. It occurs in patients without genetic predisposition to thyroid disease, but when a nodule is present a high prevalence of tumor (adenoma or carcinoma) is found, unlike non-radiated persons. It was found with a mean interval of 26 years after radiation to skin, tonsils, or thymus. Isotope findings (I-123 scan, Tc-99m scintillation camera, and fluorescent scan) included goiter, irregular labelling, iodide depltion, "cold" or rarer "hot" nodules or atrophic glands. Hashimoto's thyroiditis may be the commonest radiation-induced thyroid disease, since all other diagnoses accounted for a total of 17% of the series, and thyroiditis 20%. Many abnormalities of physical exam or thyroid imaging studies can be explained by this benign disease, but tumors are frequent in glands with discrete nodules.

RADIOIODINE THERAPY IN WELL-DIFFERENTIATED PAPILLARY AND FOLLICULAR CARCINOMA OF THE THYROID. V.M. Varma and R.C. Reba. George Washington University Medical Center, Washington, D.C.

Fourty-six patients (12 men, 34 women) with well differentiated papillary and follicular carcinoma of the thyroid were given I-131 radioiodine following thyroidectomy. Nine patients had palpable lymph nodes prior to surgery. Twenty-eight patients had metastases to cervical lymph nodes at surgery. Seven patients had evidence of lung metastasis, another 7 patients had bone metastasis. Thirty patients received one treatment

dose of 150 mCi; 6 patients received two doses; 7 patients received three doses and 3 patients had 4 or more treatments. (Four patients were lost to follow-up.) Thirty patients had negative scans from 2-10 years following treatment. Twelve patients showed persistent evidence of metastatic disease.

Patients demonstrating negative scans following radioiodine continued to do well. Follow-up scans on 4 out of 7 patients with lung metastasis treated with multiple doses of radioiodine showed clearance of functioning metastases. Scans remained poisitive in the 7 patients with bone metastases, despite multiple treatments. Seven patients had evidence of widespread metastases at the time of death. In our experience, radioiodine following total thyroidectomy should be included in the treatment of well-differentiated thyroid carcinoma.

RADIOIODINE THERAPY OF THYROID CARCINOMA. William H. Beierwaltes, University of Michigan Medical Center, Ann Arbor, MI.

THURSDAY, JUNE 29 GARDEN GROVE ROOM
1:30 p.m.-3:00 p.m.

CONTINUING EDUCATION

CURRENT STATUS OF RADIATION BIOLOGY AND SAFETY AS IT RELATES TO RADIOISOTOPE THERAPY, RADIATION WORKERS, PRE-NATAL IRRADIATION, CARCINOGENESIS, ESTIMATION OF ABSORBED DOSES, AND CURRENT FEDERAL REGULATIONS

PARTICIPANTS: Richard L. Witcofski, Chairman, Bowman Gray School of Medicine, Winston-Salem, NC; Anthony R. Benedetto, Co-Chairman, William Beaumont Army Medical Center, El Paso, TX; and Eugene L. Saenger, Cincinnati General Hospital, Cincinnati, OH.

THURSDAY, JUNE 29 ANAHEIM ROOM
1:30 p.m.-3:00 p.m.

CLINICAL SCIENCE

ONCOLOGY II

Chairman: Richard S. Benua
Co-Chairman: Steven M. Pinsky

AN IN VIVO MODEL FOR GALLIUM UPTAKE STUDIES IN TUMORS. A.A. Noujaim, B.C. Lentle, J.R. Hill, U.K. Terner, H. Wong. Cross Cancer Institute and Departments of Radiology, Pathology and Bionucleonics, University of Alberta, Edmonton, Alta., Canada

The model used for our experiments is the canine TVT (Transmissible Venereal Tumor). The tumor is believed to be cellularly transmitted, and tumor growth regularly occurs following experimental inoculation of random dogs with tumor cells. A total of 8 dogs were used in our experiments. The animals were injected with either Ga-67-citrate, Ga-67-transferrin, I-125-transferrin, Ga-68-citrate, or a mixture of the above. Dynamic uptake studies were conducted for two hours post-injection and the blood clearance as well as tumor and muscle uptake were measured using a time-sealed multi-probe system. Results indicate that the uptake of Ga-67-citrate in the tumor is related to the stage of tumor growth. However, when Ga-67-transferrin and Ga-68-citrate were injected consecutively in the same animal, the Ga-67-transferrin showed an immediate uptake by the tumor thus indicating the presence of specific transferrin receptor sites in the tumor. Dual label experiments with I-125, Ga-67-labeled transferrin, in which the I-125 and Ga-67 radioactivity were measured simultaneously, showed that the ratio of Ga-67/I-125 increased in the tumor and decreases in the blood thus leading us to believe that the role of transferrin is that of a simple carrier with no evidence of endocytosis taking place.

EFFECT OF ANEMIA ON THE BIODISTRIBUTION OF Ga-67 CITRATE. W.P. Bradley, P.O. Alderson, and J.F. Weiss. Armed Forces Radiobiology Research Institute, Bethesda, MD, and Johns Hopkins Hospital, Baltimore, MD.

The biodistribution and tumor uptake of Ga-67 is altered by exposure to whole-body irradiation, which causes increased serum iron (Fe) and saturation of unsaturated iron-binding capacity (UIBC). Iron deficiency anemia also alters UIBC. To determine if anemia alone could alter the biodistribution of Ga-67, 13 weanling Sprague-Dawley rats were fed an iron-deficient diet for 8-9 weeks. Control littermates (n = 11) received normal diet. Each animal then received 10 μCi of Ga-67 intravenously, and urine and feces were collected for 48 hr. At 48 hr, animals were sacrificed, and tissue samples were taken to determine %ID/gm. A blood sample was also obtained and hematocrit (Hct), serum Fe, and UIBC determined. Anemic rats (n = 6) had significantly decreased Hct (31.8 ± 3.1) and serum Fe, and increased UIBC and %ID/gm in liver (1.9 ± 0.2) and spleen. The %ID/gm whole blood was decreased, as was 24-hr urinary excretion (4.7 ± 1.0%). A group of 7 anemic rats given a normal diet 24 hr prior to Ga-67 had high serum Fe, low UIBC, increased urinary excretion (18.8 ± 1.6%) and normal %ID/gm in liver (0.4 ± 0.1) and spleen. These changes were apparently the result of rapid gastrointestinal absorption of Fe. There was a significant correlation ($r = 0.90$, $p < 0.001$) between UIBC and liver-spleen uptake ($n = 24$). Ga-67 biodistribution, especially liver-spleen uptake, is markedly altered by anemia and appears responsive to acute changes in Fe intake. These findings emphasize the importance of serum Fe and UIBC to Ga-67 biodistribution, and suggest that knowledge of Fe and UIBC of patients may be useful in interpreting results of clinical Ga-67 studies.

A TRANSFERRIN MEDIATED UPTAKE OF GALLIUM-67 BY EMT-6 SARCOMA. S.M. Larson, J.S. Rasey, and D.R. Allen. VA Hospital and University of Washington, Seattle, WA.

We studied Gallium-67 (^{67}Ga) uptake by EMT-6 sarcoma, a tumor with both in-vivo (BALB/c mice) and in-vitro growth forms. In-vitro studies were performed using exponentially growing cells in Waymouth's tissue culture medium. 0.5 μCi of ^{67}Ga and/or Iodine-125 (^{125}I) labeled transferrin (TF) was incubated with the cells at 37°C at 24 hrs. About 10^7 cells/flask were harvested. In-vitro, the addition of TF to the medium markedly enhanced ^{67}Ga uptake, and in fact TF was required before appreciable cell:medium concentration gradient for ^{67}Ga occurred. The uptake of ^{67}Ga by EMT-6 tumor cells was mediated by a specific cellular TF receptor. Scatchard analysis of the EMT-6 cellular binding of ^{125}I-TF showed a cellular receptor with K, association constant for TF of 5×10^6 L/M, and abundance of 500,000 receptors per cell. We correlated the observed ^{67}Ga uptake G(T) with the degree of formation of ^{67}Ga-TF, X(T), and the fraction of TF bound to the cells, Y(T). Over a 5 order magnitude range of TF medium concentration, $G(T) \alpha [X(T) \cdot Y(T)]$ with linear correlation by least squares method of $r=0.86$ ($df=69$; $p<.0001$). Since the EMT-6 tumor also grows as a solid transplantable subcutaneous tumor of BALB/c mice, we had the opportunity to determine whether the tumor

uptake of ^{67}Ga in-vitro was matched by a correspondingly active uptake in-vivo. When tracer quantities of ^{67}Ga were used, ^{67}Ga tumor uptakes at 24 hrs were as high as any reported mouse tumor (≈10%/gm tumor). Also, when tumor uptake of ^{67}Ga prelabeled to mouse serum was compared to uptake of ^{67}Ga-citrate, tumor uptakes at 24 hrs were significantly greater in the serum group ($p<.02$, $df=22$). We conclude that TF plays a significant role in ^{67}Ga tumor uptake by EMT-6 sarcoma (of BALB/c mice) in-vivo and in-vitro.

SARCOMA-180-TUMOR LOCALIZATION: In-111-OXINE AND Ga-67-OXINE COMPLEXES VERSUS In-111-CHLORIDE AND Ga-67-CITRATE. G.V.S. Rayudu, P. Clark, A.N. Sukerkar, A. Ali, D.A. Turner and E.W. Fordham, Rush University Medical Center, Chicago, IL.

Although Ga-67-citrate and In-111-chloride are being used as tumor imaging agents, their slow clearance from non-target areas poses problems in interpretation of the scans. In this communication bleomycin (Bl), trasylol (T), streptokinase (S), and plasminogen (P) were complexed with Ga-67-oxine (Ga-67-ox) and In-111-oxine (In-111-ox) which were prepared by utilizing the method introduced by McAfee and Thakur (JNM 17, 480, 1976). Some results of the tissue distribution studies in S-180 mice at 2 days post IV are:

	Tu/Muscle	Tu/Blood	Tu/Liver
Ga-67-ox-T.	3.40	3.65	0.69
Ga-67-ox-S.	9.84	7.57	0.65
Ga-67-ox-P.	6.53	2.18	0.10
Ga-67-Cit.	10.81	6.12	0.64
In-111-ox-T.	3.11	0.59	0.35
In-111-ox-S.	3.53	1.86	0.20
In-111-ox-P.	18.60	12.22	0.21
In-111-ox-Bl.	5.19	8.02	0.35
In-111-Chlo.	7.41	8.33	1.28

The results indicate Ga-67-ox-P and In-111-ox-P clear faster than Ga-67-citrate and In-111-chloride. The biodistributions of Ga-67-ox- and In-111-ox-complexes differ from those of Ga-67-citrate and In-111-chloride. In-111-ox-bleomycin is not superior to In-111-chloride in tumor localization.

STUDIES OF TUMOR LOCALIZING RADIONUCLIDES IN TRANSPLANTED HUMAN TUMORS IN NUDE MICE. S.D.J. Yeh, L. Helson. Memorial Sloan-Kettering Cancer Center & Cornell Medical College, N.Y.

Since the first demonstration of thymic aplasia in nude mice by Pantelouris in 1968, successful transplantation of various human solid tumors was achieved which maintained their original growth rate and histological characteristics. Effects of anti-cancer drugs were also successfully evaluated in such tumor bearing mice. In this paper, we wish to report our preliminary studies on tumor localizing radionuclides in the tumor bearing mice. Tumor localizing agents, Co-55 and 57 bleomycin and Ga-67 citrate were compared with Co-57 chloride and I-131 norcholesterol. The tumors were human neuroblastoma, malignant Schwannoma, testicular adenocarcinoma and non-Hodgkin's lymphoma.

The animals were sacrificed 24 to 72 hours after i.v. injection of radionuclides. The radioactivities in various tissues were measured and specific activities determined.

The Co-57 bleomycin injected animals had tumor to blood ratio (T/B) of 11.3±1.3 (Mean S.E.) and tumor to muscle ratio (T/M) of 20.4±4.3 at the end of 48 hours. The Co-55 bleomycin injected mice had T/M of only 2.32±0.81 at the end of 17 hours. In contrast, $CoCl_2$ injected animals had a T/B of 1.46±0.16 and a T/M of 3.72±0.57 at the end of 48 hours. The T/B in cholesterol injected animals was 0.78± 0.19 and the T/M was 0.79±0.15 at the end of 48 hours while the adrenal to blood ratio was 87±18. When lymphoma and Schwannoma were implanted in the same animal, the tumor uptake of Ga-67 in the lymphoma, the fast growing tumor had much higher specific activity than the slow growing Schwannoma. The difference is greater than three fold.

It is concluded that the nude mouse implanted with human tumors is an ideal model for testing tumor localizing radiopharmaceuticals.

LOCALIZATION OF INTRA-ARTERIAL VS. INTRAVENOUS H-3-ADRIAMYCIN. Bieshia Chang, R.C. Verma, M.M. Webber and T. X. O'Connell. University of California, Los Angeles, Calif.

Adriamycin is an effective chemotherapeutic agent used in man for regional intra-arterial perfusion of tumors. This study was conducted to evaluate the efficacy of intra-arterial (i.a.) versus intravenous (i.v.) administration by measuring the tissue concentrations.

Walker 256 carcinosarcoma was shown to respond very well to Adriamycin in 14 rats. The tumor was implanted in the left hind limb of a group of 19 rats. Eleven of these were selected for i.a. and 8 for i.v. administration of the drug. The H-3 Adriamycin used was 4.3 μCi/rat. The i.a. injection was made into the left femoral artery which constituted the major regional artery perfusing the tumor. The i.v. injection was made into the right femoral vein. The animals were sacrificed at approximately two hours. Multiple tissue samples from the tumor, blood, skeletal muscle, liver, small intestine, stomach, spleen, kidney, lung and myocardium were obtained and weighed. The samples were counted in a liquid scintillation counter. The tumor/tissue ratios in the two groups were as follows: the i.v. group: blood 8.7, skeletal muscle 1.9 and other tissues <0.3; the i.a. group: blood 30.2, skeletal muscle 1.7 and other tissues: 0.5-1.7.

On an average, the intra-arterial administration enhanced the uptake of the drug by the tumor by a factor of four over the i.v. route. The data also confirms that i.a. administration leads to relative dimunition of H-3-Adriamycin accumulation in other tissues, hence decreasing the tissue toxicity. This work is supported by USPHS grant #Ca-15787.

TECHNETIUM-99M PYROPHOSPHATE MYOCARDIAL IMAGING IN RABBITS WITH ADRIAMYCIN INDUCED MYOCARDIAL DAMAGE. G.A. Wilson, A. Durakovic, S. Gorton, E. Schenk, R. Sutherland and J.M. Bennett. University of Rochester Medical Center, Rochester, NY

Previous reports have noted the inconsistent localization of technetium-99m pyrophosphate (Tc-99m PPi) in the myocardium of patients receiving adriamycin. To evaluate the potential of myocardial uptake for predicting myocardial toxicity secondary to adriamycin, a group of 36 New Zealand white rabbits were treated with 2.4 mg/kg of adriamycin weekly. The rabbits were imaged weekly on a gamma camera, 1-2 hrs. post-injection of Tc-99m PPi. The images were also processed on a digital computer with ratios between the heart and bone generated. Images were graded 1-4 on the basis of myocardial uptake and adriamycin administration was either halted or the rabbits were sacrificed on the basis of the images or impending death. Prior to sacrifice, each rabbit was injected with Tc-99m PPi and tissue distribution studies were carried out.

Pathological examination of tissues including independent assessment of myocardial damage was also performed. Uptake in the myocardial images increased with the progressively severe morphological changes seen in the myocardium. Most myocardial uptake was seen in animals with both prominent vacuolization of the myocytes and fibrous changes, with lesser uptake being seen in those animals with either vacuolization of myocytes or fibrosis alone. In the animals in which the adriamycin administration was halted, most of the images promptly returned to normal. The myocardial uptake of Tc-99m PPi may be useful in the detection of adriamycin induced myocardiopathy.

Supported by United Cancer Council of Rochester and NIH CA 20329.

THURSDAY, JUNE 29
1:30 p.m.-3:00 p.m.

SANTA ANA ROOM

BASIC SCIENCE

RADIOPHARMACEUTICALS VI: CARDIOVASCULAR

Chairman: Gerald A. Bruno
Co-Chairman: Wynn A. Volkert

RADIOCHEMICALLY PURE TC-99m LABELED FATTY ACID ANALOGS. M.D. Loberg, A.T. Fields, and D.W. Porter. University of Maryland, Baltimore, Maryland 21201

Five Tc-99m labeled fatty acid analogs were developed from chelating groups chosen such that the Tc-99m complex and not the chelating group would mimic fatty acids. Four new chelating agents containing iminodiacetate (IDA) were synthesized and radiolabeled with Tc-99m: ω-carboxydecylIDA (I), undecylIDA (II) (II), N-(ω carboxydecyl)carbamoylmethylIDA (III), and N-(undecyl)carbamoylmethylIDA (IV). HPLC showed Tc-I and Tc-II to consist of a mixture of at least two radiolabeled chelates, while Tc-III and Tc-IV each existed as a single radiochemical. This and previous work have shown that the carbamoylmethyl group in III and IV is necessary for radiochemical purity. The anticipated bis structures of Tc-III and Tc-IV were confirmed by radiolabeling a mixture of III and IV. The reaction products were separated by HPLC: III-Tc-III (24%), III-Tc-IV (28%), and IV-Tc-IV (48%). This approximately 1:1:2 product ratio is indicative of mixed ligand, bis structures. III-Tc-IV has a structure most consistent with that of a fatty acid with two saturated ten carbon chains symmetrically placed around a Tc atom with a methyl group on one end and a carboxylic acid on the other. Tc-III_2, Tc-IV_2, III-Tc-IV, and ^{3}H-palmitate were compared in regards to in-vitro and in vivo stability, protein binding, octanol:H_2O partitioning, and myocardial uptake. The radiochemical structure of Tc-labeled IDA derivatives can now be predicted and Tc radiopharmaceuticals can be synthesized which are asymmetric around the central Tc-99m atom. The myocardial uptake of the fatty acid analog can now be optimized by changing hydrocarbon chain length, protein binding, lipophilicity and charge.

EVALUATION OF IODOMETHYL TRIMETHYLAMMONIUM-I-131 FOR MYOCARDIAL IMAGING. C.C. Huang and A.M. Friedman, Argonne National Laboratory, Argonne, IL, G.V.S. Rayudu, P. Clark, and E.W. Fordham, Rush University Medical Center, Chicago, IL.

The success of N-13 labeled ammonium for myocardial localization prompted us to investigate the feasibility of the tetramethyl-substituted ammonium for myocardial imaging. The use of radioiodine is economically more feasible, and the radiopharmaceutical can be made available to hospitals which do not have access to a cyclotron facility.

Iodomethyl trimethylammonium-I-131 (I-131-TMA) was prepared by the isotopic exchange of diiodomethane with sodium iodide-I-131 in acetone at 100° for 4 hr, followed by reaction with 25% trimethylamine in methanol for 1 hr. The final product was purified by ion exchange.

Tissue distributions following injection of I-131-TMA in mice showed that between 10 min and 2 hr the highest accumulation of radioactivity was in the kidney and heart. The heart to blood radio of the activity reached the peak (16) 2 hr after injection, and remained fairly high at all the time periods studied. The blood clearance was very rapid. Two min after injection, the level of activity in the blood was almost constant up to 2 hr. However, the uptake of the heart was almost immediate, but decreased as the level in the blood dropped. Nevertheless, the radioactivity in the heart was very high at all times, and remained fairly constant between 30 min and 2 hr. Whole body clearance studies in mice showed less than 1% of the injected activity was retained after 24 hr.

It is concluded that the radioiodinated TMA is potentially useful for myocardial imaging. I-123 could be easily substituted for I-131 to make a viable imaging agent.

LOCALIZATION OF STANNOUS ION FROM TECHNETIUM-99m LABELED AGENTS IN INFARCTED MYOCARDIUM. M. K. Dewanjee and H. W. Wahner. Mayo Clinic and Foundation. Rochester, MN.

Several tin-chelates are used with Tc-99m chelates in nuclear cardiology. The distribution of stannous ion in normal, ischemic and infarcted myocardium has not been determined. We have investigated the pharmacodynamics of tin-pyrophosphate (Sn-PP), tin-glucoheptonate (Sn-GH), tin-human serum albumin (Sn-HSA), and tin-dimercaptosuccinate (Sn-DMSA) in an experimental myocardial infarct model in rabbit with Sn-113 radioisotope. The animals were injected with 600 μCi of tin-chelates 24, 48, 96 and 168 hours post-infarct and sacrificed at 3 hours after injection. Myocardial mapping and organ distribution were performed. Radioactivity ratios of infarcted to normal myocardium and infarcted myocardium to blood ranged from 6.4 for Sn-DP to 10.8 for Sn-DMSA and the infarcted myocardium to blood ranged from 2.2 for Sn-PP to 6.9 for Sn-HSA. Except for Sn-DMSA, most of the tin-chelates are unstable and break down in vivo and behave as stannous ion. Binding of stannous ion with hemoglobin is higher than that of albumin. 0.2-0.5% of the stannous ion localized in infarcted and ischemic myocardium. This stannous ion might further aggravate the hypoxic tissue by oxygen depletion, caution should be exercised to minimize the amount of stannous ion injected into patients following myocardial infarction for imaging blood pool and infarct. The subcellular distribution of Sn-PP and Sn-GH in normal and infarcted myocardium suggests that (20-30)% of tin-compounds localizes in mitochondria. Hence, we investigated the effect of Sn-PP ($6x10^{-8}$M and $6x10^{-9}$M) directly on oxidative phosphorylation of isolated mitochondria of cat heart and observed State IV respiration was affected. Stannous ion at microgram level interferes with respiratory enzymes in mitochondria.

EARLY AND LATE UPTAKE IN MYOCARDIAL LESIONS. H.F. Kung, R. Ackerhalt, and M. Blau. State University of New York at Buffalo, Buffalo, NY.

As part of a search for agents capable of concentrating in early myocardial infarcts, cardiac uptake at various stages of isoproterenol-induced myocardial necrosis in rats was studied. Tc-99m-PPi, -MDP, -glucoheptonate (GH) or F-18 fluoride was injected (iv) 0-24 hours after heart tissue damage from a single subcutaneous injection of isoproterenol (30 mg/kg). All of the rats were dissected one hour after radiopharmaceutical injection. The ratio of uptake between whole damaged and whole normal heart was calculated (DH/N ratio).

For every agent studied, a curve of DH/N vs. time after isoproterenol injection was obtained. These curves all had a biphasic pattern with an early peak at 1 hour and another at 6-8 hours. For the bone agents (PPi, MDP and fluoride) the later peak is 2 or 3 times larger than the early peak. The 6-8 hour values of DH/N were 27, 17 and 4 for MDP, PPi and fluoride, respectively. The 6-8 hour peak corresponds with the time of maximum influx of Ca^{++} into these lesions, as reported by Bloom and Davis.

Tc-99m-GH, on the other hand, has its major peak (DH/N= 3.6) at 1 hour with only a small increase at 6-8 hours. This confirms reports of early myocardial lesion localization with this agent. A separate mechanism, probably cytoplasmic protein binding, must be responsible for the early uptake of GH. Agents designed to detect early infarcts should take advantage of this mechanism.

Isoproterenol-induced myocardial necrosis in rats provides a simple and useful model for studying radiopharmaceutical localization, especially for time course studies. This information is difficult to obtain with other animal models.

TECHNETIUM-99m HEPARIN: A NEW RADIOPHARMACEUTICAL TO IDENTIFY DAMAGED CORONARY ENDOTHELIUM AND DAMAGED MYOCARDIUM. P.V. Kulkarni, R.W.Parkey, L.M.Buja, J.E.Wilson, F.J.Bonte, and J.T.Willerson. U. Texas Health Science Center at Dallas, TX.

Preliminary experimental results suggested that technetium-99m heparin (TcH) may be useful for imaging damaged vascular endothelium. Both temporary occlusion (T) and permanent occlusion (P) coronary models were designed to examine TcH as a possible means to localize and scintigraphically identify damaged coronary endothelium (DCE) or myocardium (DM). Of 16 dogs, 4 had P of the proximal left anterior descending coronary artery (LAD); 12 had T of the LAD for 60-85 min followed by reflow. Three-six mCi of TcH was injected IV within 5-10 min post-release in the T and 48 hrs post-occlusion in the P dogs. Scintigrams and blood samples were taken serially to 3½ hrs and the dogs were sacrificed for histology and well counting. Of the 12 T dogs, 9 had transmural damage; 1 had subendocardial damage only; 2 had no obvious damage at all. The 9 with transmural damage showed increased uptake of TcH in the damaged tissue [ratios % injected dose to normal left ventricle (R)]. Border epicardium (BEP) 1.52 (1.14-2.10); border endocardium (BE)1.79 (1.12-2.60); damaged epicardium (DEP) 10.1 (2.04-27.4); damaged endocardium (DE) 15.5 (6.97-36.5). Four P dogs showed BEP 1.77 (1.29-2.04); BE 2.01 (1.54-2.90); DEP 3.45 (2.92-3.70); DE 4.50 (3.44-6.01). In 4 T dogs the LAD was divided into 3 parts. R above occlusion 3.45 (2.88-4.24); at occlusion 12.8 (9.82-14.1); below occlusion 5.14 (4.01-5.75). Circumflex artery 2.49 (2.04-3.04). Scintigrams were positive in vivo in T dogs; the P dogs were visualized only in vitro. Results suggest TcH may have value as a positive imaging agent when coronary arteries or myocardium is injured and blood flow is present.

16-METHYL TELLURO-Te-123m-9-HEXADECENOIC ACID: A POTENTIAL MYOCARDIAL AGENT. G. P. Basmadjian, S. L. Mills, G. R. Parker, A. S. Kirschner, R. D. Ice, and R. A. Magarian. College of Pharmacy, The University of Oklahoma Health Sciences Center, Oklahoma City, OK.

We have synthesized the Te-123m analog of the fatty acid, 16-methyl telluro-9-hexadecenoic acid as a potential myocardial imaging agent. Te-123m was selected because of its excellent physical characteristics and imaging properties (84% 159 keV photon, half-life of 117 d).

A method for solubilizing tellurium metal was developed which greatly reduces the need for hazardous reagents, is rapid and radiologically safe. The method utilizes sodium borohydride in ethanol to produce disodium ditelluride. This intermediate product was reacted with 16-bromo-9-hexadecenoic acid to form the colored ditelluride of the fatty acid, which upon reduction with sodium borohydride forms a colorless reactive intermediate. Upon the addition of methyl iodide the 16-methyl telluro-9-hexadecenoic acid is formed.

The synthesis of the Te-123m analog is accomplished within 2 hours. The Te-123m compound has the same characteristics as the "cold" tellurium fatty acid. The 16-methyl telluro-9-hexadecenoic formulation must be stabilized by the addition of ascorbic acid.

Analytical data including NMR, IR, elemental analysis, m.p. and atomic absorption indicate the compound to be 16-methyl telluro-9-hexadecenoic acid.

Biodistribution data on the Te-123m 16-methyl telluro-9-hexadecenoic acid with a specific activity of 0.2 mCi/mg. in rabbits is being evaluated and appears promising.

SELENIUM-75 LABELED HYPOTAURINE FOR MYOCARDIAL AND PANCREATIC IMAGING. D. Elmaleh, D.J. Hnatowich, R. Hinton, S. Kulprathipanja, M.A. Davis, E. Livni, R.S. Lees, and W.H. Strauss. Massachusetts General Hospital and Children's Hospital, Boston, MA.

Selenohypotaurine has been labeled with Se-75 to study its localization in pancreatic and heart tissue. The labeled amino acid was prepared by reducing selenous acid with sodium borohydrate, reacting the product with 2-bromoethylamine under nitrogen and finally oxidizing with aqueous bromine. The labeled product was separated by cation exchange and monitored throughout by HPLC. Se-75 hypotaurine was injected into mice and distributions in 8 tissue types and blood determined at 15 and 60 min. The uptake at 60 minutes in percent administered dose per gram was found to be 1.28 ± 0.17 (heart), 2.81 ± 0.26 (lung), and 5.47 ± 0.65 (liver) and was significantly different from that of Se-75 selenous acid. Pancreas/liver ratios (per gram) were determined in rats for both Se-75 labeled selenohypotaurine and selenomethionine. At 30 min. post injection the ratios were 2.59 ± 1.30 and 2.45 ± 1.29 respectively. Images obtained at 30-60 min. post injection on a gamma camera in rabbits injected with either agent were comparable in pancreatic visualization; the heart was clearly visable with selenohypotaurine. These results suggest that Se-75 selenohypotaurine may be useful for myocardial imaging, in addition, because of its ease of preparation, Se-75 hypotaurine may be useful alternative to selenomethionine for pancratic imaging. (This work supported in part by ERDA (E(11-1)-4115)).

THURSDAY, JUNE 29 CALIFORNIA B ROOM
1:30 p.m.-3:00 p.m.

IN VITRO AND CORRELATIVE TECHNIQUES

RADIOASSAY III

Chairman: John Langan
Co-Chairman: Margaret M. Iannone

TUMOR ANTIGENS. R. Nakamura, Scripps Clinical Center, La Jolla, CA.

SERUM FERRITIN: AN INDICATOR OF NEOPLASM. H.G. Greditzer, J.A. Fernandez-Pol, K.F. Witztum, F.J. Carey and R.M. Donati. St. Louis VA Hospital and St. Louis University, St. Louis, MO.

Serum levels of ferritin as measured by radioimmunoassay (RIA) are thought to accurately reflect total body iron stores. Recent reports demonstrating augmented production of ferritin by transformed cells in tissue culture coupled with reports of elevated levels of serum ferritin in patients with neoplasms provided the basis for the study of serum ferritin as a possible indicator of tumor in man. In the present study 31 patients with biopsy proven malignancy and 13 normal volunteers had serum ferritin levels quantitated by splenic ferritin RIA and the results correlated with tumor type, assessment of metastases and prior or concomitant therapy. In addition, the immunospecificity of the splenic ferritin RIA was evaluated in HeLa cell cultures which produce acidic ferritins. Elevated levels of serum splenic ferritin were found in 21 of the 31 patients with malignancy. Tumor types in this group were squamous cell, oat cell or adenocarcinoma of the lung, rectum, prostate or biliary tree. In the remaining 10 patients the serum ferritin levels were not elevated. In 6 of these patients the lack of elevation could be explained on the basis of iron deficiency, therapy, tumor type (esophageal carcinoma) or extent of the disease. Although there appeared to be cross reactivity with the HeLa cell ferritin, the explanation for the lack of elevation in the remaining patients may be related to the immunospecificity of the RIA. These results suggest that serum ferritin levels determined by RIA provide a sensitive and specific indicator of malignancy in man.

CORRELATION OF QUANTITATIVE CEA DETERMINATIONS AND ESTIMATION OF TUMOR BURDEN. M. A. Swanson, K. A. Wong, G. L.

DeNardo. Sacramento Medical Center of the University of California, Davis, School of Medicine, Sacramento, CA

To assess the predictive value of serum carcinoembryonicantigen (CEA) levels in estimating tumor burden, a retrospective analysis of 77 patients with gastrointestinal (GI) cancer was performed, comparing quantitative CEA values with stage and extent of disease. The Hoffman-LaRoche RIA kit was used to obtain CEA concentrations. The following observations were made: 1) Mean CEA level for 14 preoperative (pre-op) patients with resectable cancer was 3.7 ng/ml. 2) Mean CEA level for 13 pre-op patients with locally advanced disease was 19.1 ng/ml. 3) 20 postoperative patients without recurrent cancer had a mean CEA of 3.4 ng/ml. 4) The mean CEA value for 33 patients with distant metastases was 225 ng/ml. In the latter group, correlation existed between mean CEA concentration and total tumor burden in 26/30 of patients with well differentiated lesions, with extent of metastatic organ involvement rising directly with CEA levels. This was not the case in 3/33 patients with undifferentiated cancers.

Pre-op CEA levels differentiated early from locally advanced GI cancer. CEA levels in 86% of patients with metastatic disease correlated well with estimated tumor burden. The range of CEA levels (0-14 ng/ml) in the 20 post-op patients clinically free of disease, demonstrates the need for serial CEA determinations.

CYCLIC AMP RESPONSE TO PGE1 IN CULTURED CELLS: DIFFERENTIAL RESPONSE OF NORMAL AND TRANSFORMED CELLS.
J.A. Fernandez-Pol and R.M. Donati. Nuclear Medicine Service, VA Hospital and St. Louis University School of Medicine, St. Louis, MO.

Previous studies which demonstrated that normal rat kidney (NRK) cells synchronized in G1 by picolinic acid have a supersensitive response to prostaglandin E1 (PGE1) (FEBS Letters 74: 201-204) led to the characterization of the PGE1 response in virally transformed cells. Addition of picolinic acid to the culture medium of NRK cells transformed by Kirsten sarcoma virus, simian virus 40 and Harvey sarcoma virus with MSV coat, a treatment which predominately arrests cells in G1, G2 and G1 + G2 phases of the cell cycle, respectively, alters cyclic AMP metabolism. Cyclic AMP levels were measured after column purification by radioimmunoassay with the acetylation method which increases sensitivity a 100-fold. The basal values of cyclic AMP in NRK cells treated with picolinic acid are increased 50-60%; stimulation by PGE1 increases cyclic AMP levels 5-fold. The effects are time, PGE1 concentration and cell density dependent. In contrast, the basal values of cyclic AMP in all virally transformed cells treated with picolinic acid were low and the response to PGE1 was blunted. Furthermore, in all virally transformed cells, the PGE1 response did not show time, PGE1 concentration or cell density dependency. The findings presented here suggest that the supersensitive response may be used to evaluate the biological activity of PGE1. In addition, if the altered PGE1 response in transformed cells is an early event in the transformation process, then these studies may provide the basis for early detection of transforming viruses.

THURSDAY, JUNE 29 — CALIFORNIA A ROOM
1:30 p.m.-3:00 p.m.

CLINICAL PRACTICE

PEDIATRICS

Chairman: Hirsch Handmaker
Co-Chairman: Leonard Swanson

THE PEDIATRIC PATIENT IN A COMMUNITY HOSPITAL. J. J. Conway and S. Weiss, Children's Hospital of Chicago, Chicago, IL.

COMMON PEDIATRIC NUCLEAR MEDICINE PROBLEMS IN THE GENERAL HOSPITAL. G. F. Gates, Children's Hospital of Los Angeles, Los Angeles, CA.

THE DIFFERENTIATION OF TESTICULAR APPENDAGE, RECENT TESTICULAR AND OLD TESTICULAR TORSIONS IN CHILDREN, D.L. Gilday, J.M. Ash, J.P. Savage, B. Shandling and S. Ein, The Hospital for Sick Children, Toronto, Canada

The child who presents with a painful, erythematous and tender hemiscrotum is sometimes difficult to diagnose by physical examination. Three main possibilities are: testicular appendage torsion, epididymo-orchitis or testicular torsion. The latter requires urgent surgical correction. Scrotal imaging of the blood flow and blood pool of the scrotum has been advocated in this dilemma.

We have studied 149 boys from one month to 18 years with this technique, using a high resolution gamma camera and a converging collimator.

The appearance of testicular torsion has been described as a zone of decreased blood flow with a decreased blood pool. This occurs with an acute torsion (12 boys). The older torsion, usually with a 2 day or longer history, has a ring of hyperemia around the swollen testes due to inflammation secondary to prolonged ischemia and probably cellular necrosis (8 boys). These patients usually have an unsalvagable testis at surgery, not always predictable by the length of symptoms. However, the scan appearance is diagnostic (7 of 8). The scan appearance of testicular appendage torsion can vary from slight hypoperfusion of the hemiscrotum (3 boys) to massive hyperemia 4+ days after onset (20 boys). There is however, a characteristic appearance seen 24 to 36 hours after onset which is a mild hyperemia laterally in the scrotum which is diagnostic (12 boys).

As the field of scrotal imaging has matured, the recognition of these latter two patterns has improved the specificity of the procedure.

CURRENT STATUS OF TESTICULAR IMAGING IN PEDIATRICS. F. S. Mishkin, Martin Luther King, Jr., Hospital, Los Angeles, CA.

THURSDAY, JUNE 29 GARDEN GROVE ROOM
3:15 p.m.-4:45 p.m.

CONTINUING EDUCATION

INSTRUMENTATION: CURRENT STATUS OF CONVENTIONAL SCANNING AND IMAGING SYSTEMS

PARTICIPANTS: Robert N. Beck, Chairman, Franklin McLean Institute, Chicago, IL; Michael E. Phelps, University of California, Los Angeles, CA; Edward J. Hoffman, Hospital of the University of Pennsylvania, Philadelphia, PA; L. Stephen Graham, UCLA School of Medicine, Los Angeles, CA; and James A. Sorenson, University of Utah Medical Center, Salt Lake City, UT.

THURSDAY, JUNE 29 ANAHEIM ROOM
3:15 p.m.-4:45 p.m.

CLINICAL SCIENCE

RENAL/ELECTROLYTE/HYPERTENSION

Chairman: Peter T. Kirchner
Co-Chairman: Richard C. Reba

RENAL CLEARANCE AND EXTRACTION PARAMETERS OF I-123 O-IODO-HIPPURATE (OIH) COMPARED WITH I-131 OIH and PAH. R.C. Stadalnik*, J.M. Vogel, A-L. Jansholt, K.A. Krohn, N.M. Matolo, M. Lagunas-Solar, F. Zielinski. University of California, Davis and Los Angeles, CA, and Dominican Santa Cruz Hospital, Santa Cruz, CA.

The increased interest in I-123 as a label for hippuran, because of its high photon flux per unit of absorbed radiation dose, led us to study the renal extraction of three different I-123 hippurate preparations. Each preparation was compared to I-131 OIH and PAH by simultaneous injection into healthy dogs. A priming dose was injected, followed by constant infusion to maintain a steady state blood concentration of the test compounds at below the tubular maximum. After 30 min, arterial and renal vein blood samples were obtained at the midpoint of three 20 min collections of urine from left and right kidneys. Each I-123 hippurate preparation gave satisfactory renograms, however our experiment was primarily designed to obtain exact extraction parameters to judge whether they could be used for studies utilizing a computer renal model for estimation of perfusion and extraction parameters. After calculation of clearance rates and renal extraction ratios, we concluded that only one preparation (see table below) resulted in a product that behaved like I-131 OIH. This method involved autoclaving (90 min) a sealed ampule containing OIH and I-123 NaI from Crocker Nuclear Laboratory in the presence of iodate. (Zielinski et al, Radiology 125:753, 1977).

	I-123/I-131	I-123/PAH	I-131/PAH
Extraction Ratios	1.00 ± .11	0.89 ± .11	0.89 ± .07
Clearance Rates	0.99 ± .05	1.09 ± .09	1.11 ± .07

* Picker Scholar, James Picker Foundation

A COMPREHENSIVE COMPUTER ASSISTED RENAL FUNCTION STUDY: A ROUTINE PROCEDURE IN CLINICAL PRACTICE. W.N.Tauxe, E.V. Dubovsky, F.Kontzen, M.Tobin, A.J.Bueschen. University of Alabama and V.A. Hospital, Birmingham, AL.

Comprehensive renal function studies (CRFS) are currently being used to evaluate function of kidneys, ureters and bladder in all urology patients. 1500 computer assisted studies have been performed comprising sequential scintigraphy (after injecting 300 μCi I-131 OIH), calculation of total and differential effective renal plasma flow (ERPF), residual urine volume, urinary excretion (as a fraction of injected dose) and excretory index (ratio of the actual excretion to expected for the patient's level of ERPF) with automatic computer processing and report generation. The first 700 consecutive adult studies were compared for diagnostic accuracy with excretory urography, angiography, BUN, serum creatinine and creatinine clearances. 96 kidney donors were selected to define the normal. Differential ERPF was calculated from initial slopes of the net curves. (Normal values: ERPF: 531±46 ml/min, % dose excreted at 35 min.: 74%, EI: 0.97±.07, each kidney >45% total ERPF, maximum counts <5 min., <2 min. apart.) The CRFS provides information not obtainable from conventional radiological or biochemical methods. In diagnosis: a. Detection and quantification of non-obstructive bilateral parenchymal disease (52 patients: 7.4% of total); b. Detection of mild unilateral parenchymal or obstructive disease (138 patients 19.7% of total). In management: To assist clinician in decision making, e.g., surgical or medical treatment choice based on quantification of individual kidney function, i.e. prediction of residual function after nephrectomy. In follow-up: Quantitative evaluations of changes as a result of therapy, e.g., recurrent infections, calculi, ureteral diversions, neurogenic bladders.

QUANTITATIVE EVALUATION OF RENAL PARENCHYMAL Tc-99m HEDP UPTAKE IN EXPERIMENTAL ACUTE TUBULAR NECROSIS. K.J.Lavelle, H.M.Park, A.M.Moseman, and S.Lewis. Indiana University School of Medicine, Indianapolis, IN.

Tc-99m phosphorus compounds accumulate in non-skeletal tissues following ischemic insult, e. g., myocardial, cerebral, and splenic infarct, and hepatic necrosis. The present study was performed to assess accumulation of Tc-99m HEDP in experimental renal ischemic injury as compared with Tc-99m DMSA and Tc-99m DTPA. Acute tubular necrosis (ATN) was produced in rabbits by clamping the renal artery for 2 hr. Serial scintigraphs and activity ratio between kidney and spine were obtained in 54 animals (18 control, 18 unilateral ATN, 18 bilateral ATN). Renal uptake (radioactivity counts/gm tissue), creatinine clearance, serum and renal tissue calcium and phosphate concentrations and histology were also evaluated. Results are tabulated below.

	Control	Unilat. ATN	Bilat. ATN
Creatinine Clearance (ml/min)	8.10±1.86	0.73±0.44	0.66±0.41
Tc-99m HEDP Uptake at 1 hr (cts/gm)	223±24	2076±6.0	1835±413
Kidney/Spine ratio at 1 hr	0.6	7.5	2.8
Tissue Calcium (mg/gm)	0.09±0.016	0.548±0.096	0.685±0.102

This study indicates that ischemic renal injury causes a significant intracellular influx of calcium (6 fold, P<0.001) and increased concentration of Tc-99m HEDP (8-12 times the control at 1 to 4 hr) vs a decline for Tc-99m DMSA and Tc-99m DTPA. Tc-99m HEDP produced the best images in both unilateral and bilateral STN. Further study with Tc-99m HEDP seems warranted to explore its potential use in human renal ischemic injury.

TESTICULAR IMAGING WITH THALLIUM-201 AND COMPARISON WITH OTHER RADIONUCLIDES. F. Hosain, P. Hosain, R.P. Spencer. University of Connecticut Health Center, Farmington, CT.

There has been little progress in testicular imaging with radionuclides. Tc-99m pertechnetate has been used for the evaluation of testicular torsion and intrascrotal lesion, and Ga-67 citrate has been used for the staging of patients with testicular malignancies.

Tissue distribution of Tl-201 chloride, Tc-99m pertechnetate and Ga-67 citrate at different time intervals, was measured in mice and rats. In rats, the testes and scrota were separated. Imaging of the testicular region of dogs was carried out soon after the administration of Tl-201 and several times within 4 days. Comparative studies in the same dogs were carried out by imaging with Tc-99m pertechnetate and Ga-67 citrate. In human subjects, several

images were taken within the first 4 days (especially the initial and 1 or 2 day images), following the intravenous injection of 1.5 mCi of thallous-201 chloride.

The uptake of Tl-201 in the testes of mice and rats increased, from an initial value of 0.2-0.3%, to 0.8-1.5% in one day. There was little alteration in the scrotal activity. Initial scrotal content of Tc-99m pertechnetate was higher than that of any other agent. Uptake of Ga-67 both in the testes and the scrota was relatively low. Initial images in dogs with Tl-201 were comparable to, and sometimes better than, those obtained with Tc-99m. Images with Ga-67 were inferior. Later images with Tl-201 were far superior in outlining the testes; in all 6 dogs and 10 patients the testes were well delineated between 1-3 days. It appears that combination of an initial and a later image with Tl-201 would be valuable for testicular studies including efforts to localize undescended testes.

BODY POTASSIUM CHANGES WITH ANTIHYPERTENSIVE DIURETIC THERAPY. B.A. Burrows, S. Podolsky, J.A. Cardarelli, S.W. Burney, D.P. Morley, and S. Genna. Boston VA Hospital and VA Outpatient Clinic; Department of Medicine, Boston University School of Medicine, Boston,Mass.

Diuretic agents, an important component of antihypertensive therapy, sometimes produce potassium depletion. Percentage changes in serial body K-40 measurements were determined in male patients with mild to moderate hypertension randomly assigned to two diuretic regimens in a double-blind study over a 6-month interval. Hydrochlorothiazide, 50 mg b.i.d., resulted in a significant mean decrease in body K-40 from 47.19 mEq/kg to 43.88 mEq/kg (range +8% to -26%) and in serum K from 4.46 to 3.97 mEq/L ($p<0.01$) in 18 patients, 12 of whom had a body K-40 decrease of more than 5%. A "K-sparing" regimen (hydrochlorothiazide 25 mg + triamterene 50 mg b.i.d.) did not result in a significant mean change in body K-40 (45.11 to 45.13 mEq/kg, range +9% to -15%) or serum K (4.45 to 4.26 mEq/L) in 19 patients. Although 9 patients showed a decrease in body K-40 of more than 5%, it was usually less than with hydrochlorothiazide alone. Three patients with hydrochlorothiazide alone showed a drop in serum K on monthly determinations to below 3.5 mEq/L, one to 2.9 mEq/L at the 5th month and he was removed from the study. No clinical or other laboratory evidence of potassium depletion was observed. The influence of other factors, such as insulin-dependent diabetes, could not be excluded.

Although the clinical significance of such body K changes is not known, the need for individualized management of patients on antihypertensive diuretics is suggested by these findings.

(Supported by Veterans Administration Research Funds)

CORRELATION OF DIFFERENTIAL RENAL FUNCTION DETERMINATION BY Tc-99m DMSA IMAGING AND URETERAL CATHETERIZATION. M.L. Born, R.B. Grove, J.P. Jones, J.H. Nadeau, R.R. Price, J.J. Touya, and F.D. Rollo. Vanderbilt University Hospital, Nashville, TN.

The proportion of total renal function provided by each kidney is important in the evaluation and therapy of many forms of renal disease. The purpose of this study was to determine if quantitation of relative Tc-99m DMSA uptake in the kidneys can provide an accurate index of differential renal function. Thirty-nine patients being evaluated for renovascular hypertension underwent Tc-99m DMSA imaging and split ureteral catheterization studies. Computer quantitation of the percent differential DMSA uptake was performed based on the geometric mean of anterior and posterior views and using the posterior view alone. These values were compared to the relative percent creatinine clearance of each kidney determined by bilateral ureteral catheterization. In the 39 patients, the relative percent DMSA localization in the kidneys correlated with the relative percent creatinine clearance with R = 0.97 ($m = .996 \pm 0.04$, $b = 0.08 \pm 2.13$). In this group of patients, geometric mean correction of the DMSA data for differing renal depth had no effect. Similar results were obtained when patients with asymmetric and symmetric impairment of renal function were evaluated separately. The high correlation between relative DMSA concentration and the relative creatinine clearances from ureteral catheterization studies suggests that this noninvasive radionuclide technique may be able to replace invasive catheter studies for the determination of differential renal function. It may be possible to extend this technique to the measurement of absolute differential GFR.

EMERGENCY RADIONUCLIDE STUDIES IN ACUTE RENAL TRAUMA. H. Hekmat-Ravan, Richard T. Chopp and J. K. Siemsen, University of Southern California School of Medicine, Los Angeles, California, CA

The purpose of this study is to compare the sensitivity of renal radionuclide studies (RNS) with I.V. pyelography and angiography in renal trauma.

23 patients with suspected renal trauma were studied by these techniques in close time sequence. 20 mCi of Tc-99m Glucoheptonate were used for a "flow study" followed by immediate and 1 hour delayed imaging in posterior and oblique projections with large field cameras.

Of 16 cases of proven renal injury, 8 had definitely positive IVP, 15 had abnormal RNS and 15 abnormal angiograms. In only 6 of these did the angiogram provide additional information essential for patient management. If the RNS shows a peripheral lesion and the patient's condition is stable, or if the RNS is negative with an equivocal IVP, angiography does not appear to be necessary.

Of 7 patients who turned out to have no renal injury, IVP was definitely negative in 3, equivocal in 3 and positive in one. RNS were normal in 6 and abnormal in 1 case, showing diffuse underperfusion of one kidney immediately after angiography.

In 5 cases with gross evidence of injury on IVP and angiographic confirmation, RNS did not add essential information.

We conclude that RNS are useful in renal trauma evaluation and more sensitive than IVP. When they are used in conjunction with IVP as primary work-up, about 70% of unnecessary angiography may be avoided.

THURSDAY, JUNE 29 — SANTA ANA ROOM
3:15 p.m.-4:45 p.m.

BASIC SCIENCE

DATA PROCESSING I: MINI-SYMPOSIUM ON NUCLEAR MEDICINE IMAGE PROCESSING AND DISPLAY

Chairman: W. Gordon Monahan
Co-Chairman: Patrick T. Cahill

CONCEPTS IN DISPLAY TECHNIQUES--AN OVERVIEW. E. Lyons, Stanford Technical Program Corporation, Sunnyvale, CA.

CURRENT STATUS OF DISPLAYS IN NUCLEAR MEDICINE IMAGING. D. L. Kirch, V.A. Hospital, Denver, CO.

DIGITAL IMAGE PROCESSING TECHNIQUES. H. Andrews, Image Processing Laboratories, University of Southern California, Los Angeles, CA.

VISUAL PERCEPTION OF IMAGES. D. Fender, California Institute of Technology, Los Angeles, CA.

THURSDAY, JUNE 29 CALIFORNIA B ROOM
3:15 p.m.-4:45 p.m.

IN VITRO AND CORRELATIVE TECHNIQUES

RADIOASSAY IV

Chairman: Howard J. Dworkin
Co-Chairman: Danielle J. Battaglia

TUMOR RECEPTORS. S. Korenman, University of California, San Fernando Valley, San Fernando, CA.

GRANULOCYTE CHEMOTAXIS USING A RADIOASSAY OF LEUKOCYTES LABELED WITH INDIUM-111. R. E. Coleman, M. Portas, R. Beightol, M. Kitahara, W. Baker, H. R. Hill. University of Utah Medical Center, Salt Lake City, UT

The methods for measuring chemotaxis using Boyden chambers take significant time for staining and counting and have considerable variability. Chromium-51 labeled leukocytes have been used to overcome these problems but only a 6% labeling efficiency is obtained and elution of the radioactivity has been demonstrated. Leukocytes labeled with indium-111 oxine have little elution from the cells and the label has no demonstrable effect on viability. We have evaluated a method for studying granulocyte chemotaxis using leukocytes labeled with indium-111 oxine in the presence of plasma, saline or Medium 199.

The mean labeling efficiencies for the cells in plasma, saline and Medium 199 are 35%, 88% and 85% respectively. The percent activity associated with granulocytes averaged 64% by the Ficoll-Hypaque gradient technique with the average percent of granulocytes on differential counting being 63%. Chemotaxis is measured with a 5 micron pore size top filter on which the cells are deposited and an identical bottom filter closer to the chemoattractant bacterial factor (BF) or Medium 199 (random migration). Clear separation was obtained between random migration and chemotaxis toward BF with the leukocytes labeled in plasma, saline and Medium 199 with the best separation being the cells labeled in plasma. The results compare favorably with the visual method of determining granulocyte chemotaxis, and this technique eliminates many of the problems associated with the visual method.

COMPARISON OF ISOTOPIC AND CONVENTIONAL ASSAYS FOR DELAYED TYPE HYPERSENSITIVITY IN OLD AND YOUNG MICE. W.A. Baumgartner, T. Makinodan, and W.H. Blahd, Veterans Administration, Wadsworth Hospital Center, Los Angeles, CA.

The effectiveness of a recently developed isotopic method utilizing 5-{I-125}iodo-2'-deoxyuridine for the measurement of delayed type hypersensitivity (DTH) was compared to the conventional method based on the earswelling index. DTH was measured in young and old C57Bl6 mice (4-6 months vs 20-26 months) under conditions of normal health, Sendai virus infection, occurrence of spontaneous reticular cell sarcoma, and under the above conditions while being treated with an immunorestorative agent, mercaptoethanol. The DTH assay consists of sensitizing animals with dinitrofluorobenzene, followed by rechallenging in the left ear after 5 days. Fifteen hours later 2 μCi of 5-{I-125}iodo-2'-deoxyuridine are injected into the tail vein, followed after 24 hours by the determination of isotope content and swelling of the sensitized vs. the unsensitized ear. We found that the isotope-index is more sensitive than the earswelling index for detecting depressions in DTH due to advanced age (55% depression); Sendai virus infections (90% max. depression); and reticular cell sarcoma (75% depression). Reticular cell sarcomas were found with a frequency of 17% in the old mice. Depressions of DTH due to Sendai virus infection was found to be significantly greater in young animals than in old ones. Both the isotope and earswelling indeces were unaffected over a wide range of sensitizing doses (1.5 to .04mg) thereby reducing the possibility of accentuating differences in DTH between young and old animals. With the following regime of mercaptoethanol administration (0.5 mg/mouse, once a week for three weeks), it was possible to restore partially DTH only in virus infected animals.

NON-DESTRUCTIVE RADIOASSAY OF SPERM VIABILITY. A.H. Gobuty and W.J. Cameron, Kansas University Medical Center, Kansas City, KS.

We here present data on a radioassay of sperm viability in which [U C-14] D-Glucose (C-14 glucose) is consumed and [C-14] carbon dioxide is released and counted.

Sperm were collected from human donors in the usual way and their count per ml semen adjusted as required. One microcurie C-14 glucose in 0.1 ml was added to each 2 ml sterile, pyrogen-free vial used. The required number of sperm in 1.5 ml semen was then added. The vials were placed inside liquid scintillation vials previously lined with Whatman No. 42 filter paper impregnated with sodium hydroxide and 1,4-dioxane. The vials were capped, incubated, and the evolved [C-14] carbon dioxide was counted.

Counts from semen alone did not differ from background up to 24 hours. Semen incubated with viable sperm in the presence of C-14 glucose gave count rates of 690 ± 41 cpm at 1 hour, 4800 ± 310 cpm at 3 hours, and 98,210 ± 5601 cpm at 24 hours. At 24 hours semen, sperm and C-14 glucose gave 7410 ± 410 cpm at 25°C and 121,210 ± 5212 cpm at 37°C. At 3 hours counts from 1.0E 06 sperm were lower than counts from 5.0E 07 sperm (814 ± 22 cpm vs. 18,310 ± 3125 cpm). At 24 hours 1.0E 06 sperm have 14,250 ± 2101 cpm while 5.0E 07 sperm gave 269,410 ± 11,202 cpm. Counts from six 15 minute intervals demonstrated the reproducibility of this assay.

The data indicate that the count rate increases with the absolute number of viable sperm up to 24 hours. The count rate was lower with 25°C incubation than with 37°C incubation. This simple, non-destructive sperm viability assay permits sequential counts on the same sample and should prove useful in the evaluation of infertility.

THURSDAY, JUNE 29 CALIFORNIA A ROOM
3:15 p.m.-4:45 p.m.

CLINICAL PRACTICE

PULMONARY

Chairman: Victor J. H. Sharpe
Co-Chairman: Richard W. Meyers

REGIONAL LUNG FUNCTION IN BRONCHIECTASIS. R. Secker-Walker C. Tansuwan and J. Ho. St. Louis University School of Medicine, St. Louis, Mo.

There is little available information on the patterns of regional ventilation and blood flow found in patients with bronchiectasis. We have studied 10 patients with bronchiectasis, all of whom had bronchographic evidence of this condition. Regional ventilation was studied in the upright position during the 3-4 minute washin of Xe-133, and its subsequent washout, while breathing air. A four view perfusion scan was then performed using labeled macroaggregates or human albumin microspheres. Four patients were known to have bronchiectasis prior to the study. Four patients were thought to have pulmonary embolism, one a tumor and one bronchial asthma - but each was subsequently shown to have bronchiectasis. The findings in all the patients were remarkably similar. At the end of the washin the bronchiectatic regions contained very little Xe-133 compared to the rest of the lungs and the defects appeared segmental or lobar depending on the extent of the bronchiectasis. During the washout, there was prolonged retention of what little Xe-133 entered the region (perhaps through the bronchial circulation) which again conformed to the extent of the bronchiectasis. In 4 patients other regions

of less severely impaired ventilation were seen. The perfusion scans showed clearly defined defects in blood flow which corresponded to the bronchiectatic segments or lobes, and precisely matched the extent of the defects in ventilation. In conclusion, perfusion scans in bronchiectasis show absent pulmonary arterial blood flow to the affected region and thus mimic pulmonary embolism. A ventilation study shows that such regions have virtually no ventilation and thus present the appearance of lobar or segmental bronchial obstruction.

DETECTION OF UREMIC PULMONARY CALCIFICATION WITH BONE SCINTIGRAPHY. P. de Graaf, I.M.Schicht, E.K.J. Pauwels and J. de Graeff. University Hospital, Leiden, Holland.

The value of Tc-99m EHDP bone scintigraphy in detecting uremic pulmonary calcification was studied in 30 chronic dialysis patients. All patients had histologically proven renal osteodystrophy. Ca/PO_4 product was elevated in 60%, $Ca/Mg/PO_4$ product in 83%. Non-specific chest X-ray abnormalities were present in 3 patients. PO_2 values were within normal range. Using varying methods, ocular (63%), arterial (33%), periarticular (23%) and gastric (60%) calcification was found. Prior to scintigraphy, elevated background activity due to absence of renal radionuclide excretion was reduced with hemodialysis to levels found in normals. Scintigraphy was performed after 6 hr, chest and spine activity quantitated and the activity ratios calculated. Scintigraphic evidence of pulmonary calcification was found only in one patient and histologic proof of extensive calcifications was obtained. Although chest-to-spine activity ratios, compared to normals, were elevated in 66% of the patients, evidence of significant increased pulmonary radionuclide uptake could not be obtained, except for the patient with proven calcification.

The incidence of pulmonary calcification in dialysis patients is known from autopsy studies to be 60-70%. This serious complication is rarely diagnosed antemortem, due to absence or nonspecificity of X-ray abnormalities. This study suggests that uremic pulmonary calcification, with the exception of severe calcification, is not detected with bone seeking radionuclides either. This is probably due to the different crystalline and chemical composition of uremic pulmonary calcification, which is not hydroxyapatite but an amorphous compound with a high magnesium and pyrophosphate content.

IV INJECTED XENON-133 FOR DIAGNOSIS OF PULMONARY EMBOLISM (PE). M.L. Maayan, J. Eisenberg, E. Lopez, A. Kyriakakos, S. Majid and K. Pohutsky, VA Hospital and Downstate Medical Center, Bklyn, NY.

Performance of Xenon-133 ventilation scans, greatly enhancing the diagnostic accuracy of perfusion scans in PE, is hampered by the inability of a large number of patients to perform correctly the radioactive gas inhalation-retention step. The present study circumvents this problem by applying the Mishkin technique for washout studies to the early ventilation stages; namely, injecting 20 mCi Xenon-133 in a saline suspension IV with the patient breathing in a mask connected with a trap and recording the ventilation phase between 2 to 5 minutes after injection. Of 548 ventilation-perfusion lung studies in suspected PE over a 4 year period, 148 (27%) of cases had a positive diagnosis. Of these 9 (6.08%) died immediately or shortly after a PE and presented confirmatory autopsy findings. 12 (8.11%) had angiography, 11 with confirmatory results. 89 (60.14%) presented confirmatory serial lung scan changes. 12 (8.11%) had non-confirmatory serial lung scans. 17.56% were followed-up by clinical findings alone. Conclusion: This study suggests an alternative modality for performance of ventilation studies for diagnosis of PE yielding a positive correlation with the available pathology, angiography and clinical data.

ACCURACY OF CURRENT TECHNIQUES IN LUNG IMAGING FOR PULMONARY EMBOLISM. H.H.Lo, K.A.McKusick, H.W. Strauss, C.A. Athanasoulis, A.C. Waltman, A.J.Greenfield. Dept. of Radiology, Massachusetts General Hospital, Boston, MA.

Xe-133 ventilation imaging (V) can be performed immediately following Tc-99m-perfusion imaging (Q) on a routine basis. In order to assess the accuracy, sensitivity, and specificity of this technique, we compared a series of 27 patients with pre-Q ventilation studies (6/'75-12/'76),and an additional 58 patients with post-Q ventilation studies (1-9/'77), retrospectively. All patients underwent selective pulmonary arteriography, 79% within 24 hrs. and 94% within 48 hrs.

Perfusion imaging was performed on a large field of view camera with low energy parallel hole collimator,4mCi Tc-99m-Human Albumin Microspheres was injected with patients in supine position. All Q-images were obtained in upright position whenever possible, including the obliques. Pre-Q ventilation studies were done in posterior view only; post-Q ventilation studies were done with 10% window in projection(s) best delineated the defects. Single breath, equilibrium and washout data were obtained following inhalation of 20 mCi Xe-133. Two observers independently analyzed all V and Q studies without clinical history, chest radiograph or result of pulmonary arteriogram; and scored studies as negative, positive or indeterminate for pulmonary emboli. Results can be summarized as:

	Accuracy		Sensitivity		Specificity	
	Obs.1	Obs.2	Obs.1	Obs.2	Obs.1	Obs.2
Pre-Q	56%	41%	62%	71%	62%	54%
Post-Q	74%	78%	73%	82%	86%	91%

Post-Q ventilation studies resulted in increased certainty of diagnosis and specificity. The data thus indicated that V should preferably follow Q, which includes oblique views.

ASSESSMENT OF POSTOPERATIVE PULMONARY EMBOLISM BY SERIAL VENTILATION-PERFUSION SCINTIGRAPHY. I.T. Sakimura, L.D. Dorr, S. Lapin, J.K. Siemsen, and R.S. Rosen. Univ. of So. CA. and Rancho Los Amigos Hospital, Downey, CA.

Risk of pulmonary embolism (PE) following major surgery is recognized to be increased, but its reported incidence is widely variable.

Postoperative pulmonary embolism in 25 patients undergoing elective total hip arthroplasty (THA) and 24 primarily diabetic patients undergoing 25 amputation, bone graft or debridement of lower extremities was assessed by preop and postop follow-up perfusion and ventilation scintigraphy within 7 -10 days. Average age of each group was 54 and 59. Chest X-rays were available in all and pulmonary angiography in 3 patients. Two patients died postop and autopsy was obtained in one.

Scan criteria for high probability of pulmonary embolism were new postop perfusion defects without matching ventilation defects. Results are tabulated below:

PERFUSION SCAN	CHANGE	NO.PTS	INTERPRETATION
Normal pre and post	None	21	No PE
Abnormal pre and post	None	17	PE unlikely
Abnormal pre and post	Improved	6	PE unlikely
Abnormal pre, died post	?	1	Autopsy: No PE
Abnormal pre and post	New defects	2	1 PE (+ angio)
			1 CHF (died, stroke)
Normal pre, abnormal post	New defects	3	2 PE (1+ angio)
			1 No PE (+V,-angio)

The incidence of PE in the THA group was 1/25 or 4% and in the amputation group 2/25 or 8%. Note the high incidence of abnormal postop perfusion scans in this series (28/50). Variability in reported incidence of postop pulmonary embolism may in part be due to patient selection as well as specificity of the diagnostic tests used.

LUNGS AND LEGS. T. A. Verdon, Penrose Hospital, Colorado Springs, CO.

THURSDAY, JUNE 29 ANAHEIM ROOM
5:00 p.m.-5:30 p.m.

NUCLEAR PIONEER LECTURE HONORING BENEDICT CASSEN

LECTURER: Joseph F. Ross, UCLA School of Medicine, Los Angeles, CA.

THURSDAY, JUNE 29 SOUTH EXHIBITION HALL
8:00 p.m.-9:45 p.m.

CLINICAL SCIENCE

CARDIOVASCULAR IV: POSTER SESSION

Chairman: Heinrich R. Schelbert
Co-Chairman: David M. Shames

CLINICOPATHOLOGIC FINDINGS IN FIFTY-TWO PATIENTS STUDIED BY TECHNETIUM-99m STANNOUS PYROPHOSPHATE MYOCARDIAL SCINTIGRAPHY. R.W.Parkey, L.R.Poliner, L.M.Buja, F.J.Bonte, and J.T.Willerson. U. Texas Hlth. Sci. Ctr. at Dallas, TX.

Scintigraphic, clinical and pathological findings were correlated in 52 patients who had technetium-99m stannous pyrophosphate (Tc-99m PYP) myocardial scintigrams (Sc) prior to death or surgical resection of myocardium. A total of 59 clinical events were studied with Sc in the 52 patients; 41 of 59 were associated with one or more abnormal Sc and 18 with normal Sc. Sc were positive in 29 of 31 cases with clinicopathological evidence of a corresponding discrete, grossly obvious acute myocardial infarct (MI), including 16 of 16 transmural MI and 13 of 15 subendocardial MI. In 16 of 18 cases negative Sc correlated with the absence of acute MI as determined by clinicopathological evidence. In 2 cases small subendocardial MI (< 3 gms) were not detected by Sc. Of the 12 additional instances of positive Sc, 5 were associated with clinical unstable angina pectoris and 7 were in the category of persistently positive Sc since the scans were obtained 2½ months or longer after proven or suspected acute MI. In all 12 instances, the positive Sc were associated with evidence of multifocal irreversible myocardial damage consisting of myocytolysis, coagulation necrosis, and/or fibrosis, and the histological age of the lesions was compatible with acute injury corresponding to the time of Sc. The findings indicate that a positive Tc-99m Sc is a sensitive indicator of significant myocardial injury which may occur as confluent coagulation necrosis corresponding to clinical acute MI or as multifocal coagulation necrosis or myocytolysis associated with unstable angina pectoris or recurrent ischemic heart disease, especially after previous MI.

INFARCT INDUCED WALL MOTION ABNORMALITIES IN AORTOCORONARY BYPASS PATIENTS. E.G. DePuey, J.A. Burdine, P.H. Murphy, and R.J. Hall. Baylor College of Medicine, St. Luke's Episcopal Hospital, Clayton Foundation, Houston, TX.

Perioperative myocardial infarction (POMI) is suspected in approximately 10% of aortocoronary bypass (ACB) patients but the hemodynamic consequences are variable and frequently difficult to predict by enzymatic and electrocardiographic criteria. To determine the relationship between POMI and subsequent ventricular kinetic abnormalities, multigated cardiac blood pool scintigrams were obtained in 41 patients 7-12 days postoperatively and compared to preoperative contrast ventriculograms. Each of these patients had a clinical diagnosis of POMI based on signs and symptoms and the results of Tc-99m pyrophosphate (PYP) scans, serial ECG's, and serial cardiac enzyme studies. Five patients (12%) demonstrated no new regional wall motion changes (Group I); 9 (22%) demonstrated new areas of hypokinesis (Group II); and 24 (66%) exhibited new and more severe abnormalities including regional akinesis, dyskinesis, or aneurysm formation (Group III). No patient in Group I had a significant decrease in left ventricular ejection fraction (LVEF), 4 (44%) of Group II, and 15 (56%) of Group III sustained greater than a 20% decrease. No patient in Group I had greater than 2+ PYP myocardial uptake, whereas all patients in Group III had either 3+ or 4+ PYP uptakes. Interestingly, the degree of CPK elevation did not parallel the severity of regional or global wall motion changes. Due to normal perioperative changes, the ECG was often difficult to interpret and diagnostic in only 63% of these patients. It is concluded that POMI frequently results in significant changes in left ventricular kinetics. Of the standard techniques utilized, the PYP scan had the greatest predictive value.

PROGNOSTIC VALUE OF DOUGHNUT PATTERN Tc-99m PYROPHOSPHATE MYOCARDIAL UPTAKE IN ACUTE MYOCARDIAL INFARCTION. M. Ahmad, K.W. Logan, and R.H. Martin. VA Hospital and University Medical Center, Columbia, MO.

We followed 30 patients (pts) with acute myocardial infarction (MI) and positive Tc-99m pyrophosphate (Tc-99m PYP) myocardial scintigrams for a mean time of 25 months. None of the pts had previous MI and all survived the initial hospitalization. Development of angina, congestive failure, ventricular arrhythmias and recurrent MI were listed as complications. The intensity of uptake in all scintigrams was equal to or greater than the uptake in the sternum. Scintigrams were classified as Type A: localized uptake; Type B: doughnut pattern uptake; Type C: diffuse uptake. Data in various pt groups based on the type of scintigram are tabulated below:

Scintigram	# of pts	% Complications	% Mortality	Time+ to Death
Type A	16	50	6	14.0 mo.
" B	6	100	83	9.8 "
" C	8	12	0	---

+ Mean time post initial MI

The high complication and mortality rates in pts with a Type B scintigram were significant as compared to pts with Types A and C ($p<0.001$ Fisher's exact test).

These data indicate a poor long term prognosis for patients with acute myocardial infarction and a doughnut pattern Tc-99m pyrophosphate uptake.

Tl-201 VERSUS Tc-99m-ALBUMIN MICROSPHERES IN THE EVALUATION OF MYOCARDIAL PERFUSION IN ASYMPTOMATIC PATIENTS WITH ABNORMAL ECG'S AND NORMAL CORONARY ARTERIES. P.J. Ell, S. Joseph, R. Donaldson, P. Ross, I. Marcomichaelaidis, P. Taggart, E.S. Williams, W. Somerville. Departments of Nuclear Medicine and Cardiology, The Middlesex Hospital Medical School, London, UK.

A highly selective group of 9 patients were investigated with the following common features: (1) Asymptomatic pilots in active service (2) Abnormal rest electrocardiograms (3) Normal coronary arteries as judged by contrast coronary angiography and normal ventriculograms (4) Normal echocardiograms as judged by T-M mode ultrasonography.

All patients were submitted to a rest and stress Tl-201 perfusion study and a Tc-99m-microsphere coronary perfusion investigation. Accepted and standard doses of the radiopharmaceuticals were given, routine 3-projection Gamma Camera imaging was undertaken, and a standard protocol for the Tl-201 image during stress was followed.

5 out of 9 patients had a positive Tl-201 stress scan with a perfusion defect confirmed by the Tc-99m coronary microsphere study in 3 out of these 5 cases. In 3 cases the microsphere study was non contributory. All patients with abnormal ECG's reversed to normal after medication (β-blockade). This study highlights the sensitivity of Tl-201 stress imaging in the detection of ischaemic heart disease in a group of patients where the expected incidence of this disease is very low. Transient ischaemia during stress is the most likely cause for the observed results.

COMPARISON OF DEFECT DETECTION ON UNGATED VS. GATED THALLIUM-201 CARDIAC IMAGES. K.A. McKusick, J. Bingham, G. Pohost, and H.W. Strauss. Massachusetts General Hospital, Boston, MA.

End-diastolic Tl-201 cardiac images should be of higher resolution than ungated images, because of edge blurring and loss of contrast normally induced by cardiac contraction. An ECG-gating device which provides simultaneous end-diastolic, end-systolic and ungated intensity corrected images from a gamma camera scope was evaluated on studies performed on fifteen patients undergoing exercise stress testing.

Following injection of 2mCi of Tl-201 at peak exercise, six sequential 7 minute (approximately 300K full field) anterior and 50 degree and 70 degree LAO projection images were obtained with the gate set for a window of 190 msec for end-systole, and a variable end-diastolic window which covered the slow phase of ventricular filling. Recording was on 70mm film from a high resolution gamma camera, utilizing a 35% window around the Hg-K x-ray peak, and a low energy parallel hole collimator. The heart was divided into three segments on each projection, and each segment analyzed for the presence of a defect or for wall thinning. In total, 270 segments were evaluated individually for abnormalities on the ungated, end-diastolic and end-systolic images. Total segments concluded abnormal were as follows: ungated, 58; end-diastolic, 64; end-systolic, 13. Inadequate end-diastolic count rates were obtained in two patients who had rapid heart rates, and hence, shortened end-diastolic intervals. End-diastolic images tended to provide improved edge detection, increased apparent wall thinning, and certainty of defect detection; but, no defect was seen on gated images, not first appreciated on ungated images.

THALLIUM-201 REDISTRIBUTION AFTER TRANSIENT MYOCARDIAL ISCHEMIA IN DOGS. G.A. Beller, D.D. Watson, J.F. Irving, and G.M. Pohost. University of Virginia Hospital, Charlottesville, VA, and Massachusetts General Hospital, Boston, MA.

Diminished myocardial uptake of thallium-201 (Tl) has been observed clinically with administration of the tracer during exercise-induced malperfusion, spontaneous angina, or at rest in patients with coronary artery disease. Those defects which fill in with Tl activity over time may represent viable but underperfused or transiently ischemia areas. The mechanism for this redistribution (RD) phenomenon was investigated in 21 anesthetized dogs receiving 1.5 mCi of Tl intravenously 10 min after occlusion (occl) of the left anterior descending coronary artery. Coronary reperfusion (RP) was accomplished 10 min after Tl administration. Transmural biopsies were obtained in situ from normal (N) and ischemic (IS) regions during occl and 5 min (n=4), 20 min (n=8), 4 hr (n=5) and 6 hr (n=4) after RP. Tl activity (counts/10 min/mg) was 14±6% of N in the IS zone during occl and increased to 25±5% ($P<0.05$) in dogs undergoing 5 min of RP. In the 20 min group, Tl activity increased from 12±3% of N during occlusion to 43±6% ($P<0.001$) after RP. In the 4 hr group, Tl activity in the IS zone increased from 19±4% of N during occl to 77±6% ($P<0.001$) after RP. In dogs undergoing 6 hr of RP, Tl activity increased from 25±4% of N to 86±4% ($P<0.001$). In the 4 and 6 hr groups activity in the N zone decreased by 24±9% and 37±6%, respectively, indicating the magnitude of Tl washout during the post-ischemic period. These findings indicate that the mechanism for resolution of myocardial defects in Tl uptake over time is related to both early redistribution of Tl into ischemic zones and more rapid washout from normally perfused areas.

CORRELATION IN THE DIAGNOSIS OF INFARCTION BY THALLIUM, ECG AND ANGIOGRAPHY WITH THE SURGICAL FINDINGS. J. Leppo, T. Yipintsoi, R. Bontemps and L. M. Freeman. Montefiore Hospital-Albert Einstein College of Medicine, Bronx, NY.

The use of Thallium 201 (Tl) imaging post-exercise to identify areas of myocardial ischemia and infarct has been compared to ECG and cardiac angiography. 24 pts. with angina and triple (20) and double (4) vessel coronary disease (>70% stenosis) were studied before coronary bypass surgery. Tl was given IV at peak exercise and followed by Anger camera imaging within 10 minutes and at 4 hours. Perfusion defects on the post-stress scan that disappeared after 4 hours were termed ischemic, while defects persisting 4 hours were termed infarction. Epicardial scars were verified independently at surgery in Group I and were absent in Group II. Tl demonstrated better sensitivity for infarction in Group I than ECG and angio.

	ECG		Angio	Thallium	
	Qwaves	+ Ex. Test	Akinesis	Ischemia	Infarct
Gr. I(15)	6	12	8	12	15
Gr. II(9)	1	9	1	8	5

Since intramural damage can occur without surface scars, specificity cannot be assessed. The combination of Tl ischemia and infarction in the same area did not lessen the accuracy of scar detection. 19 of 20 Tl infarcts involved the inferior-apical region, suggesting that this area is particularly vulnerable in pts. with multiple proximal stenotic arteries. Conclusion: The observation of persistent Tl perfusion defects is frequently associated with epicardial scars even without corroboration by ECG or angio.

OPERATING POSITION ON THALLIUM-201 MYOCARDIAL PERFUSION IMAGING (TMPI) RECEIVER OPERATING CHARACTERISTIC (ROC) CURVE FOR SELECTION OF PATIENTS FOR CORONARY ARTERIOGRAPHY (CA). M.L. Nusynowitz, R.E. Sonnemaker, J.L. Floyd. William Beaumont Army Medical Center, El Paso, TX and The University of Texas Health Science Center, San Antonio, TX.

Selection of patients with suspected ischemia-producing coronary artery disease (CAD) for CA using stress electrocardiography (ECG) is not wholly satisfactory because many series show that at the prevalence of CAD in the population undergoing study, the negative predictive value P(D-/T-) of stress ECG (proportion of patients without disease with a negative test) is low. TMPI is being extensively evaluated for its utility in the selection process. Our TMPI studies in 36 patients undergoing CA were interpreted using a lesion enhancement technic, with resultant sensitivity = 100% and specificity = 56%. Analysis of 5 reported series showed sensitivities of 59-93% and specificities of 71-100%. Prevalence of CAD in all 6 series was remarkably similar (mean = 75%, range = 68-78%). Bayesian analysis at this prevalence showed positive predictive values P(D+/T+) ranging from 87-100% and negative predictive values P(D-/T-) varying from 45-100%. Sensitivity and specificity data from the 6 series allowed construction of a ROC curve. Qualitative cost estimates, prevalence data, and information content analysis of the operating positions on the ROC curve all indicated the use of an operating position where sensitivity and negative predictive value are highest for maximum test utility. The lesion enhancement technic employed produces an operating position in this range, and a normal TMPI study based on this operating position results in effectively ruling out significant CAD and eliminating unnecessary CA.

MYOCARDIAL UPTAKE OF THALLIUM-201 FOR ESTIMATION OF RIGHT VENTRICULAR PRESSURES. Keith C. Fischer, Marlene Rabinovitch, and S. Treves. Children's Hospital Medical Center and Harvard Medical School, Boston, MA.

This study was undertaken to determine if measurement of the myocardial accumulation of Tl-201 could predict the right ventricular pressure in patients with congenital heart disease (CHD). Initial laboratory studies using chronically hypoxic rats with right ventricular (RV) hypertrophy showed a high degree of correlation ($r = 0.969$) between directly measured ventricular activity and mass ratios. This link between muscle mass and Tl-201 activity having been established, we proceeded to clinical trials. Six patients with CHD (age 4-30 years) with varying levels of RV peak systolic pressures (PSP) (range 27-128 mm Hg) had Tl-201 myocardial scintigraphy at the time of cardiac catheterization. Each patient received 30 μCi/kg. Tl-201 IV at rest and imaging was begun immediately in the 45 degree LAO pos-

ition for 500 k counts in a computer. Regions of interest that included each ventricle and background areas were selected and a simple program calculated accumulated activities in each ventricle as a percentage of the injected dose. There was a good correlation between level of RV PSP and percentage of Tl-201 RV uptake ($r = 0.91$, $p < 0.01$). Our results in the laboratory and clinic indicate that this technique may be a reliable, non-invasive method for determining right ventricular pressure in certain patients.

ACCURACY OF LEFT VENTRICULAR END-DIASTOLIC VOLUME DETERMINATIONS USING FIRST PASS RADIONUCLIDE TECHNIQUE. S.K. Rerych, P.A.W. Anderson, P.M. Scholz, G.E. Newman, R.H. Jones. Duke University Medical Center, Durham, NC.

This investigation compared the accuracy of left ventricular end-diastolic volume obtained with biplane cine angiography to planimetry of radionuclide end-diastolic volume images in 33 patients. In addition, 20 studies were performed in conscious dogs with implanted endocardial sonar crystals in the minor axis of the left ventricle. All measurements were performed in the anterior projection using the first pass technique. Counts were obtained at 50 msec intervals using a Baird-Atomic System 77 gamma camera. Twenty-five millicuries of technetium-99m pertechnetate were used in all patients. Dogs were given doses ranging from 6.9 to 25 mCi. The appropriate activity level and activity range for edge detection was determined for each collimator by ellipsoid phantoms of known volume. The length area relationship implied by the prolated ellipsoid model was used in all studies. The correlation coefficient of 0.89 was obtained in the 33 patient studies. A comparison of minor axis dimensions and end-diastolic volumes in 20 dog studies revealed a correlation coefficient of 0.92 and 0.95 respectively. This study demonstrates the accuracy of end-diastolic volume determinations obtained with radionuclide angiocardiography.

APPLICATION OF RADIONUCLIDE LEFT VENTRICULAR SYSTOLIC EJECTION RATE (dV/dt). J.A. Bianco, D.G. Makey, and R.B. Shafer. V.A. Hospital, Nuclear Medicine Service, Minneapolis, MN.

Although a relationship between radionuclide left ventricular ejection fraction and dV/dt has been shown by radionuclide angiocardiography, the overall relevancy of left ventricular dV/dt at present remains tentative. Radionuclide left ventricular dV/dt was determined in a prospective series of 10 normal subjects and 21 patients with ischemic heart disease. Left ventricular ejection fraction and left ventricular dV/dt were computed by multiple gating of the cardiac blood-pool. The range of left ventricular ejection fractions for the series was 6-88%. The correlation between radionuclide and angiographic left ventricular ejection fraction was 0.82 ($n = 24$). The correlations between peak and average radionuclide left ventricular dV/dt normalized to end-diastolic counts, and radionuclide left ventricular ejection fraction were 0.90 and 0.92 ($n = 31$). Analysis of the data demonstrates that the usefulness of these derived indexes of ventricular systole is independent of heart rate, aortic pressure and diastolic volume. Left ventricular ejection fraction and left ventricular dV/dt equally reflect the basal contractile state of the left ventricle. Peak and/or mean radionuclide dV/dt offer comparable information. Findings will be discussed relative to observed responses of left ventricular ejection fraction and dV/dt to inotropic interventions.

QUANTITATIVE ANALYSIS OF CARDIAC WALL MOTION AND SELF-ABSORPTION EFFECTS IN DETERMINING EJECTION FRACTIONS. K. W. Logan, R. R. Hurst, R. A. Holmes. V. A. Hospital, Columbia, MO.

The limitations of accurately diagnosing ventricular wall motion and ejection fractions using radiopharmaceuticals, the gamma scintillation camera and a dedicated computer are due to problems of sensitivity, resolution and the apparent negative effects of self-absorption on the cardiac image. To quantitate the finite detection of ventricular wall motion and the effect of intra-cardiac radionuclide self-absorption on determining ejection fractions a multipurpose mechanical heart model called DUHMY (Diagnostic Universal Heart Model You'all) was constructed Precise wall motion and change of ventricular volume were determined by imaging the synchronized balloon expansion with different collimators (high resolution and high sensitivity) and analyzing the data with the computer using various pixel sizes. The high sensitivity collimator gave superior qualitative images compared to the high resolution collimator for typical count-rates and sampling times. In the assessment of pixel size both the 2 and 4mm pixels showed good resolution for detecting 2mm wall excursions.

Varying path lengths (blood pool depth) and ventricular volumes showed little change in the accuracy of determining ejection fractions even when the simulated ventricular volume was well over 200 ml. Apparent intra-cardiac absorption loses previously reported were not observed at low count rates. Our conclusions include the following: a) In determining ventricular wall motion, increased sensitivity is the primary determinate. b) Optimum pixel size for wall motion determination is 2 to 4 mm. c) Self-absorption within large ventricles is insignificant for ejection fraction measurement.

QUANTITATIVE SEGMENTAL WALL MOTION ANALYSIS OF GATED BLOOD POOL IMAGES. J. W. Verba, V. Bhargava, N. P. Alazraki, A. Taylor, I. Bornstein. Veterans Administration Hospital, San Diego and University of California, San Diego, CA.

Many authors have reported techniques for obtaining volume curves from equilibrium blood pool imaging and multiple images throughout the cardiac cycle for the subjective interpretation of wall motion. Computer filtering and edge definition programs improve accurate boundary determination. However, to define and evaluate the wall motion for entire ventricle requires multiple projections and in some views the ventricle is masked by overlying cardiac structures. To circumvent these problems we have developed a computer program for the quantitative evaluation of segmental motion based on the number of counts in a 15 degree segment of an isolated left ventricle. Proper handling of the background and the effects of the left atrium are critical. Not only the magnitude, but an estimate of the detailed distribution across the ventricular silhouette is obtained by using the distribution of counts around the ventricle and the point spread function of various gamma cameras. The resulting background is subtracted from the raw data giving a very symmetric and very clean ventricular count distribution. The images are segmented and the segmental counts used to produce a picture of the average wall motion, quantitative numbers on the percent change in radius and the ejection fraction of each 15 degree segment. Global ejection fractions are also calculated and atrial contributions estimated.

The program requires a minimum amount of operator intervention and as a result is very reproducible. The program runs on a small nuclear medicine type computer in a very reasonable amount of time. Preliminary results on 10 patients studied with drug interventions will be presented.

REGIONAL MYOCARDIAL BLOOD FLOW IN MAN DURING CONTRAST INDUCED HYPEREMIA. Samir E. Alam, Marvin I. Friedman, Harvey G. Kemp, and Richard N. Pierson, Jr., St. Luke's Hospital Center, Columbia University, NYC, NY.

The need for quantitative assessment of the functional significance of coronary artery obstructions has become more compelling in light of the widely recognized lack of reproducibility in interpreting angiographic data. 133-Xenon measurement of resting myocardial blood flow (MBF) has not served this need because of the significant overlap between normal and diseased states. In 23 patients undergoing coronary arteriography, intracoronary injections of 133-Xenon (both in saline, and mixed with and flushed with Renografin 76) provided measurements of MBF at rest and during contrast induced hyperemia.

An Anger gamma camera/minicomputer was used to collect and analyze data in 2 sec intervals during the first 40 sec of washout from pixcels approximately 1.0 cm^2. MBF was averaged in the regions supplied by the proximal and distal left anterior descending and circumflex arteries, and was analyzed in conjunction with the extent of the lesion and the segmental wall motion (SWM).

Regional MBF, measured in 73 segments, was grouped as follows:

	CAD	SWM	n	Control	Hyperemic Response
I	None	Normal	36	69 ± 14	148 ± 30
II	<50%	Normal	9	62 ± 15	*111 ± 41
III	<75%	Normal	18	59 ± 12	*100 ± 30
IV	>75%	Abnormal	10	*45 ± 9	* 76 ± 17

There was significant reduction (* $p<.01$) in MBF during contrast induced hyperemia in the presence of obstructive coronary artery disease (CAD), particularly when associated with contraction abnormalities.

Regional MBF is reduced in CAD in relation to severity, as graded by coronary narrowing and SWM abnormality. Hyperemic response to an intracoronary contrast injection increases the sensitivity of MBF measurement to disclose CAD, and provides an assessment of the functional significance of obstructive CAD.

NONINVASIVE ESTIMATION OF PULMONARY ARTERIAL PRESSURE (Pa) BY ANALYSIS OF PULMONARY BLOOD FLOW DISTRIBUTION (PBFD). M.A. Konstam, H.W. Strauss, N. Alpert, S. Miller, R.X. Murphy, and K.A. McKusick. Massachusetts General Hospital, Boston, MA.

To determine whether a correlation exists between Pa and PBFD, PBFD was measured in upright dogs before and during infusion of epinephrine and prostaglandin F2α (PGF2α). Four dogs were placed upright in front of a scintilation camera, and Pa was monitored with a Swan-Ganz catheter. During suspension of respiration, 15mCi of Xe-133 were injected intravenously, and a 30 second lung perfusion image was recorded. After one minute of rebreathing, an equilibration image was obtained. Following a recovery period epinephrine or PGF2α was infused at a rate sufficient to increase Pa by 5 to 50 cm H20, at which time Xe injection and imaging were repeated. The procedure was performed multiple times on each dog, using varying infusion rates of epinephrine or PGF2α. A slice profile of each scan was obtained in the long axis of the lungs, yielding a plot of relative blood flow per unit lung volume (RBF) vs. distance above the hilum (h, cm). Pa was derived from each curve, assuming the relation $Pa = \sqrt{RBF/B} + Dh$ where B= constant and D= specific gravity of blood. Calculated Pa correlated strongly with measured Pa (R=β0). Our findings suggest that upright injection of Xe-133 and analysis of the distribution of pulmonary blood flow may be used to determine Pa in humans.

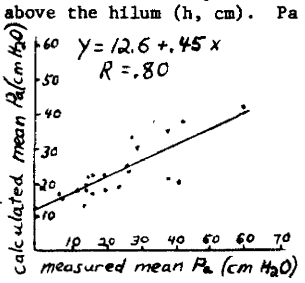

FRIDAY, JUNE 30, 1978

FRIDAY, JUNE 30 — GARDEN GROVE ROOM
8:30 a.m.-10:00 a.m.

CONTINUING EDUCATION

HIGHLIGHTS OF THE SCIENTIFIC SESSIONS: A REVIEW OF SELECTED SCIENTIFIC PAPERS PRESENTED DURING THE COURSE OF THE MEETING WITH AN EMPHASIS ON NEW AND INNOVATIVE APPLICATIONS

RAPPORTEUR: Henry N. Wagner, Jr., The Johns Hopkins Medical Institutions, Baltimore, MD.

FRIDAY, JUNE 30 — ANAHEIM ROOM
8:30 a.m.-10:00 a.m.

CLINICAL SCIENCE

PULMONARY II

Chairman: Naomi P. Alazraki
Co-Chairman: Edgar L. Suprenant

TOMOGRAPHIC IMAGING OF REGIONAL LUNG DENSITY BY COMPTON SCATTER: CLINICAL EVALUATION. M. Pistolesi, S. Solfanelli, R. Guzzardi, M. Mey, and C. Giuntini. CNR Clinical Physiology and 2nd Medical Clinic University of Pisa, Pisa, Italy.

The purpose of this study was to evaluate the performance of Compton scatter tomograms in detecting regional lung density changes due to pathologic processes. Lung visualization according to density is obtained employing a collimated linear source (3 mm id glass tube, 80 cm long, containing 1.5 Ci of Hg-203) and a gamma camera to detect scattering at 90° of primary gamma rays (279 KeV). Imaging 90° scattered rays (180 KeV) provides a view of the anatomical cross-section corresponding to the path of the primary rays through chest tissues. Frontal and sagittal lung tomographic views are obtained in 3 to 5 min at the spatial resolution of the camera, with tissue density discrimination of 10% on the average. The radiation dose is 0.09 rads for each view. We performed 41 studies in patients with various lung disorders. When the lung density was either reduced such as in emphysema or increased such as in pulmonary edema, the technic visualized density changes over the entire lung. In patients with focal lesions such as bullous emphysema, lung tumor, pneumonia, interstitial fibrosis and localized effusion, the technic provides images comparable to those of x-ray tomography but with better visualization of the lung structures surrounding the lesion. This may be of interest for patients who undergo surgery. The low radiation dose permits application in children and monitoring of lung edema in cardiac patients.

QUANTITATIVE ANALYSIS OF Xe-133 WASHOUT IN ACUTE INHALATION INJURIES: AN ANIMAL MODEL. **R.J. Lull, G.W. Welch. Brooke Army Medical Center, San Antonio, TX.**

Xe-133 ventilation washout studies in burn patients provide accurate diagnosis of inhalation injury in its earliest stages, often 2-4 days before changes on physical examination or x-ray. Such early diagnosis enables initiation of therapy before onset of clinically apparent disease. The purpose of this investigation was to develop an animal

model of inhalation injury that could measure the effect of early therapeutic measures on the developing lung lesions.

Typical pulmonary changes of inhalation injury were consistently produced in anesthetized goats by injecting 60 ml nitrogen tetroxide gas down an endotracheal tube. Baseline and post-injury intravenous Xe-133 pulmonary washout studies were performed on 4 control animals and 4 animals treated with intravenous steroids (500 mg methylprednisolone at 1, 6, and 12 hours post-injury). All animals developed regional Xe-133 retention after nitrogen tetroxide. The area under the time-activity washout curve for both lungs was used to quantitate Xe-133 retention severity. When individual components of the biexponential washout curves were analized, the area under the slow component was the most sensitive indicator of early inhalation injury. The fast component showed accelerated Xe-133 clearance after injury, probably due to hyperventilation.

The steroid treated group had significantly greater Xe-133 retention than control animals ($p < 0.05$). Thus, steroid therapy seemed to worsen the obstructive changes typical of early inhalation injury.

Quantitative analysis of slow component changes in Xe-133 washout can provide a useful method for monitoring therapy of acute inhalation injury.

REGIONAL VENTILATION STUDIED WITH KR-81M IN ILLINOIS COAL WORKERS. R. Secker-Walker, A. Friedman, P.Sanjabi, J. Fletcher, L. Mayron, J. Gindler, E. Kaplan, R. Donati. St. Louis University, St. Louis, Mo., Hines V.A. Hospital, Hines, Il. and Argonne National Laboratories, Argonne, Il.

The inhalation of Kr-81m provides a unique way of examining regional ventilation during tidal breathing, because the distribution of activity is proportional to the regional exchange of air. We have studied regional ventilation using Kr-81m in 14 coal workers receiving Black Lung compensation. Rb-81m generators were made at the Argonne National Laboratories and flown to Marion V.A. Hospital in Illinois. The studies were performed in the upright position during tidal breathing, and recorded by a digital computer interfaced to the gamma camera. The digitized images were transmitted via the V.A. computer network to St. Louis for analysis. The abnormalities seen in regional ventilation have been compared to the occupational history, pulmonary function tests and chest radiographs. Increasingly abnormal regional ventilation was directly related to: 1) increased residual volume, 2) greater reductions in forced vital capacity, (FVC), forced expiratory volume in one second (FEV1), FEV1/FVC ratio , maximum mid flow rate and maximum voluntary ventilation, 3) increasing pack-years of smoking. Eight chest radiographs showed evidence of emphysema, but only 4 showed a few nodular opacities.

In general those coal miners who smoked the most had worked the least time in mines, so that there was an inverse relationship between the severity of the abnormalities of regional ventilation and the length of time spent working with coal. We conclude that in these coal miners cigarette smoking is a more important cause of regional pulmonary dysfunction than working with coal.

REGIONAL VENTILATION-PERFUSION RELATIONSHIPS STUDIED WITH KR-81M. R. Secker-Walker, A. Friedman, P. Sanjabi, J. Fletcher, L. Mayron, J. Gindler, E. Kaplan, R. Donati. St. Louis University, St. Louis, Mo., Hines V.A. Hospital, Hines, Il. and Argonne National Laboratories, Argonne, Il.

We have studied regional ventilation-perfusion relationships in ten coal miners who had blood gas analyses and pulmonary function tests. Images of regional ventilation were made in the 4 standard projections while breathing Kr-81m in the upright position. Images of regional perfusion were made in the same projections, following the administration of Tc-99m HAM. The regional relationship of ventilation ($\dot{V}$) to blood flow ($\dot{Q}$) was determined by visual inspection of the ventilation and perfusion images, without knowledge of the blood gas analyses. These results were then compared to the calculated alveolar-arterial oxygen tension differences (PA-aO2). Two miners had normal ventilation and perfusion images, but increased PA-aO2 of 34 and 39 mmHg. One was 36 Kg. overweight. The other was obese and in mild congestive heart failure. Three miners with abnormal regional function, had either matched abnormalities of $\dot{V}$ and $\dot{Q}$ or regions in their upper lobes with high $\dot{V}/\dot{Q}$ ratios. Their PA-aO2 were normal at 10, 11 and 12 mmHg. Five miners had low $\dot{V}/\dot{Q}$ regions in their lower lobes, two also had low $\dot{V}/\dot{Q}$ regions in the upper lobes and two had high $\dot{V}/\dot{Q}$ regions in their upper lobes. Their PA-aO2 ranged from 18 to 55 mmHg. The two greatest differences, 54 and 55 mmHg., were seen in two more obese subjects. We conclude that a visual comparison of Kr-81m ventilation and Tc-99m HAM perfusion images is a sensitive method of recognizing altered ventilation-perfusion relationships, but that the magnitude of the resulting PA-aO2 is underestimated in obese subjects.

THE USE OF Kr-81m LUNG VENTILATION STUDIES FOR THE DIAGNOSIS OF PULMONARY EMBOLI: A REVIEW OF 156 CASES. M.L. Goris and S. G. Daspit. Stanford University Medical Center, Stanford, CA.

The role of ventilation studies in the diagnosis of pulmonary embolism has been defined by B. McNeil (J Nucl Med 17: 613, 1976) using Xenon-133 for the ventilation study: the combined perfusion-ventilation study should be judged according to the size of the defects (SL = segmental or lobar, SS = subsegmental) and the ventilation in corresponding sites (UU = all perfusion defects unmatched by ventilation defects, MU = mixed pattern, MM = all matched). Of the 6 possible outcomes only 3 are diagnostic (SLMM, SSMM, SLUU). The value of the study depends on the prevalence of each outcome. Using Kr-81m, we found our results to correspond in general, except that the category SSUU seems equally diagnostic, and that the prevalence of this category is low. Of the 156 studies, only 23 were considered unequivocally normal in the perfusion study. The remaining 133 were distributed as follows: SLMM = 38%, SSMM = 31%, SLMU = 6%, SSMU = 7%, SLUU = 12%, SSUU = 5%. The frequency of positive pulmonary angiographies in each category is shown in the table:

	MM	MU	UU
SL	0/7	1/2	5/5
SS	0/5	-	2/2

Our results seem to indicate that small ventilatory abnormalities are missed with the usual Xe-133 technique but not with Kr-81m, and that the diagnostic specificity of the UU cases is high (larger than 65% at $p = 0.05$).

Failure to perform the ventilation study and the exclusive use of defect size as discriminating characteristic would have reduced the specificity to less than 50% and the sensitivity to less than 95%.

RAPID DYNAMIC VENTILATION IMAGING WITH KRYPTON-81m. P.M. Johnson, N.M.T. Braun, N.A. Skultety, and P.D. Esser. College of Physicians and Surgeons, Columbia University, New York, NY.

The use of Krypton-81m gas in millicurie doses for pulmonary ventilation studies permits rapid dynamic imaging.

Eight normal volunteers and 20 patients with pulmonary diseases including embolism, chronic obstructive disease, carcinoma, fibrosis and sarcoidosis were examined, seated, using a scintillation camera interfaced to an MDS computer. The Rb-81/Kr-81m generator outlet was secured to a mouthpiece inlet. Air was pumped through the generator at rates of 8.5 or 15 ml/min, delivering 10-20 mCi/min of Kr-81m admixed with inspired air. Serial posterior images were obtained at the rate of 1 or 2/sec for 90 sec; Kr-81m flow was stopped after 60 sec. Analog images (200 K/view) during equilibration, perfusion images and chest x-ray were obtained.

Time-activity curves were generated for both lungs together. Multiple images during peak inspiration and expiration were summed separately and subtracted to yield a "difference" image which displayed dynamic regional ventilatory excursion. Well-ventilated areas were indicated by larger excursions.

Normals showed homogeneous perfusion and ventilation with maximum ventilatory excursions at the bases. Patients showed variabilities depending on the disease state. A

positive perfusion scan could be rapidly assessed by an immediate ventilation study. Further analysis of the "difference" image may yield a semiquantitative index of ventilation abnormality in patients with abnormal gas exchange. Such an index may have potential value in planning for pulmonary surgery and evaluating physiotherapy.

COMPARISON OF GALLIUM, VENTILATION AND PERFUSION SCANNING WITH CHEST X-RAY AND PULMONARY FUNCTION TESTS IN SARCOIDOSIS. B.R. Line, J.D. Fulmer, J.S. Nagel, A.E. Jones, and R.G. Crystal. National Institutes of Health, Bethesda, MD.

Sarcoidosis, a disease with protean manifestations, involves the lung more commonly than any other organ. Although classical staging of disease severity relies on chest x-rays (CXR) and clinical findings, these standards often show poor correlation with tests of lung function. In 19 patients with biopsy proven sarcoidosis, we have compared Gallium-67 evidence of disease activity, Xenon-127 evidence of airway or alveolar ventilatory dysfunction, and Tc-99m MAA perfusion scan evidence of capillary disease with routine CXR and pulmonary function tests (PFT). Scans and the CXR were graded on a scale of 0 to 3, according to the presence of thoracic nodal disease (ND) and parenchymal disease (PD) (0: no disease; 1: ND only; 2: ND and PD; 3: PD only). Perfusion scans with abnormal hilar prominence were interpreted as showing ND, and abnormal airway resistance or alveolar compliance as indicated by ventilation scan washout delay was considered evidence of parenchymal disease. Grading results (patients in each group) for CXR (4,2,9,4), gallium (4,0,13,2), ventilation (3,0,0,16) and perfusion (2,0,13,4) studies, indicated greater scan sensitivity for PD. Standard PFT measurements failed to show a significant rank correlation with CXR, ventilation, or perfusion scan grade. The gallium scan grade, however, correlated with total lung capacity ($p<.005$), vital capacity ($p<.05$), functional residual capacity ($p=.001$), and carbon monoxide diffusing capacity ($p<.05$). These studies suggest that assessment of regional ventilation or perfusion dysfunction is an important complement to CXR structural information; and that grading of gallium scans most accurately reflects physiological severity as indicated by PFT.

REGIONAL VENTILATORY CLEARANCE TIME: VALIDATION STUDIES IN IDIOPATHIC PULMONARY FIBROSIS. B.R. Line, A.E. Jones, J.J. Bailey, R.G. Crystal, and J.D. Fulmer. NIH, Bethesda, MD.

Delay of xenon clearance in washout images is widely used as a qualitative indicator of ventilatory dysfunction. Because regional lung volume and image intensity can affect detection accuracy, we present a procedure which provides images and quantitative estimates of regional clearance time constants (CTC).

Idiopathic pulmonary fibrosis (IPF) is a disease of alveoli and small airways. Frequency dependence of dynamic compliance (FCdyn), when present, has been shown to accurately predict small airways abnormalities in IPF. To test the CTC procedure sensitivity, 13 patients with IPF were studied who had normal large airways by standard pulmonary function tests. Each patient was studied with lung biopsy (8/13 patients with >50% airways >50% narrowed), dynamic compliance measurements (8/13 with FCdyn), and Xenon-127 washout scans. Regional clearance time was determined during tidal respiration, in both IPF patients and in 17 non-pulmonary disease controls, by fitting a single exponential equation to washout curves associated with each of 1200 posterior lung locations. A plot of the total lung volume associated with each clearance time was produced. The standard deviation (SD) of this plot was used to estimate the homogeneity of pulmonary clearance times. The SD separated IPF patients from controls ($p<.02$) and, in the IPF group, was significantly higher in patients with FCdyn ($p<.05$). Further, the IPF patients with a SD greater than 12 seconds showed both significant (Chi square) FCdyn ($p<.005$), and airways narrowing ($p=.05$). This data suggests that this regional CTC procedure can detect small airways disease in IPF, and therefore should be valuable in other patients to quantitate ventilatory dysfunction.

COMPARISON OF METHODS FOR IMAGING REGIONAL VENTILATION. P.O. Alderson, H. Lee, W. Summer, A. Motazedi, P. Rigo, K. Stolz, J. Gomez, and H.N. Wagner, Jr., Johns Hopkins Medical Institutions, Baltimore, Md.

The optimal tracer gas and breathing maneuvers for imaging regional ventilation have not been determined. Posterior Xe-133 ventilation (V) studies were performed prior to Tc-99m microsphere perfusion (P) imaging in 150 patients. Each patient had a single breath (SB) study and equilibrium image, plus early (5 sec images x 12) and late (60 sec images x 7) washout studies. Fifty of these patients had standard spirometry. Twenty additional patients with spirometry had Xe-127 V studies and multiple-view Kr-81m V studies. In the posterior Xe-133 studies the T1/2 of early washout correlated significantly with Fev 1.0% ($r=0.50$, $p < 0.01$). The late washout provided the only evidence of V abnormalities matching P defects in 42% of patients. The SB image provided similar information in 5% of patients, and the equilibrium phase in 3%. Other V defects were seen in at least two phases of the study. Multiple-view Kr-81m studies provided evidence for V defects matching each P defect in 20 patients. However, Kr-81m V studies were normal in 2 of 3 patients who had mild airways obstruction by spirometry; Xe-127 studies showed uneven ventilation and retention in late washout. Kr-81m studies were abnormal in all other patients with obstruction (O) or restrictive (R) lung disease, but could not distinguish O from R. Xe-127 clearly distinguished patients with O from others. Kr-81m provides excellent information about V-P matching, while Xe-127 is a sensitive detector of airway obstruction. Xe-127 or Xe-133 studies should include both a SB and late washout phase to maximize detection of regional airways disease.

UTILITY OF GATED AND CINEMATIC PERFUSION LUNG IMAGING IN DETECTING EXPERIMENTAL PULMONARY EMBOLI. P.O. Alderson, F. Vieras, D.F. Housholder, K.G. Mendenhall, and H.N. Wagner, Jr. Johns Hopkins Hospital, Baltimore, Md. and Armed Forces Radiobiology Research Institute, Bethesda, Md.

To determine how blurring caused by pulmonary motion during perfusion (P) lung imaging effects detection of pulmonary emboli (PE), 12 dogs had routine lung scans and gated or cinematic P studies after receiving autologous experimental PE. Six dogs had end-inspiratory (IN) and end-expiratory (EX) 6-view P studies performed using a Brattle synchronizer set to 80% threshold. Six other dogs had ungated and cinematic 3-view (Post, LPO, RPO) P studies. Cinematic studies were acquired using a camera-computer system synchronized to a Harvard respirator. Prior to sacrifice all animals received intravenous India Ink to outline pulmonary perfusion defects. Post-mortem lung dissection verified sites of emboli. Three independent observers rated unidentified noncinematic images for clarity of defects. The ungated images were scored lowest by all three. An ROC curve analysis of randomized, unidentified images yielded true-positive (TP) rates 5-10% higher for IN than ungated or EX images at all levels of confidence, without increasing false-positive rates. Five documented emboli were seen on In-gated studies which were not seen on multiple-view routine images. Cinematic images yielded slight increases in TP rates and documented expansion of embolic P defects during inspiration. Gating P lung images improved image clarity and observer confidence in detecting PE. The results suggest that stop-motion techniques might be useful as a selective (i.e., certain views in certain patients) adjunct to routine P imaging.

FRIDAY, JUNE 30 SANTA ANA ROOM
8:30 a.m.-10:00 a.m.

BASIC SCIENCE

INSTRUMENTATION III: CARDIOVASCULAR

Chairman: Thomas F. Budinger
Co-Chairman: Ronald R. Price

DUAL ANGLE SIMULTANEOUS IMAGING: A NEW CONCEPT IN COLLIMATION. J.L. Tatum, J.W. Beck, J.K. Goodrich, and R.H. Jones. Duke University Medical Center, Durham, N.C.

Noninvasive radionuclide studies for evaluation of cardiac function are rapidly finding acceptance as a routine diagnostic procedure. Peformance of these evaluations has developed by two dissimilar techniques, the first-pass radioangiocardiogram and the equilibrium blood-pool gated study. Although both techniques evaluate similar parameters, mainly left ventricular ejection fraction and wall motion, each method has its disadvantages. The first-pass study does not allow imaging from multiple projections and is therefore felt to be less reliable in evaluation of wall motion. On the other hand, the blood pool study requires long imaging times which is a significant disadvantage when performing studies under exercise stress.

A possible partial solution to both disadvantages may be found in a new collimator design* which allows one to obtain simultaneous views in planes 60° apart. Initial evaluation at our institution has been performed with the collimator on an Ohio-Nuclear large field camera. As anticipated, collimator efficiency is improved while resolution is comparable to that of a parallel-hole medium sensitivity collimator. The collimator allows acquisition of two simultaneous views on the first-pass study; it also shortens acquisition time of multiple views on the blood-pool gated studies. An additional advantage is the ability to obtain images with a fixed planar relationship. Operational concerns with this collimator are the requirements for critical positioning and short collimator-to-target distance; however, neither is intolerable.
(*Cardiac Medical Systems.)

A ONE-DIMENSIONAL IMAGING DEVICE FOR NUCLEAR MEDICINE APPLICATIONS. M. W. Groch, Group Research, Searle Diagnostics Inc., Des Plaines, IL.

A one-dimensional scintillation camera based on the Anger principle has been developed. The device provides a sectional image, with good spatial resolution along the imaging axis, while maintaining high efficiency in the segment under study. The linear imager is used to generate high resolution nuclear kymograms, portably at the bedside. Nuclear kymograms are unidimensional position events swept in time, synchronized with the R-wave of the patient's ECG. The motion of a regional myocardial wall segment can be directly assessed from the kymogram after administration of Tc-99m human serum albumin.

The linear imager incorporates a 9 inch by 1/2 inch bar of NaI (Tl) with 11-3/4 inch photomultiplier tubes in a highly compact head weighing 35 pounds. Electronics necessary for accumulation, positioning, and display of gamma photon events, are housed in a mobile stand. The rectangular NaI (Tl) bar exhibits complex optical properties due to multiple reflections and scattering of light within the crystal, and light response functions were obtained to study its optical properties. The resolution of the one-dimensional collimator is 35% better than that of a conventional high resolution collimator. The collimator is converged in the second dimension to maintain good sensitivity (twice that of an equivalent strip of high resolution collimator), while restricting the slice width to less than 2 cm at 3 inches. The camera's system resolution with Tc-99m was measured to be 8 mm at 4 inches. Uniformity of the device is excellent (±5%).

CODED APERTURE IMAGING OF THE HEART. W.L. Rogers, K.F. Koral, R. Mayans, P.F. Leonard and J.W. Keyes, Jr. University of Michigan Medical Center, Ann Arbor MI.

Accurate sizing and morphologic localization of acute infarcts is of clinical value both in managing patients and determining their prognosis. Because the heart is a small organ lying close to the body surface, coded aperture imaging (CAI) offers the potential of high resolution, good sensitivity, tomographic presentation, accurate size scaling, and portability (allowing bedside use).

Preliminary studies of this application of CAI were undertaken using a coded aperture designed for thyroid imaging and a dog model of acute myocardial infarction. On the basis of these results, a new two-pass aperture with optimized code was designed specifically for imaging the heart. For both apertures longitudinal tomograms are computed using a modified algebraic reconstruction technique (ART).

The preliminary studies with the thyroid aperture produced good images of the dog heart with both pyrophosphate and thallium, however, the field of view and depth resolution were limited by the small aperture size. The field of view of the new heart aperture ranges from 20 cm at 3 cm to 46 cm at 11 cm. The new aperture produces seven tomographic images spaced approximately equally between 2.2 and 11 cm with measured transverse resolution varying from 4 mm FWHM at 3 cm to 9 mm FWHM at 11 cm and estimated depth resolution of about 1 cm at 6 cm. Images of a myocardial phantom and of dogs with acute infarcts show excellent detail and constrast.

CAI is a good technique for myocardial imaging. It is suitable for both hot spot and cold spot imaging and produces tomographic images superior in resolution to conventional techniques. Further development and clinical trials are warranted.

LONGITUDINAL SECTION TOMOGRAPHY WITH A HIGH PURITY GERMANIUM ARRAY. J.A. Patton, R.R. Price, F.D. Rollo and A.B. Brill, Vanderbilt University Medical Center, Nashville TN.

A nine element array of high purity germanium with dual-isotope capability is being evaluated in conjunction with a computer-driven scanning bed for diagnostic nuclear medicine imaging studies. For longitudinal section tomography a collimator system has been fabricated in which the fields of view of the 9 detectors intersect at a point 2.5 inches directly below the center of the collimator. Data are collected separately from each of the 9 detectors and recombined after suitable transformations have been performed to reinforce data from a particular plane.

The system is currently being evaluated in selected patients whose scintillation camera studies were equivocal. It is also being used in conjunction with on-going studies in the Division of Cardiology in quantitating the size of induced infarcts in dogs by imaging with Tl-201 chloride and Tc-99m pyrophosphate. From the studies performed to date, the Tl-201 images obtained with the germanium array in the tomographic mode are of higher contrast than those routinely obtained by the scintillation camera. Also, the Tc-99m pyrophosphate images obtained with this instrument appear to be superior due to the separation of the infarcted heart muscle from the sternum and ribs that lie in planes above and below the plane of interest.

Techniques are also being developed for using the point spread function and the methods of deconvolution analysis to further improve the quality of the longitudinal section images obtained with the system. Preliminary results offer encouragement in our attempts at high resolution imaging of selected planes within the body.

IMPROVED DIAGNOSTIC RESULTS OF MYOCARDIAL PERFUSION TOMOGRAPHY USING A NEW RAPID INEXPENSIVE TECHNIQUE. R.A. Vogel, D.L. Kirch, M.T. LeFree, and P.P. Steele. Denver Veterans Administration Hospital, Denver, CO.

A new method of thallium-201 myocardial perfusion tomography was developed using a seven pinhole collimator, a standard 37.5 cm crystal Anger camera, and a digital computer. Forty-two patients, 16 without and 26 with angiographically demonstrated coronary artery stenosis

(>70%) underwent stress thallium-201 scintigraphy using graded treadmill exercise. Tomography and standard parallel-hole collimator imaging were performed 10 minutes following injection of 1.5 mCi thallium-201. Using the seven pinhole collimator, each study's single projection 750,000 count data acquisition and computer reconstruction required approximately 10 and 5 minutes, respectively. Both the regular and tomographic studies were interpreted through use of a computerized program which determines maximal circumferential cardiac wall count densities and compares these profiles to normalized mean ± 2 standard deviation values obtained from 25 individuals without coronary disease. Of the 16 normal individuals tested by both techniques, one had abnormal standard scintigraphy and none had abnormal tomography. Of the 26 patients with coronary disease, 19 had abnormal standard scintigraphy and 24 had abnormal tomography ($P<.05$). These results suggest that this technique of myocardial perfusion tomography using an ordinary radionuclide and Anger camera is more sensitive to the presence of coronary artery disease than is standard imaging, and can be performed including data processing in less time.

CLINICAL STANDARDIZATION OF THE NEW DUAL CARDIAC PROBE. E. DePuey, V. Mathur, and P. Werp. Baylor College of Medicine, St. Luke's Episcopal Hospital, Clayton Foundation, Houston, TX, and Searle Diagnostics, Des Plaines, IL.

A new mobile dual cardiac probe has recently been introduced to measure left ventricular ejection fraction (LVEF). Following the intravenous administration of a 1.5 mCi bolus, first pass time-activity (radiocardiogram = RCG) curves are generated from the left ventricle and a surrounding background area. From these LVEF is calculated. To evaluate the clinical feasibility of this technique, its accuracy, reproducibility, and the optimal route of injection were determined. In 28 patients correlation between LVEF determined by the dual probe technique and by single plane and biplane contrast ventriculography was 0.87 and 0.83 respectively. Calculations of two independent observers were virtually identical (R=0.99). Central and peripheral injections yielded comparable curves, and the resultant LVEF's correlated well (R=0.95). In 43 patients LVEF was determined from RCG curves and from left ventricular volume curves generated by computer from multigated Tc-99m albumin blood pool images. Correlation between these two isotope methods was 0.83. LVEF's calculated following three serial bolus injections of Tc-99m albumin in 20 patients indicated excellent reproducibility of the technique. However, in another 21 patients who received serial injections of Tc-99m sulfur colloid, the LVEF increased artifactually by approximately 7% with each injection due to sequestration of the radionuclide by the liver, which is in the field of view of the annular background detector. These results indicate that LVEF may be simply, accurately, and reproducibly determined using the dual cardiac probe and a small peripheral bolus of a blood pool radiopharmaceutical.

SPATIAL RESOLUTION OF LARGE FIELD OF VIEW GAMMA CAMERAS FOR THALLIUM-201 MYOCARDIAL IMAGING. R. Sarper, W.A. Fajman, J. Witkowski, and Y.A. Tarcan. Emory University School of Medicine, Atlanta, Ga.

Large field of view camera might be considered to be the most desirable system for multipurpose imaging, However, due to the increasing popularity of thallium-201, the question arises as to whether its usefulness could be extended to optimal thallium myocardial imaging. The answer to this question depends on the spatial resolution of a camera system at approximately 80 keV. In this study, Ohio-Nuclear, Picker, Searle and Toshiba large view cameras have been evaluated. Comparable collimators were used to resolve different low energy line sources at depths of 0, 1, 2, and 3 inches from the collimator surface. It has been found that one of the cameras had superior spatial resolution.

FRIDAY, JUNE 30
8:30 a.m.-10:00 a.m.

CALIFORNIA B ROOM

IN VITRO AND CORRELATIVE TECHNIQUES

RADIOPHARMACEUTICALS VII (BASIC SCIENCE)

Chairman: Walter Wolf
Co-Chairman: Robert H. Rohrer

C-14 ORNITHINE AS A MARKER OF MALIGNANCY. D.C. Buffkin and M.M. Webber. UCLA, School of Medicine, Los Angeles, Calif.

The polyamines, putrescine→spermidine→spermine, are small, organic cations which have been implicated as prime candidates for the regulatory control of the growth processes in mammalian physiological systems. Increased urinary polyamine levels have been demonstrated in humans with varied types of malignancies. The non-protein amino acid ornithine is the principal source of polyamines in mammals.

The metabolism of DL-1-C-14-ornithine monohydrochloride in rats with either Walker 256 carcinoma or chemically induced methylcholanthrene (MCA) tumors was studied. Following the intraperitoneal injection of 3 μCi C-14 ornithine/100 gm body weight, the decarboxylation of ornithine - yielding C-14 O_2 - was monitored by using the vibrating reed electrometer-ionization chamber model of Davidson and Schwabe. Tumor-bearing animals (T-B) showed significant increases in ornithine metabolism as compared to controls (C); for Walker 256, T-B/C rose from 1.16 to 1.78; for MCA implants, T-B/C rose from 1.19 to 1.82; and MCA paintings rose from 1.00 to 2.29. With tumor regression, ornithine levels of metabolism in T-B animals returned to baseline or near-baseline levels. These results encourage us in our pursuit of developing ornithine as a biological marker of malignancy because of the demonstrated positive correlation between tumor growth and ornithine metabolism.

(This project was supported by USPHS Grant 5 RO1 CA 15787).

BIODISTRIBUTION OF Fe-59-IRON II-BIS-2-PYRIDINECARBOXALDEHYDE THIOSEMICARBAZONES. Michael A. Davis and Robert N. Hanson, Joint Program in Nuclear Medicine, Harvard Medical School, Boston, Massachusetts 02115.

In spite of the volume of work published regarding the antineoplastic activity of the α-N-heterocyclic carboxaldehyde thiosemicarbazones, few studies have examined the biologic activity of the iron complexes of these compounds, even though these complexes are hypothesized to be the active species in vivo. Only three papers have described the use of radiolabeled (C-14, H-3 and S-35) thiosemicarbazones for determining the distribution and metabolism of the drugs. None of the studies used radiolabeled preformed chelates. In this study we have examined the biodistribution of three Fe-59-iron II-bis-5-substituted-2-pyridinecarboxaldehyde thiosemicarbazones I-III in normal rats. The effect of the 5-substituent and time upon distribution were the two main parameters of interest. The resulting data indicated that the distribution of the preformed chelates differed from that reported for the beta-labeled compounds. The labeled complexes were rapidly distributed to the fat and muscle within 5 minutes, but whereas I and II were also taken up rapidly by the liver and subsequently into the gut, III was only slowly accumulated in the liver and only to a slight extent in the gut. No correlations between the reported antineoplastic activity and the tissue distributions are apparent, however, the significant accumulation in the gut may account for the reported gastrointestinal side effects that are observed with some members of this class of drugs.

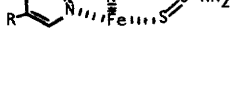

I R= H
II R= $N(CH_3)_2$
III R= OH

RADIOPHARMACOKINETIC STUDIES WITH PT-195m LABELED Cis-PLATIN
R.C. Manaka and W. Wolf. Radiopharmacy Program, University of Southern California, Los Angeles, CA.

The recent introduction of diuretics,mannitol and/or high hydration has dramatically enhanced the clinical use of cis-platin (cis-dichlorodiammine platinum (II)) in the treatment of a range of tumors refractary to other antitumor drugs.

In previous studies (J.Clin.Hematol.Oncol.7,79,1977) we had described the blood loop technique and documented preliminary data on the radiopharmacokinetics of cis-platin. A more careful analysis of the data showed that, following an intravenous bolus injection, the blood levels of cis-platin could be analyzed as a 3 compartment model. The $t_{\frac{1}{2}}$ of Sprague Dawley male rats,(untreated), when compared with rats having been treated with mannitol, are: $t_{\frac{1}{2}}\gamma$, 0.8 & 0.36 min; $t_{\frac{1}{2}}\alpha$, 6.6 & 5.3 min; and $t_{\frac{1}{2}}\beta$, 2.1 and 3.0 hrs, respectively.

To analyze these data further, it became necessary to determine the distribution of cis-platin among the various blood components. However, preliminary results were so variable as to suggest a series of rapid equilibria in vivo, rapidly distorted when blood is withdrawn. Following the use of rapid analysis, it was noted that at 2 min post injection 11% of the activity in the blood is bound to the RBC, and that at 1 hr this had increased to 66%. All of this activity is cell bound and apparently removed from the available drug pool. Of the activity in the plasma, already 22% is bound at 2 min post injection, and 45% at 1 hr. However, at 5 min this binding occurs preferentially to the γ-globulins, where as at 40 min the main bound activity is associated with the albumins and prealbumins.

These data are of significance in evaluating the desirable drug level for a given patient, and perhaps of "titrating" patients non-invasively with radiolabeled drugs for individualized chemotherapy.

LOCALIZATION OF COLD INSOLUBLE GLOBULIN IN DAMAGED TISSUE.
F.B. Gelder, C.J. Reese, A.R. Moosa, V. Stark, and P.V. Harper. University of Chicago, Chicago, IL.

Cold Insoluble Globulin (CIG) is a poorly understood normal plasma protein with a molecular wt of 300,000 to 320,000 which binds avidly to denatured collagen and damaged tissue, where it promotes phagocytosis of tissue debris. This material has been purified from plasma using an immobilized antibody column and labeled with iodine-125 by the Chloramine T method without significantly damaging its biologic activity. One-fourth of a milligram of the material was injected into rats one hour after they were given a 2 cm diameter full thickness burn. Fifteen to 30% of the label was localized in the burned area within 90 minutes after injection. Scintillation scanning of the animals five hrs after injury demonstrated clear uptake in the liver and burned area with very little elsewhere. The serum level of CIG dropped sharply to around 0.03 mg/ml (normal $\sim$ 0.3 mg/ml) during 8-12 hours after the burn. In similar experiments, 5% of the injected dose of I-125-CIG was localized in an 0.5 cm surgical flank incision. Radioactivity over the incision was 10 times higher than that over the adjacent tissue. This minor injury did not significantly reduce the serum level of CIG indicating that serum depletion is not a prerequisite for tissue localization in measurable amounts. These studies suggest that the natural avidity of CIG for denatured collagen and damaged tissue may make it a valuable scanning agent to detect certain types of injury, such as infarction where it appears to circumvent some of the intrinsic limitations of Tc-99m-PyP. The labeling of CIG with Tc-99m using a bifunctional chelating agent is currently under investigation. (Supported in part by CA14599)

THE EFFECT OF DEFEROXAMINE-MESYLATE (DESFERAL) ON THE BIODISTRIBUTION OF GALLIUM-67 CITRATE.
Zvi H. Oster, Tel Hashomer Hospital,Israel.

The use of Ga-67 citrate for tumor and abscess detection is hindered by the high soft tissue concentration in the first hours after injection.Deferoxamine-mesylate (Desferal), a chelating agent used in acute and chronic iron intoxication was found to form a stable complex with Ga-67 citrate.The effect of Desferal on the biodistribution of Ga-67 citrate was studied in rabbits.Two 1.2 Kg. rabbits were placed under a gamma camera connected to a dedicated computor system.Ga-67 citrate 0.3 mCi,was administered intravenously and was followed 20 minutes later by 50 mg of Desferal to one rabbit of the pair.Simultaneous acquisition of data from the two rabbits in dynamic mode served as a basis for the generation of time/activity curves from the heart, kidney, bladder, muscle and soft tissue abscess regions.It was found in six paired experiments that 5-8 minutes after the Desferal injection Ga-67 concentration in the kidneys increased by 53% over the previous level and the concentration in the heart decreased by 35%.The activity in the kidneys of the control animals decreased by 13% and in the heart by 12%.The soft tissue activity in the Desferal treated animals decreased markedly enabling the distinction between it and the skeletal activity while in the control animals this was not possible.In turpentine-induced abscesses Ga-67 continues to accumulate in the presence of Desferal.These observations suggest that Desferal could be used to increase the target/non-target ratio and to reduce the radiation dose from gallium studies if given after the scan was performed.

IDENTIFICATION OF Ga-67 BINDING COMPONENT IN HUMAN NEUTROPHILS.
R.E. Weiner, P.B. Hoffer, and M.L. Thakur. Yale University School of Medicine, New Haven, CT.

This study was undertaken to elucidate the mechanism by which Ga-67 accumulates in abscesses and inflammatory lesions. Human neutrophils contain a significant concentration of iron binding protein, Lactoferrin, a likely candidate for Ga-67 localization.

6.7×10^7 human neutrophils isolated from peripheral healthy human blood were suspended in normal saline and 7.8 μCi of carrier free Ga-67 citrate was added. The preparation was incubated at room temperature for 30 min. After repeated washings the final cell pellet contained 27.9% of the original radioactivity. The cells were resuspended in 1M NaCl and sonicated. The sonicate was centrifuged and the supernatant contained 85.1% and the pellet 12.5% of the original activity. The supernatant was split into two aliquots and applied to columns containing rabbit anti Human Lactoferrin and anti Human Transferrin antibodies. The anti Human Lactoferrin antibody column retained 87.3% of the activity in the sample. In contrast, the anti Human Transferrin column, which served as a control, retained only 5.3%. Moreover, antigen-antibody dissociating agents eluted 97.6% of the bound CPM from the anti Human Lactoferrin column substantiating the specific nature of Ga-67-Lactoferrin complex.

While it is not clear whether Ga-67 is absorbed on the surface or interior of the human neutrophil, it is clear Ga-67 is ultimately bound to Lactoferrin. These data also support the concept that Ga(III) is an Fe(III) analogue.

USE OF AN AFFINITY CHROMATOGRAPHIC METHOD TO DETERMINE RELATIVE BINDING OF ^{67}Ga TO LACTOFERRIN AND TRANSFERRIN IN TEAR FLUID.
P.B. Hoffer, J. Huberty and A. Samuel. Yale Univ., New Haven, CT & Univ. of California, San Francisco, CA.

^{67}Ga in lacrimal glands and tear fluid is bound to transferrin (TF). Tear fluid is also rich in lactoferrin (LF). Both proteins have similar molecular weights and may be difficult to distinguish electrophoretically. We have developed a method to determine the relative binding of ^{67}Ga to LF and TF. Affinity chromatographic columns were prepared using excess anti-human TF and anti-human LF bound to Sepharose-4B columns by the cyanobromine method. Tear specimens were obtained from 6 patients 24 to 48 hrs following intravenous injection of ^{67}Ga. An aliquot of each specimen was run through anti-LF and anti-TF columns to determine relative binding with the following results:

Patient	% Activity bound to TF	% Activity bound to LF
1	0	97
2	15	93
3	7	57
4	32	77
5	5	80
6	18	81
AVG.	13±11	81±14

These results indicate that most of the ^{67}Ga in tears is bound to LF. The affinity chromatographic method is practical for determining ^{67}Ga binding to TF and LF.

COMPARATIVE BIOKINETICS OF RADIOGALLIUM AND RADIOINDIUM IN MICE. B.M.W. Tsui and K.A. Lathrop. The University of Chicago, Chicago, IL.

Radionuclides of two chemically similar elements, Ga and In, have proved useful in nuclear medicine. These have similar nuclear decay properties so that it is not entirely clear which nuclide may be the best choice unless a comparison is made of the biokinetic behavior. We have determined distributions in mice for 12 tissues at intervals between 15m and 2d after i.v. injection of carrier-free Ga-chloride (same as citrate) and In-chloride. The data were used to construct linear compartment models and the rate constants (k) are compared. Initial rapid blood clearances are the same but after 15m In clears more slowly than Ga. This is related in the smaller summed blood→tissue and excretion rate constants for In. Concentration in kidney exceeds all organs and is ∿3 times higher for In than for Ga. The kidney/blood ratio increases rapidly from ∿2 at 6h to ∿45 at 2d for Ga, and from ∿6 to ∿60 for In. The liver/ and spleen/blood ratios are similar up to ∿1d, then increase more rapidly for Ga. The low gallbladder activity for both indicates no secretion from liver to intestine. Considerable activity is found in intestinal wall at 15m; wall/content ratio is ∿10 and decreases to ∿3 by 6h. Blood clearance in pregnancy is faster than in normals which seemed to be the result of additional high ks for blood→placenta and for In a higher summed k for blood→tissue, for Ga a lower summed k for tissue→blood. The biokinetic models will be used as guides for collection of critical data in humans. Use of these models for the collective consideration of characteristics such as photon imaging properties, radiation absorbed doses, tissue-to-background ratios should be an aid in the design and evaluation of radiopharmaceuticals prepared with Ga-67, -68 and In-111, -113m.

FRIDAY, JUNE 30 — CALIFORNIA A ROOM
8:30 a.m.-10:00 a.m.

CLINICAL PRACTICE

GASTROENTEROLOGY AND GALLIUM

Chairman: George W. Evans
Co-Chairman: John J. Sziklas

EVALUATION OF BOWEL ACTIVITY IN EARLY GALLIUM-67 IMAGING OF THE ABDOMEN P.J.Perkins Salem Hospital, Salem OR

58 patient referred for Ga-67 imaging were evaluated for appearance of bowel activity on early imaging. Imaging was performed at 5-9 hours post injection; 48 were imaged at 6 hours. No colon cleansing was used. The study was performed as a whole body image with a moving detector camera system; an ID of 150 was achieved over the liver. Selected spot images were obtained. Bowel activity was classified thus: 0-no bowel activity; 1-focal activity less intense than liver; 2-focal activity equal to liver; 3-focal activity greater than liver; 4-diffuse segment of bowel uptake. Bowel activity was identified by inspection of the initial image in conjunction with delayed follow-up images. Patients with early positive studies due to disease and not bowel activity were excluded. The results were: Class 0 - 22/58 (38%); Class 1 - 2/58 (<1%);Class 2 - 15/58 (26%); Class 3 - 13/58 (22%); Class 4 - 6/58 (10%). Early imaging of the abdomen with Ga-67 for the detection of inflammatory disease has been advocated to avoid confusion of pathologic activity with bowel activity. This study shows that 50% (Class 2+3) of patients show focally increased physiologic uptake on early imaging which could be confused with a pathologic lesion if early imaging were relied upon exclusively.

Ga-67-CITRATE SCANNING IN THE DETECTION OF INFLAMMATORY DISEASE OF THE COLON. S.Sarkar, S.Nacianceno, R.Joseph, and D.Woodbury. Wayne County General Hospital, Eloise, MI.

Demonstration of bowel inflammation aids in differentiating ulcerative (U.C.) or granulomatous colitis (G.C.) from irritable colon (I.C.) and in diagnosing active disease in chronic cases. We investigated, prospectively, the value of Ga-67-citrate scanning in these disorders.

Nine patients with suspected inflammatory disease of the colon had at least 3 rectilinear scans, using standard technique, between 6 and 120 hours after a 3 mCi dose of Ga-67-citrate I.V. Endoscopy, barium enema, and/or biopsy were performed within 1-15 days of the scan. Additionally, 3 patients, previously diagnosed as having irritable bowel syndrome, were also scanned. Bowel preparation with laxatives, attempted in only 2 patients, was inconsequential.

To avoid erroneous interpretation of normal gallium activity in feces, only intense uptake in colon persisting over at least 3 successive days was considered positive for active inflammation.

In all, 12 patients had 14 Ga-67-citrate studies; 13 of these correctly demonstrated presence or absence of inflammation in 11 patients with the following proved diagnoses: a) Acute U.C., 3 patients (2 of these had negative follow-up scans during remission); b) Inactive U.C., 2 patients; c) Active G.C., 1 patient; d) Chronic regional ileitis with G.C. ruled out, 1 patient; e) I.C.,4 patients. There was 1 false negative scan in a patient with acute exacerbation of chronic U.C. and no false positives.

Adequate endoscopic and/or barium enema studies are not always possible because of risk to the patient or noncompliance. In these instances a positive gallium scan will help to establish the diagnosis and initiate therapy.

ONE WEEK POST-INJECTION GALLIUM-67 SCAN - IS IT OF ANY ADDED ADVANTAGE? W. H. Beal and T. K. Chaudhuri. University of Texas Health Science Center and Bexar County Hospital; University of Texas Health Science Center and VA Hospital, San Antonio, TX.

This study was undertaken to find if one-week delayed Ga-67 scan is of any more diagnostic value over the conventional 3-day post-injection scans. Sequential whole body scans were obtained in 45 patients at 6-hr, 1-day, 3-day, and 7-day post-injection of 2.5 mCi of Ga-67-citrate. Except for the 6-hr scans, all other scans were performed following a bowel preparation. Scan findings were compared with other clinical and laboratory findings.

There was not a single 3-day negative scan turning positive on day-7. There were 30 cases showing definitely abnormally increased uptake in the 3-day scans and persisting the abnormality on the 7-day scans. Only in 5 cases did the 7-day scans appear to be more convincingly positive. All 30 cases were shown to be diagnostically positive. Fifteen cases appeared to be positive at day-3 scans but became negative on day-7, ten of which were proven to be clinically negative and five remained undetermined. In most of the 3-day false positive cases, the abdominal area was the affected anatomical region. Localized area of questionably abnormal uptake ranged from cecal to rectal radioactivity accumulation. Although the total count rate declined significantly on day 7, substantial decrease in the background count helped to interpret the 7-day scans.

It is concluded that, irrespective of claimed good cleansing enema, faintly positive or equivocal 3-day Ga-67 scans, specifically of the abdominal area, should be repeated with a 7-day scan. Emergency nature of the inflamatory or neoplastic conditions precludes avoidance of earlier scans.

GALLIUM-67-CITRATE SCANNING IN EXTRAPULMONARY TUBERCULOSIS. S.D. Sarkar and K.P. Ravikrishnan. Wayne County General Hospital, Eloise, MI.

The uptake of Ga-67 in peritoneal tuberculosis (T.B.) has been recently reported. We wish to report the results to date of an ongoing study concerning the value of Ga-67-citrate scanning in the diagnosis and follow-up of extrapulmonary T.B.

Patients clinically suspected of having T.B. of the bone, kidneys, bowel or peritoneum, had 2-4 sequential whole-body rectilinear scans using standard technique, between 6 and 120 hours after intravenous injection of 3 mCi of Ga-67-citrate. For a definitive diagnosis, all patients underwent 2 or more conventional tests, including radiography, echography, tissue biopsy and bacteriologic examination. Follow-up scans were performed in those with abnormal initial studies.

Over a period of 7 months, we have studied 5 patients. Three of these had the following proved extrapulmonary lesions correctly demonstrated by the scan: 1) Pott's abscess of spine; the Ga-67 scan provided the only direct evidence of the abscess; 2) left renal tuberculosis, first detected on the scan performed for possible active bowel T.B. (past history of ileocecal T.B.); 3) peritoneal T.B. In all 3 patients, the Ga-67 scan not only demonstrated the extent of the involvement, but also, dramatic changes with improvement following therapy. The 2 remaining patients with negative scans had no extrapulmonary involvement.

Our preliminary data show that Ga-67 scanning may be a useful adjuvant in screening for suspected extrapulmonary T.B. and in assessing the results of therapy.

THE DIAGNOSTIC EFFICACY OF GALLIUM-67 IN THE LOCALIZATION OF ABSCESSES OR INFLAMMATORY PROCESSES: A REVIEW OF 300 CONSECUTIVE CASES. R.F. Carretta, F.L. Weiland, W.C. Harvey, and D.A. Podoloff, Wilford Hall USAF Medical Center, Lackland AFB, Texas.

The etiology of temperature elevation in the post-operative, immunosuppressed, or septic patient is often difficult to ascertain on clinical grounds, and/or routine non-invasive diagnostic tests. The presence of an abscess or hidden inflammatory process is often considered in the differential diagnosis. A retrospective study of 300 consecutive gallium-67 citrate scans done to evaluate abscess or inflammatory processes were reviewed to evaluate the accuracy and sensitivity of gallium-67 as a non-invasive diagnostic study. All patients received between 1 and 3 millicuries of gallium-67 citrate. Using a 5-inch dual probe rectilinear scanner, patients were scanned at 48 hours post injection and serial scans were obtained in selected patients when clinically indicated. Patients' hospital records were then reviewed for clinical correlation. Thirty per cent (89/300) of the scans were positive for occult infections. Sixty-three per cent (189/300) were negative for occult infections. One per cent (4/300) of the scans were false positive, and six per cent (18/300) of the scans were false negative. Gallium-67 citrate scanning at this institution has proven to be a useful non-invasive diagnostic procedure for the localization of occult infection.

COMPREHENSIVE REVIEW OF GALLIUM SCANNING FOR INFLAMMATORY LESIONS. R.C. Verma, L. Ramanna and M.M. Webber. UCLA-San Fernando Valley Medical Program, Los Angeles, California.

Although the role of Gallium-67 scintigraphy in detection of tumors is well established, its use for inflammatory processes is not as well recognized. The paucity of large series (dealing with the entire spectrum of inflammations and infections studied by Gallium scanning) prompted this systematic in-depth review of 36 reports published in the English literature from 1970 to 1976. Detailed analyses of all reports yielded 910 cases who had a histopathological or strong clinical confirmation and these constitute the population for this review.

Of 545 known inflammatory lesions, 437 were correctly localized by Gallium scans. The true positive rate (sensitivity) therefore is 80%. Of 365 scans showing normal Gallium distribution, 350 did not reveal any abnormality at surgery or on thorough clinical evaluation. Since these reports did not include oncology patients, there were only 15 false positives. These data yield a true negative rate (specificity) of 96% and an overall accuracy of 88%.

The accuracy for detection of intracranial, pulmonary, subphrenic, abdominal, renal/perinephric, and localised wound infections was very good and fair for liver and gall bladder lesions. The number of bone and pelvic infections reported were too few to draw any definitive conclusions. In two relatively large series in which 45 patients had early and delayed scans, the 6 hr. scans did not miss any of the abscesses demonstrated at the 48 hr. studies.

In conclusion, with an overall accuracy of 88%, Gallium scintigraphy is a very useful technique in detection of most inflammatory lesions. Further work is needed to define its role in evaluation of bone and pelvic infections.

ASSESSMENT OF GASTRIC EMPTYING OF A SOLID MEAL UTILIZING A SCINTILLATION CAMERA-COMPUTER SYSTEM. W.A. Fajman, M.S. Perkel, T. Hersh, R. Sarper and Y.A. Tarcan. Emory University School of Medicine, Atlanta, Ga.

Assessment of gastric emptying of a solid meal is being performed utilizing a large field of view scintillation camera-computer system which requires less than 45 minutes total camera-computer time and incorporates measurement of values late in the emptying sequence. After a breakfast of eggs, bacon, toast and coffee mixed with .25-.50 mCi of Tc-99m sulfur colloid, a 5 minute camera-computer image is obtained, followed by at least 6 similar 5 minute images (30, 60, 90, 120, 240 and 360 min.). Utilizing light pen flagging of the stomach, individual images are quantitated and, via computer, the data is corrected for decay and plotted. Gastric emptying may be expressed as half time (T50), 95% emptying time (T95) and percent residual at 2, 4 and 6 hours. Ten normals were evaluated (T50 = 97 $\pm$ 18 min, T95 = 286 $\pm$ 60 min, percent at 2 hr = 38 $\pm$ 9, 4 hr = 10 $\pm$ 4, 6 hr = 1 $\pm$ 2). Patients with gastric atony or with gastric outlet obstruction have prolonged studies compared to controls. The study has demonstrated improvement after surgical treatment in two cases of outlet obstruction. In a group of clinically selected patients with gastric atony, the effect of a drug, metoclopramide, which enhances gastrointestinal motor activity, was investigated and improvement was shown on T50 in 14 of 19 and T95 in 18 of 19 cases. This technique requires less than 45 minutes total imaging time and allows proper assessment of gastric emptying of a solid meal. It is also useful in evaluation of therapy, providing an objective measurement of gastric emptying.

RADIONUCLIDE IMAGING IN THE NON-SURGICAL TREATMENT OF LIVER-SPLEEN INJURY. L.G. Lutzker and J. Chun. Albert Einstein College of Medicine, Bronx, NY.

The study was undertaken because of recent interest in avoiding splenectomy after trauma, particularly in children, to eliminate the risk of overwhelming sepsis. 19 children and 2 adults had defects in the spleen or liver on Tc-99mSC imaging performed immediately after abdominal trauma. All were clinically stable on admission or became so after receiving 1 unit of blood or RBCs. None had surgery.

Follow-up scans, sometimes multiple, were obtained in 17 patients 1-13 months later. They showed resolution that was complete in 8, nearly so in 4, and significant though partial in 3; 2 studies were unchanged, so pre-existing acquired or congenital defect could not be differentiated from acute injury progressing to scar formation. No defects enlarged.

All but 2 patients were asymptomatic vis a vis the abdomen 1-15 months after initial examination. 2 children with occasional unexplained upper abdomen pain had spleen images showing progressive resolution of the traumatic defect. No defects enlarged during this time.

This study confirms work by others suggesting

that surgery may not always be necessary for liver-spleen injury, and documents the utility of imaging in the initial diagnosis and subsequent evaluation of such injuries.

FRIDAY, JUNE 30 GARDEN GROVE ROOM
10:30 a.m.-12:00 p.m.

CONTINUING EDUCATION

CARDIOVASCULAR V (CLINICAL SCIENCE)

Chairman: Robert H. Jones
Co-Chairman: James W. Fletcher

RADIONUCLIDE ANGIOGRAPHY: SERIAL ASSESSMENT OF CARDIAC OUTPUT AND EJECTION FRACTION FOLLOWING NITROGLYCERIN. S.G. Sorensen, J.L. Ritchie, G.W. Hamilton, and J.W. Kennedy. Veterans Administration Hospital, Seattle, WA.

For a given patient (pt), the hemodynamic effects of arterial or venous vasodilators are unpredictable. Invasive studies have been used to document improvement. Gated radionuclide angiography (RNA) allows serial determinations of ejection fraction (EF), end-diastolic counts (EDC), end-systolic counts (ESC), stroke counts (SC), and radionuclide cardiac output [RNCO= heart rate (HR) x SC].

Serial 1 min hemodynamic responses to 0.6 mg sublinqual nitroglycerin (NTG) were studied in 26 pts for 6 min before and 14 min after NTG, utilizing RNA. Diagnoses were coronary artery disease - 21, normal - 3, cardiomyopathy - 1, and aortic regurgitation - 1. Following NTG, mean HR increased 6% (p=.001), blood pressure (BP) fell 11% (p=.001), EDC fell 11% (p=.001), ESC fell 18% (p=.001), EF increased 18% (p=.001), and RNCO increased 10% (p=.02). Mean time of onset for all hemodynamic changes was 3 min post-NTG; changes persisted through 14 min after NTG. Change in EF and RNCO did not correlate with change in HR or BP, but did relate to change in ESC (p=.01). Although changes in RNCO correlated with changes in EF (r=.65), EF change in individual pts was not predictive of improved CO. In 12 pts, both EF and RNCO increased; however, EF increased in 5 pts with no change in RNCO. RNCO fell in 2 pts (9% and 36%) with no change in EF.

We conclude that RNA provides noninvasive quantitation of changes in CO which are not predicted by other parameters (BP, HR, EF). Rapid acquisition RNA may also serially define temporal and hemodynamic interrelationships and document drug efficacy.

SCINTIGRAPHIC AND HEMODYNAMIC DEMONSTRATION OF TRANSIENT LEFT VENTRICULAR DYSFUNCTION IMMEDIATELY AFTER UNCOMPLICATED CORONARY ARTERY BYPASS GRAFT SURGERY: Jamshid Maddahi, Richard Gray, Daniel Berman, Marjorie Raymond, Alan Waxman, William Ganz, Jack Matloff, H.J.C. Swan, Cedars-Sinai Medical Center, Los Angeles, California.

The immediate effects of elective coronary bypass graft (CABG) on left ventricular (LV) function were assessed by serial hemodynamic and scintigraphic (Sc) measurements obtained before, immediately (1 to 5 hours), and up to 3 days after surgery in 29 patients (PT). Multiple gated Sc ejection fractions (EF) were obtained in 22 of the 29 PTs using Sc camera, computer, and in-vitro tagged RBCs. Surgical technique included moderate hypothermia (23 to 29°C) and intermittent aortic cross clamping without chemical cardioplegia. One PT had a perioperative myocardial infarction (peri-op MI).

Cardiac index decreased (2.38 ± .08, mean ± SEM, to 2.12 ± 0.07 L/m/m^2, p<.05) in spite of unchanged systemic vascular resistance (1583 ± 91 to 1571 ± 90 dyne·sec·cm^{-5}, p=NS) and increased pulmonary wedge pressure (9.7 ± 0.7 to 12.3 ± 0.8 mmHg, p<.05) immediately after surgery. Left ventricular stroke work index decreased from 53 ± 3 to 33 ± 2 gm·m/m^2 (p<.05). Ventricular function curves indicating response to volume infusion showed flattening and displacement downward in 22 of 29 PTs. The Sc EF decreased from 57 ± 2 to 42 ± 3% (p<.05). All parameters improved to preoperative or higher levels by the second postoperative day. Thus immediately after CABG: (1) LV function deteriorates significantly as measured hemodynamically and by EF. (2) These changes occur consistently even in the absence of peri-op MI, but, (3) show spontaneous improvement within 2 days and are compatible with a benign clinical course.

THALLIUM SCANNING IN THE EVALUATION OF CORONARY ARTERY BYPASS GRAFTING. D.E. Blumfield, H.S. Hecht, R.A. Cukingnan and W.H. Blahd. Wadsworth VA Hospital Center, University of California, Los Angeles, CA.

Exercise and rest Thallium - 201 scanning (TS) was used to evaluate the results of coronary artery bypass surgery (CABG) in 15 patients with 46 grafts. Before CABG all had positive TS for ischemia; 14 had positive exercise testing (ET) on the basis of ST depression (ST) and/or chest pain. Thirteen were NYHA FC II - III, 2 were FC I. Three months after CABG 6 had positive TS for ischemia; 1 in an area that was negative and 5 in areas that were positive before CABG. All were FC I. Fourteen had negative ET and 1 had positive ET on the basis of chest pain. Thirteen had increased exercise duration and 14 had improved pressure rate product. There was evidence of improved perfusion without worsening of other areas in 8 patients. The remaining 7 patients had areas of new myocardial infarction (MI) by scan. Four of the patients with new MI had other areas of improved perfusion and 2 had EKG and/or enzyme evidence for perioperative MI. Five patients had a new MI by scan alone. One patient with positive enzymes had improved perfusion without evidence for new MI. There was no significant correlation between operative graft flow and change in regional perfusion. Thus, improvement in FC and/or exercise performance after CABG was associated with improved perfusion in 8 patients, with new MI and improved perfusion in 4 patients, and with new MI alone in 3 patients.

We conclude that TS is a physiologic, non-invasive means for evaluating the results of CABG. It offers insight into the mechanism of relief of angina by CABG by determining the relative contributions of improved perfusion and new MI.

SCINTIGRAPHIC, ELECTROCARDIOGRAPHIC, AND ENZYMATIC DIAGNOSIS OF PERIOPERATIVE MYOCARDIAL INFARCTION IN PATIENTS UNDERGOING CORONARY ARTERY REVASCULARIZATION. J. Burdine, E. DePuey, F. Orzan, and V. Mathur. Baylor College of Medicine, St. Luke's Episcopal Hospital, Clayton Foundation for Research, Houston, TX.

Two hundred fourteen consecutive patients were evaluated 24-120 hrs after coronary bypass surgery with Tc-99m pyrophosphate (PYP) myocardial imaging, serial electrocardiograms (ECG) and enzymes (SGOT, LDH, CPK) to detect the incidence of perioperative myocardial infarction (POMI).

Based on clinical course and scintigraphic, enzymatic, and ECG changes, the incidence of definite POMI was 17/214 (7.9%), and probable POMI 6/214 (2.8%). In all of these 23 patients PYP scans were abnormal; 4 additional patients had false positive scans. Only 13 of the 23 patients had ECG evidence of infarction, but there were no false positives. The threshold for abnormality of enzyme changes was set quite high based upon experience in more than 900 postoperative patients (SGOT >200, LDH> 500, CPK >500 on the same day). Using these criteria, 22 of the 23 infarct patients had abnormal enzymes, and six others were falsely positive.

These results indicate a relatively low sensitivity (57%) of the ECG in diagnosing perioperative infarction, but the lack of false positives suggests high specificity. The calculated accuracy (validity) of the three diagnostic modalities in this series is ECG-95%, serial enzymes-97%, and pyrophosphate scanning-98%. Considering its sensitivity, specificity, and ability to localize and to a certain extent quantitate necrosis, pyrophosphate scanning is likely the most valuable means of diagnosing POMI.

RIGHT VENTRICULAR PERFORMANCE FOLLOWING SURGICAL RELIEF OF PULMONARY HYPERTENSION. G. Schuler, K. Peterson, W. Ashburn, A.D. Johnson, R. Slutsky, G. Dennish, J. Utley, P.O. Daily, and J. Ross, Jr., University of California Medical Center, San Diego, California.

The response of right ventricular (RV) performance to surgical relief of pulmonary hypertension has not been documented. We measured RV ejection fraction (EF) by radionuclide angiography in 15 normals and in 33 patients (pts) before and following mitral or aortic valve surgery; RV-EF was calculated from first pass high frequency time activity curves. Preoperatively (preop), all pts had right and left heart catheterization and postoperatively (postop) right heart data were obtained by balloon-flotation catheters in 20 pts. Preop, the average peak systolic pulmonary artery (PA) pressure was 53 ± 18 [SD] mmHg and mean pulmonary artery wedge pressure (PAW) was 24 ± 9 mmHg. RV-EF (range 68% to 31%) correlated inversely with peak PA pressure (range 28-96 mmHg) ($r = -0.75$). In pts with PAP > 45 mmHg (Group A, n = 21) preop average RV-EF was depressed (41% ± 7, $p < 0.001$) as compared to normal (average 50%, lower limit 45%); in pts with PAP < 45 mmHg (Group B, n = 10) RV-EF was normal (53% ± 8, p:ns). Average PAW fell in 19 pts post-op from 27 ± 7 to 16 ± 7 mmHg ($p < 0.001$). Including both early postop (average 1.5 weeks) and late postop studies (n = 15, average 12 months) RV-EF in Group A increased to 51% ± 7 ($p < 0.01$) and was no longer different from normal; in Group B RV-EF remained unchanged at 54% ± 8, (p:ns). In 3 of the pts studied late (mitral valve replacement in all), RV-EF failed to improve suggesting persistent pulmonary hypertension. We conclude that peak PA pressure >45 mmHg preop is associated with impaired RV shortening, likely due to an afterload excess. Surgical correction of the valve lesion usually restores RV function to normal.

MYOCARDIAL PERFUSION ABNORMALITIES IN PATIENTS WITH MITRAL VALVE PROLAPSE. J.S. Soin, D.D. Tresch, R. Siegel, M.H. Keelan, Milwaukee County Medical Complex, Milwaukee, Wisconsin.

Twenty patients, 15 females and 5 males, ages 16-50 years (mean age-30) with ECHO documented MVP, had combined treadmill stress test (ST) and myocardial perfusion imaging (MPI). At peak exercise, 1 mCi of T1-201 (Sn) chloride was injected I.V. and myocardial perfusion images were obtained in multiple views, using a gamma camera. The clinical, Echocardiographic, resting and stress EKG findings were analyzed independently and later correlated with MPI. In nine subjects, contrast coronary arteriography and ventriculography was performed.

Twelve subjects (60%) had abnormal stress MPI, showing decreased perfusion in the apical diaphragmatic and lateral wall of the left ventricle. Ten (90%) of these either had loud systolic click, angina-like pain or arrhythmia. Seven (58%) had abnormal resting EKG, and six (50%) had positive stress EKG. Nine (75%) of the 12 subjects with abnormal MPI had severe MVP on ECHO (4mm prolapse). In seven subjects where repeat T1-201 MPI at resting was done, the same perfusion abnormalities were seen. All 9 subjects had normal coronary arteries and ventriculogram, except for findings of MVP. Of the 8 subjects with normal T1-MPI, six (75%) were asymptomatic, two (25%) had abnormal resting EKG, none had abnormal stress EKG, seven (87%) had mild MVP on ECHO.

In conclusion, a high incidence (60%) of myocardial perfusion abnormalities are demonstrated in patients with severe MVP and normal coronary arteries. This study supports the hypothesis that decreased regional myocardial blood flow or abnormal cellular function occurs in MVP, and may offer an explanation for the clinical manifestation of this abnormality.

EFFECT OF EXERCISE ON LEFT VENTRICULAR PERFORMANCE: COMPARISON BETWEEN ATHLETES AND NON-ATHLETES. Hajime Murata, Masahiro Iio, Katsumi Asano, Hinako Toyama, Shinichiro Kawagichi, Kazuo Chiba, Hideo Yamada and Kengo Matsui. Tokyo Metropolitan Geriatric Hosp.& The Univ. of Tsukuba, Japan.

Left ventricular function was examined before and immediately after the exercise with bicycle ergometer. Two cases of non-athlete and 10 cases of amateur athlete were evaluated, the latter group had history of daily road training for years. ECG gated analysis was performed with Tc-99m albumin. Using gamma camera-computer system and LIST mode data acquisition, sequential events during 20msec intervals were continuously recorded for 1800 cardiac cycles before the exercise and for 350 cycles immediately after the exercise. From these sequential data, such indeces were obtained as relative volume curve($V(t)/V_{ED}$), ejection fraction(EF), dV/dt curve, max.systolic volume velocity(MSVV) and max.diastolic volume velocity(MDVV).

The mean values of EF before and after the exercise were 70.4 and 68.2% for middle-aged athletes, 61.3 and 70.6% for aged athletes, 70.1 and 77.8% for middle-aged non-athletes. The mean MSVV before and after the exercise were 3.7 and 5.6/sec in middle-aged athletes, 3.7 and 4.6/sec in aged athletes, 5.0 and 7.0/sec in non-athletes. The mean MDVV before and after the exercise for three groups were 3.8 and 5.1/sec, 3.0 and 3.9/sec, 4.3 and 4.5/sec, respectively. EF after the exercise showed significant increase in non-athletes and aged athletes, whereas it remained normal in middle-aged athletes. These results showed the significant effect of continuous athletic training on the left ventricular performance and the method proved to be of value for the evaluation of physiological functions of the left ventricle.

FRIDAY, JUNE 30 ANAHEIM ROOM
10:30 a.m.-12:00 p.m.

CLINICAL SCIENCE

GASTROENTEROLOGY II

Chairman: Leon S. Malmud
Co-Chairman: Harry J. Lessig

TRANSPORT OF Tc-99m BY THE GASTROINTESTINAL SYSTEM. K.A. Lathrop, B.M.W. Tsui, I.V. Gloria, T.A. Aitkin, and P.V. Harper. University of Chicago, Chicago, IL.

Some clinical use has been made of the gastric and intestinal accumulation of Tc-99m after i.v. administration as sodium pertechnetate. Large differences between individuals have been noted and some attempt has been made to correlate these with the intake of food or with changes in the intestinal environment. For the most part, however, little systematic investigation of the localization has been undertaken. A clearer understanding of the G-I transport of Tc-99m might result in furtherance of clinical application. The mouse has been shown to be a good animal model for the study of pertechnetate biokinetics, with the exception of a shortened time scale. In order to study the passage of Tc-99m into and out of the G-I tract mice were sacrificed after intragastric, intraintestinal, and intravenous injection of Tc-99m-pertechnetate. Ligatures were placed around the stomach, segments of the small intestine, and portions of the large intestine, so that the accumulation or loss of Tc-99m could be determined for each. Wall and content were assayed separately. Twenty-three other tissues and organs were assayed. Inspection and analysis of the data allows deductions concerning the accumulation and source of Tc-99m, from which a compartmental mathematical model is constructed to relate processes for the stomach and intestine, and to observe the influence of impaired function on accumulation of Tc-99m in other compartments. The mouse model will be used as a guide to the collection of critical data in humans. Absorption of Tc-99m occurs throughout the tract; at 10 min, it is ~20% from the stomach and LI, between 50-75% from the SI, except for 90% from the ileum. Only about one-half of intestinal Tc-99m (i.v.) comes from salivary and gastric accumulation.

* * *

The following four papers constitute a Rapporteur Session. The Rapporteur for this session is Alexander Gottschalk, Yale University School of Medicine, New Haven, CT.

EVALUATION OF LIVER HEMATOMAS IN DOGS WITH THREE IMAGING MODALITIES. M. P. Frick, L.C. Knight, R.A. Ponto, and M.K. Loken. University of Minnesota, Minneapolis, MN.

Single gamma emission computerized tomography (ECT) was compared to transmission computerized tomography (TCT) and scintillation camera (SC) imaging in eight dogs with acute solitary hematomas in the left liver lobe. These hematomas were induced by instillation of 20-30 cc of nonheparinized blood at laparatomy. All eight of the hematomas were detected by TCT imaging. Four were clearly demonstrated by ECT with the remaining four being questionably positive either as a filling defect or as a distortion of the left lobe of the liver. Only two of the hematomas could be identified on camera scintiphotos with an additional two being questionably positive. The optimal performance of TCT in this study is attributed to its inherent spatial resolution being better than ECT or SC and, that studies with TCT could be performed during apnea (20 sec.), whereas the SC study or one slice with ECT required several minutes. In addition, the Hounsfield number for blood is significantly different from that of liver parenchyma. We do find the ECT to be more sensitive than SC to small changes in the spatial distribution of radionuclides. In addition, the ECT, by virtue of its sectioning capability, is more sensitive to differences in radionuclide concentrations at some depth in an organ than is true for SC or for conventional scanners. However, until such time as the photon yield in ECT permits a shortening of the examination to a period of apnea, it is apparent that TCT will be the modality of choice in instances in which density differences are identifiable. In instances in which a study is performed to assess organ function or blood flow, ECT or SC techniques will continue to be useful.

UTILITY OF Tc-99m SULFUR COLLOID LIVER SCANS IN DIRECTING PERCUTANEOUS LIVER BIOPSY. R.S. Johannes, J.K. Boitnott, P.O. Alderson, W.C. Maddrey, and H.N. Wagner, Jr., Johns Hopkins Medical Institutions, Baltimore, Md.

Routine percutaneous liver biopsy results in a specific histologic diagnosis in approximately 70% of patients. Because of this yield the utility of guided biopsy has been questioned. Over a 12 month period 10 patients with Tc-99m sulfur colloid (SC) liver scans showing focal defects had a negative routine biopsy. The unguided biopsies were performed through the intercostal space in the mid-axillary line with two passes of a Klatskin needle. No less than 4 cm of tissue was obtained. These 10 patients then had a guided biopsy. Following the intravenous injection of 3 mCi of Tc-99m SC, multiple views of the liver were obtained using a camera-computer system. High resolution images were rapidly displayed on the computer oscilloscope and a radioactive source was used to mark the lesion in at least three planes each 45° apart. Thus the location and depth of the lesion were recorded. Nine of the 10 guided biopsies established a specific histologic diagnosis. The diagnoses included metastatic carcinoma (5), cirrhotic nodule (2), hepatoma (1) and hemangioma (1). Six of these lesions were located in the left lobe of the liver and 3 were in the right lobe. In one patient with a left lobe lesion, guided biopsy failed to yield diagnostic tissue. A subsequent rib biopsy yielded undifferentiated adenocarcinoma. None of these patients had biopsy-related complications, including the patient with the hemangioma. The results demonstrate that scintigraphically guided percutaneous liver biopsy is a safe and useful technique for determining histologic diagnoses in patients with focal hepatic disease.

LIVER MASS ESTIMATION FROM THE RIGHT LATERAL PROJECTION OF THE RADIOCOLLOID LIVER SCAN. E.A. Eikman, G.A. Mack, V.K. Jain, and J.A. Madden. College of Medicine and College of Engineering, University of South Florida, and Veterans Administration Hospital, Tampa, FL

The purpose of this work was to devise a means for objective, reproducible estimation of liver mass. Gamma camera Tc-99m sulfur colloid liver images were digitized, preprocessed, and stored in computer memory. The liver was then adaptively defined for area measurement by means of a Laplacian operator that reproducibly measures change in radioactivity slope associated with the liver margin. Individual thresholds are calculated for each of sixteen subregions of the area-normalized image. A liver mass index was derived from a linear regression model correlating the area of the right lateral projection with liver mass at autopsy in 50 patients. The correlation coefficient found for this method was 0.83 using the equation:

Liver mass = 0.0542 (right lateral liver area) - 0.215

between about 0.8 to 3 Kg.

An alternate computer assisted method and representative manual methods adapted for gamma camera images all showed lower correlation with liver mass at autopsy. Experiments show that the superiority of the computer assisted method over the adapted manual methods may be attributable in part to freedom from the effects of observer variation and to freedom from the effects of changes in gamma camera intensity settings.(Supported by NIH Grant GM22890)

ELECTRONIC MOTION-CORRECTION IN EQUIVOCAL LIVER SCANS. R.D. Neumann, A. Gottschalk, P.B. Hoffer. Yale University School of Medicine, New Haven, CT.

Turner, et. al. have previously determined that the electronic motion-correction device for gamma cameras increases the detection of hepatic lesions in liver scintigraphy. Accurate diagnosis of equivocal liver scans is aided by combined nuclear medicine-ultrasound examination as described by Sullivan, et. al. The purpose of this study was to determine whether the motion correction device would be of value in improving the accuracy of diagnosis in equivocal liver scans.

Fifty cases termed equivocal at initial interpretation were selected for the study. Observers were asked to score the anterior image alone for the presence of focal lesions and/or diffuse disease. The initial scoring was done without observer knowledge of which image was motion-corrected. A second reading scored the same images now labeled as corrected or uncorrected.

The data were evaluated using a receiver operating characteristic (ROC) curve; a plot of the true-positive ratio against the false-positive ratio for varying confidence points. No significant difference was observed between curves representing scoring of corrected and uncorrected images with or without observer knowledge of the corrected image.

These results indicate that although electronic motion-correction may aid in the detection of hepatic lesions in unselected cases, it does not appear to increase accuracy in equivocal studies. This result may be expected since motion-correction is designed to enhance defect borders and image margins. Thus the corrected image aids the observer in detecting defects but does not help to characterize them.

* * *

The following two papers constitute a Rapporteur Session. The Rapporteur for this session is Peter M. Ronai, University of Kansas Medical Center, Kansas City, KS.

CLINICAL COMPARISON OF ^{99m}Tc-DIETHYL-IDA AND ^{99m}Tc-PYRIDOXYLIDENEGLUTAMATE FOR EVALUATION OF THE HEPATOBILIARY

SYSTEM. W.C. Klingensmith III, A.R. Fritzberg, and L.J. Koep. U. of Colorado Medical Center, Denver, CO.

The relative merits of ^{99m}Tc-diethyl-iminodiacetic acid (^{99m}Tc-diethyl-IDA) and ^{99m}Tc-pyridoxylideneglutamate (^{99m}Tc-PG) for evaluation of the hepatobiliary system were determined by performing 12 paired studies in 9 patients. The paired studies were performed an average of 1.8 days apart and a maximum of four days apart. Eight patients had liver transplants and the ninth patient had a cholangiocarcinoma. Images were obtained in the anterior and right lateral projections at 15, 30, 45, and 60 minutes and at 24 hours. ^{99m}Tc-diethyl-IDA images were superior to ^{99m}Tc-PG images in demonstrating: 1) the liver parenchyma, 2) the intrahepatic ducts, 3) small bowel activity early after injection, 4) colonic activity at 24 hours after injection, and 5) less renal and bladder activity. The relative merits of the two radiopharmaceuticals for evaluation of hepatocyte clearance by the 20 min/5 min blood retention method were compared using total blood bilirubin levels as the standard. The correlation coefficient between ^{99m}Tc-diethyl-IDA retention values and total blood bilirubin levels in 19 determinations was 0.33 and between ^{99m}Tc-PG retention values and total blood bilirubin levels in 82 determinations was 0.30. In conclusion, ^{99m}Tc-diethyl-IDA is clearly superior to ^{99m}Tc-PG for imaging the hepatobiliary system; using the blood retention method, neither radiopharmaceutical was a reliable indicator of hepatocyte clearance.

CORRELATION OF Tc-99m HIDA WITH ANATOMIC IMAGING IN PATIENTS WITH HEPATOBILIARY DISEASE. H. Weissmann, M. Frank, R. Rosenblatt, M. Goldman, L. M. Freeman. Montefiore Hospital-Albert Einstein College of Medicine, Bronx, NY

Several studies have attempted to correlate computerized tomography (CT) and ultrasound (US) with Tc-99m colloid imaging of the liver, particularly in space occupying disease. In this prospective study, the information obtained by studying 80 patients for suspected biliary tract disease with the new functional parenchymal cell agent, Tc-99m iminodiacetic acid (HIDA), was correlated with anatomic CT and US studies. In this series, 55 had US, 18 had CT and 15 had all three procedures.

In 43 scans done for suspected acute cholecystitis, it was determined that HIDA should be the initial study. Nonvisualization of the gallbladder (GB) was diagnostic of cholecystitis in all cases. Oral cholecystography (OCG) or US is necessary to determine if calculi are present in the few patients who have gallstones without acute inflammation. Patients with pain who have calculi demonstrated by OCG, US or CT should have a HIDA scan since the former modalities cannot determine whether visualized stones are the cause of the acute symptoms or an incidental finding, whereas, nonvisualization of the GB on a HIDA study effectively diagnoses cholecystitis.

17 patients were done to evaluate cholestasis. Visualization of dilated bile ducts and delayed intestinal activity strongly suggests extrahepatic obstruction. CT or US help establish the cause by locating calculi, pancreatic masses, etc. Dilated bile ducts on US or CT are purely anatomic findings and may represent residua of old disease. HIDA will establish whether any acute functional obstruction exists. Photon deficient areas seen in the region of the pancreas on the HIDA study were confirmed as pancreatic masses on CT.

* * *

The following four papers constitute a Rapporteur Session. The Rapporteur for this session is Leon S. Malmud, Temple University School of Medicine, Philadelphia, PA.

RADIONUCLIDE MARSHMALLOW SWALLOW FOR EVALUATION OF DYSPHAGIA. H.W. Henry, D. Staples, R.J. Lull, S.R. Kiser, B.D. Kehn, D. Yuille, R.J. Telepak, R.W. Lambrecht, R. Mc Auley. Letterman Army Medical Center, San Francisco, CA.

A nuclear imaging method for evaluating symptomatic esophageal motility disorders is described. The images obtained depict a composite representation of the transit of a solid bolus through the esophagus and into the stomach.

Each patient or control volunteer was placed in a 45° RPO position standing in front of a large field of view camera. A transmission source was used for delineation of the lungs and hemidiaphragms. Halved regular marshmallows containing a central capsule with approximately 500 uCi Tc-99m sulfur colloid were prepared. Each individual was studied with three consecutive marshmallow swallows. The total transit time was recorded for each swallow. Scintiphotos were obtained with at least 30 sec. exposure time. Intensity indicates the relative time which the bolus required to traverse each portion of the esophagus.

Ten control volunteers had a mean transit time of 18.0 sec. (standard error of mean = ± 2.2 sec.). Three patients with dysphagia have been studied. In each case the average total transit time was significantly prolonged (77.3 sec. for one patient, 46 sec. for another patient, and the third patient could only tolerate two swallows in which one bolus required greater than 3 min. to pass through the lower esophageal sphincter and the second bolus required 44 sec.). The studies also reproduced the patients' symptoms. Prior liquid barium esophagrams had shown normal motilities.

These results demonstrate that this technique will produce a scintiphoto representation of the region of abnormal motility and may be a sensitive method for evaluation of dysphagia.

PRELIMINARY EVALUATION OF A RADIOLABELED FIBER MARKER FOR GASTRIC EMPTYING. M.L. Brown, G.L. Carlson, and J.R. Malagelada. Mayo Clinic and Foundation. Rochester, MN.

Methods for studying gastric emptying of solid foods have suffered from poor label stability or being unphysiological. A natural fiber marker was selected for labeling with radioiodine.

The method of labeling α-cellulose involves 3 successive steps: 1) decrystallization and limited substitution with benzhydryl bromide to give benzhydrylcellulose (BHC); 2) iodination of BHC in trifluoroacetic acid; and 3) elution of unreacted radioiodine and other by-products by repeated washing in 5% $NaHCO_3$.

Chemical stability as determined by exposure of the radiolabeled fiber to 1N NaOH or 1N HCl over 48 hours showed elution of less than 0.3% of the iodine. Biological stability was assessed by balance studies over 5 days in 2 dogs using I-131 as a label. Total fecal recovery was 93.5% and 91.8%; urinary excretion was 1.3% and 0.6%, and serum levels were not detectable. Scanning demonstrated activity only in the abdomen. Thyroid activity was never above background levels. Tissue distribution studies of dog 1 revealed only background levels with the exception of the thyroid which contained 0.002% of the administered dose. In two other dogs with duodenal fistulae, the gastric emptying pattern of I-125 labeled fiber was compared to the liquid phase marker polyethylene glycol (PEG). Clear separation of the emptying pattern was observed with the $T_{\frac{1}{2}}$ emptying for PEG being 40 minutes and for I-125 being 2 hours.

This material appears to be a valuable tool for studying gastric emptying. Further evaluation is underway to study gastric transit and emptying in humans with radiolabeled (I-123 or I-131) fiber and gamma camera detection.

A NEW DUAL ISOTOPE TECHNIQUE TO CORRELATE GALL BLADDER AND GASTRIC EMPTYING. R. Tolin, L.S. Malmud, R. Menin, P.T. Makler, J. Reilley, R.S. Fisher. Temple University Hospital, Philadelphia, PA.

Coordination between gastric emptying and delivery of bile into the duodenum is important for proper absorption of fats. The purpose of this study was to develop a technique to visualize and quantitate gall bladder (GB) emptying and correlate it with gastric emptying in normal volunteers (10), and patients with gallstones (5), with hemigastrectomy and gastrojejunostomy (10), and with functional dyspepsia (3). One hour following I.V. administration 5 mCi Tc-99m HIDA, fasting subjects were given a liquid meal consisting of 80 gm fat, 72 gm protein, 138 gm carbohydrate in 300 ml, and containing 250 μCi

In-111 DTPA. In-111 and Tc-99m activity was recorded at 15 minute intervals for 2 hours over the stomach and GB using a gamma camera on line to a digital computer. Compared to the normal controls, patients with gallstones and functional dyspepsia had slow and incomplete GB emptying. In patients with gastrojejunostomy, the GB emptying rate was normal for the first 15 minutes, but slowed thereafter. The temporal correlation of GB emptying and gastric emptying was expressed as the ratio (R) of the rate of each: $R > 1$ in normals; $R < 1$ at all times in patients with jejunostomy, and in the second postprandial hour in patients with gallstones. This study suggests that 1) GB emptying is abnormal in patients with gallstones, functional dyspepsia, and following gastrojejunostomy; 2) the gastric emptying rate is rapid following gastrojejunostomy; 3) gastric and GB emptying coordination is disrupted in patients with gallstones, and gastrojejunostomy and 4) functional dyspepsia may be due to abnormal GB emptying.

DETECTION AND QUANTITATION OF ENTEROGASTRIC REFLUX FOLLOWING BILLROTH II SURGERY. R. Tolin, L.S. Malmud, R. Menin, J. Reilley, P.T. Makler and R.S. Fisher. Temple University Hospital, Philadelphia, PA.

Enterogastric reflux of bile and/or gastric stasis may underlie the postprandial nausea, bilious vomiting and abdominal pain which occur frequently in patients following Billroth II anastomosis. Bile reflux has been observed endoscopically in both symptomatic and asymptomatic patients following Billroth II surgery. To date, a noninvasive, quantitative test for enterogastric reflux has not been available. The purpose of this study was to develop a noninvasive technique for the simultaneous detection and quantitation of enterogastric reflux and gastric emptying for the evaluation of peptic ulcer patients before and after surgery. Following oral administration of 120 ml of potassium perchlorate, 5 mCi of Tc-99m-HIDA (5mg) were administered intravenously to fasted patients. One hour later a standard liquid meal labelled with 250 µCi In-111 DTPA was given. The Tc-99m and In-111 activity was recorded simultaneously for 1 minute periods at 15 minutes intervals for 2 hours over the liver, gall bladder, and gastric areas of interest. Enterogastric reflux indices (EGRI) and gastric emptying (GE) were determined for each consecutive 15 minute period. Three patients were studied following Billroth II procedures.
Conclusions: 1. Gastric emptying and enterogastric reflux are able to be visualized and quantitated simultaneously. 2. Patients with abdominal pain and bilious vomiting due to gastric stasis may be distinguished from those with bile gastritis, and 3. The technique is applicable to the evaluation of the postgastrectomy syndrome and to its treatment.

FRIDAY, JUNE 30 SANTA ANA ROOM
10:30 a.m.-12:00 p.m.

BASIC SCIENCE

DATA PROCESSING II: COMPUTER-ASSISTED IMAGING PROCEDURES

Chairman: David A. Weber
Co-Chairman: Valerie A. Brookeman

AN ANATOMIC-PHYSIOLOGICAL RENAL MODEL. **B.E. Oppenheim and C.R. Appledorn. Indiana University School of Medicine, Indianapolis, IN.**

We have constructed a realistic model for simulating the uptake and excretion of radioiodinated orthoiodohippurate (OIH) by the kidneys as imaged with the scintillation camera. We call this the Dynamic Renal Simulator (DRS). The DRS is an anatomic model of the components of the urinary tract combined with a physiological model describing the passage of OIH through these components.

The anatomic model consists of ten structures, four for each kidney (cortex, medulla, pelvis and proximal ureter), the bladder and the extrarenal tissues (liver and spleen superimposed on a uniform background). These are simulated realistically by mathematical expressions, which are parameterized to allow complete flexibility in specifying size, shape, orientation and location.

The physiological model is based on the seven-compartment model of DeGrazia et al. (J. Nucl. Med. 15:102,1974). The various physiological compartments are assigned to anatomic structures. The mixing compartment is assigned to renal cortex to represent diffusion from proximal tubular cells into the tubular lumen. The delay compartment is subdivided as follows: medulla → cortex → medulla → pelvis → ureter, with a separate transit time for each compartment to represent passage through the tubular lumen and upper collecting system.

Values are assigned to the parameters of the physiological model to simulate normality or various disease states. Time-activity curves are then generated for each anatomic structure. Sequential images are formed representing the composite activity distribution at different times. Finally, Poisson random noise is added, and a realistic simulation of a dynamic renal scan is obtained.

QUANTIFICATION OF FIRST PASS Tc-99m DTPA BLOOD FLOW IN TRANSPLANTED KIDNEYS. P.Cahill, S. Ho, J. Hurley, E.Ornstein P. Nikolich The New York Hospital-Cornell Medical Center New York, NY and Polytechnic Institute of New York, NY

Improved edge detection and deconvolution methods have been developed to quantitate effective renal blood flow in transplanted kidneys using first pass bolus injections of Tc-99m DTPA. Using list mode acquisition from scintillation camera and subsequent generation of 140 activity histograms at 0.2 second intervals, areas of interest over the aorta, both descending iliacs, kidney and background regions are flagged. By use of a nearest neighbor edge detection algorithm, the activity in these regions are calculated by computer. A deconvolution of the activity in the iliac artery is performed from a knowledge of the effective path of the iliac underlying the kidney and transit time delay between the iliac and the aorta areas. The effect of the aortic bolus is also deconvolved from the observed activity in the kidney. By use of a phantom, tracer counts are expressed as % of dose, and conservation of tracer activity within 2 to 5% is normally obtained. This analysis has also been applied to 10 renal transplant patients undergoing rejection therapy with methylprednisolone. The rate of tracer accumulation by the kidney remained statistically similar before and after 3 days of therapy, but the venous return from the kidney increased by a factor of 1.8 ($p > .98$). The increased rate of transport clearance of tracer is most marked in the effective cortex of the kidney. Equally, the results of the measurement of blood flow in the kidney without using these image analysis methods and high data framing rates are highly variable. In summary, we have been able to measure effective renal blood flow using Tc-99m DTPA in transplanted kidneys and have demonstrated modification of blood flow in kidneys undergoing therapy.

VELOCITY IMAGING: APPLICATION TO MULTIGATED CARDIAC STUDIES AND LIVER AND BRAIN FLOW STUDIES. A.S. Johnston, T. Gulick, I. Kim, and S. Pinsky. Michael Reese Medical Center, Chicago, IL.

The rate of change of counts in the image during a flow study was computed for each pixel, normalized and converted into a scale of gray for each pixel, and presented as scale of gray image on a television screen. A 64 x 64 matrix was used for all images.

The rate of change of the counts is the first derivative of the counts which collect in a particular pixel as a function of time. The derivative is the physiological velocity, hence velocity image.

The derivative of the counts in each pixel was computed by a least squares fit of a straight line to the counts in each pixel (4096 fits) versus time (slope =

derivative).

Physiologically significant information can be extracted from a velocity image. In multigated cardiac studies with a blood pool agent the counts in a pixel change for two reasons: the blood in the LV is squeezed away from the particular pixel; the boundary of the heart moves away from the pixel. The derivative image of the heart taken during contraction gives a view of the "velocity" of the heart.

Velocity images have been made from brain flows, liver flows, and cardiac multigated studies.

Results are that velocity images in liver flows give an improved visualization of structures vascularized by the hepatic artery. Velocity images in brain flows must be carefully interpreted because they are almost too sensitive to give reliable data on asymmetry of flow. Velocity images in cardiac multigated studies give a good indication of where changes in counts occur due to blood ejection and wall motion.

AN EVALUATION OF SEVERAL TECHNIQUES FOR THE MEASUREMENT OF PULMONARY AND CARDIAC CHAMBER TRANSIT TIMES. L.S. Graham, B. Horn, T. Nelson, F.E. Holly, and L.R. Bennett. UCLA School of Medicine, University of California, Los Angeles, CA.

Pulmonary and cardiac chamber mean transit times are often useful parameters in the evaluation of disease. The purpose of this study was to evaluate several methods of estimating transit times. These methods were compared to a Fourier-based deconvolution technique by which the transit time spectrum (transfer function) and mean transit time were computed. Time-activity (T-A) curves were generated using areas-of-interest over the right and left ventricles to obtain "pulmonary" transit times, and the left lung and aorta to obtain "left ventricular" transit times.

The peak-to-peak technique involved visual inspection of the T-A curves and selection of the peak time. The difference between the peak times for the two curves was defined as the mean transit time. Regression analysis yielded a correlation coefficient of 0.93 with the mean "left ventricular" transit time computed by deconvolution.

The T-A curves were also fitted with gamma variate functions and two other methods were used for computing the mean transit time. The times of maximum count rate were determined analytically; the difference was defined as the mean transit time. The correlation coefficient was 0.99. The difference between the centroids of the fitted curves a correlation coefficient of 0.992 for the "pulmonary" curves and 0.998 for the "ventricular" curves.

On the basis of this evaluation we have concluded that "pulmonary" and "ventricular" mean transit times can be accurately assessed using the difference between the centroids of the appropriate T-A curves without the use of deconvolution techniques.

IMPROVED PRECISION IN THE QUANTITATION OF Qp/Qs IN LEFT-TO-RIGHT SHUNTS. P.D. Esser. College of Physicians and Surgeons, Columbia University, New York, NY.

Improvements have been made in the technique of gamma-variate-analysis of pulmonary time-activity curves acquired with a scintillation camera. These have been incorporated into an assembly language algorithm for an on-line computer.

The time of first appearance of the activity in the lungs is treated as a variable. Since the shape of the gamma-variate curve is sensitive to time, this procedure permits further optimization of the fit to the initial pulmonic activity peak. Next, when indicated, the leading edge of the primary systemic recirculation curve is fitted with a gamma-variate function, a procedure verified on data from normals. This isolates the early recirculation ("shunt") peak which can then be fitted in the usual manner. All fitting is done by the method of weighted-least-squares with weighting factors corresponding to Poisson statistics.

The curve-stripping procedure appears to be particularly useful when the Qp/Qs ratio is less than ~1.6. In these cases, the shunt peak is often a small shoulder on the leading edge of the recirculation curve and, consequently, the area of the shunt curve is difficult to determine accurately. In addition, the introduction of the variance and the multiple-correlation coefficient in the printout provides an objective criterion for determining the goodness-of-fit and comparing fits.

COMPUTERIZED KINETIC ANALYSIS OF TWO 99m-Tc-Sn-DIPHOSPHONATES DEMONSTRATING DIFFERENT BINDING CHARACTERISTICS. J.S. Arnold, W.E. Barnes, N. Khedkar, and M. Nelson. Hines VA Hospital, Hines, IL.

Marked differences in the kinetic behavior of two similar diphosphonate compounds, EHDP and MDP, have been observed in human clinical bone imaging studies. We have developed a computerized technique for subtracting the blood and soft tissue backgrounds from sequential images of bone made over a period of 4 hours following I.V. injection of 99m-Tc-Sn complexed agent. The bone activity stripped of its background activity can be plotted for any imaged area of the skeleton. The time course of activity in vertebrae, pelvis, and femurs has been studied in 3 patients imaged with MDP and 6 with EHDP. The bone and blood time activity curves have been fit by a kinetic model in which bone is represented by two compartments, one exchanging with the blood and the other being non-exchangeable. The blood to bone fractional transfer constants were almost identical for the two agents. For Tc-99m-EHDP, the mean exchangeable bone to blood transfer constant was 6% per minute while that to non-exchangeable bone was 3% per minute. On the other hand, Tc-99m-MDP bone activity was virtually entirely irreversibly bound. The Tc-99m-EHDP transfer from exchangeable to non-exchangeable bone was greater in hot lesions than in normal bone, suggesting that Tc-99m-MDP may be a better imaging agent of the skeleton, but EHDP may image osteoblastic lesions better. It is suggested that the methyl and hydroxyl groups on the linking carbon of Tc-99m-EHDP may alter the configuration of the phosphonate groups so as to decrease their binding energy to mineral surfaces and making binding a reversible process. In newly depositing bone, the binding sites may be different where binding is irreversible.

A SPIROMETRIC METHOD FOR VOLUME GATING VENTILATION STUDIES. B.R. Line, R.G. Dunham, J.A. Cooper, T.R. Kushner, S.L. Bacharach, and G.S. Johnston. NIH, Bethesda, MD.

ECG gating has been critically important to the scintigraphic study of cardiac function, yet no similar technology for gating ventilation scans exists. Unfortunately, respiratory volume cycles are characterized by wide physiologic variations in cycle time and waveform, and also by the absence of a clear counterpart to the R wave as a cycle delimiter. We have overcome these difficulties with a computer program which generates image sequences reflecting changes in lung volume over an average tidal breath.

The respiratory cycle is obtained during equilibrium ventilation by sampling (100Hz) the volume in a water sealed spirometer. We store this information in list mode along with scintigraphic data and 10 msec. timing marks. The spirometer volume data must be corrected both for drifts due to constant oxygen input and carbon dioxide removal, and for sudden changes due to leaks at the patient mouthpiece. To make these corrections, a least squares technique is used to compute a reference line with respect to which all tidal breath volumes are measured. Respiration cycles are discarded if they show breath amplitudes greater than one standard deviation from the mean amplitude for all breaths. The scintigraphic data from the remaining tidal respirations is partitioned into 8-12 volume range images for both the inspiratory and expiratory phase of the breath cycle. We display the resulting image sequence in cinematic format for visual assessment of pulmonary volume dynamics. Initial experience with this program suggests that volume gating will provide a practical means of studying the intra-cycle distribution of ventilatory volume.

FRIDAY, JUNE 30
10:30 a.m.-12:00 p.m.

CALIFORNIA B ROOM

IN VITRO AND CORRELATIVE TECHNIQUES

ENDOCRINOLOGY III (CLINICAL SCIENCE)

Chairman: Hee-Myung Park
Co-Chairman: John G. Weir

CONTINUING OCCURRENCE OF THYROID ABNORMALITIES IN PATIENTS WHO RECEIVED HEAD AND NECK IRRADIATION. S.M. Pinsky, C. Bekerman, U.Y. Ryo, L.A. Frohman, M.J. Favus, and A.B.Schneider. Michael Reese Medical Center, Chicago, IL.

A relationship between head and neck irradiation in childhood and the development of thyroid abnormalities many years later has been established. In order to determine if these abnormalities are continuing to occur, patients who had normal neck palpation and thyroid image during their first evaluation, were re-examined 27 to 42 months after their initial study.

One-hundred twelve patients underwent Tc-99m thyroid image and neck palpation. The original and follow-up thyroid scans were compared without knowledge of the order in which they were obtained. The reviewer was to determine if the scans had changed and if so was to select the worst. Ninety-nine patients were determined to have unchanged scans, while eleven had scans that became worse and two had scans that became better.

Of the eleven abnormal patients, seven had palpable abnormalities not found at the initial examination. Three of these patients have undergone surgery to date. Two were found to have thyroid carcinoma and one a colloid cyst. Two patients had scans that were considered improved although the initial study had been called normal. This is probably on the basis of thyroiditis.

The incidence of thyroid scans becoming abnormal approximately three years after initial evaluation is 10%. Thus, it would appear that thyroid abnormalities are continuing to appear in adults who underwent head and neck irradiation in childhood.

TIME-CODED-APERTURE THYROID SCINTIGRAPHY. K.F. Koral, J.E. Freitas, W.L. Rogers and J.W. Keyes, Jr. University of Michigan Medical Center, Ann Arbor, MI.

Multiple view pinhole imaging (MVPI) has been shown to enhance the detectability of small thyroid nodules. Because of its tomographic response and its higher efficiency for small organs, coded-aperture imaging (CAI) of the thyroid should offer equal or improved performance.

Fifteen patients with known or suspected thyroid nodules received 3-5 mCi of TcO4 intravenously and standard anterior, LAO, and RAO pinhole images were obtained. CAI data were then obtained with the aperture 1 cm from the neck for the same time as for one pinhole image. Longitudinal planes were reconstructed at a depth of 1.2, 1.7, 2.3, and 3.3 cm from the skin using a modified algebraic reconstruction technique (ART).

One surgically confirmed 5 mm cold nodule was clearly shown by CAI but not seen by MVPI, while one cystic nodule was better visualized by MVPI. Subjective evaluation of the images showed the following:

CAI Better	MVPI Better	Equal
5	1	9

CAI offered the following advantages to MVPI: 1) Patient repositioning is avoided and total imaging time is reduced a factor of 3 to 4, 2) images are reconstructed to scale and are free of pinhole image distortion, and 3) resolution is improved. Disadvantages are: 1) CAI is motion sensitive and 2) a computer is required for image reconstruction.

The advantages of CAI appear to be significant and to warrant a full clinical trial of the technique.

VALIDITY OF THREE-DAY T-3 SUPPRESSION TEST. R.C. Verma, N.M. Panagiotis, L. Ramanna. UCLA-San Fernando Valley Medical Program, Los Angeles, CA.

The one week wait and the poor patient compliance are major drawbacks of the conventional Tri-iodothyronine (T-3) Suppression Test. Nicoloff et al (NEJM 283:402-5, 1970) advocate repeat RAIU a week after a single oral dose of 3mg of thyroxine but this still does not obviate the 7-day wait.

The present study was conducted to evaluate the accuracy of thyroid suppression induced by 100 ugm of T-3/day for 3 versus the conventional 6 days. Baseline RAIU's were obtained in 12 normal volunteers and 12 patients with thyroid disorders following 100 uCi of I-123 orally. Repeat RAIU's were obtained on the 4th & 7th day of T-3 administration.

The mean baseline 6- and 24- hour RAIU's in normal subjects were 10.4% and 18.3% respectively. After 3 days of T-3 ingestion, the 6- and 24-hour RAIU's dropped by 59% and 66% respectively; an additional fall of $\simeq$15% in the 6- and 24-hour RAIU's was recorded after 6 days of T-3.

In 8 suppressible thyroid disorders (including multinodular goiters), the 6- and the 24-hour RAIU's dropped by 60% and 69% respectively after 3days and by 65% and 73% respectively after 6 days. Three nonsuppressible glands demonstrated less tha 50% (range -6%to 23%) suppression after 3 and 6 days. One patient, whose 6- and 24-hour RAIU's dropped by 65% and 70% respectively after 6 days, failed to adequately suppress both RAIU's after 3 days.

In conclusion, preliminary studies indicate that adequate suppressibility ($>$ 50% fall in RAIU) of the thyroid can be assessed on the 4th day of T-3 administration and that the 6 hour uptake alone can be a good predictor of suppression in a majority (22/24 in this series) of the patients.

"REBOUND" ENDOGENOUS STIMULATION OF THYROIDAL UPTAKE IN EVALUATION OF AUTONOMOUS NODULAR GOITER (TRIIODOTHYRONINE SUPPRESSION TEST WITHDRAWAL). E.V. Kotlyarov and M.A. Quaife University of Nebraska Medical Center, Omaha, NB.

In order to evaluate suppressed perinodular thyroid tissue in patients with autonomous nodular goiter (toxic or nontoxic) TSH stimulation test is commonly employed. The possibility of allergic reaction to bovine TSH and some inconvenience of additional visits for patients led us to study the time course of "rebound" phenomenon after cessation of T-3 suppression. The 2 hour thyroid uptake of iodine (I-131 or I-132) and/or Tc-99m Pertechnetate was accomplished daily for 12 days immediately following completion of the suppression test in 24 euthyroid patients. The study demonstrated that maximal increased of 2 hour thyroid uptake of I-132 (I-131) was on 7th day after cessation supression test and was equal 140$\pm$ 25% (115-165%) of original uptake before suppression test. The maximal increased of 2 hour thyroid uptake of Tc-99m pertechnetate was observed on 6th day after cessation supression test and was equal 200$\pm$6% (155-270%) of original uptake before suppression test. Using these parameters we evaluated endogenous stimulation of thyroid uptake in 22 patients with toxic autonomous nodule with initally suppressed perinodular tissue. The suppressed thyroid tissue could be visualized with rectilinear scanning in 19 patients from 22 using described above technique. In our opinion, the repeat scan 6-7 days after cessation of "T-3 suppression" test could be used as a method of choice in evaluation of the suppressed perionodular thyroid tissue. This study suggests that in evaluation of suppressed perionodular thyroid tissue, the "rebound" endogenous stimulation offers advantages of safety as well as effacacy for patients with autonomous nodular goiter.

SIMULTANEOUS I-123 AND "EARLY" Tc-99m EHDP SCINTIMAGING IN THE DIFFERENTIAL DIAGNOSIS OF SOLID VS. CYST THYROID NODULES. H.N. Wellman, A.R. Siddiqui, R.W. Burt, H.M. Park, B.E. Oppenheim and B.T. Burney. Indiana University School of Medicine, Indianapolis, IN.

Initial observations that bone imaging agents transiently "localize" in thyroid nodules has lead to a correlation study with multiview I-123 thyroid scintimaging. 49 patients have been studied with follow-up in 28, 16 by sur-

gery (S) alone, 15 by ultrasound (US) alone and 3 by both.

Pinhole oblique I-123 thyroid images are followed by an anterior view and without moving the patient a 20 mCi I.V. dose of Tc-99m EHDP is injected obtaining superimposition anterior images 0-3, 3-6, 6-9 minutes post injection.

EHDP thyroid nodule uptake was interpreted as less than (18), equal to (20), greater than (9) or mixed (2) compared to I-123 normal uptake. All cystic lesions (9) by US or S were found to have less than I-123 uptake while all solid lesions (19) had equal to or greater than I-123 uptake. 2 mixed lesions were found to be mixed cystic and solid at S. 4 of the solid or mixed lesions were found to be thyroid carcinoma and 13 adenomas, the rest being multinodular glands. Two carcinomas had mixed uptake and 2 had uptake equal to I-123. One patient found to have less uptake than I-123 and interpreted as cystic was found to be solid by US leading to surgery where the lesion was found to be a cyst.

Thus simultaneous I-123 with Tc-99m EHDP thyroid imaging has been as accurate in separating solid vs. cystic lesions as US. However, solid lesions cannot be differentiated as to being benign or malignant. In the absence of US technique or as another independent assessment, simultaneous thyroid imaging can be helpful in the differential diagnosis of thyroid nodules.

THE ROUTINE USE OF THE OBLIQUE THYROID SCAN IMAGE. S. Pinsky, U.Y. Ryo, C. Bekerman, M. Creditor, and M. Colman. Michael Reese Medical Center, Chicago, IL.

One of the advantages of using the gamma camera with a pin-hole collimator is the availability of oblique views which enhance the diagnostic accuracy of the thyroid scan. But is the routine use of both oblique views necessary?

Eighty-four patients had Tc-99m thyroid studies consisting of an anterior and both oblique views. The images were reviewed without knowledge of the physical findings. The anterior view alone was reviewed initially and later all three views were analyzed in random order. The data were recorded as normal, abnormal or suspicious for each of seven regions of the thyroid.

Of 43 regions considered abnormal on the anterior view six became normal and three suspicious when all three views were studied. None of these nine had palpable lesions. Of 31 regions initially considered suspicious, 12 became normal, nine abnormal, and 10 remained suspicious. There were 514 regions initially called normal, of which six became abnormal and 19 suspicious when all three views were reviewed. Of the six that became abnormal all occurred in patients with other lesions that were suspicious or definite on anterior view and three were palpable.

In this series patients with normal anterior thyroid image and normal palpation, oblique views were not necessary. Those patients with abnormal or suspicious studies should have oblique views.

SERIAL THYROID IODIDE CONTENT IN HYPERTHYROID PATIENTS TREATED WITH RADIOIODINE. G.S. Lee, J.A. Patton, A.B. Brill. Vanderbilt University Medical Center. Nashville, TN.

Sixty consecutive hyperthyroid patients referred to the Nuclear Medicine Division for radioiodine therapy were studied using quantitative x-ray fluorescent scanning techniques to measure the thyroidal iodide pool. Forty-eight patients returned for serial follow-up studies after the radioiodine dose. Follow-ups were correlated with estimations of T3, T4, and TSH radioimmunoassays.

Initial iodide content before radioiodine therapy was generally normal or high in untreated cases and in those who had previously received drug therapy. Iodide content was low in those who had undergone previous surgery or radioiodine therapy.

Follow-up studies show a sharp decline of iodide content in the first 3 months post-therapy irrespective of type of management before or after radioiodine. Thereafter, the values tended to fluctuate at a low to low-normal level. In patients who ultimately became hypothyroid, a low iodide value preceeded the rise in TSH and the drop in T4.

It was shown that when thyroid iodide content is 2 mg. or less between 2-3 months after radioiodine therapy, there is close to 90% chance of developing hypothyroidism in the next 4-5 months. The low iodide value generally preceeded biochemical changes of hypothyroidism by an average of 2 months. Also, contrary to expectation, the mean initial iodide content was found to be no different in the untreated group compared to the drug-treated group.

FRIDAY, JUNE 30 CALIFORNIA A ROOM
10:30 a.m.-12:00 p.m.

CLINICAL PRACTICE

RADIOPHARMACY AND HEMATOLOGY

Chairman: Thomas A. Verdon
Co-Chairman: Albert S. Hale

PLAYING THE ODDS: WHEN TO USE GALLIUM AND WHEN TO LEAVE IT ON THE SHELF. S. L. Rosenthal, Holladay Park Hospital, Portland, OR.

INDIUM-111 OXINE LABELED AUTOLOGOUS LEUKOCYTES IN THE DIAGNOSIS OF INFLAMMATORY DISEASE. P. Doherty and D.A. Goodwin. Veterans Administration Hospital and Stanford University School of Medicine, Palo Alto, CA.

To determine the clinical usefulness of leukocyte scanning we studied 33 patients with suspected inflammatory disease. The cells were isolated using either 2% methylcellulose or 5% Hetastarch and labeled in saline with 0.5-1 mCi of In-111 oxine. The average labeling yield was >80% with a labeling time of 2 hours. Cell distribution was studied using whole body scans and spot views obtained at 4, 24 and 48 hours following reinjection.

In patients with positive scans (n=16) there was a good correlation between amount of white cell accumulation on scan and the intensity of inflammatory response being mild in healing wounds and intense in abscesses. The lack of normal bowel and bladder activity facilitated the diagnosis of abdominal and pelvic abscesses. In patients with positive bone scans and suspected osteomyelitis (n=9), the white cell scan was positive in those with acute osteomyelitis (n=3) and negative in those with chronic osteomyelitis, fractures or bone grafts. In 4 patients with acute myocardial infarction and positive PYP scans studied 4-7 days post infarction, all had normal white cell scans. On follow-up of patients with negative scans there were no false negatives.

White cell scanning is very sensitive in the detection of acute inflammation but has the disadvantage that cell preparation is required and repeat scans cannot be performed with the same isotope for 5-7 days.

THIN LAYER CHROMATOGRAPHY (TLC) OF TECHNETIUM RADIOPHARMACEUTICALS: CLINICAL VALUE. B. Markus and S.J. Goldsmith. Mount Sinai Medical Center, New York.

Radiopharmaceutical (RP) kits for in-hospital labeling with 99m-Tc have become commonplace in nuclear medicine practice. TLC of preparations (prep) has been recommended to assay radiochemical purity. TLC, either with acetone or normal saline was performed on 99m-Tc Sulfur Colloid, 99m-Tc MAA, 99m-Tc DTPA, and 99m-Tc PYP prep. to detect 99m-TcO4 and TcO2. For 99m-Tc MAA, 99m-TcO4 values varied up to 15%; no gastric or thyroid activity was noted. For 99m-Tc Sulfur Colloid, up to 20% 99m-TcO4 was detected; no evidence of 99m-TcO4 was seen in images. 99m-TcO4 in 99m-Tc DTPA prep. usually varied up to 13% without imaging evidence of parotid, thyroid, or gastric activity. In one instance, parotid activity was seen in a sample later found to contain 58% 99m-TcO4.

Estimates of 99m-TcO4 in 99m-Tc PYP prep, depended upon media used. Up to 44% 99m-TcO4 was found with ITLC-

SA; < 1% with ITLC-SG with no 99m-TcO4 in images. 99m-TcO2 content varied in different systems and increased dilution of RP: 0 dil.(60 mCi/mL), 8-12%; 1/10 dil., 13-19%; 1/100 dil.,64-75%; 1/1000 dil., 80-87%. Dilution did not effect 99m-Tc DTPA results. In a two solvent system (acetone, normal saline), estimates of 99m-Tc PYP prep. depended upon the solvent sequence. Initial development in normal saline increased 99m-TcO4 up to 87%. Other RP were more resistent to this effect.

We conclude that (1) freshly prepared 99m-Tc RP kits regularly meet quality standards when used as directed; (2) TLC is subject to a variety of artefacts; and (3) the advantage of routine TLC is questionable.

DRUG INTERACTIONS AND INCOMPATIBILITIES WITH Tc-99m RADIOPHARMACEUTICALS. R.L. Hodges, St. Vincents Infirmary, Little Rock, AR.

This is a literature survey to summarize reports of the effects of drugs and disease states on the distribution and excretion of Tc-99m radiopharmaceuticals. There are several physiologic effects of drugs which could alter the expected behavior of Tc-99m. Drugs may alter interstitial fluid volumes, electrolyte content or protein levels. They may also alter the extent that Tc-99m is bound to available serum protein. Drugs which alter capillary permeability may influence the degree of uptake at and around a tumor site. Thus, false nagative interpretations of brain scans may occur when large doses of dexamethasone are given prior to scanning. Any drug which blocks the available routes of secretion or excretion can influence the radiation exposure of patients. For example, there appears to be marked changes in gastric content of Tc-99m in relation to food intake. Rapid accumulation of radioactivity in the small intestine of individuals with low urinary excretion occurs. Gastric secretion of Tc-99m was found to be directly dependent on HCl production and parietal cell stimulation. The valence of Tc-99m can easily be altered by many agents which can lead to drastic changes in the in vivo behavior. In conclusion, there are significant drug interactions with Tc-99m. Most of these go unnoticed or are excused as being due to poor labeling or some other defect in preparation.

IATROGENIC ALTERATIONS IN THE BIODISTRIBUTION OF RADIOTRACERS. B.C. Lentle, R. Schmidt, and A.A. Noujaim. Department of Nuclear Medicine, Cross Cancer Institute and University of Alberta, Edmonton, Alta., Canada

The problem of drug interactions and drug incompatibilities are of increasing importance in clinical pharmacy. It must also be recognized that there may be alterations in radionuclide biodistributions resulting from treatment. Some of these are not widely known.

The subject will be reviewed with particular reference to the following observations:

chemotherapy:	bleomycin - pulmonary uptake of radiogallium
	cis-platinum- absence of hepatic activity-and marked renal uptake of radiogallium
	adriamycin toxicity- myocardial uptake of bone scanning agents
anesthesia:	reversal of liver/spleen uptake ratios of radiocolloid
surgery:	localization of radiogallium at operative sites
radiation therapy:	uptake of bone scanning agents in pulmonary radiation fibrosis
immunotherapy:	uptake of radiogallium in pulmonary BCG granulomatosis

These and other iatrogenic changes in the blood distribution of radiotracers are important variables to be considered in interpreting radionuclide images and in dosimetric determinations.

PROBLEMS ASSOCIATED WITH THE USE OF IN VIVO RADIOPHARMACEUTICALS. E. L. Holmes, Mallinckrodt Incorporated, St. Louis, MO.

PITFALLS IN IMAGING DUE TO RADIOPHARMACEUTICALS (PANEL). MODERATOR: A. S. Hale, Wilford Hall, USAF Medical Center, Lakeland AFB, TX. PANELISTS: F. H. Allen, Virginia Mason Clinic, Seattle, WA; S. L. Rosenthal, Holladay Park Hospital, Portland, OR; and T. H. Ravin, Rose Medical Center, Denver, CO.

FRIDAY, JUNE 30 — ANAHEIM ROOM
2:00 p.m.-3:30 p.m.

CLINICAL SCIENCE

CARDIOVASCULAR VI

Chairman: Robert W. Parkey
Co-Chairman: Michael L. Goris

ASSESSMENT OF REGIONAL MYOCARDIAL PERFUSION WITH N-13 AMMONIA AND POSITRON EMISSION COMPUTERIZED AXIAL TOMOGRAPHY ECT). H.R. Schelbert, M. Phelps, E. Hoffman, C. Selin, H. Huang, D. Kuhl. UCLA School of Medicine, Los Angeles, CA.

The feasibility to assess regional myocardial perfusion with N-13 ammonia (AM) and ECT was studied in 5 open chest dogs, each instrumented with flow probes around the left circumflex (LCx) and anterior descending (LAD) coronary artery and placed under the ECT camera. In each dog, AM (10 mCi) was injected together with radioactive microspheres (15μ) into the left atrium at 1 hr intervals while LCx flow was increased 2 to 5 times by intracoronary Papaverine (1 mg) and ECT was performed. On the ECT images the AM activity in myocardium supplied by the LAD and the LCx were determined and compared to the regional myocardial microsphere activity after sacrificing the animal. No significant AM redistribution was observed by delayed imaging. An increase LCx flow by 56% above control raised the ratio AM activity LCx/LAD from 1.01±0.21 to 1.31±0.27 ($p<0.05$); a LCx flow increase by 224% and by 369% above control raised the ratios AM activity LCx/LAD to 2.15±0.47 ($p<0.001$) and 2.01±0.11 ($p<0.001$). Myocardial AM uptake was related to myocardial perfusion in a non-linear fashion, e.g. as flow was increased by 56% above control, AM uptake increased by 29.6% ($p<0.02$). A further increase in flow by 107.7% and by 48.8% resulted in relatively smaller increases in AM uptake by 40.9% ($p>0.001$) and by 8.6% (NS). As flow increased AM extraction fell, e.g. by 40% for a 2.2 fold flow increase. Thus, myocardial AM uptake increases with flow. This relationship, however, is not linear because AM extraction falls as flow increases. Although AM uptake increases little in the extremely high flow range, it sufficiently increases within the physiologic range of flow and should prove useful for assessing regional myocardial perfusion by ECT.

NONINVASIVE ASSESSMENT OF CORONARY DISEASE IN MAN BY MYOCARDIAL IMAGING DURING PHARMACOLOGIC VASODILATATION. P.C. Albro, K.L. Gould, R.J. Westcott, and G.W. Hamilton. Veterans Administration Hospital, Seattle, WA.

^{201}Tl myocardial imaging was performed at rest, following maximal treadmill exercise, and during coronary vasodilatation induced by intravenous (IV) dipyridamole (D) in 41 patients (pts) who underwent coronary angiography. Dipyridamole 0.142 mg/kg/min was infused for 4 minutes with ECG and BP monitoring. Four minutes after infusion, the pts stood and walked in place, and ^{201}Tl was injected IV.

Myocardial images following D infusion were compared with rest and exercise (E) ^{201}Tl images. Myocardial/background (M/B) count ratios of 2.3±0.5 after D were significantly higher than M/B ratios for E images (2.1±0.4; p <

.02). Defects were identified in 21/31 (68%) of D and E images in pts with >50% stenosis of one or more coronary arteries. 13/31 (42%) had abnormal rest images; in 9 pts image defects increased with E (8/9) or D (9/9). One of 10 pts with no stenosis >50% had a defect on D and E images.

Following D infusion BP decreased significantly from 130±14/81±10 supine to 121±18/73±10 standing ($p < .001$). M/B ratios in D images increased compared to rest and these increases were significantly greater in pts with larger increments in supine HR, suggesting individual variation in drug effect at this fixed dose. However, sensitivity did not increase in the group with larger increases in M/B ratios. 12 pts (29%) had mild angina. 2 pts (5%) had the gradual onset of significant angina, terminated immediately by IV aminophylline, an antagonist of D, after ^{201}Tl injection. Intravenous infusion of D is a safe, effective method of inducing coronary vasodilatation and identifying regional perfusion abnormalities without E in pts with coronary artery disease.

"CIRCUMFERENTIAL PROFILE": A NEW METHOD FOR ANALYZING THALLIUM-201 MYOCARDIAL PERFUSION IMAGES. R. Burow, M. Pond, A.W. Schafer, and L. Becker, Johns Hopkins Hospital, Baltimore, MD.

Visual interpretation of thallium-201 myocardial perfusion images (MPI) is a subjective task influenced by image quality, background correction, contrast enhancement, and video display. We have developed a computer technique called "circumferential profile" (CP) for objective, quantitative analysis of MPI.

For each MPI an elliptical region of interest (ROI) is placed around the left ventricle and the geometric center is identified. The ventricular edge is defined by those points having a selected percent of peak activity within the ROI. Radii are extended from the center to each circumference point. Mean isotope activity along every radius is computed, normalized, and depicted as a graph of activity versus circumference point, thereby describing a CP for that MPI.

Rest and exercise imaging was performed in three projections in 15 volunteers and 20 patients with coronary disease. A composite CP with 2 standard deviation normal limits was constructed from volunteers' CPs. For volunteers, mean image radius was 12.8+1.0 points and circumference was 84.6+6.6 points. Mean radius (13.4+1.5 points) and circumference (106.0+15.9 points) were larger for patients with coronary disease ($p < .005$). CP fell outside normal limits of the composite curves for 96 of 100 visually perceived MPI defects and for 7 of 19 MPI without defects ($p < .005$). Abnormal CP regions averaged 30+14 percent of image circumference and represented at least 20 percent reduction of maximum activity.

Our studies indicate that computer-generated CPs may be a useful method for objective analysis of thallium-201 myocardial images.

INDIUM-111 LABELED PLATELETS FOR IMAGING BACTERIAL ENDOCARDITIS. M.L. Thakur, A.L. Riba, J. Downs, V.T. Andriole, B.L. Zaret, and A. Gottschalk. Yale University School of Medicine, New Haven, CT.

The cellular component of bacterial endocarditis (BE) has been found to be composed largely of platelets. The ability of In-111-labeled platelets to detect BE by cardiac imaging was investigated in an experimental model. BE was induced in rabbits by abrading the aortic valve with a catheter followed by the intravenous injection of Streptococcus sanguis. Three to seven days later each animal received 150 μCi of In-111 heterologous rabbit platelets. In vivo cardiac scintigraphy was performed on each animal daily for 3 days with a gamma camera equipped with a pinhole collimator. Following in vivo imaging, animals were sacrified, the extirpated hearts were imaged and concomitant radioactivity in the lesion and in normal left ventricle tissue samples were determined and compared.

Cardiac images obtained within 24 hrs post-injection of the platelets reflected blood pool activity while images obtained at 48-72 hrs demonstrated abnormal uptake in the region of the aortic valve in all animals. Hot spot images of excised hearts anatomically correlated with the site of vegetative lesions. Histopathological and microbiological examination of these lesions revealed the presence of platelets and bacteria. In-111 uptake in the BE lesion from 13 animals averaged 271 ± 48 (range 80-532) times greater than in normal myocardium. In contrast 4 normal rabbits failed to demonstrate either abnormal images or radioactivity uptake.

This study demonstrates the ability of In-111 platelets to image the lesions of experimental BE.

INDIUM-111 LABELED LEUKOCYTES FOR IMAGING ACUTE MYOCARDIAL INFARCTION: INFLUENCE OF REGIONAL MYOCARDIAL BLOOD FLOW, AND AGE OF INFARCT IN CANINE MODELS. M.L. Thakur, B.L. Zaret, A. Gottschalk. Yale University School of Medicine, New Haven, CT.

The ability of In-111 oxine labeled autologous leukocytes (PMN) to image acute myocardial infarct (MI) was investigated in dogs with closed chest embolic anterior MI. Groups of 4 to 6 animals each received autologous In-111-PMN i.v. either at 2, 24, 48, 72 or 96 hrs post-MI. In vivo cardiac imaging was performed 20 hrs after injection. Following imaging thoracotomy was performed and Sr-85 labeled microspheres were administered into left atrium to measure regional myocardial blood flow (RMBF). Sr-85 and In-111 activity in 50 samples per animal, obtained from normal and MI zones allowed measurement of RMBF and uptake of In-111 PMN. Controls consisted of sham operated animals given In-111 PMN and MI animals given In-111 oxine.

Focal uptake of In-111 was observed in MI in all animals imaged between 24-96 hrs, while at 120 hrs images were normal. In-111 uptake occurred primarily in transmural MI area of less than 40% of normal RMBF. At 24 and 48 hrs In-111 uptake was 9 X greater than normal myocardium (NM) and was evenly distributed across the ventricular wall. At 72 hrs the radioactivity in MI zones increased to 27 X (NM) and was localized in the endocardium with less than 10% RMBF. At 92 hrs the ratio decreased to 15 X NM but was still localized in the endocardium. The ratios were negligible at 120 hrs. In control animals there was no evidence of increased radioactivity in myocardium.

The study demonstrates that In-111 labeled PMN is a potential agent for imaging acute MI and that leukocytic infiltration in MI zone is independent of RMBF.

TECHNETIUM-99m PERTECHNETATE SEQUENTIAL SCINTIPHOTOGRAPHY: AID IN DIFFERENTIATING BETWEEN EXUDATIVE AND TRANSUDATIVE PERICARDIAL EFFUSIONS. S. H. Yeh, R. S. Liu and O. K. Liu Veterans General Hospital, Taipei, Taiwan

Since exudates are different from transudates in their contents and the mechanism of their formation, it would be feasible to determine the type of pericardial effusions by their diffusion patterns after I.V. injection of a diffusible tracer. Accordingly, Tc-99m pertechnetate sequential scintiphotography has been used to differentiate pericardial exudates from pericardial transudates.

Sequential cardiac blood pool scintiphotos were recorded at 5, 15, 30, and 60 min after I.V. injection of 10 mCi of Tc-99m pertechnetate with the patient in the same position. The results were divided into two categories: (A) fast diffusion when there was final complete obscuration of "holo" of decreased radioactivity surrounding the cardiac blood pool within 1 hr; and (B) slow diffusion when the "holo" was still discernible clearly at 1 hr.

In 7 cases studied, the correlation of the type of pericardial effusions as confirmed by pericardiocentesis or pericardiostomy and the assigned degree of diffusion in each case is shown in the table:

Type of effusion	Degree of diffusion	
	Fast	Slow
Transudate	2	
Exudate		5

Ongoing studies continue. Initial results suggest that the delayed sequential study would extend the applications of radionuclide angiocardiography to differentiating pericardial exudates from pericardial transudates. Thus it may provide additional information to alert the physician to the possible type of disease process present.

QUANTITATIVE PULMONARY RADIOANGIOGRAPHY: A RELIABLE METHOD FOR MEASURING LEFT-TO-RIGHT SHUNTS. P.M. Johnson, R.A. Boxer, P.D. Esser, R.A. Fawwaz, and C.N. Steeg. College of Physicians and Surgeons, Columbia University, New York, NY.

The accuracy and interobserver variability of quantitative pulmonary radioangiography (QPR) in detecting and quantifying left-to-right (L→R) shunts was evaluated in 23 patients aged 5 months - 16 yrs, within 2 hrs of cardiac catheterization (CC). During CC, L→R shunts were detected in 18 of these patients by oximetry (Ox) and angiocardiography.

Each patient underwent QPR while supine, using Tc-99m pertechnetate (200 μCi/kg) injected rapidly into the external jugular or antecubital vein or superior cava. Chest images were acquired at a rate of 2/sec for 45 sec, using an Anger-type camera with parallel-hole collimator and an MDS computer. The pulmonary-to-systemic shunt ratio (Qp/Qs) was determined by pulmonary transit curve analysis using the gamma variate model of Maltz and Treves. Qp/Qs values, calculated independently by 3 observers, were matched to each other and to CC data.

Qp/Qs values by QPR and by CC correlated well (r=+0.93). Discrepancy in 2 patients may reflect the inadequacy of Ox. Every patient with Qp/Qs greater than 1.2/1 by Ox had a positive QPR. There were no false positive QPR data and no significant interobserver differences.

QPR is an accurate noninvasive technique to quantify L→R shunts and may, with other appropriate data, preclude the need for CC in selected patients.

FRIDAY, JUNE 30 SANTA ANA ROOM
2:00 p.m.-3:30 p.m.

BASIC SCIENCE

DATA PROCESSING III: COMPUTER-ASSISTED RECONSTRUCTION TECHNIQUES AND IMAGE PROCESSING

Chairman: Ronald R. Price
Co-Chairman: K. William Logan

EFFECTS OF INACCURATE ATTENUATION CORRECTION IN EMISSION COMPUTED TOMOGRAPHY (ECT). S.C. Huang, M.E. Phelps, E.J. Hoffman, D.E. Kuhl. UCLA School of Medicine, Los Angeles, California.

In ECT, inaccurate attenuation correction would introduce error on reconstructed images. As more and more emphasis is placed on the quantitative aspect of ECT, this error needs to be carefully evaluated. By computer simulation of a 20 cm diameter cylinder of μ=0.088 cm^{-1} and of uniform activity, the effect of the following realistic types of errors are studied. (1) Incorrect size of attenuation object; (2) incorrect location of attenuation object; (3) incorrect shape of attenuation object; (4) incorrect attenuation coefficient; (5) non-uniformity of attenuation coefficient; (6) non-zero background level due to scattering and random coincidence. After attenuation correction, a filtered back-projection algorithm with the ramp filter function is used for final image reconstruction.

It is found that errors due to types 2 and 5 have strong visual artifacts on the reconstructed image and distort the true regional distribution of radioactivity in the cylinder. Errors due to the other types introduce relatively smaller artifacts and appear only as uneven shadings on the cylinder. For all the error types studied, the reconstructed activity level on the cylinder deviate significantly from the true values. For example, a 5% error in cylinder diameter causes the activity level at the center to be affected by 5.5%. A 2.3% error in attenuation coefficient causes an error of 5%. A background to total count ratio of 17% causes an error of 8%. These percentage error of the reconstructed activity is also found to be larger, as the size of the cylinder increases. It is concluded from this study that, in ECT, reliable quantitative results can be obtained only if the attenuation correction is accurate.

ATTENUATION INDUCED SPREAD FUNCTIONS IN E-CAT. S.C. Pang and S. Genna. Boston VA Hospital and Boston University School of Medicine, Boston, MA.

Previously (J.Nucl.Med. 17:552, 1976 and IAEA Symposium on Medical Radionuclide Imaging, 1976) we demonstrated the effects of attenuation on E-CAT by means of computer simulation of "brain-like" elliptical phantoms. One conclusion was that a point source, which transmits nonisotropically along different angular directions, reconstructs as a point spread function having nonisotropically positive (or negative) tails along paths having higher (or lower) transmissions than the average. Since reconstruction is a linear process, attenuation can be expressed in terms of these spread functions. This paper shows that in general a spread function is derivable from the angular distribution of the transmissions from the source point, with a peak equal to the average value of the transmission and tails functionally dependent on the angular transmission distribution, falling as $1/r^2$ from the source center. Positron reconstructions have more highly attenuated spread functions with larger more anisotropic tails than do ^{99m}Tc-reconstructions.

We have also studied the effect of attenuation on noise by direct reconstruction of the variance distribution of simulated phantoms. This is required for single photon (gamma-ray) sources for which variance reconstruction is non-linear with respect to the source distribution. For positrons this reconstruction is linear; hence, variance spread function analysis is applicable. These variance spread functions have a peak value dependent on the average inverse transmission, tails which fall as 1/r, and the same angular nonisotropicity as the inverse transmission.
(Supported by Veterans Administration Research Funds)

SIMULTANEOUS MULTIPLE ANGLE RECONSTRUCTION TECHNIQUE (SMART) FOR EMMISSIVE TOMOGRAPHY. D.L. Kirch, R.A. Vogel, M.T. LeFree, and P.P. Steele. VA Hospital, Denver, CO.

The computational method reported here provides first estimate tomographic reconstruction values which are sufficiently accurate to minimize the number of iterations required to reach a satisfactory convergence by the ray sums. The basis for this method is a new arithmetic operator which computes an estimate for each reconstructed volume element (voxel) from the corresponding values of the original planar picture elements (pixels) in a set of multiple angular views. This estimate is modulated so that when all the pixels corresponding to a given voxel are large in magnitude the reconstructed voxel is assigned a large relative value. When one or more of the pixels have a small magnitude, the voxel is assigned a correspondingly smaller value. This estimator has been found to have excellent performance characteristics. The count-rate linearity has been measured using a stackable ring phantom which simulates myocardial perfusion imaging and found to be within statistical limits. The estimator has very little tendency to produce "ringing" artifacts as associated with many reconstruction techniques and the smoothness of the resultance reconstructions is much improved over other methods. We have applied SMART to the problem of reconstructing a set of 12 tomographic myocardial perfusion images from 7 simultaneous images made using a multiple pinhole collimator on a large field Anger camera. The tomographic results were visually graded (VG) and statistically graded (SG) by the computer and the probability of detection in patients with known coronary artery disease was improved from .92 (VG) to .95 (SG). The speed and accuracy of this method is essential for a clinically practical tomographic system.

REAL-TIME CORRECTION OF RADIOISTOPE CAMERA SIGNALS FOR NONUNIFORMITY AND NONLINEARITY. G.F. Knoll, M.C. Bennett, and D.R. Strange. Medical Data Systems, Ann Arbor, MI.

We have developed and tested a microprocessor-based device which allows the position and energy signals from an Anger-type gamma ray camera to be digitized and processed in real time to eliminate the image distortions and nonuniformities which result from imperfections in these signals. The correction is applied to each event from the camera and takes two distinct forms: a position shift and a more exact energy selection. The X and Y position signals are transformed into real position coordinates which are shifted as required to account for camera nonlinearity. The extent of the shift is derived from an initial calibration image of a phantom consisting of parallel lines oriented sequentially in the vertical and horizontal directions. Energy selection is accomplished by replacing the conventional fixed pulse height window with a spatially-dependent window which can follow variations in the energy signal amplitude with position. Calibration data for this operation are obtained under "flood" conditions. All calibration data are acquired and processed in an associated minicomputer system, and can easily be updated to accomodate changes in camera operating characteristics. The system will handle counting rates up to 200,000/s without data loss. The method not only eliminates nonlinearities or curvature apparent in bar phantom images, but also greatly improves field flood uniformity by correcting for the two major contributors to nonuniformity: spatial distortion and imperfect energy windowing. It should be emphasized that the uniformity is achieved without discarding events or upsetting the constant sensitivity to a point source everywhere within the field of view.

IMAGE RECONSTRUCTION FROM ORTHOGONAL VIEWS USING A POSITRON CAMERA. F.B. Atkins and P.V. Harper. Department of Radiology and The Franklin McLean Memorial Research Institute, The University of Chicago, Chicago, IL.

Positron cameras consisting of two large area, position sensitive detectors have been successfully used to reconstruct longitudinal tomograms from coincident information obtained from a single limited angle view of an object. The depth of axial resolution of such a device depends very strongly on the maximum coincident angle accepted, which in turn is a function of the dimensions and separation of the detectors. In fact, the most serious limitation of longitudinal reconstruction tomography is the inability to adequately locate large, low spatial frequency objects in depth.

With this limitation in mind, we have investigated the use of combining information from orthogonal views. This geometry is of interest because of its implications in terms of a possible design of a positron imaging system consisting of four stationary large area detectors. The reconstruction algorithm developed for this purpose involves an iterative deconvolution of conical projection data obtained with the positron camera from right angle views of the object. Such processing is capable of producing both longitudinal and transverse sections. Evaluations of this technique indicate that accurate reconstructions of the activity distribution in the two sets of orthogonal longitudinal planes are possible. Some distortion does however remain in the transverse sections which depends upon the detector diameter to separation ratio.

A SIMPLE WAY TO DIGITIZE CONTRAST RADIOGRAPHIC AND TOMOGRAPHIC SCANNER IMAGES FOR MINICOMPUTER PROCESSING. J.M. Uszler, J.A. Jengo, P. Briandet, V. Oren. Harbor General Hospital, Torrance, CA.

There is known value in processing digitized scintillation camera images for standardization, objective analysis and semiquantitation. To achieve these same ends we developed a simplified method to digitize (256 x 256 matrix) x-ray contrast ventriculographic and emission tomographic scanner (Pho/Con) images. Each contrast ventriculogram image from the cine series was projected, subsequently viewed by the video camera and digitized into a 256 x 256 matrix. This process required 2 seconds. It was condensed to a 64 x 64 matrix for background subtraction, calculation of ejection fraction by area-length method and determination of segmental wall motion using second derivative approach for edge definition. Background subtraction was done by comparing the image density over a rib to that of the ventricle, and subtracting this percentage of the pre-contrast image. In like manner each Pho/Con tomoplane was imaged while transilluminated and accumulated into a 256 x 256 matrix. Then it was condensed to a 128 and 64 matrices for trials of smoothing, filtering background subtraction and determination of regional count rates.

EF and SWM determined from digitized "cine" were not significantly different from the values calculated from ventriculogram tracings or by first pass radionuclide angiography at the same time as the contrast study.

Filtering, background correction and smoothing in 64 and 128 matrices of the Pho/Con images did not improve the tomographic data. However a method was developed for semiquanitated description (regional count rate) so that lesion to reference or background area comparisons could be made on the tomoplane showing best definition of lesion(s).

A TECHNIQUE FOR GENERATING AND STORING IMAGES USED IN OBSERVER PERFORMANCE STUDIES. R.T. Overman, J.L. Daly and R.M. Donati. Veterans Administration Hospital and St. Louis University, St. Louis, MO.

A technique for computer generation of images useful in observer performance studies by receiver operating characteristic (ROC) analysis was developed using a minicomputer. Focal areas of variably increased or decreased activity were produced in random locations in a flood field image by extracting two circular regions of interest, multiplying the counts in those regions by 0.1, 0.15 and 0.2, "smoothing" them and adding or subtracting them in the original location. Areas of increased activity simulated "hot spots"; areas of decreased activity simulated "cold spots". Twelve of the 40 images were defined as abnormal on the basis of the presence of two areas of increased or decreased activity; the remaining 28 were considered normal. The images were photographed and displayed in a 35 mm projection slide format to 29 physicians, eight of whom were familiar with nuclear images, in a workshop in Medical Decision Making. The physicians were asked to rate the images by two scoring methods: variable criteria and a certainty level. Both scoring methods used scoring forms and graph paper which translated responses directly into true positive and true negative fractions used as the basis for plotting conventional ROC curves. Differences in ROC curves were obtained by experienced and non-experienced readers and the exercise was shown to be an effective vehicle for teaching concepts of observer performance variations. The technique can be used in training and suggests the possibility of quantifying reader performance using clinical images based on known pathology.

FRIDAY, JUNE 30 — CALIFORNIA B ROOM
2:00 p.m.-3:30 p.m.

IN VITRO AND CORRELATIVE TECHNIQUES

RADIOASSAY V

Chairman: Bernard J. Shapiro
Co-Chairman: Benjamin Rothfeld

A COMPARISON OF THREE RADIOIMMUNOASSAY TECHNIQUES FOR THE MEASUREMENT OF SERUM FOLATE. Mary L. Brown and Robert F. Carretta. Wilford Hall USAF Medical Center,

Lackland AFB, TX. and Roseville Community Hospital, Roseville, CA.

Three commercially available kits employing three different radionuclides were studied in order to determine: 1) the precision and accuracy of each, and 2) differences that may exist in serum folate levels using different radionuclides. The Diagnostic Products Corporation kit uses ^{3}H-folic acid as the tracer, methyl THFA as the standard, and dextron-coated charcoal to separate bound and free fractions. New England Nuclear Company uses a ^{125}I-histamine-folic acid conjugate as the radioligand, PGA as the standard, and a charcoal separation method. ^{75}Se-selenofolate is the radioligand employed by Amersham/Searle Corporation. Reference standards were supplied as methyl THFA and, albumin-coated charcoal was used for separating free from bound folate. The validity of the assays was studied by determining the per cent recovery of exogenous folate added to serum and by measuring the serum folate concentrations obtained by assaying various dilutions of serum from a patient with an elevated folate level. Serum folate determinations were performed in duplicate on serum samples containing 5 mg/ml of ascorbic acid as an antioxidant. The assay performance of the Diagnostic Products ^{3}H kit was superior in all areas tested, although the assay procedure has all the difficulties associated with liquid scintillation counting.

RADIOASSAY (RIA) DETECTION OF ANTIBODY TO HEPATITIS A ANTIGEN IN BLOOD DONORS AND HOSPITAL ADMISSIONS. F. Ashkar and F. Block, Jackson Memorial Hospital, Miami, FL.

Conservative estimates place the incidence of type A (infectious) hepatitis at 50,000 cases/year in U.S.; (non-B hepatitis cases may actually number tenfold greater.) Our investigation for the presence of antibody to Hepatitis A by RIA has enabled identification of "high risk" cases and establish the feasibility of general screening. The method, a direct solid phase assay, is based on competitive binding of patient serum anti-HA Ab., with I-125-labelled anti-HA Ab for known amount of A antigen. Gamma counter is used after overnight incubation at room temperature. In addition to a standard panel of sera, we examined 941 donors of John Elliott Blood Bank (JEBB) and 441 random admissions to Jackson Memorial Hospital, Miami, Fl. The survey also included radioassays for HB_sA_g, HB_sAb, HB_cAb. Presence of Ab to Hepatitis A was found in 298 JEBB donors (31.6%) similar in profile to general population. Hospital admissions, however, were positive in 308 cases (67.6%), compatible with the previously suspected increased Anti-A Ab presence in areas of crowding, poor hygiene, debilitation. Results by RIA compare more favorably than prior immune-adherence method, detecting specific Ab for Hepatitis A, days earlier. Prompt identification during the early communicable phase is now possible for arresting further transmission during outbreaks of the disease.

STAT PROCEDURE FOR DIGOXIN RADIOASSAY, I.W. Chen, M. Sperling and C. Volle. Radioisotope Laboratory, University of Cincinnati, Cincinnati, OH

A short, simple and precise digoxin radioassay suitable for stat determinations was developed by using optimum conditions for the antigen-antibody interaction and was compared with our routine procedure (Beckton Dickinson). The binding of antigen (I-125 labelled digoxin) to its specific antibody was maximum at temperatures between 35 to 45°C. A two-fold increase in the concentrations of antigen and antibody resulted in about a 30% increase in the rate of their interaction at 37°C. Under these conditions, the binding was 80% maximum after 10 min. of incubation and the change in the binding with time at this point was sufficiently small to allow precise radioassay of digoxin. Separation of free antigen from antibody-bound antigen could be accomplished instantaneously by dextran-coated charcoal.

The stat procedure involved a 10 min. incubation at 37°C of antigen, antibody and standard or serum in duplicate (three standards, 1, 2 and 3 ng/ml, and two control sera), followed by charcoal addition, centrifugation at 1,500 x g for 5 min. at 4°C and counting the supernatant fluid for 0.5 min. A semi-logarithmic plot of percent binding against digoxin concentration gave a linear standard curve (r=0.9951, n=15). The digoxin values obtained by the stat procedure correlated extremely well with those obtained by the routine procedure (r=0.9737, y=0.0356 + 0.9915x, n=40). The recovery of added pure digoxin was better than 94%. The within and between assay coefficients of variation were less than 8.4%. With this stat procedure, the result could be reported out in less than one hour after the receipt of the specimen.

OPTIMIZATION OF ANTIGEN-ANTIBODY REACTION FOR MEASUREMENT OF ANGIOTENSIN I. L.R. Witherspoon, S.E. Shuler, M.M. Garcia, L.A. Zollinger. Ochsner Medical Institutions, New Orleans, LA.

Measurement of plasma renin activity - the renin dependent generation of Angiotensin I from renin substrate, inhibition of conversion to Angiotensin II and the subsequent radioimmunoassay of Angiotensin I - has been helpful in the clinical assessment of hypertension. Overnight generation may be required to achieve the sensitivity necessary to distinguish low from normal renin patients. Identification of those samples requiring longer generation is facilitated by a rapid radioimmunoassay rather than one requiring overnight incubations. We have investigated the kinetics of Angiotensin I - antibody interaction at 4, 22 and 37° C. Displacement produced by added standard (15-500pg) was measured after incubation for 1/2-22 hrs. at each temperature. Labelled and unlabelled antigen were added simultaneously to antibody and "bound" antigen separated from "free" by charcoal. Synthetic Angiotensin I (WHO 71/328) was measured in all assays at two dilutions. Equilibrium (no further change in % B/T) was reached in 6 hrs. at 37°, 18-22 hrs. at 22° and not achieved in 22 hrs. at 4°. Percent B/T of the zero standard at equilibrium was 32% at 37°, 45% at 22° and 45% in 22 hrs. at 4°. Plots of B/F vs dose permitted estimation of the apparent K_a and assessment of sensitivity loss at higher temperatures or shorter incubation times. Nonspecific binding (incubational damage) was not increased by higher temperature or longer incubations. At 22° B/T was 65% of equilibrium in 3 hrs. Assays at these conditions reproducibly yielded results similar to the 4° 22 hr. assay with negligable loss of sensitivity. This modification permits same day results and earlier identification of low renin specimens.

DIRECT COMPARISON OF RADIOIMMUNOASSAY AND IMMUNORADIOMETRIC ASSAY FOR THE MEASUREMENT OF HUMAN GROWTH HORMONE. M. A. Wilson, Y. Kao, and L. E. M. Miles. Stanford University Medical Center, Stanford, CA

Two general immunological methods exist for measuring antigens or haptens. These are the radioimmunoassay (RIA) and the immunoradiometric or labeled antibody technique. The immunoradiometric assay (IRMA) is a reagent excess system that allows all the unknown antigen to combine with the labeled antibody, resulting in a direct assay system. This contrasts with the competitive inhibition (indirect) assay system of RIA. On the basis of several theoretical and experimental considerations it has been claimed that the IRMA technique has significant advantages. This study was undertaken to test this claim. A rigorous comparison of the two techniques using the same anti(HGH)serum ($K=0.4x10^{11}$ liters/mole), standards and quality control samples was performed. The assay conditions were identical in both methods and the same incubation times, volumes and temperatures were used. The average coefficient of variation (CV) of the response of the standards was 1.9% in 2-site IRMA and 2.9% in RIA. The 2-site IRMA technique had a lower minimal detectable dose (6pg/ml plasma versus 77 pg/ml) and the assay range (defined by a CV less than 20%) was wider (113-fold versus 19-fold). These results confirm the superiority of the 2-site IRMA technique with regard to precision, sensitivity, and assay range.

AN IMMUNORADIOMETRIC ASSAY USING A TERMINAL LABELING AND A DOUBLE ANTIBODY TECHNIQUE. A.Gükce, R.Nakamura, T.O'Brien, M.Tubis and W.Wolf. Radiopharmacy Program and Department of Obstetrics and Gynecology, University of Southern California Los Angeles, CA.

Present methods of radioimmunoassay and related techniques are primarily based on the use of I-125 labeled agents. While this radionuclide has many advantages, the iodination reaction and its $t_{\frac{1}{2}}$ limit the sensitivity, the shelf life and sometimes the immunological integrity of the labeled protein.

A method has been proposed by one of us (M.T.) (JNM 15, 526,1974) that suggested the use of a labeled antibody by conjugating it with a metal chelator, followed by binding this conjugated complex with In-111. We wish to describe here further development of this work, using a double antibody immunoradiometric assay, where the second antibody will carry the metal chelating group. This reagent now becomes a "universal reagent", as it will react with any unoccupied antibody site. Labeling will proceed after the specific antibody has been bound to the modified second antibody, and short lived and generator produced radionuclides such as In-113m and Ga-68 can be used.

In addition to the increased sensitivity, no chemical modification of the primary specific ingredients, such as the antibody and the antigen, are required, and no radioactive waste is generated in the procedure.

A GENERAL PURPOSE RADIOASSAY PROGRAM FOR OBTAINING THE BEST FIT IN CONSTRUCTING THE STANDARD RADIOASSAY CURVE. S.R. Kiser, H.G. Lehman, R.J. Lull, D.L. Yuille, B.T. Dewey, B.D. Kehn. Letterman Army Medical Center, San Francisco, CA.

A general purpose program for obtaining the best fit for radioassay standard curve construction has been developed. The program will yield 96 fits to the standard points based on 6 polynomial regressions on the transformed data according to the method of least squares. Curves exhibiting non-monotonic behavior or inflection points over the range of the standard points are rejected as best fits by using the first and second derivatives of the curve. The best fit is chosen from the remaining curves as the one with the highest correlation coefficient. We show that if the rejection capability is not included, curves with very high correlation coefficients may not be suitable and that a plot of the standard curve is highly desirable.

In a busy radioassay laboratory using automated data reduction methods, the choice of a mathematical function for obtaining the dose from a measured response variable utilizing the standard curve is essential for rapid evaluation. In recent years some manufacturers have recommended such functions while others have not. We have found the general program to be very useful in developing such functions where none are recommended, or in assessing the accuracy of the manufacturer's recommended fit.

We have analyzed several assays with the program and present a comparison of fits recommended by the manufacturer and by the general program. We conclude that in most of the cases, improved clinical accuracy may be obtained by estimating dose from response using the result of the general program.

FRIDAY, JUNE 30 GARDEN GROVE ROOM
2:00 p.m.-3:30 p.m.

CLINICAL PRACTICE

GOVERNMENTAL AFFAIRS

Chairman: Gilbert Greenspan
Co-Chairman: John B. Richards

RIGHTING THE LIABILITY BALANCE. E. Hamilton, Chairman, California Citizens' Commission on Tort Reform.

MEDICAL PRACTICE UNDER A GOVERNMENT-SPONSORED PROGRAM: THE CANADIAN EXPERIENCE. D. L. Gilday, Hospital for Sic Children, Toronto, Ontario, Canada.

MEDICAL PRACTICE UNDER A GOVERNMENT-SPONSORED PROGRAM: THE AUSTRALIAN EXPERIENCE. I. P. Murray, Prince of Wales Hospital, Randwick, New South Wales, Australia.

FRIDAY, JUNE 30 SANTA ANA ROOM
3:45 p.m.-5:15 p.m.

BASIC SCIENCE

DATA PROCESSING IV: CARDIOVASCULAR

Chairman: Stephen L. Bacharach
Co-Chairman: David L. Gilday

KINETICS OF MYOCARDIAL INFARCT GROWTH IN DOGS: COMPARTMENTAL MODEL AND EFFECTS OF DRUG INTERVENTION. P.Cahill, S. Ho, J. Jacobstein, D. Alonso, S. Kline, and M. Post. The New York Hospital-Cornell Medical Center, New York, NY and Polytechnic Institute of New York, Brooklyn, NY

Tc-99m glucoheptonate (TcGH) is currently the only "hot spot" imaging agent capable of demonstrating the growth of myocardial infarction (MI) within the first hours after onset of infarction when presumably salvageable myocardium still remains. By use of "nearest neighbor" edge detection algorithms and deconvolution procedures, TcGH radioactivity was measured in the total area of uptake over the ischemic myocardium and it's outer and middle regions over 12 to 14 hours following infarction in 10 dogs with acute MI's produced by occulsion of the left anterior descending coronary artery. The middle region of TcGH uptake, a probable necrotic region, shows a relatively constant amount of TcGH, while the outer region of ischemic but presumably salvageable myocardium, shows a rapid and continuing uptake of TcGH. TcGH activity in all control dogs showed a constant accumulation for at least 8 to 10 hours following MI.

Pulse doses of propranolol 4 to 6 hours after MI dramatically decreased the total activity of TcGH uptake along with changes in activity in the "necrotic" and "ischemic" regions. Pulse doses of propranolol given 24 hours after infarction produced no effect on MI. A six compartment model has been developed to describe the kinetics of MI and the distribution of TcGH. The analytical description of the dynamics of MI growth is essential in order to evaluate quantitatively the effects of interventions.

A METHOD FOR COMPUTERIZED INTERPRETATION OF MYOCARDIAL PERFUSION SCINTIGRAPHIC IMAGES. M.T. LeFree, R.A. Vogel, D.L. Kirch, and P.P. Steele. VA Hospital, Denver, CO.

A method for interpretation of myocardial perfusion images using a minicomputer was developed and used to evaluate planar and tomographic Tl-201 images. Scintigraphy was performed following intravenous injection of 1.5 mCi of Tl-201 during exercise on a graded treadmill. Parallel hole collimator images were taken in AP and 40 degree LAO projections. Tomographic images in the 40 degree LAO projection were obtained from data taken with a seven pinhole collimator and a large field Anger camera using an iterative least-squares reconstruction algorithm. All images were smoothed, background corrected, and normalized for maximum counts. Maximum myocardial wall counts were determined along 60 rays extending radially from the geographic center of each myocardial image at 6 degree intervals around the myocardial silhouette. Mean and standard deviation from the mean values were calculated for the 60 angles in each individual image for a group of 27 angiographically normal individuals. The lower limit of normal was defined

to be the mean normal distribution minus two standard deviations from the mean for each angle. Distributions from a series of 51 patients (including the 27 normals) were then compared to this limiting distribution. Any patient curve falling below this lower limit was called abnormal. Results from computer interpretation (CI) and visual interpretation were compared to results from coronary angiography. In our controlled patient population, CI demonstrated an increase of approximately 15% in sensitivity and 10% in specificity for both parallel hole and tomographic imaging. Thus it is shown that myocardial perfusion images can be interpreted with greater accuracy by this computer implemented numerical technique.

COMPUTERIZED CARDIAC NUCLEAR KYMOGRAPHY. P.H. Murphy, J.A. Burdine, M.L. Moore, M.W. Groch, and P.L. Von Behren. Baylor College of Medicine, St. Luke's Episcopal/Texas Children's Hospitals, Houston, TX, Group Research, Searle Diagnostics Inc, Des Plaines, IL.

Nuclear kymography is a data processing and display technique which permits quantitative assessment of boundary movement for cyclic functions such as ventricular contraction. A one-dimensional scintigraphic image in time, synchronized to the patient's ECG, is obtained from a narrow rectangular region of interest (ROI) across the boundary under study. Kymograms may be produced using a gamma camera-minicomputer combination. Computerization allows rapid evaluation of multiple ROI's across different boundaries from data collected from multigated ventricular wall motion images.

Multigated equilibrium Tc-99m albumin images at a rate of 40 frames per cardiac cycle are collected using a Gamma-11 system synchronizing the collection with the R-wave. Kymograms are extracted from multigated images along any rectangular ROI, 32 cells long, and a minimum of one cell wide within the 32 x 32 matrix. The magnitude of segmental wall motion is measured from the kymogram after calibration of the system for distance.

A correlation coefficient greater than 0.90 in the magnitude of wall motion by kymography has been obtained in comparison to contrast ventriculography. The time rate of change of wall position can also be obtained from the kymogram and is presently being analyzed for the evaluation of systolic ejection and diastolic filling rates.

Computerized cardiac kymography is an effective mechanism to add quantitative information to multigated wall motion images.

THE MEDIAN WINDOW FILTER AS A SMOOTHING/EDGE PRESERVING TECHNIQUE. R. Scott, F. Atkins, and P.V. Harper. University of Chicago, Chicago, IL.

A central problem in radionuclide imaging is the definition of edges (e.g., cardiac blood pool or myocardial uptake defects). Most edge detection computer routines use information contained in 1st or 2nd derivatives to locate edges, with the image first smoothed to suppress the effects of quantum noise on the derivatives. The most commonly used techniques (weighted averaging and least squares fitting) have the disadvantage that smoothing is accomplished at the expense of blurring the edges. We have investigated a smoothing method used in optics - a median window filter (MWF) - in which an N x N (N is an odd integer) "window" is moved through all the pixels of the digitized image, and the count density at the midpoint of the window is replaced by the median value of the count densities of the N x N pixels. We have compared the performance of the MWF, a least squares technique, and a weighted average technique in smoothing low contrast, low count density, noisy computer generated images and clinical images. Results show that the MWF preserves edges much better than the weighted average method and slightly better than the least squares method, while suppressing statistical noise much better than the least squares method and somewhat better than the weighted averages method. The use of this approach should be helpful particularly in objective estimation of the size of defects in thallium imaging and in wall motion studies in the heart using gated blood pool images.

A CURVILINEAR COUNT PROFILE PROGRAM FOR NUCLEAR MEDICINE IMAGES. E.C. Glass, H.H. Hines, G.L. DeNardo. University of California, Davis, CA.

Most organs have curvilinear anatomy, for example, myocardium. Conventional computer techniques that generate count profile curves (CPC) along straight lines are therefore of limited value in evaluating regional distributions of radioactivity. We developed a program to generate CPC from curved lines (CL). CL were drawn with a light pen on a 64x64 image matrix. The operator flagged a starting pixel on the CL and the program advanced pixel by pixel along the CL to generate a CPC. The value of each point of the CPC was based on an adjusted average of counts in the corresponding CL pixel and in the greatest 5 of 8 surrounding pixels, normalized to the value of a single pixel. Only 5 of 8 pixels were included in the adjusted average so that pixels beyond the edge of an organ were excluded from consideration if the CL were drawn near the edge. The number of points in the generated CPC equaled the number of pixels flagged by light pen in the initial CL.

We performed a preliminary study to illustrate the utility of this technique in 12 patients (pts) who underwent both coronary angiography and exercise (Ex) and rest (R) Tl-201 myocardial scintigraphy. Ex and R CPC interpretations agreed with independent angiographic interpretations in 10/12 pts as to the presence or absence of significant coronary artery disease. Interpretations of Tl scans on film by independent observers showed agreement with angiography in 9/12 pts. Changes in segmental perfusion between Ex and R were more clearly displayed by CPC than by scans.

CPC generated by this technique from CL provide additional quantitative information from imaging studies that is not available from conventional nonlinear photographic displays or from CPC generated from straight lines.

A COMPUTERIZED PATIENT RECORD SYSTEM FOR CARDIO-NUCLEAR DATA. A.L. Pai, J.M. Zaid, J. Sbarbaro, H. Karunaratne, L. Resnekov, and P.V. Harper. Department of Medicine, (Cardiology), The University of Chicago, Chicago, Il.

This paper describes an on-line, interactive computerized patient record system for the entry, correction, storage, search and retrieval of clinical cardio-nuclear data especially from patients with ischemic heart disease. This system uses a minicomputer interfaced with a video terminal for data entry, a disk drive for data storage, and a high speed line printer for producing copies of patient reports. The modular software has been written in FORTRAN IV, and runs under a real time operating system.

The physician requesting a cardio-nuclear study fills out the appropriate sections of a four page computer form indicating: type of study (static, dynamic, list, ECG gated etc.), the radionuclide to be used, clinical interventions, ECG analysis data, and initial diagnosis. The imaging study is then conducted, and its technical aspects filled out on the form including: gamma camera switch settings, types of views, total counts and time per view, etc. The clinician then reviews the scintigrams, indicates the final diagnosis, and writes the free text conclusions. This alphanumeric data is entered into the computer and can easily be corrected or updated if desired.

A special in-house text editor enables insertions, deletions, or corrections of the free text portions of the patient record. Also, this system allows on-line search operations in any combination on its total data base. System advantages include: 1) ease of data entry, correction, and retrieval of patient reports; 2) interactive search capabilities on its total data base for obtaining selective patient populations for both routine clinical and specialized research protocols in nuclear cardiology.

QUANTITATIVE ANALYSIS OF RADIOCARDIOGRAM (RCG) BY DIGITAL SIMULATION METHOD. Y. Yonekura, Y. Ishii, K. Minato, M. Kuwahara, and K. Torizuka. School of Medicine and Automation Research Laboratory, Kyoto University, Kyoto, Japan.

The purpose of this study is to extract various quantitative parameters concerning flow/volume relations in the RCG curve by digital simu-

lation method using a minicomputer automatically.

RCG and input curve were obtained by a multicrystal gamma camera injecting Tc-99m human serum albumin intravenously, and transferred to a minicomputer with 24kw by a magnetic tape. The principal model of the transport process in the circulatory system is made up of four compartments of first order lag system; right heart lungs, left heart and body; and two transport delays, one for the pulmonary and the other for the systemic circulation. After the simulation of input curve, RCG was transformed into a frequency domain by Fourier transformation and curve fitting was performed, where we cut off the high frequency components as a noise.

Many useful parameters were obtained through this simulation study, namely cardiac output, intracardiac shunt flow, mean transit times of four compartments and so forth. The parameter values showed a good agreement with those by the conventional analog simulation method (1). It takes about 5 minutes for this simulation, and it is fast enough for the routine clinical use.

1. Ishii Y, et al., J Nucl Med 12: 792, 1971

FRIDAY, JUNE 30 GARDEN GROVE ROOM
3:45 p.m.-5:15 p.m.

CLINICAL PRACTICE

CARDIOVASCULAR II

Chairman: Donald A. Podoloff
Co-Chairman: William Turner Harris

PREVENTION OF UNNECESSARY AMPUTATION OR PROLONGED HOSPITALIZATION: THE PERIPHERAL ULCER PERFUSION STUDY. M.E. Siegel. LAC/USC Medical Center, Los Angeles, CA

The purpose of this paper is to present and review a clinically useful procedure to determine the healing ability of an "ischemic ulcer" thus aiding in the prevention of unnecessary amputation or unnecessarily prolonged hospitalization.

Peripheral vascular perfusion scans, using Tc-99m labelled albumin microspheres, have been performed in over 100 patients with ischemic ulcers of the lower extremities. They can be administered via a catheter already in place as part of a contrast angiogram, or via a femoral artery puncture with a 20 gauge needle, which makes the procedure suitable for outpatient studies. After administration, the distribution of perfusion is subjectively evaluated via leg scans and objectively evaluated via point counting over the ulcer and surrounding normal tissue. From the point counting, the degree of hyperemia, associated with the inflammatory response of healing, is determined.

When the degree of hyperemia in the patient's ulcer bed compared to surrounding tissue is at least 3.5:1 there is approximately a 90% chance of the ulcer healing while in those patients whose ulcers do not have this degree of hyperemia, approximately 90% eventually required an amputative procedure. Little correlation was noted between the presence of diabetes, palpable peripheral pulses or the status on the trifurcation vessels, as seen on the ateriogram and the ability of the lesions to heal.

The presence and degree of hyperemia in an ulcer is a clinically useful indicator of healing.

IMPROVED DATA COLLECTION EFFICIENCY BY SHIELDING IN CARDIAC BLOOD POOL IMAGING. J.H. Thrall, J.M. Clare, W.L. Rogers. University Hospital, Ann Arbor, MI.

Two factors limit data acquisition rates in heart blood pool studies: (1) camera/computer count rate limitations due to deadtime and (2) absolute acquisition rate limitations in some computer systems. Shielding of extracardiac structures offers a method of approaching both problems.

A cardiac shield has been fabricated for 10" field of view cameras from a 1.0 mm thick lead disk with a 12" outside diameter and a central 6.5" diameter viewing aperture. For stability the shield is sandwiched in plexiglass and attaches to the collimator face via Velcro strips. In 200 clinical studies in adults, the 6.5" aperture was large enough to encompass the left ventricle in 98% of cases and both ventricles in approximately 90%. The oversized 12" outside diameter facilitates positioning.

In a series of 20 patients studied with and without the shield using 15 mCi Tc-99m Red Blood Cells and a 10" field of view camera with low energy parallel hole collimator (Searle Pho/Gamma HP), the shield reduced the total count rate in the field of view by an average of 35.8%±5.7 S.D. and at the same time the net count rate from the left ventricle increased 12.6%±4.5 S. D. (greater counting benefits would be anticipated with higher administered activity). Although not included in this study, image resolution should theoretically improve with lower total processed events and reconstruction times for list mode acquisitions should be reduced.

For negligible extra cost, shielding of non-cardiac activity significantly improves data collection efficiency in heart blood pool studies.

ROLE OF TECHNETIUM-99m PYROPHOSPHATE MYOCARDIAL IMAGING: APPLICATION OF BAYE'S THEOREM. G.T. Krishnamurthy, W.H. Blahd, R. Taylor, S. Kazmi, E.L. Rolett. Wadsworth VA Hospital & UCLA School of Medicine, Los Angeles, Ca

The role of Tc-99m pyrophosphate imaging in the evaluation of infarction was studied in 100 patients admitted to CCU for suspicion of acute myocardial infarction (MI). Images were obtained within 48 hours & repeated at 5-7 days and 9-11 days after the onset of chest pain. Imaging abnormalities were correlated with serial EKG & enzyme analysis. Sixty-one patients were found to have acute infarction (10 subendocardial). In the studies obtained within 48 hours considering only 2+ and 3+ (equal to or greater than rib uptake) myocardial uptake as abnormal, the sensitivity and specificity of the imaging tests were 84% and 61% with an overall accuracy of 75%. When combined with the initial EKG, the overall accuracy of imaging test was 70% as against a combined overall accuracy by EKG and enzyme of only 39%. In 55% of the patients with infarction, the EKG and imaging studies showed identical location of lesion and in the remaining 45% a discordant or an additional location was found in the imaging study. Only the decrease in intensity of myocardial uptake in the serial imaging studies is suggestive of acute MI. Either no change or increase in intensity has less discriminating value.

It was found that myocardial imaging has the best discriminant value (Baye's theorem) when the frequency of infarction in the population under study is from 0.4 to 0.7 and the discriminant value decrease at the rates below and above these levels. With a frequency rate of infarction of 0.61 in CCU patients, the probability of infarction increases to 0.77 in the presence of an abnormal imaging and decreases to 0.28 in the presence of a normal imaging study.

ATRIAL SEPTAL DEFECT - PRE AND POSTOPERATIVE EVALUATION BY GATED CARDIAC SCANNING. R.R. Libertheon, G.M. Pohost, R. E. Dinsmore, K.A. McKusick, W.H. Shea, and H. W. Strauss. Massachusetts General Hospital, Boston, MA.

Seventeen patients (pts) with secundum atrial septal defect (ASD) were evaluated sequentially by gated cardiac scan preoperatively, and in operated pts after 2 weeks and 6 months. Two groups were evaluated. (1) 10 pts with uncomplicated ASD (age 18-58 yrs): normal rhythm, pulmonary artery systolic pressure (PAP) < 30mmHg, right ventricular end-diastolic pressure (RVED) < 8mmHg, pulmonary-systemic flow ratio (QP/QS) 2-5/1; and (2) 7 pts with complicated ASD (age 36-75 yrs): atrial fibrillation - 4 pts, PAP 40-70mmHg - 4 pts, RVED ≥ 10mmHg - 3 pts, and QP/QS 1.7-3.0/1. Group 1 had marked preoperative right atrial (RA) and RV dilatation, mild RA and RV hypokinesis (HYPO) and inter-

ventricular septal akinesis or paradox; and 2 weeks post-op ASD closure, mild RV HYPO AND RA dilatation with new RA akinesis in all; and at 6 months, some RA and RV HYPO and septal akinesis or paradox remained in spite of absence of clinical heart failure. In group 2, all had marked pre-op RA and RV dilatation which persisted in 3 unoperated pts inspite of cardioversion or medical therapy. Four pts had ASD closure; 3 had no post-operative failure but mild RA and RV HYPO; the fourth pt had severe post-operative failure with marked residual RA and RV dilatation and HYPO on scan. In summary, gated scan delineated functional changes pre and post ASD closure, and persistant mild post-op RA and RV HYPO even in uncomplicated, asymptomatic pts. In complicated ASD, severe HYPO may be refractory to management, although milder abnormalities improved post-op.

THALLIUM-201 CLEARANCE FROM HUMAN MYOCARDIUM AND LUNGS FOLLOWING INJECTION AT STRESS. J.B.Bingham, H.W.Strauss, K.A.McKusick and G.M.Pohost. Massachusetts General Hospital, Boston, Ma.

Tl-201 myocardial imaging following injection at stress has been used to detect zones of ischemia. We have studied a series of patients following injection of Tl-201 at peak exercise with sequential, preset time imaging for up to 3 hours to define the rate of Tl-201 clearance from the heart and lung and to determine the effects of propranalol and ischemia on clearance rates. All images were recorded in a computer system and analysed by measurement of changes in counts in regions of interest placed over segments of myocardium and lung. Myocardial clearance of Tl-201 in 25 patients without stress induced ischemia averaged 7% ± 3.5% at 40 min. and 28% ± 8.5% at 150 min. In 13 patients with transient perfusion abnormalities, corresponding clearances were 7% ± 8% and 25% ± 7.5%. In the ischemic patients, intercomparison of normal with abnormal areas of myocardium showed clearances of 8% ± 4.5% and 28% ± 8% in normal segments and 4% ± 4% and 21.5% ± 7% in ischemic segments. The rate of lung clearance in the ischemic group was not different from the non-ischemic group, but the absolute uptake in lung was greater. When patients on propranalol were compared with those on no therapy, no significant difference was observed in the clearance from either heart or lung. These data suggest that the clearance of Tl-201 from the myocardium is not altered by propranalol and that the appearances of redistribution in ischemic areas are in part due to slower clearance in those ischemic areas of myocardium.

COMPARATIVE USEFULNESS OF EXERCISE THALLIUM 201 IMAGING AND RESTING INTRACORONARY PARTICLE DISTRIBUTION. A.J. Kolibash, T.D. Call, C.A. Bush, M.R. Tetalman, J. Olsen, and J. Scheu. Ohio State University Hospital, Columbus, OH.

This study was designed to assess the combined usefulness of stress thallium images and resting myocardial perfusion distribution using direct intracoronary instillation of In-111 and Tc-99m macroaggregated albumin particles (MAA). Of 56 patients with chest pain who underwent coronary arteriography, 18 were normal and 38 had coronary artery disease (equal to or greater than 50% narrowing). All eighteen patients (Group A) without coronary artery disease had normal thallium and particle distribution images. Of the 38 patients with coronary artery disease, 30 (Group B) had abnormal thallium images; however, only 13 patients had abnormal resting myocardial perfusion images. The other 17 patients had resting myocardial perfusion distribution scans without perfusion defects; the perfusion was maintained by native vessels in 8 and collateral vessels in 9. The remaining 8 patients (Group C) had normal thallium images; 7 had normal MAA images and 1 demonstrated a perfusion defect. In all patients myocardial perfusion imaging more clearly delineated perfusion from each coronary artery; in 9 patients a perfusion defect to a specific vessel was localized which was not possible with thallium. Thallium identified 79% (30/38) of the patients with coronary artery disease. Particle distribution imaging added valuable information as to: whether a perfusion defect was present at rest 43% (13/30); localization of a perfusion defect to a specific artery 30% (9/30); perfusion distribution pattern of each coronary artery; significance of collateral vessels. In assessing the physiological significance of coronary lesions, myocardial perfusion distribution with MAA plays a complementary role to exercise thallium.

AUTHOR/LECTURER INDEX

C

D

SCIENTIFIC EXHIBITS

All Scientific Exhibits to be presented at the 25th Annual Meeting of the Society are listed below by title and author. Submitted Exhibits are listed alphabetically by last name of first author and Teaching Exhibits by subject categories. All exhibits will be on display in the North Exhibition Hall, Anaheim Convention Center. For full abstracts, exhibit numbers and locations, and times for viewing and Scientific Exhibit Rounds, please consult the Exhibit Program for the meeting.

SUBMITTED EXHIBITS

IMAGING I-125 WITH A SCINTILLATION CAMERA. Ralph Adams, Gerald A. Kirk, Eloy Schulz, and Barbara Snell, Loma Linda University, Loma Linda, CA.

HOW HARD IS A ROC? Alan B. Ashare, Wright State University School of Medicine, Dayton, OH.

HEPATOBILIARY IMAGING: ROLE OF TECHNETIUM-99m HIDA. V.R. Bobba, M. Eklem, A. Jansen, D.J. Mahler, and G.T. Krishnamurthy, V.A. Hospital and University of Oregon Health Sciences Center, Portland, OR.

CLINICAL UTILITY: METHODOLOGY REQUIRED FOR THE CRITICAL EVALUATION OF DIAGNOSTIC PROCEDURES. Gary L. Carden, Robert E. Sonnemaker, John L. Floyd, and Martin L. Nusynowitz, William Beaumont Army Medical Center, El Paso, TX.

EFFICACY OF I-125 FIBRINOGEN IN THE DIAGNOSIS OF DEEP VEIN THROMBOPHLEBITIS: A MULTI-INSTITUTIONAL EVALUATION. R.F. Carretta, Roseville Community Hospital, Roseville, CA.

SKELETAL IMAGING WITH Tc-99m-Sn-METHYLENE DIPHOSPHONATE (MDP). H.M. Chilton, Robert J. Cowan, Nat E. Watson, Jr., Richard L. Witcofski, Richard J. Kelly, and C. Douglas Maynard, Bowman Gray School of Medicine, Winston-Salem, NC.

RADIOIMMUNOASSAY OF URINARY FREE CORTISOL WITH AGGREGATED ANTIBODY. Sonia Collins, Marianne Klonowski, Edward Bermes, and Marion Brooks, Loyola University Medical Center, Maywood, IL.

NP-59 ADRENAL IMAGING. John E. Freitas, James H. Thrall, William H. Beierwaltes, Dennis P. Swanson, Milton D. Gross, and Jean M. Clare, University of Michigan Medical Center, Ann Arbor, MI.

THE HOMEMADE BAR PHANTOM. David L. George, Cooper Medical Center, Camden, NJ.

BATCH PROCESSING ON A NUCLEAR MEDICINE COMPUTER. David L. George and Louis S. Zeiger, Cooper Medical Center, Camden, NJ.

THYROID FUNCTION TESTS--WHAT SHOULD I ORDER? George L. Jackson, Joseph S. Burkle, Him Gan Kwee, and Fred W. Flickinger, Harrisburg Hospital, Harrisburg, PA.

SINGLE PHOTON EMISSION COMPUTED TOMOGRAPHY USING MULTI-SLICE FAN BEAM COLLIMATORS. Ronald J. Jaszczak, Lee-Tzuu Chang, Anton M. Smudde, and Paul H. Murphy, Searle Diagnostics Inc., Des Plaines, IL, and St. Luke's Episcopal-Texas Children's Hospitals, Baylor College of Medicine, Houston, TX.

IMPROVED DIAGNOSTIC RESULTS OF MYOCARDIAL PERFUSION SCINTIGRAPHY BY LARGE FIELD ANGER CAMERA TOMOGRAPHY. M.T. LeFree, R.A. Vogel, D.L. Kirch, and P.P. Steele, V.A. Hospital, Denver, CO.

GLUCOHEPTONATE RENAL IMAGING. Joe C. Leonard, E. William Allen, Robert S. Chercorski, and Carl W. Smith, Oklahoma Children's Memorial Hospital, Oklahoma City, OK.

DETERMINATION OF BODY CONTOUR FOR ATTENUATION CORRECTION OF Tc-99m EMISSION COMPUTED TOMOGRAPHIC IMAGES. Fergus E. Moore, Neil A. Stein, and Eric G. Hawman, Searle Diagnostics Inc., Des Plaines, IL.

THE NATIONAL COUNCIL ON RADIATION PROTECTION AND MEASUREMENTS. W. Roger Ney and James A. Spahn, Jr., NCRP, Washington, DC.

CLINICOPATHOLOGIC FINDINGS IN FIFTY-TWO PATIENTS STUDIED BY TECHNETIUM-99m STANNOUS PYROPHOSPHATE MYOCARDIAL SCINTIGRAPHY. R.W. Parkey, L.R. Poliner, L.M. Buja, F.J. Bonte, and J.T. Willerson, U. Texas Health Science Center at Dallas, Dallas, TX.

THE BONE METASTASIS THAT WASN'T. Robert M. Sodaro, Santa Ana-Tustin Community Hospital, Nuclear Medicine Section, Santa Ana, CA, and University of California at Irvine Medical School, Irvine, CA.

NUCLEAR MEDICINE AND NUCLEAR MEDICINE TECHNOLOGY: A SHORT FILM. John Saban, Edward B. Stockham, Jerome Wagner, and Margaret T. Jaconski, Rochester Institute of Technology, Rochester, NY.

PROBE RADIOCARDIOGRAPHY: A CLINICAL REALITY. Robert E. Sonnemaker, John L. Floyd, and Anthony R. Benedetto, William Beaumont Army Medical Center, El Paso, TX.

PROBLEMS ENCOUNTERED WHEN PERFORMING A CALIBRATION CHECK OF DOSE CALIBRATORS USING CERIUM-141 AND VARIOUS OTHER STANDARDS. Ann Warbick, Princess Margaret Hospital, Toronto, Ontario, Canada, and Frank Taylor, St. Joseph's Hospital, London, Ontario, Canada.

GAMMA CAMERA ACCEPTANCE TESTING AND ROUTINE QUALITY CONTROL. David A. Weber, Linda A. Decker, Robert E. O'Mara, Azu Owunwanne, and George A. Wilson, University of Rochester Medical Center, Rochester, NY.

BONE SCANNING WITH 24-HOUR DELAYED IMAGES TO ELIMINATE URINARY TRACT ACTIVITY. Peter F. Winter, Lahey Clinic Foundation, Boston, MA.

TEACHING EXHIBITS

CARDIOVASCULAR

MULTIPLE GATED EQUILIBRIUM CARDIAC BLOOD POOL SCINTIGRAPHY: VALIDATION OF TECHNIQUE AND CLINICAL APPLICATIONS. D.S. Berman, J. Maddahi, A.D. Waxman, R. Gray, P.K. Shah, and J. Forrester, Cedars-Sinai Medical Center, Los Angeles, CA.

INVENTIVE EQUILIBRIUM CARDIAC STUDIES. R. Henkin, W. Chang, and A. Woodruff, Loyola University, Chicago, IL.

MYOCARDIAL INFARCT IMAGING WITH Tc-99m PHOSPHATES. R.W. Parkey, F.J. Bonte, L.M. Buja, E.M. Stokely, and J.T. Willerson, University of Texas Health Science Center, Dallas, TX.

ASSESSMENT OF CARDIAC FUNCTION BY RADIONUCLIDE TECHNIQUES. Heinrich Schelbert, John W. Verba, and William L. Ashburn, University of California at San Diego, San Diego, CA.

RADIONUCLIDE ANGIOCARDIOGRAPHY IN CONGENITAL HEART DISEASE. Peter M. Scholz, Stephen K. Rerych, and Robert H. Jones, Duke University Medical Center, Durham, NC.

INSTRUMENTATION

THE MULTIPLANE TOMOGRAPHIC EMISSION SCANNER: PRINCIPLES OF OPERATION. Hal O. Anger, Donner Laboratories, University of California, Berkeley, CA.

DISPLAY SYSTEMS FOR GAMMA CAMERAS. Robert T. Anger and John G. Allen, Methodist Hospital, Indianapolis, IN, and James E. Carey, University of Michigan, Ann Arbor, MI.

INSIDE THE GAMMA CAMERA. R.E. Johnston and F. Chan, University of North Carolina, Chapel Hill, NC.

MICROPROCESSORS IN NUCLEAR MEDICINE. D.S. Kearns and J.W. Steidley, Picker Corporation, Northford, CT, F.D. Rollo, Vanderbilt University Hospital, Nashville, TN, and E. Prokop, St. Raphael's Hospital, New Haven, CT.

EMISSION COMPUTERIZED TOMOGRAPHY TECHNIQUES. J.A. Patton, R.R. Price, and F.D. Rollo, Vanderbilt University Hospital, Nashville, TN, and L.S. Graham, UCLA School of Medicine, Los Angeles, CA.

PROPERTIES AND CLINICAL APPLICATIONS OF COLLIMATORS IN NUCLEAR MEDICINE. J.A. Patton, R.R. Price, and F.D. Rollo, Vanderbilt University Hospital, Nashville, TN.

PRACTICAL APPLICATIONS OF THE COMPUTER IN THE NUCLEAR MEDICINE LABORATORY. R.R. Price, J.A. Patton, J. Erickson, J.P. Jones, E. Lagan, and F.D. Rollo, Vanderbilt University Medical Center, Nashville, TN.

QUALITY CONTROL PROCEDURES FOR SCINTILLATION CAMERAS. Edward M. Smith, Walland, TN, and James Larose, Baptist Medical Center, Birmingham, AL.

PRINCIPLES OF SINGLE PHOTON EMISSION RECONSTRUCTIVE TOMOGRAPHY. Edward M. Smith, Walland, TN.

BONE IMAGING

THE TECHNIQUE OF BONE IMAGING AND SOME VARIATIONS OF EPIPHYSEAL LATE UPTAKE. Paul Denhartog, The Hospital for Sick Children, Toronto, Ontario, Canada.

THE "THREE-PHASE BONE SCAN" IN ASSESSING TRAUMA OF THE HAND AND WRIST. N.D. Greyson, E. Urowitz, A.E. Gross, and F. Langer, Mt. Sinai Hospital, Toronto, Ontario, Canada.

BONE IMAGING IN MALIGNANT DISEASE. Brian Lentle, Cross Cancer Institute, Edmonton, Alberta, Canada.

RADIONUCLIDE SKELETAL IMAGING IN INFLAMMATORY AND ISCHEMIC DISEASE. Massoud Majid, Children's Hospital, National Medical Center, Washington, DC.